



LUND UNIVERSITY

The variability in Salix BVOC emissions and possible consequences for managed SRC plantations

Karlsson, Tomas

2021

[Link to publication](#)

Citation for published version (APA):

Karlsson, T. (2021). *The variability in Salix BVOC emissions and possible consequences for managed SRC plantations*. [Doctoral Thesis (compilation), Dept of Physical Geography and Ecosystem Science]. Department of Physical Geography and Ecosystem Science, Lund University.

Total number of authors:

1

General rights

Unless other specific re-use rights are stated the following general rights apply:

Copyright and moral rights for the publications made accessible in the public portal are retained by the authors and/or other copyright owners and it is a condition of accessing publications that users recognise and abide by the legal requirements associated with these rights.

- Users may download and print one copy of any publication from the public portal for the purpose of private study or research.
- You may not further distribute the material or use it for any profit-making activity or commercial gain
- You may freely distribute the URL identifying the publication in the public portal

Read more about Creative commons licenses: <https://creativecommons.org/licenses/>

Take down policy

If you believe that this document breaches copyright please contact us providing details, and we will remove access to the work immediately and investigate your claim.

LUND UNIVERSITY

PO Box 117
221 00 Lund
+46 46-222 00 00



The variability in *Salix* BVOC emissions and possible consequences for managed SRC plantations

TOMAS KARLSSON

DEPARTMENT OF PHYSICAL GEOGRAPHY AND ECOSYSTEM SCIENCE | LUND UNIVERSITY





Salix plantation in Skrehalla November 2016. Even though they seem to be sad like weeping willows they are standing tall.

The variability in *Salix* BVOC emissions and possible consequences for managed SRC plantations

The variability in *Salix* BVOC emissions and possible consequences for managed SRC plantations

Tomas Karlsson



LUND
UNIVERSITY

DOCTORAL DISSERTATION

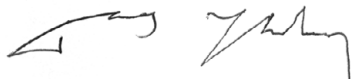
by due permission of the Faculty of Science, Lund University, Sweden.
To be defended at Lundmarksalen, Astronomihuset, Sölvegatan 27, Lund.
Friday 19 November, 2021 at 09:00.

Faculty opponent
Prof. Dr. Robert R. Junker

Organization LUND UNIVERSITY Department of Physical Geography and Ecosystem Science Author: Tomas Karlsson		Document name DOCTORAL DISSERTATION	
		Date of issue 2021-11-19	
		Sponsoring organization FORMAS	
Title and subtitle The variability in <i>Salix</i> BVOC emissions and possible consequences for managed SRC plantations			
Abstract Willow (<i>Salix</i> spp.) trees have been used commercially since the 1980s to produce renewable energy. Some benefits with these trees are that they can clean soil from heavy metals, reduce the risk of nutrient leakage and eutrophication. They could be an alternative to reduce carbon dioxide emissions from fossil fuel, but they are known to emit high rates of biogenic volatile organic compounds (BVOCs). Many thousands of different compounds are included in this group and they can be divided into terpenes, alcohols, alkanes and esters, to mention a few. These compounds are important. For instance, BVOCs help plants to attract pollinators. They serve as a protection to different kinds of stress, e.g., herbivores, heat and pollutions. Once they are released into the atmosphere, they will be involved in many chemical processes. Hydroxyl radicals, which are known to clean the air from pollutions, are depleted by BVOCs leading to increased lifetime of methane. Emissions of BVOCs could also act as precursors for aerosol formation, which in turn might lead to changes in cloud properties and radiative forcing. Photochemical smog like ozone (O ₃) is another result of the reactions in the atmosphere where BVOCs are involved, which impairs regional air quality. The reported range of emission rates from <i>Salix</i> is wide. Details about age, canopy position of leaves and how commercially used <i>Salix</i> varieties differ in their emission potentials are lacking, which lead to large errors if modelled emissions are based on too simple assumptions. Therefore, the aim of the work in this thesis was to investigate how the emissions vary with height, age, variety and during the growing season to get more reliable emission rates that can be used in models to better assess the impacts on the regional air quality. Measurements of aerosol formation were conducted to be able to determine the potential particle production near the <i>Salix</i> site. The outcome from the <i>Salix</i> measurements was then combined with BVOC measurements on spruce to assess how an expansion of <i>Salix</i> plantations could affect the regional air quality if a conversion of the land was shifted into these plantations, e.g., by using more arable and forest land. The study between 2015 and 2016, and the measurements in 2017, showed that <i>Salix</i> mainly emitted isoprene, which peaked during summer. Emissions of monoterpenes (MTs) showed a decreasing trend through the growing season. The BVOC emission rates differed depending on if the leaves were acclimatized to sunlit or shaded conditions, where the sun-adapted leaves emitted twice as much isoprene as the shaded. There was also a significant difference among the studied varieties, where Wilhelm emitted approx. three times more isoprene than Tora. Age influenced the emission rates. The emissions of non-terpenes from younger trees were substantially higher than from the older trees. Emissions of MTs were higher from younger trees compared to older as well. When comparing isoprene emissions, the emission rates from the older trees were almost five times larger than from the younger. Induced emissions of stress-related compounds like hexanal was observed due to an outbreak of <i>Melampsora</i> in 2015. Together with some other compounds, these emissions increased several times. All these results highlight the complexity of BVOC emissions and existing models need to be improved by including parameters like season, age, microclimate adaption and stress to better predict and estimate BVOC emissions. No particle enhancement could be observed from the <i>Salix</i> plantation near the site in 2015. The explanation for this result was the lack of precursors, e.g., MTs. However, spruce trees emitted higher rates of MTs and are probably more prone to generate particles compared to <i>Salix</i> trees. The high isoprene emissions from <i>Salix</i> is more likely to produce O ₃ if sources of anthropogenic NO _x are sufficiently close. An expansion of <i>Salix</i> plantations where spruce forest and traditional agriculture are converted into willow fields would lead to considerably more regional isoprene in the atmosphere. Thus, plantations of <i>Salix</i> should be strategically located to avoid prerequisites to form O ₃ , and preferably the variety Tora should be chosen since it emitted the lowest rates of isoprene.			
Key words: <i>Salix</i> , BVOCs, varieties, age, branch chamber, leaf chamber, GC-MS, aerosols			
Classification system and/or index terms (if any)			
Supplementary bibliographical information		Language: English	
ISSN and key title		ISBN (print): 978-91-89187-09-2 ISBN (PDF): 978-91-89187-10-8	
Recipient's notes	Number of pages: 174		Price
	Security classification		

I, the undersigned, being the copyright owner of the abstract of the above-mentioned dissertation, hereby grant to all reference sources permission to publish and disseminate the abstract of the above-mentioned dissertation.

Signature



Date 2021-10-11

The variability in *Salix* BVOC emissions and possible consequences for managed SRC plantations

Tomas Karlsson



LUND
UNIVERSITY

Front and back cover photos by Tomas Karlsson

Copyright pp 1–69 (Tomas Karlsson)

Paper 1 © by the Authors (Manuscript unpublished)

Paper 2 © MDPI

Paper 3 © MDPI

Paper 4 © Elsevier

Faculty of Science

Department of Physical Geography and Ecosystem Science

ISBN (print): 978-91-89187-09-2

ISSN (pdf): 978-91-89187-10-8

Printed in Sweden by Media-Tryck, Lund University
Lund 2021



Media-Tryck is a Nordic Swan Ecolabel
certified provider of printed material.
Read more about our environmental
work at www.mediatryck.lu.se

MADE IN SWEDEN 

*Dedicated to Kim and Gunde
(and the rest who R.I.P.,
but I dunno if they care...)*

List of papers

- I. **Karlsson, T.**, Klemedtsson, L., Rinnan, R., Holst, T. (2021). Leaf-scale Study of Biogenic Volatile Organic Compound Emissions from Willow (*Salix* spp.) Short Rotation Coppices Covering Two Seasons. *Accepted for publication in Atmosphere-Basel*.
- II. **Karlsson, T.**, Rinnan, R., Holst, T. (2020). Variability of BVOC Emissions from Commercially Used Willow (*Salix* spp.) Varieties. *Atmosphere-Basel*, 11, 356.
- III. Ahlberg, E., Ausmeel, S., Eriksson, A. C., Holst, T., **Karlsson, T.**, Brune, W. H., Roldin, P., Kristensson, A., Svenningsson, B. (2019). No Particle Mass Enhancement from Induced Atmospheric Ageing at a Rural Site in Northern Europe. *Atmosphere-Basel*, 10, 408.
- IV. van Meeningen, Y., Wang, M., **Karlsson, T.**, Seifert, A., Schurgers, G., Rinnan, R., Holst, T. (2017). Isoprenoid emission variation of Norway spruce across a European latitudinal transect. *Atmospheric Environment*, 170, 45–47.

Contributions

- I. TK contributed to the design of the study, collected all field data, performed all data analysis and led the writing of the manuscript.
- II. TK contributed to the design of the study, collected all field data, performed all data analysis and led the writing of the manuscript.
- III. TK participated in the discussion and the writing of the manuscript.
- IV. TK contributed to the design of the study, collected field data, performed data analysis, participated in the discussion and writing of the manuscript.

Abstract

Willow (*Salix* spp.) trees have been used commercially since the 1980s to produce renewable energy. Some benefits with these trees are that they can clean soil from heavy metals, reduce the risk of nutrient leakage and eutrophication. They could be an alternative to reduce carbon dioxide emissions from fossil fuel, but they are known to emit high rates of biogenic volatile organic compounds (BVOCs). Many thousands of different compounds are included in this group and they can be divided into terpenes, alcohols, alkanes and esters, to mention a few. These compounds are important. For instance, BVOCs help plants to attract pollinators. They serve as a protection to different kinds of stress, e.g., herbivores, heat and pollutions. Once they are released into the atmosphere, they will be involved in many chemical processes. Hydroxyl radicals, which are known to clean the air from pollutions, are depleted by BVOCs leading to increased lifetime of methane. Emissions of BVOCs could also act as precursors for aerosol formation, which in turn might lead to changes in cloud properties and radiative forcing. Photochemical smog like ozone (O_3) is another result of the reactions in the atmosphere where BVOCs are involved, which impairs regional air quality. The reported range of emission rates from *Salix* is wide. Details about age, canopy position of leaves and how commercially used *Salix* varieties differ in their emission potentials are lacking, which lead to large errors if modelled emissions are based on too simple assumptions. Therefore, the aim of the work in this thesis was to investigate how the emissions vary with height, age, variety and during the growing season to get more reliable emission rates that can be used in models to better assess the impacts on the regional air quality. Measurements of aerosol formation were conducted to be able to determine the potential particle production near the *Salix* site. The outcome from the *Salix* measurements was then combined with BVOC measurements on spruce to assess how an expansion of *Salix* plantations could affect the regional air quality if a conversion of the land was shifted into these plantations, e.g., by using more arable and forest land.

The study between 2015 and 2016, and the measurements in 2017, showed that *Salix* mainly emitted isoprene, which peaked during summer. Emissions of monoterpenes (MTs) showed a decreasing trend through the growing season. The BVOC emission rates differed depending on if the leaves were acclimatized to sunlit or shaded conditions, where the sun-adapted leaves emitted twice as much isoprene as the shaded. There was also a significant difference among the studied varieties, where Wilhelm emitted approx. three times more isoprene than Tora. Age

influenced the emission rates. The emissions of non-terpenes from younger trees were substantially higher than from the older trees. Emissions of MTs were higher from younger trees compared to older as well. When comparing isoprene emissions, the emission rates from the older trees were almost five times larger than from the younger. Induced emissions of stress-related compounds like hexanal was observed due to an outbreak of *Melampsora* in 2015. Together with some other compounds, these emissions increased several times. All these results highlight the complexity of BVOC emissions and existing models need to be improved by including parameters like season, age, microclimate adaption and stress to better predict and estimate BVOC emissions.

No particle enhancement could be observed from the *Salix* plantation near the site in 2015. The explanation for this result was the lack of precursors, e.g., MTs. However, spruce trees emitted higher rates of MTs and are probably more prone to generate particles compared to *Salix* trees. The high isoprene emissions from *Salix* is more likely to produce O₃ if sources of anthropogenic NO_x are sufficiently close. An expansion of *Salix* plantations where spruce forest and traditional agriculture are converted into willow fields would lead to considerably more regional isoprene in the atmosphere. Thus, plantations of *Salix* should be strategically located to avoid prerequisites to form O₃, and preferably the variety Tora should be chosen since it emitted the lowest rates of isoprene.

Populärvetenskaplig sammanfattning

Salix (vide eller pil) har använts kommersiellt sedan 1980-talet för att producera förnybar energi. Det finns många fördelar med dessa träd, bland annat kan de rena jord från tungmetaller och minska risken för kväveläckage och övergödning. De kan vara ett alternativ till fossilt bränsle men är också kända för att avge höga flöden av flyktiga organiska föreningar (eng. biogenic volatile organic compounds; BVOCs). Tusentals olika ämnen ingår i denna grupp, vilka kan delas in i terpenener, alkoholer, alkaner och estrar för att nämna några. Dessa ämnen är viktiga. Till exempel så hjälper BVOCs växterna att attrahera pollinerare men kan också skydda växterna emot olika typer av stress såsom växtätare, värme och luftföroreningar. De ingår också i många kemiska processer i atmosfären. Hydroxilradikaler, vilka kallas för luftens renare, bryts ned av BVOCs och detta i sin tur kan leda till ökad livslängd för metan. BVOCs kan också generera aerosoler, vilka påverkar egenskaper hos moln och jordens albedo. Fotokemiska föroreningar som ozon (O_3) är också ett resultat av reaktioner där BVOCs är inblandade och kan leda till försämrad luftkvalitet. Det finns mycket som påverkar BVOC emissionerna och information om ålder, lövposition och hur emissionerna varierar för de olika kommersiella salixklonerna saknas, vilket kan leda till stora fel om modellerade emissioner baseras på alltför enkla antaganden. Syftet med studierna i denna avhandling var således att undersöka hur BVOC emissionerna varierar med lövets position i trädkronan, ålder, för de olika salixsorter samt över växtsäsongen, för att få mer tillförlitliga emissionsvärden som kan användas i modeller för att bättre kunna bedöma påverkan på den regionala luftkvaliteten. Mätningar av aerosolbildning vid en av salixplanteringarna var också en del av studien. Därtill studerades även emissioner av BVOCs från gran för att bedöma hur luftkvaliteten skulle påverkas om mer landyta ändras från till exempel skogs- och åkermark till salixplantage.

Studien mellan 2015 och 2016, och mätningarna från 2017 visade att salix emitterade till största delen isoprene där de högsta värdena inträffade under sommaren. Emissioner av monoterpenener (MTs) avtog allteftersom växtsäsongen fortlöpte. BVOC emissionerna varierade beroende på om löven var acklimatiserade till solljus eller skugga där de solljusanpassade löven emitterade dubbelt så mycket isopren. Det fanns också en betydande skillnad mellan de olika salixsorterna och Wilhelm emitterade ungefär tre gånger mer isopren än Tora. Åldern påverkade också emissionerna. Både emissioner av icke-terpenener och MTs var högre från de yngre träden medan isopren var nästan fem gånger så hög från de äldre träden. Stressinducerade emissioner av ämnen som hexanal inträffade under ett utbrott av

svampen *Melampsora* 2015 och tillsammans med några andra ämnen så ökade emissionerna för dessa flertalet gånger. Alla dessa resultat understryker svårigheten med att simulera emissioner av BVOCs och nuvarande modeller behöver förbättras genom att inkludera parametrar som tid på säsongen, ålder, anpassning till rådande mikroklimat och stress för att bättre förutse och beräkna BVOC emissioner.

Ingen partikelökning kunde observeras vid salixplanteringen 2015. Förklaringen till detta var för låga halter av bland annat MTs. Däremot så emitterade gran högre halter av MTs och är förmodligen mer benägna att generera partiklar i förhållande till salix. Det är mer troligt att salix istället kan ge upphov till O₃ på grund av de höga emissionerna av isopren, om utsläpp av NO_x är tillräckligt nära. Att ändra landytans markanvändning från granskog och traditionellt jordbruk till salixplantage skulle därför kunna ge upphov till betydande högre halter av isopren lokalt. Därför behöver dessa salixplanteringar vara strategiskt placerade så att förutsättningar till O₃ produktion undviks, och sorten Tora bör därmed väljas eftersom denna emitterade de lägsta halterna av isopren.

Table of contents

List of papers	9
Contributions.....	9
Abstract	11
Populärvetenskaplig sammanfattning	13
Table of contents	15
Introduction	17
<i>Salix</i> trees	17
BVOCs	18
Why plants emit BVOCs.....	20
Production and emission of BVOCs	20
BVOCs influence on air chemistry	22
BVOC emission and climate feedback.....	23
Aims and objectives	24
Material and methods	25
Study sites	25
<i>Salix</i> sites (Paper I–III).....	25
Spruce sites (Paper IV).....	27
Plant material	28
Equipment	29
Setup of branch chamber	29
Setup of leaf chamber.....	30
Sampling of BVOCs.....	31
PTR-MS measurements.....	31
Particle measurements	32
Field measurements on <i>Salix</i>	33
Analysis of BVOC chamber measurements from <i>Salix</i>	34
GC-MS analysis.....	34
Calculations of BVOC emissions.....	34

Results and discussion	37
Phenological and genetical influences on BVOC emissions from <i>Salix</i> (Papers I and II).....	37
Comparison between different heights and light conditions (Papers I and IV)	42
Impact of age on BVOC emissions (Paper I and II).....	44
LUCC and impact on air quality from <i>Salix</i> (Paper I–IV)	46
Conclusions and outlook	49
Acknowledgments	53
References	55

Introduction

Salix trees

Because of the rapid increase of greenhouse gases (GHGs), i.e., carbon dioxide (CO₂), methane (CH₄) and nitrous oxide (N₂O), and temperature in the atmosphere (IPCC, 2014; IPCC, 2018, IPCC, 2021), mitigation strategies have been suggested to decrease the use of fossil fuel and to limit the global average temperature increase below 2°C (European Commission, 2014; Paris Agreement, 2015). In the long run, a reduction between 80–95% of GHG emissions in 2050 compared to 1990 will be necessary by the developed countries (Gupta et al., 2007; European Commission, 2014). Additionally, Sweden has the goal to achieve zero net emissions of GHGs by the year 2045 (Swedish EPA, 2019; Bonde et al., 2020). To solve the future energy demand, more focus has been put on renewable energy and one way to meet these goals could be to produce energy from plant biomass. The benefit of using plants is that they do not add any extra carbon (C) to the atmosphere compared to fossil fuel, since the C released from plants in combustion is basically the same amount that is taken up by the plants. By using biorefineries, the shift toward a more C neutral society could be achieved (Ragauskas et al., 2006).

Perennial biomass crops, also known as short rotation coppices (SRCs), are suitable for producing renewable energy and can be grown directly on agricultural land, i.e., short rotation plantations (SRPs). The SRCs do not require as much management as annually harvested crops, and trees might be one of the least nutrient-intensive bioenergy, resulting in less emitted GHGs compared to using annual crops as bioenergy (Kägi et al., 2008; Hillier et al., 2009). One suitable tree species for this purpose is willow (*Salix* spp.). However, even if it has been shown that using willow as a renewable energy source can reduce CO₂ emission compared to fossil fuel (Kimming et al., 2011; Therasme et al., 2021), it is still not clear how it will influence the concentrations of GHGs in the atmosphere. High emissions of CH₄ and N₂O from the SRPs could compensate for the uptake of CO₂ (Zenone et al., 2016), but more life cycle assessment (LCA) studies are needed, which cover the whole growing life span of the plantations.

Together with *Populus* (poplars, cottonwoods and aspens), *Salix* (willows, sallows and osiers) belong to the Salicaceae family. It is relatively easy to propagate and hybridize these plants, which have made them suitable as bioenergy crops (Isebrands and Richardson, 2014). They were probably already used more than

10 000 years ago in the Middle East for cooking, heating and construction (Stettler, 2009). *Salix* has been grown in Sweden since the early 1970s and was first used to produce new plant material for the paper industry (Hollsten et al., 2013). The research has continued since then to establish new species with desired features and since the 1980s, willow trees have been intensively used as energy crop (Lindegaard et al., 2016). The earlier *Salix* varieties used in Sweden for bioenergy production were clones from the European willow species *Salix viminalis*. Unfortunately, these older clones were susceptible to rust and new hybrids have been developed using *Salix* from, e.g., Siberia (*Salix schwerinii*) to create new varieties with improved resistance to rust and better yield (Åhman and Larsson, 1999). Currently, *Salix* plantations are growing on crop land and the majority of the plantations in Sweden are mostly located in the southern part, e.g., in Scania or near the lakes Mälaren and Hjälmaren. The current land use for SRPs in Sweden is around 10 000 ha, whereof *Salix* comprises approx. 50%, but the potential has been estimated to be between 200 000 and 300 000 ha (Fredga et al., 2008).

Managed *Salix* trees grow between 3 and 5 years before they are harvested. Compared to annual crops, *Salix* trees do not need as much management even though some fertilization is common to increase the plant growth (Kägi et al., 2008). For instance, the ratio between how much energy is put in and how much is gained is only 5–6% for *Salix*, while it is 10–17% for annual crops (SOU 2007:36). When it comes to C uptake, *Salix* trees assimilate approx. 5.5 times more C than normally managed spruce forest (Grelle et al., 2007). There are many environmental advantages with growing *Salix* (Kägi et al., 2008). Studies have shown that *Salix* could be beneficial to enhance biodiversity in arable environments (Baum et al., 2009; Karp et al., 2009). *Salix* has the ability to clean the soil by taking up heavy metals, e.g., cadmium and zinc (Landberg and Greger, 1996; Meers et al., 2007; Baum et al., 2009; Mleczek et al., 2010). *Salix* plantations can also be used to clean effluents from nitrogen and phosphorus after application of sludge and waste water treatments (SOU 2007:36; Fredga et al., 2008; McCracken and Johnston, 2015). The increase in soil C stock, mulch, and reduced risk of nutrient leakage and erosion are other positive effects on the environment with *Salix* compared to annual crops (SOU 2007:36; Fredga et al., 2008). However, like other broad leaf trees, such as oaks, aspens and eucalypti, *Salix* species have shown to be high emitters of biogenic volatile organic compounds (BVOCs) (Hakola et al., 1998; Isebrands et al., 1999; Kesselmeier and Staudt 1999; Owen and Hewitt, 2000).

BVOCs

Ever since Went (1960) stated the hypothesis about blue haze originating from plant emitted terpenes, more attention and efforts have been carried out to explain this phenomenon, leading to new discoveries and eventually to an increased

understanding of a group of compounds called volatile organic compounds (VOCs). They were believed to be involved in photochemical smog formation in the 1950s (Haagen-Smit, 1952) and their production and emission by plants were also discussed by Sanadze et al. (1956). These molecules can either come from natural sources, referred to as BVOCs, or from human activities, i.e., anthropogenic volatile organic compounds (AVOCs). Attempts have been made to estimate the global emissions of VOCs, where the natural emission is estimated to be more than 10^{15} g C a year, which is many times higher than the emissions of AVOCs (Hough and Johnson, 1991; Müller, 1992; Guenther et al., 1995; Guenther, 2002; Peñuelas and Llusà 2003; Guenther et al., 2012).

There exists no clear definition of VOCs but according to the Environmental Protection Agency (EPA) in the US, they are defined as any compound of C that participate in atmospheric photochemical reactions except carbon monoxide, CO₂, carbonic acid, metallic carbides, carbonates, and ammonium carbonate. This definition also excludes several other compounds such as CH₄, which lead to the establishment of the abbreviation NMHCs (nonmethane hydrocarbons) or NMVOCs (nonmethane VOCs) (Kesselmeier and Staudt, 1999). Attempts have been made to state a clearer definition, which resulted in that VOCs are those organic compounds with a vapour pressure >10 Pa at 25°C, a boiling point up to 260°C at atmospheric pressure and consist of not more than 15 C atoms (Williams and Koppmann, 2007). The definition has become blurred, new groups or compounds have been included and now there exist VOCs with far more than 15 C atoms.

In living organisms, more than 60 000 terpenoids have been described and plants emit more than 30 000 different BVOCs (Niinemets et al., 2004; Xie et al., 2012; Niinemets and Monson, 2013). The compounds can be divided into different groups depending on their chemical structure and characteristics. Terpenes (e.g., hemiterpenes, monoterpenes (MTs) and sesquiterpenes (SQTs)) share the same carbon and hydrogen structure, which is built up by multiples of C₅H₈. Thus, hemiterpenes contain one C₅H₈ chain, MTs contain two (i.e., C₁₀H₁₆) and so on. The group terpenes are sometimes interchangeable with terpenoids (also known as isoprenoids), although the latter contains additional functional groups like oxygen. Other groups are alkanes, alkenes, carbonyls, alcohols, ester, ethers and acids (Kesselmeier and Staudt, 1999). Green leaves volatiles (GLVs) is another important group, which can induce plant defense and help plants against herbivores and pathogens (Ameye et al., 2018). They are released when plants are hurt and damaged and originate from the lipoxygenase (LOX) pathway (Hatanaka et al., 1993; Laothawornkitkul et al., 2009; Ameye et al., 2018). Everyone that has mowed the lawn has got acquainted with this certain smell from GLVs (Olofsson et al., 2003; Watkins et al., 2006; Dombrowski et al., 2019). One of the most important and common compounds is isoprene, which belong to the group hemiterpenes. The production and emission of isoprene was first discussed by Sanadze (1956) and has been estimated to comprise around 50% or more of all emitted BVOCs (approx. 500

$\times 10^{12}$ g C year⁻¹) followed by methanol (approx. 100×10^{12} g C year⁻¹), by using the MEGAN model (Guenther et al., 2006; Guenther et al., 2012).

Why plants emit BVOCs

The reasons why plants emit BVOCs are manifold but simply put, the main reason is to help the plants to survive and reproduce themselves. These compounds serve as communication between plant-plant and plant-animal, and play critical roles in plant defense (Yuan et al., 2009). For instance, BVOCs can attract pollinators (Peñuelas and Staudt, 2010). They act as protection against biotic stress (e.g. insects and pathogens), either by direct defense (repel or deter herbivores) or by indirectly induced defense (attract parasitoids or predators of herbivores) (Dicke and Vet, 1999; Llusià and Peñuelas, 2001; Dicke et al., 2003a; Dicke et al., 2003b). They also act as protection against abiotic stress (e.g., extreme temperature, drought, intense sunlight, mechanical damage and pollutants) (Beauchamp et al., 2005; Capitani et al., 2009; Vickers et al., 2009; Loreto and Schnitzler, 2010; Brillì et al., 2012; Copolovici et al., 2012). The major part of the photosynthesized C is used in primary production and only a few percent is reemitted back to the atmosphere as, e.g., isoprene (Kesselmeier et al., 2002; Bracho-Nunez et al., 2013). However, the emission of stress-induced BVOCs can result in significantly larger fraction of reemitted C (Sharkey and Loreto, 1993; Sharkey et al., 1996).

Production and emission of BVOCs

The production of the different BVOCs in plants are complex and since it is related to secondary metabolism, the plants need to balance the investment in C between primary production, i.e., biomass, and the production of BVOCs (Paiva, 2000). The pathways are interlinked and not fully understood. In general, it starts with photosynthesis and the Calvin cycle where C atoms later on are distributed to different pathways, depending on which kind of compound that is produced in the end (Laothawornkitkul et al., 2009). There is also indication that starch and respiratory CO₂ could be an alternative C source to isoprene formation besides recently photosynthesized CO₂ (Loreto et al., 2004; Schnitzler et al., 2004). Isoprene, together with the other terpenes, share some of the similar production pathways, i.e., isoprenoid pathways. They are produced from the same substrate, isopentenyl pyrophosphate (IPP) and its isomer dimethylallyl diphosphate (DMAPP) (Vickers et al., 2009). Two different isoprenoid pathways have been found that produce IPP and DMAPP; the cytosolic mevalonic acid pathway (MVA) and the plastidic 2-C-methyl-D-erythritol 4-phosphate pathway/1-deoxy-D-

xylulose 5-phosphate pathway (MEP/DOXP) (Lichtenthaler et al., 1999; Rohmer 1999; Lange et al., 2000; Humphrey and Beale, 2006). The MEP/DOXP pathway is responsible for producing isoprene, MTs, diterpenes and other higher orders of terpenes, while homoterpenes, SQTs and triterpenes are produced through the MVA pathway (Vickers et al., 2009) (Figure 1). Compounds that are released directly after they are produced, such as isoprene, are emitted from de novo synthesis. Other compounds are stored in pools, e.g., in resin ducts and glandular trichomes (Kesselmeier and Staudt, 1999), and emitted when they are needed.

The emissions of BVOCs can be divided into two categories; constitutive and induced emissions. The former is considered as normal state emissions, which continuously occurs to build up a barrier against herbivore attacks (Paiva 2000; Walling, 2000). Constitutive production and emissions of BVOCs are sensitive and influenced by different stress factors, such as temperature, light, herbivores and pathogens (Niinemets et al., 2004; Loreto et al., 2006; Loreto and Schnitzler, 2010, Joó et al., 2011). Induced emissions, on the other hand, are a response to a direct impact from, e.g., herbivores causing wounds on the leaf tissue (Loreto and Schnitzler, 2010; Possell and Loreto, 2013).

Instantaneous emission rates of BVOCs are mainly controlled by temperature and sunlight. Thus, the two of the most commonly used models that describe the emissions for many terpenes are based on the temperature-dependent algorithm (used for, e.g., for MTs and SQTs that are stored in pools) or the light- and temperature-dependent algorithm (used for, e.g., isoprene) (Guenther et al., 1991; Guenther et al., 1993; Helmig et al., 2007). But these algorithms poorly reflect long-term effects (e.g., phenological changes) and they also do not include stress-induced emissions of BVOCs. The algorithms also rely on emission potentials, which varies a lot among and within species (Kesselmeier and Staudt, 1999). This diversity points out the need for accurate and representative emission potentials when scaling up the BVOC emissions.

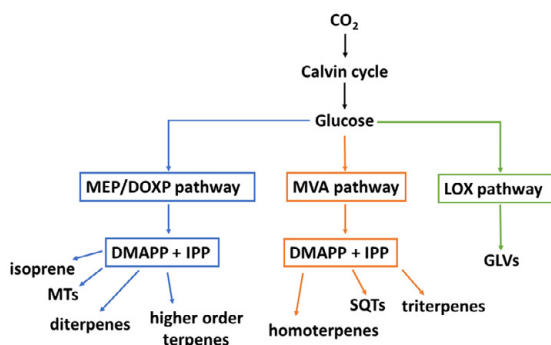


Figure 1. A simplified description of the production pathways for terpenes (blue and orange arrows) and green leaf volatiles (GLVs, green arrows). Redrawn from Laothawornkitkul et al. (2009) and Vickers et al. (2009).

BVOCs influence on air chemistry

Even though the concentration of BVOCs in the atmosphere is much lower than, e.g., CO₂, they play an important role for atmospheric chemistry and oxidation processes since they are very reactive (Monks et al., 2010).

The most crucial initiators for oxidation reactions in atmosphere are hydroxyl (OH) radicals produced by photochemical processes (Olofsson et al., 2005). Many BVOCs react with OH radicals (Atkinson and Arey, 2003), but depending on which compound that is involved in the reaction, both production and consumption of OH are possible. For instance, isoprene and MTs are possible consumers of OH whilst alkenes could be a source (Paulson and Orlando, 1996; Atkinson, 1997; Folberth et al., 2005; Olofsson et al., 2005). When OH radicals are consumed, they will not be able to react with CH₄ and consequently, a depletion of these radicals will lead to a prolonged atmospheric lifetime of CH₄ and increased global warming (Folberth et al., 2006; Kaplan et al., 2006; Arneth et al., 2008).

Oxidation of BVOCs can also lead to production of ozone (O₃) and peroxyacetyl nitrates (PANs) in the troposphere (Roselle et al., 1991; Ryerson et al., 2001; Kleinman et al., 2002; Atkinson and Arey, 2003; Watson et al., 2006; Pike and Young, 2009). High concentrations of O₃ and PAN can be harmful for humans and vegetation (Lovelock, 1977; Temple and Taylor, 1983; Sakaki, 1998; Vyskocil et al., 1998; Fumigalli et al., 2001; Ashmore, 2005; Sun et al., 2014; Emberson et al., 2018). The prevailing conditions in the atmosphere determine if there will be a production or a depletion of O₃. The chemical reaction that produces O₃ occurs via formation of nitrogen dioxide (NO₂) (Kleinman et al., 2002; Atkinson and Arey, 2003). If the concentrations of NO_x (NO and NO₂) are sufficiently high, then this process will lead to enhanced levels of tropospheric O₃ (Ryerson et al., 2001; Kleinman et al., 2002; Calafapietra et al., 2013). On the other hand, when NO_x concentrations are too low, O₃ will react directly with BVOCs and a depletion of O₃ will instead occur (Fehsenfeld et al., 1992; Laothawornkitkul et al., 2009). Since O₃ is a GHG, increased concentrations of O₃ will enhance global warming. Increased concentrations of O₃ could also result in a reduced plant productivity and indirectly lead to more CO₂ in the atmosphere and to an increased radiative forcing (Sitch et al., 2007; Wittig et al., 2009).

Another important mechanism that BVOCs are responsible for is the formation of secondary organic aerosols (SOAs). Aerosols, which are airborne particles suspended in the atmosphere, affect the climate by scattering and absorbing radiation from the sun (Kulmala et al., 2004). These particles are produced in two different ways. The first one occurs via gas-phase oxidation products, which condensate onto pre-existing particles. The other alternative is via nucleation, or new particle formation. To be able to quantify the SOA formation, these processes need to be modelled and one way to do it is to divide them into the following steps: gaseous emissions, gas-phase chemistry, nucleation/gas-particle partitioning and aerosol-phase/aqueous phase chemistry/cloud processing (Kanakidou et al., 2005).

Many studies have shown that oxidation products from isoprene, MTs and SQTs act as precursors for condensable products that are required to create SOAs (Pandis et al., 1991; Hoffmann et al., 1997; O'Dowd et al., 2002; Clayes et al., 2004; Kulmala et al., 2004; VanReken et al., 2006; Ehn et al., 2014). Aerosols in turn, can lead to enhanced cloud condensation nuclei (CCN) production (O'Dowd et al., 2002; Paasonen et al., 2013; Ehn et al., 2014) and have an impact on cloud formation and precipitation, and thereby change the properties of the clouds (Kulmala et al., 2004; Holzinger et al., 2005; Spracklen et al., 2008; Paasonen et al., 2013). More SOAs and CCN will consequently lead to an increased albedo, which in turn is believed to counteract global warming (Kulmala et al., 2004; Peñuelas and Staudt 2010; Boucher et al., 2013).

Although the overall agreement is that SOAs and CCN cool the earth, all the mechanisms behind these processes are complicated and not completely understood (Boucher et al., 2013; Rosenfeld et al., 2014; Fan et al., 2016; Seinfeld et al., 2016). This uncertainty is represented by the large error bar in the estimation of the radiative forcing from aerosols by IPCC (Stocker et al., 2013). In addition, atmospheric aerosols are considered to impair human health and together with other pollutions, they cause several millions premature deaths globally (Pope and Dockery, 2006; Kuehn, 2014; Landrigan et al., 2017).

BVOC emission and climate feedback

The global warming during the last 30 years could be responsible of 10% additional BVOC emissions (Peñuelas and Llusia, 2003). Increased global temperatures will likely result in longer plant growing season (Peñuelas and Filella, 2001). Phenological events such as leafing, flowering and senescence are plant processes that will be affected by a changed climate and could contribute to changed BVOC emissions. A temperature increase between 2 and 3°C could generate additional 30–45% BVOC emissions globally (Peñuelas and Llusia, 2003), but these estimations are based on models with fixed emission factors and could overestimate regional emissions. The net effect of BVOC emissions on the climate is difficult to quantify because of all the complex feedback processes. Elevated atmospheric concentrations of CO₂ and extreme weather events add complexity to the emissions but need to be considered to better estimate future BVOC emission scenarios (Llusia and Peñuelas, 1998; Staudt et al., 2008; Taylor et al., 2008; Peñuelas et al., 2009). A simplified description of how increased BVOC emissions could affect the global warming can be seen in Figure 2, where depletion of OH and production of O₃ (in high NO_x areas) are believed to enhance global warming, whereas increased consumption of O₃ (in low NO_x areas), production of SOAs and CCN may reduce global warming.

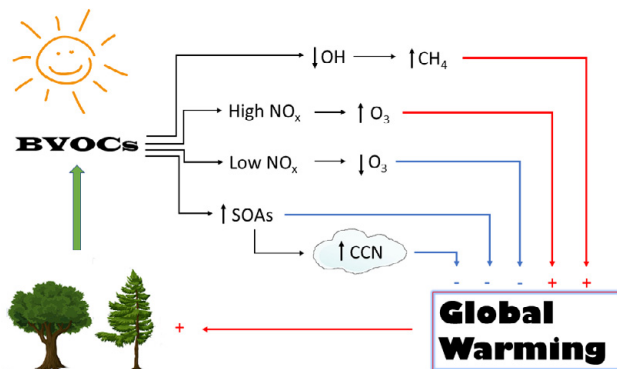


Figure 2. Schematic picture on how emission of BVOCs are coupled to climate warming by processes in the atmosphere. Redrawn from Laothawornkitkul et al. (2009) and Peñuelas and Staudt, 2010.

Aims and objectives

While a large expansion of *Salix* plantations may be good for mitigating climate change, local air quality could be negatively affected. Due to the wide range of published emission potentials among *Salix* species, new reliable emission potentials are needed to better estimate the emission on an ecosystem scale. The newer *Salix* varieties that are used commercially might differ in their emission rates and compound mixture compared to the reported older species.

The overarching aim of the work presented in this thesis was to study some of the important factors that influence the emission rates from managed *Salix* trees. These results are then combined with measurements on aerosol formation near a *Salix* plantation, and with BVOC emissions from spruce, to assess what the possible outcome could be for the regional air quality if land use and cover change (LUCC) shifts the current land use into SRPs with *Salix* in areas like Sweden.

The specific objectives were:

- To study and quantify how seasonality and different varieties influence BVOC emissions from commercial *Salix* trees (Paper I and II).
- To study and quantify how position within canopy height influences the BVOC emissions (Paper I and IV).
- To study and quantify how the age of the *Salix* trees influences the BVOC emissions (Paper I and II).
- To investigate how BVOC emissions from *Salix* plantations could impact the local air quality compared to traditional agriculture and spruce forest (Paper I–IV).

Material and methods

Study sites

The study sites can be divided into two categories, the first one contains sites that have been subjected to BVOC measurements at *Salix* plantations and these are located in Sweden (Skrehalla and Billeberga). The second has been related to BVOC measurements from spruce and these sites were found both in Sweden (Hyltemossa, Skogaryd and Norunda), and in other parts of Europe (Ljubljana (Slovenia), Grafrath (Germany), Taastrup (Denmark) and Piikkiö (Finland)), whereof these four latter sites were a part of the International Phenological Garden (IPG).

***Salix* sites (Paper I–III)**

Skrehalla

Most of the *Salix* measurements were done in Skrehalla, which is located in the municipality of Grästorps and about 80 km north-east of Gothenburg. Two plots were chosen at this site (plot 1 (P1), 58°16'55'' N 12°46'20'' E and plot 2 (P2), 58°17'09'' N 12°45'31'' E) (Figure 3). Mean annual temperature was 6.1°C (1961–1990) and annual precipitation was 683 mm (1961–1990) (Karlsson et al., 2020). An older variety of *S. viminalis* was established in 1994 on P1 but was replaced with a new one called Wilhelm in 2017, which means that measurements in 2015 (Paper I and III) was conducted on two older varieties in their third growing season after the last harvest, and measurements in 2017 (Paper II) was conducted on Wilhelm (first growing season). On P2, a variety called Tora was planted in 2003 and in 2016 they had their fourth growing season after the last harvest. The area of P1 was approx. 6 ha and P2 was around 5 ha. All trees on P1 and P2 were planted in double rows, separated with 1.25 m. The distance between the rows in each double row was 0.75 m and the trees were planted with 0.4 m intervals in the rows.

Billeberga

This site is located approx. 300 km south of Skrehalla, outside a community called Billeberga in the municipality of Svalöv. Two plots were studied at this location (plot 3 (P3), 55°52'32.9'' N 13°1'18.2'' E and plot 4 (P4), 55°52'11.7'' N 13°1'33.3'' E) (Figure 3). *Salix* trees growing here were used in field trails for

producing new commercial varieties suitable for biomass production. These field trials were run by a commercial company (European Willow Breeding AB). Mean annual temperature and precipitation for this site were 7.7°C (1961–1990) and 687 mm (1961–1990), respectively (Karlsson et al., 2020). Several different *Salix* varieties were growing on P3 and P4 but the ones chosen to be studied were Wilhelm, Tora, Inger and Ester. On P3, the varieties were planted in 2014 and cut down before growing season in 2016, which implies that these trees had their second growing season in 2017 (Paper II). The varieties on P4 were planted in 2017 and had their first growing season when measurements were done in 2017. Each variety on P3 and P4 was growing in approx. 5 m long rows and the rows were separated by approx. 0.7 m. In the rows, trees had been planted at 0.5 m intervals.



Figure 3. The two sites (black circles) in Sweden represent Skrehalla (P1 and P2) and Billeberga (P3 and P4) where measurements on *Salix* trees were performed. The picture is taken and modified from Lantmäteriet.

Spruce sites (Paper IV)

Hyltemossa

Hyltemossa is a site run by the Integrated Carbon Observation System (ICOS) in Sweden (<http://www.icos-sweden.se/hyltemossa>) and is located in the southern part of Sweden (56°06' N 13°25' E) (Figure 4). This site is a forest dominated by Norway spruce (*Picea abies*) but it also contains small amounts of other species such as birch (*Betula* sp.) and Scots pine (*Pinus sylvestris*). When the BVOC measurements were done here in 2016, the age of the trees was around 30 years. Annual mean temperature and precipitation (1961–1990) for the area was 6.9°C and 831 mm, respectively (Alexandersson and Eggertsson Karlström, 2000).

Skogaryd

Skogaryd research site is a part of the Swedish Infrastructure for Ecosystem Science (SITES), established in 2013 (<https://www.gu.se/en/earth-sciences/skogaryd-research-catchment-0>). It is located in the south-western part of Sweden (58°23' N 12°09' E) and about 40 km west of Skrehalla (Figure 4). The measurements were done on subsite F (Forest on mineral soils) according to the classification on the webpage. The forest contained mainly coniferous trees, dominated by Norway spruce and Scots Pine with a stand age of approx. 50 years old trees. The mean annual temperature was 6.2°C and mean annual precipitation was 709 mm (1961–1990) (Alexandersson and Eggertsson Karlström, 2000).

Norunda

The location of Norunda (60°05' N 17°29' E) is around 30 km north of Uppsala (Figure 4). It is part of the ICOS network in Sweden (<http://www.icos-sweden.se/norunda>). It was established in 1994 and the forest is dominated by Norway spruce and Scots pine but with some deciduous trees like birch. The age of the trees varies mostly between 60 and 110 years. Annual temperature and precipitation were 5.6°C and 544 mm (1961–1990), respectively.

IPG sites

The four remaining sites were located in Ljubljana (Slovenia, 46°04' N 14°30' E), Grafrath (Germany, 48°18' N 11°17' E), Taastrup (Denmark, 55°40' N 12°18' E) and Piikkiö (Finland, 60°23' N 22°30' E) (Figure 4). The advantage with these IPG sites is that they contain clones of different species, which makes it possible to exclude the genetic influence and consequently, study the impact of climate change and environmental adaption in the species (Chmielewski et al., 2013). The sites were established more than 50 years ago. Since they are located in a wide latitudinal range, mean annual temperature and precipitation varied from 5.9–10.9°C and 583–1362 mm, respectively (van Meeningen et al., 2017).



Figure 4. The black circles mark the Norway spruce sites where BVOC measurements were done 2014–2016. Image from van Meening et al. (2017).

Plant material

The older varieties used for biomass production originated from species such as *S. viminalis* and the names usually contained letters followed by digits. Since commercial willow varieties are easy to breed, many new clones have been propagated the last decades. A short description of the four varieties studied in 2016 and 2017 is given below. The family tree for these varieties can be seen in Figure 5.

Tora was produced in 1989 from the clone L 79069 (*S. schwerinii* originating from Siberia) and the variety Orm, and is a female hybrid. Tora is one of the most successful varieties growing in northern latitudes since it is resistance to frost and rust.

Inger was produced in 1994 and is a female hybrid cross between the clone SW 911096 (*S. triandra* originating from Siberia) and the variety Jorr. Inger is suitable for mild or warm climates with normal water supply.

Wilhelm is a male hybrid and a cross between the varieties Sherwood and Björn. Wilhelm was produced in 2011. The biomass productivity from Wilhelm is somewhere between Tora and Inger.

Ester is a female hybrid and was produced in 2012 from the variety Linnéa and a clone of “Shrubby willow” (*S. miyabeana*). The yield from Ester is similar to Inger and it is suited for dry and hot climates. Among these four varieties, Ester is the only one that is almost completely free from leaf beetle attacks.

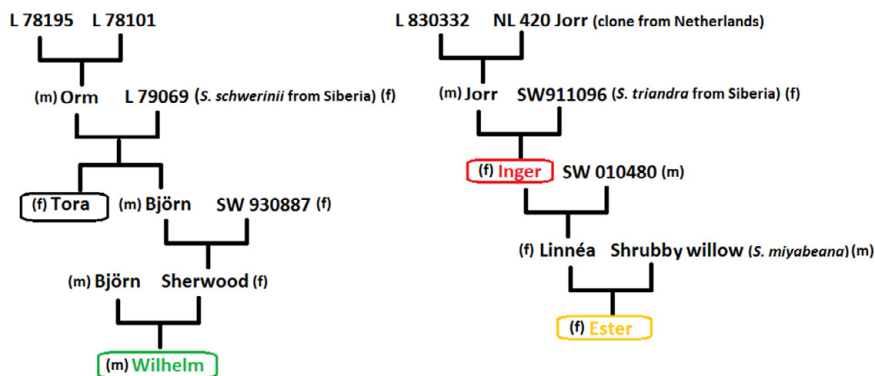


Figure 5. Family tree for the produced *Salix* varieties studied on P1 (Wilhelm), P2 (Tora) and P3–P4 (Tora, Inger, Wilhelm and Ester). Letters in parentheses represent gender; male (m) or female (f).

Equipment

Measuring volatile organic compounds can be done in different ways. One common approach is to use vegetation enclosures (e.g., bags or chambers). From these enclosures, samples can be taken by using adsorbent cartridges, which are later on analyzed with gas chromatography mass spectrometry (GC-MS). This method has high spatial resolution but lacking in the temporal resolution. Instead, using a technique based on proton transfer reaction mass spectrometry (PTR-MS) makes it possible to directly monitor and observe the emissions in the field. Additionally, when using vegetation enclosures, two techniques can be used, static (no purge flow) or dynamic (flow-through). In case of static, CO₂ concentration together with temperature could change dramatically resulting in non-realistic conditions, making this technique less preferably (Ortega and Helmig, 2008). The dynamic enclosure makes it easier to keep the conditions closer to ambient and this technique has been used throughout all manual measurements between 2015 and 2017. Two types of chambers were used, a leaf chamber and branch chamber.

Setup of branch chamber

The branch chamber had a cylindrical shape. It was made of stainless steel, Teflon (PFA) and covered with a transparent PFA film (Figure 6A). The volume was approx. 13 l. The day before the measurements started, the tip of the tree branch was inserted into the chamber. The chamber was closed and flushed one hour before the measurements started. Purge air was continuously flowing into the chamber. The purge air passed through a hydrocarbon trap (Alltech, Associates Inc., US), containing activated carbon and MnO₂-coated copper nets, providing BVOC- and

O₃-free air entering the chamber. Air temperature (T, °C) and relative humidity (RH) were measured inside (chamber T and RH denoted as T_C and RH_C) and outside of the chamber (CS215, Campbell Scientific, UT, US). Measurements of photosynthetically active radiation (PAR, μmol m⁻² s⁻¹) was measured close to the chamber (PAR_C) and at canopy level (Li-190, LI-COR, NE, US) and recorded together with T and RH on a data logger (CR1000, Campbell Scientific, UT, US). Only one branch chamber was used in 2015, but from June–October in 2016, two identical branch chambers were used in parallel at different heights.

Setup of leaf chamber

The leaf chamber system consisted of two parts, a portable photosynthesis system (LI-6400XT, LI-COR, NE, US) and a leaf chamber with a LED source (6400-02B) (Figure 6B). One advantage with this system is that it is possible to control PAR, T, RH and CO₂ while doing measurements. To control RH, water vapor is removed by using Drierite. Soda lime, a mixture of calcium oxide and sodium hydroxide, was used to remove CO₂. Using cartridges of CO₂ then made it possible to regulate concentration of incoming CO₂ into the chamber. Purge air into the leaf chamber passed through a similar hydrocarbon trap as in the branch chamber setup. The leaf chamber system was modified to be able to measure BVOCs by adding an extra outlet between the leaf chamber and the infra-red gas analyzer (IRGA). The maximum leaf area that is possible to measure with the leaf chamber is 6 cm² (2x3 cm²). While doing measurements, ambient conditions were maintained inside the chamber of CO₂ (400 ppm), T (20–25°C) and RH (30–70%). Emissions of BVOCs were measured at different light levels and changed in the following order 0, 150, 300, 450, 600, 1000 and 1500 μmol m⁻² s⁻¹. Along with BVOC emissions, net assimilation (A, μmol CO₂ m⁻² s⁻¹), transpiration (Tr, mmol H₂O m⁻² s⁻¹) and stomatal conductance (g_s, mol H₂O m⁻² s⁻¹) were measured.

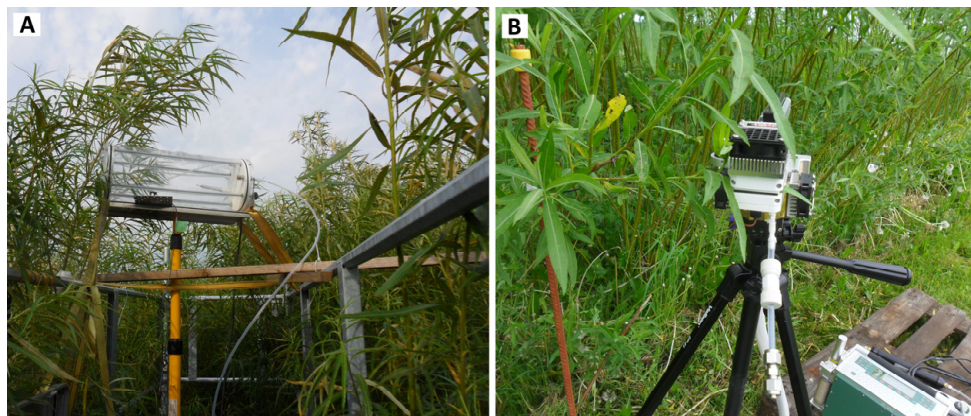


Figure 6. A) Setup of branch chamber measurements on P1 in Skrehalla 2015. B) Setup of leaf chamber measurements on P3 in Billeberga 2017.

Sampling of BVOCs

All samples were taken by using a flow-controlled pump (Pocket Pump, SKC Ltd., Dorset, UK). Sample air was pulled from the chambers and through an adsorbent cartridge containing Tenax TA (a porous organic polymer) and Carbograph 1TD (graphitized black carbon) (Markes International Ltd., Mid Glamorgan, UK) during 20 min with a flow rate of 0.2 l min^{-1} . Samples were taken during daytime (8:00–18:00) with approx. one-hour intervals. In the case of the leaf chamber, measurements started one hour after the insertion of the leaf into the chamber, to avoid any stress-induced BVOC emissions. After each new light level was set in the leaf chamber, 30 min passed before the measurement started to provide time for the leaf to acclimatize to the new conditions. To acknowledge possible contamination from the instruments, background samples were taken each day from the purge air in the branch chamber system and from the empty leaf chamber. All sample cartridges were sealed with caps made of Teflon-coated brass and stored at 3°C until analysis. At the end of each campaign, the measured leaves were collected and dried at 75°C for two days to measure dry weight.

PTR-MS measurements

A convenient way to measure BVOCs with high temporal resolution is to use PTR-MS technique. This method results in a fast response on-line measurement. By combining a time-of-flight (TOF) detector, i.e., PTR-TOF-MS, the time resolution is further improved. This instrument is capable of measuring full mass spectra 10 Hz time series, which is necessary for combining PTR-MS with direct eddy covariance technique (Müller et al., 2010; Ruuskanen et al., 2011). During field

campaigns in 2015, a PTR-TOF-MS (8000, Ionicon Analytik GmbH, Tyrol, Austria) was used to measure emissions of BVOCs on an ecosystem scale from P1. The idea behind PTR-MS technique is that it requires an ionization of the studied compound, which can be done by producing hydronium (H_3O^+) from pure water vapor in high voltage (Hansel et al., 1995; Lindinger et al., 1998; Ammann et al., 2004). Detection of masses and raw data analysis were done by the software PTRwid (Holzinger, 2015).

Particle measurements

Measurements of SOAs have traditionally been made by using larger smog chambers but during the last decades more attention has been put on the oxidation flow reactor (OFR). Compared to the smog chambers, OFRs are smaller, which make them suitable for field measurements. The smaller volume in OFRs, which could lead to more wall losses, is compensated with a shorter residence time in the chamber and studies have shown that measurements of chemical composition and mass yield by OFRs agree well to smog chambers (Bruns et al., 2015).

Oxidation flow reactor

A common OFR is the potential aerosol mass (PAM) reactor (designed at Pennsylvania State University), and in 2015 this type reactor was used to measure aerosol formation from P1 in Skrehalla. This PAM reactor consisted of a horizontal aluminum cylinder with a volume of approx. 13 l. An ultraviolet lamp produced OH and O_3 from oxygen and water, which later on oxidize incoming air. This process makes it possible to study aging of the atmospheric composition in a faster manner than it would take in the atmosphere.

Scanning mobility particle sizer

After the oxidative aging in the PAM reactor, the air flow from the reactor entered a scanning mobility particle sizer (SMPS) (Wiedensohler et al., 2012) and a high-resolution time-of-flight aerosol mass spectrometer (AMS) (Aerodyne Research Inc., MA, US) (DeCarlo et al., 2006). The SMPS measured the particle number size distribution in the range 11–600 nm (electrical mobility diameter). The SMPS consisted of a differential mobility analyzer (DMA) (TSI 3071, TSI Inc., MN, US) and a condensation particle counter (CPC) (TSI 3775, TSI Inc., MN, US). The AMS measured chemically resolved mass concentration in the interval of approx. 50–1000 nm (vacuum aerodynamic diameter).

Field measurements on *Salix*

Measurements of BVOC emissions from *Salix* trees were done between 2015 and 2017 (Table 1). The measurements in 2015 started in July and ended in September. In total, 142 samples were taken with the branch chamber during this growing season, where the major part of the measurements was done on an unknown variety of *S. viminalis* growing on P1. Campaigns done during 2016 were performed from May to October at different heights with both branch and leaf chambers on the variety Tora, growing on P2. Measurements with branch chambers resulted in 427 samples, and with the leaf chamber, 94 samples were taken and used for further analysis. The heights of the leaves were divided into three categories, lower (z_L , up to approx. 70% of the total canopy height (TCH) and representing shade-adapted leaves), higher (z_H , leaves growing above z_L and representing sun-adapted leaves) and middle (z_M , up to approx. 70% of TCH but growing at the edge of the plantation and assumed to experience similar conditions as z_H).

From May to September in 2017, 299 leaf chamber measurements were performed on P1–P4. The varieties studied in 2017 were Wilhelm, Tora, Inger and Ester.

Table 1. Details about field campaigns with leaf and branch chambers on *Salix* trees including year, period, height, location, plots, varieties, number of samples and in which paper they were used.

Year	Campaigns	Heights	Location	Plots/varieties	Chamber	Samples	Paper
2015	16–17 July	z_H	Skrehalla/	P1 & P2/ unknown <i>S.</i> <i>viminalis</i> and Tora	Branch	142	I
	28–31 July	z_H	58°16'55"N				
	4–7 Aug.	z_H	12°46'20"E				
	18–21 Aug.	z_H	and				
	1–4 Sep.	z_H	58°17'09"N				
	8 & 10–11 Sep.	z_M ; z_H	12°45'31"E				
2016	4–5 May	z_M	Skrehalla/	P2/Tora	Branch & leaf	427+94	I
	24 May	z_H	58°17'09"N				
	6–10 June	z_M ; z_H	12°45'31"E				
	19–23 June	z_M ; z_H					
	11–15 July	z_M ; z_H					
	26–29 July	z_L ; z_M ; z_H					
	15–17 Aug.	z_L ; z_M ; z_H					
	6–9 Sep.	z_L ; z_M ; z_H					
	10–13 Oct.	z_M ; z_H					
	2017	29 & 31 May					
2 & 5 June			and				
13 & 15 June			Billeberga/				
28 June			58°16'55"N				
5–6 & 9–10 July			12°46'20"E				
12–14 & 15 July			and				
22, 25–26 & 28 July			58°17'09"N				
1–2 Aug.			12°45'31"E				
28–31 Aug.			and				
5 & 7 Sep.			55°52'32.9"N				
			13°1'18.2"E				
			and				
			55°52'11.7"N				
		13°1'33.3"E					

Analysis of BVOC chamber measurements from *Salix*

GC-MS analysis

Adsorbent cartridge samples from the chamber measurements were analyzed with thermal desorption GC-MS (TD-GC-MS) instrument (UNITY2 thermal desorber, Markes International Ltd., Mid Glamorgan, UK) in combination with an ULTRA autosampler and GC-MS (7890A Series GC coupled with a 5975C inert MSD/DS Performance Turbo EI System, Agilent Technologies Inc., CA, US). Helium was used as carrier gas. Analysis of BVOCs was done using the software Enhanced ChemStation (MSD ChemStation E.02.01.1177, Agilent Technologies Inc., CA, US). Identification of the peaks in the mass spectra were done by injected pure standards or by the NIST 8.0 database. Concentrations of measured BVOCs were calculated by using ratios between the sample peak areas and standard peak areas. Only compounds with at least an area twice as large as the area in the background samples were included for further analysis.

Calculations of BVOC emissions

BVOC emission rates E ($\mu\text{g g}_{\text{dw}}^{-1} \text{h}^{-1}$) was calculated as (Ortega and Helmig, 2008):

$$E = \frac{C_2 - C_1}{m} \times Q \quad (1)$$

where C_2 ($\mu\text{g l}^{-1}$) is the concentration of the compounds taken out from the chamber, C_1 ($\mu\text{g l}^{-1}$) is the concentration of the compounds entering the branch chamber or in the empty leaf chamber, Q (l h^{-1}) is the flow rate of the purge air and m (g_{dw}) is the dried mass of the leaves.

Standardization of compounds that are dependent on both T and PAR were calculated according to Guenther et al. (1993). Standardized (STD) values for T and PAR were 303.15 K and $1000 \mu\text{mol m}^{-2} \text{s}^{-1}$ respectively:

$$E = E_s \times C_T \times C_L \quad (2)$$

where E ($\mu\text{g g}_{\text{dw}}^{-1} \text{h}^{-1}$) is the measured emission at T (K) and PAR ($\mu\text{mol m}^{-2} \text{s}^{-1}$) inside the chamber. E_s ($\mu\text{g g}_{\text{dw}}^{-1} \text{h}^{-1}$) is the STD emission, C_T and C_L are correction factors for temperature and light, which are defined by

$$C_L = \frac{\alpha C_{L1} PAR}{\sqrt{1 + \alpha^2 PAR^2}} \quad (3)$$

where α (=0.0027) and C_{L1} (=1.066) are empirical coefficients (Guenther et al., 1993), and

$$C_T = \frac{\exp\left(\frac{C_{T1}(T-T_s)}{RT_s T}\right)}{1 + \exp\left(\frac{C_{T2}(T-T_M)}{RT_s T}\right)} \quad (4)$$

where C_{T1} (=95 000 J mol⁻¹), C_{T2} (=230 000 J mol⁻¹) and T_M (=314 K) are empirical coefficients (Guenther et al., 1993). The parameter T_s (=303.15 K) is STD temperature and R (=8.314 J K⁻¹ mol⁻¹) is the universal gas constant.

Standardization of temperature-dependent compounds were done as

$$E = E_s \times e^{\beta(T-T_s)} \quad (5)$$

where E (μg g_{dw}⁻¹ h⁻¹) is the measured emission rate and E_s (μg g_{dw}⁻¹ h⁻¹) is the STD emission rate at temperature T (K). The parameter T_s (=303.15 K) is STD temperature and β (=0.09 K⁻¹ for MTs and 0.17 K⁻¹ for SQTs) is an empirical constant (Guenther et al., 1993; Helmig et al., 2007).

Results and discussion

Phenological and genetical influences on BVOC emissions from *Salix* (Papers I and II)

As studies have pointed out, many factors are involved when it comes to affect the BVOC emission rates from plants (Guenther et al., 1997; Laothawornkitkul et al., 2009). For *Salix*, a mix of different STD emission factors exist in the published literature. The STD emission factor for isoprene, which has so far been the most studied compound from *Salix*, varies almost 20-fold when considering *Salix* varieties used in biofuel plantation (Olofsson et al., 2005; Copeland et al., 2012; Morrison et al., 2016). The average STD isoprene emission for the study in 2015 and 2016 was $45.2 (\pm 42.9) \mu\text{g g}_{\text{dw}}^{-1} \text{h}^{-1}$, which is almost twice as much as the highest reported value from commercial *Salix* trees (Copeland et al., 2012). The STD emission for the varieties in 2017 was $33.2 (53.4 \pm \mu\text{g g}_{\text{dw}}^{-1} \text{h}^{-1})$. One reason to the variability in the STD emission rates can be related to the different technique employed (e.g., leaf-scale or canopy-scale) for measuring the fluxes. Further, the physiological changes in the plants related to different phenological stages is another factor that influence the emission rates. The development for isoprene emission has been suggested to vary in at least four stages (Monson et al., 1994; Guenther et al., 1997; Pétron et al., 2001), which is one of explanations for how the average STD isoprene emission varied during 2016 at P2 for the different months ($1.6\text{--}42.4 \mu\text{g g}_{\text{dw}}^{-1} \text{h}^{-1}$). The summer months (June–August) had similar average STD emission rates and the autumn months (September–October) had considerably lower STD emission rates (Table 2). A decreasing isoprene trend for the STD emission was also observed between July and September at P1 during 2015. The plant physiological processes behind the isoprene emissions are suggested to depend on isoprene synthase activity (Monson et al., 1992; Kuzma and Fall, 1993). This synthase activity changes through the season (Schnitzler et al., 1997), and long-term predictions should be corrected for this influence. Even though T and PAR were the main factors that influenced the isoprene emissions and is the reason why eq. 2 has been widely used to describe these emissions, this equation cannot explain why average STD isoprene emission was lower in May compared to June and July, despite that T_{C} and PAR_{C} were higher in May. An additional correction factor in eq. 2 has been applied by, e.g., Guenther et al. (1997) and Schnitzler et al. (1997), which takes long-term processes into account. But since this factor could be species-

dependent, more emphasis needs to be put on how it varies for different plants, and conducted in natural growing conditions.

The STD MT emission at P2 in 2016 decreased from May ($0.590 \pm 0.306 \mu\text{g g}_{\text{dw}}^{-1} \text{h}^{-1}$) to October ($0.022 \pm 0.028 \mu\text{g g}_{\text{dw}}^{-1} \text{h}^{-1}$) and a decreasing trend was found in 2017 for the other site (P3–P4) as well. Studies conducted on *Salix* have shown that close after budbreak, enhanced emissions of MTs have been observed (Hakola et al., 1998; Hakola et al., 1999), but since the budbreak was not recorded in these years, it is difficult to confirm this result. No SQTs were emitted in May and October at P2 in 2016, which indicates that these compounds are emitted during a shorter season compared to, e.g., isoprene and MTs, and also points out the need for a parameter that takes the seasonality into account.

Table 2. Average emission (mean and standard deviation, $\mu\text{g g}_{\text{dw}}^{-1} \text{h}^{-1}$) for isoprene, monoterpenes (MTs), sesquiterpenes (SQTs) and other VOCs, and average standardized (STD) emission (mean and standard deviation, $\mu\text{g g}_{\text{dw}}^{-1} \text{h}^{-1}$) for isoprene, MTs and SQTs during 2015 and 2016. Average T_c ($^{\circ}\text{C}$) and PAR_c ($\mu\text{mol m}^{-2} \text{s}^{-1}$) together with standard deviation for each month.

	2015			2016					
	July	Aug.	Sep.	May	June	July	Aug.	Sep.	Oct.
Isoprene	38.3 (43.3)	49.8 (37.2)	5.1 (5.4)	17.4 (12.4)	26.0 (21.5)	16.2 (16.9)	34.4 (34.9)	7.3 (9.5)	0.1 (0.3)
MTs	0.317 (0.228)	0.219 (0.145)	0.068 (0.045)	0.305 (0.140)	0.291 (0.209)	0.129 (0.078)	0.051 (0.020)	0.063 (0.037)	0.003 (0.004)
SQTs	0.031 (0.024)	0.035 (0.033)	0.023 (0.014)	0 (0)	0.003 (0.005)	0.015 (0.018)	0.084 (0.057)	0.001 (0.002)	0 (0)
other VOCs	0.441 (0.039)	1.640 (0.149)	0.207 (0.021)	0.330 (0.034)	0.114 (0.016)	0.499 (0.083)	0.398 (0.052)	0.232 (0.033)	0.092 (0.017)
STD isoprene	74.8 (42.8)	70.4 (43.0)	19.2 (16.1)	29.9 (20.4)	42.4 (23.5)	35.8 (25.4)	42.0 (35.0)	13.8 (12.9)	1.6 (4.8)
STD	0.580 (0.292)	0.268 (0.163)	0.286 (0.182)	0.590 (0.306)	0.488 (0.330)	0.257 (0.186)	0.065 (0.032)	0.139 (0.075)	0.022 (0.028)
STD	0.076 (0.044)	0.040 (0.038)	0.171 (0.113)	0 (0)	0.004 (0.007)	0.021 (0.026)	0.054 (0.046)	0.003 (0.009)	0 (0)
T_c	23.2 (4.7)	28.9 (2.9)	19.3 (3.4)	26.1 (2.5)	25.1 (5.8)	24.2 (4.5)	31.1 (6.8)	25.0 (4.6)	8.7 (2.7)
PAR_c	562 (397)	467 (230)	329 (192)	951 (448)	710 (479)	461 (354)	704 (459)	403 (307)	89 (125)

Previous studies have put little focus on finding emission potentials for non-terpenes, and how they differ through the season since their emission rates only have been less significant when studying SRCs (Copeland et al., 2012). Grouped together as other VOCs, the average emission during the different months in 2015 and 2016 were usually lower than $0.500 \mu\text{g g}_{\text{dw}}^{-1} \text{h}^{-1}$ for this group, except in the beginning of August 2015 (Table 2 and Figure 7). During this month, emissions of compounds like benzaldehyde, hexanal and nonanal increased approx. 4-fold. Due to the outbreak of *Melampsora* in 2015, it is likely that the fungus influenced the emission rates of these compounds. Many studies have shown that stress-induced compounds, such as benzaldehyde, nonanal, octanal, decanal and hexanal have been emitted when the plants were suffering from abiotic and biotic stresses (Hilderbrand, 1989; Andersen et al., 1994; Wildt et al., 2003; Misztal et al., 2015; Jiang et al., 2016). Especially, nonanal and hexanal have been observed from many plant species

affected by pathogens (Hilderbrand 1989; Andersen et al., 1994; Wildt et al., 2003). Green leaf volatiles (e.g., hexanal) are known to act as a defense against pathogens (Hilderbrand, 1989), and Toome et al. (2010) showed that willow trees emitted GLVs when they were infected by *Melampsora*. Besides this, it was harder to relate the emissions of other VOCs to a seasonal trend but like the terpenes, other VOCs had substantially lower emissions in the late growing season. This was also the case in 2017 for P3 and P4, where the emissions of other VOCs were many times lower in September compared to May. *Melampsora* was believed to have caused the higher emissions of caryophyllene in August 2015, and may have suppressed the isoprene emissions (Toome et al., 2010). Stress-induced emission is harder to include in algorithms but would be required to better estimate the emissions from vegetation.

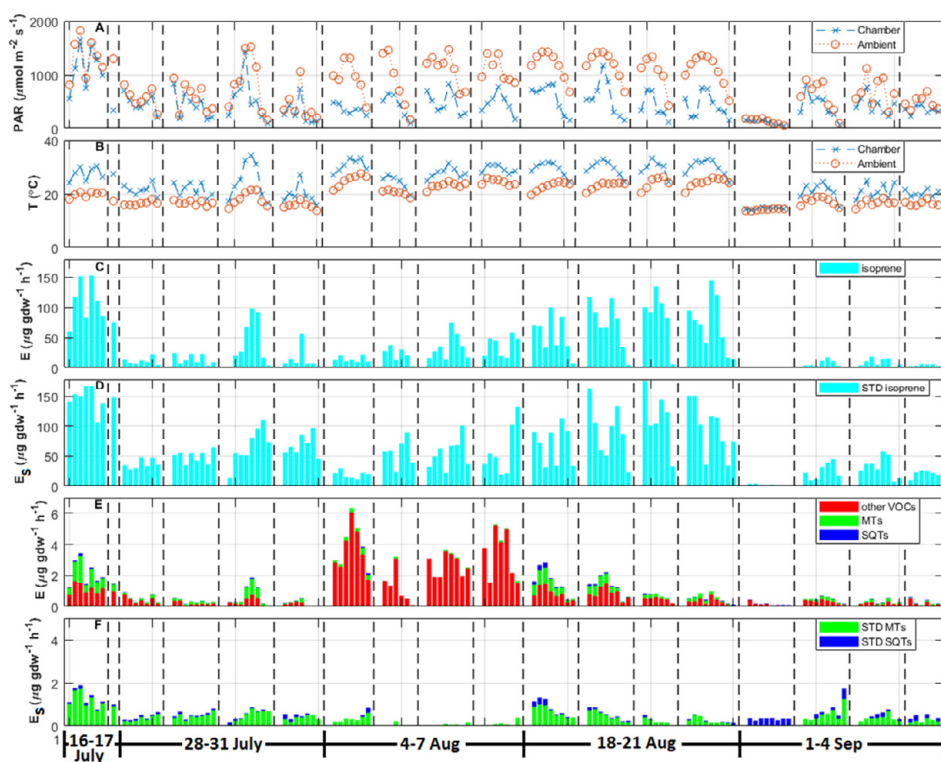


Figure 7. Measurements from P1 in 2015. A) PAR ($\mu\text{mol m}^{-2} \text{s}^{-1}$) values for chamber condition (PAR_c , blue cross and dashed line) and ambient condition (red circle and dotted line). B) Temperature ($^{\circ}\text{C}$) values for chamber condition (T_c , blue cross and dashed line) and ambient condition (red circle and dotted line). C) Emission rates ($\mu\text{g g}_{\text{dw}}^{-1} \text{h}^{-1}$) for isoprene (cyan). D) Standardized (STD) emission rates ($\mu\text{g g}_{\text{dw}}^{-1} \text{h}^{-1}$) for isoprene (cyan). E) Emission rates ($\mu\text{g g}_{\text{dw}}^{-1} \text{h}^{-1}$) of other VOCs (red), monoterpenes (MTs, green) and sesquiterpenes (SQTs, blue). F) STD emission rates ($\mu\text{g g}_{\text{dw}}^{-1} \text{h}^{-1}$) for monoterpenes (MTs, green) and sesquiterpenes (SQTs, blue). Vertical dashed lines separate the different days. Each bar represents individual measurements.

A clear difference was observed when comparing the different varieties in 2017. The STD isoprene emission from Wilhelm (50.33 ± 72.63 μg g_{dw}⁻¹) was almost three times higher and statistically significant compared to Tora (17.99 ± 27.18 μg g_{dw}⁻¹) (Table 3). The STD average isoprene emissions from Ester and Inger differed less, and their emission rates followed the same curve up to 450 μmol m² s⁻¹, thereafter emissions from Ester levelled out faster than for Inger (Figure 8 A,B). Isoprene emission from Wilhelm showed a strong increase for the measured light levels and no tendency of leveling out, even after 1000 μmol m² s⁻¹. In this sense, Wilhelm are the least appropriate variety for SRPs among these four varieties if planted near pollution sources (e.g., trafficked roads or industrial areas) because of the higher risk to produce O₃ and PAN (Folberth et al., 2005; Watson et al., 2006).

Table 3. Isoprene, monoterpenes (MTs), sesquiterpenes (SQTs) and total terpenoid emissions (μg g_{dw}⁻¹ h⁻¹, mean and standard deviation) for the different *Salix* varieties. Standardized (STD) emission rates for isoprene, MTs and SQTs (μg g_{dw}⁻¹ h⁻¹, mean and standard deviation) for the different varieties. Average and standard deviation for temperature (T_c, °C), photosynthetically active radiation (PAR_c, μmol m⁻² s⁻¹) and relative humidity (RH_c, %) in the leaf chamber.

	Tora, n = 90	Wilhelm, n = 104	Ester, n = 53	Inger, n = 52
isoprene (μg g _{dw} ⁻¹ h ⁻¹)	4.00 (7.05)	12.66 (20.63)	6.11 (9.06)	7.77 (11.65)
MTs (μg g _{dw} ⁻¹ h ⁻¹)	1.56 (0.62)	0.80 (0.28)	1.25 (1.01)	1.87 (1.24)
SQTs (μg g _{dw} ⁻¹ h ⁻¹)	0.40 (0.28)	0.22 (0.24)	0.57 (0.44)	0.56 (0.26)
Sum (μg g _{dw} ⁻¹ h ⁻¹)	5.96 (2.06)	13.68 (5.84)	7.93 (2.73)	10.02 (3.32)
STD isoprene (μg g _{dw} ⁻¹ h ⁻¹)	17.99 (27.18)	50.53 (72.63)	25.84 (34.36)	32.75 (47.82)
STD MTs (μg g _{dw} ⁻¹ h ⁻¹)	5.84 (1.90)	3.09 (0.99)	3.44 (2.35)	6.00 (3.21)
STD SQTs (μg g _{dw} ⁻¹ h ⁻¹)	2.43 (1.63)	1.30 (1.53)	3.76 (3.20)	3.71 (1.91)
T _c (°C)	19.0 (2.1)	19.0 (2.0)	18.9 (2.2)	19.0 (2.3)
PAR _c (μmol m ⁻² s ⁻¹)	571 (487)	551 (477)	561 (477)	573 (494)
RH _c (%)	61.5 (13.0)	53.9 (16.9)	48.2 (9.5)	51.4 (8.9)

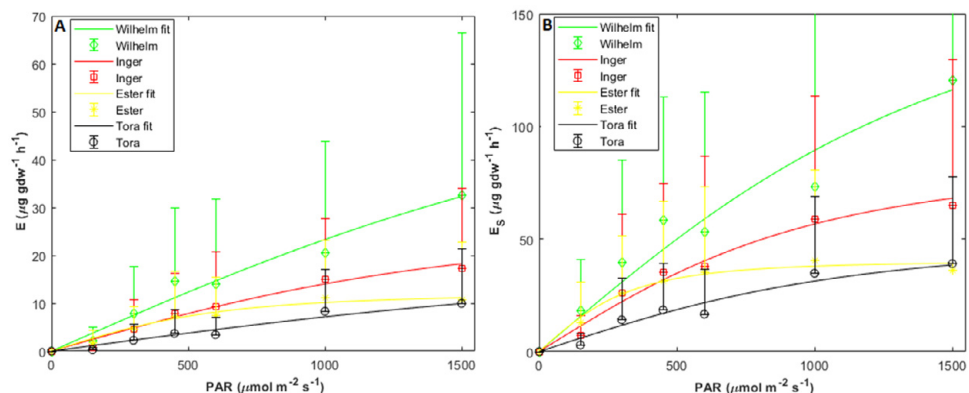


Figure 8. A) Isoprene emission rates (μg g_{dw}⁻¹ h⁻¹, mean + standard deviation, n = 7–16) and fitted curves for Wilhelm (green diamonds and line), Inger (red boxes and line), Ester (yellow stars and line) and Tora (black circles and line) at different PAR values (μmol m² s⁻¹). B) Standardized isoprene emission rates (μg g_{dw}⁻¹ h⁻¹, mean + standard deviation, n = 7–16) and fitted curves for Wilhelm (green diamonds and line), Inger (red boxes and line) and Tora (black circles and line) at different PAR (μmol m² s⁻¹) values.

Average measured MT emission (0.8 ± 0.3 μg g_{dw}⁻¹ h⁻¹) and SQT emission (0.2 ± 0.2 μg g_{dw}⁻¹ h⁻¹) from Wilhelm were lower than from the other varieties (1.25–1.87

$\mu\text{g g}_{\text{dw}}^{-1} \text{h}^{-1}$ (MTs) and $0.40\text{--}0.57 \mu\text{g g}_{\text{dw}}^{-1} \text{h}^{-1}$ (SQTs)). This was also the case for the average STD MT and SQT emissions. Ocimene was a dominant MT for all varieties except for Ester. Instead, camphene and limonene were the dominantly emitted MTs from this variety (Figure 9A). Limonene was also the most abundant MT from Inger. Emissions of linalool was abundant from Wilhelm and Tora but not from Ester and Inger. No caryophyllene was observed from Wilhelm (Figure 9B). Response to light for MTs and SQTs varied as well for the varieties. No correlation between PAR and the compounds ocimene and linalool was seen for Ester, but all the other varieties showed an increasing emission rate trend with PAR. Inger was the only variety that showed a clear light response for the emission of caryophyllene. These results point out how important the genetical influence can be for BVOC emissions even within the same genus or species, which has been reported previously (Staudt et al., 2004). Genetical influence on BVOC emission has been found for other deciduous and coniferous trees, and plants with same provenances do not necessarily respond in the same way. For instance, oak species have been considered mainly as isoprene emitters but some can be significant MT emitters (Pio et al., 1993; Kesselmeier et al., 1996). How the emission is influenced by light is another trait that can differ within the same species. According to Evans et al. (1985), MT emission from spruce was little influenced by PAR, whilst Steinbrecher et al. (1993) reported a significant dependence. Tingey et al. (1980) found no influence of PAR on MT emissions from pine but Tarvainen et al. (2005) reported that 1,8-cineole was affected by light. Extrapolating emissions among species must be done prudently and based on representative measurements (Kesselmeier et al., 1996).

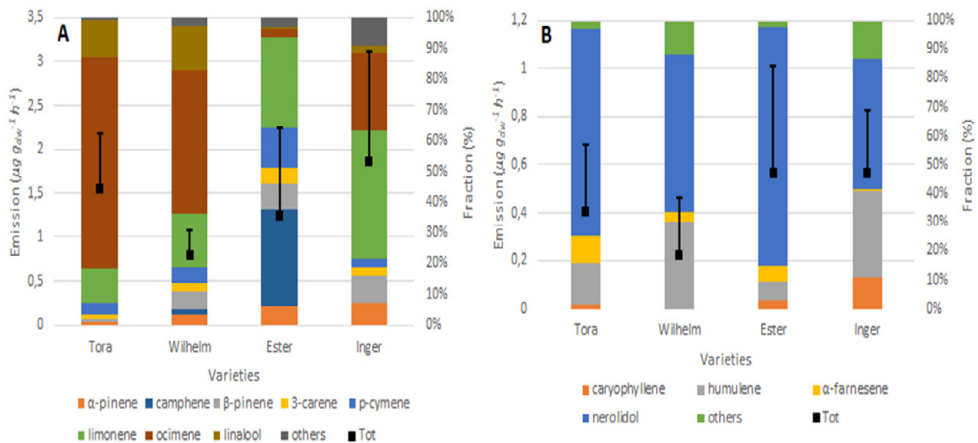


Figure 9. A) Total MT emissions (black square, $\mu\text{g g}_{\text{dw}}^{-1} \text{h}^{-1}$, mean + standard deviation, $n = 52\text{--}104$) and the contribution from each MT for the different varieties. Others includes eucalyptol, d-phellandrene, terpinolene, γ -terpinene and one unknown compound. B) Total SQT emissions (black square, $\mu\text{g g}_{\text{dw}}^{-1} \text{h}^{-1}$, mean + standard deviation, $n = 52\text{--}104$) and the contribution from each SQT for the different varieties. Others includes copaene and one unknown compound.

Comparison between different heights and light conditions (Papers I and IV)

Light response curves during 2016 showed that the height within the canopy had a large impact on the BVOC emission rates. The emission of isoprene, both measured and STD, differed a factor two when comparing more sun-adapted leaves (z_H and z_M) to shade-adapted leaves (z_L). This light response resulted in that the average STD isoprene emission rate was $96.1 (\pm 64.6) \mu\text{g g}_{\text{dw}}^{-1} \text{h}^{-1}$ (or $5.47 \pm 0.26 \text{ mgC g}_{\text{dw}}^{-1} \text{h}^{-1}$) at z_H and $51.8 (\pm 32.9) \mu\text{g g}_{\text{dw}}^{-1}$ (or $2.88 \pm 1.57 \text{ mgC g}_{\text{dw}}^{-1} \text{h}^{-1}$) at z_L . The difference between the emission rates was especially pronounced for the lower PAR values, and the emissions at z_H increased all the way up to $1000 \mu\text{mol m}^{-2} \text{s}^{-1}$ (Figure 10A,B). This pattern has been reported by others (Sharkey et al., 1991; Niinemets et al., 2010), which points out that light acclimatization is an important factor for emissions of, e.g., isoprene. Therefore, estimating isoprene emissions on a landscape or regional level can be misleading if simulations are based on an emission potential that represents only one height level. The shape of the isoprene curves followed a hyperbolic curve similar to the one that can be observed for A (Monson and Fall, 1989), but since the ratio between emitted isoprene and A (E/A) increased with PAR (Figure 11), the leaves lost more C as isoprene for the higher PAR values compare to the lower PAR values. Moreover, leaves at z_H had a higher E/A ratio compared to leaves at z_L , showing that the light-adapted leaves in the upper part of the canopy lost more C as isoprene than less light adapted leaves.

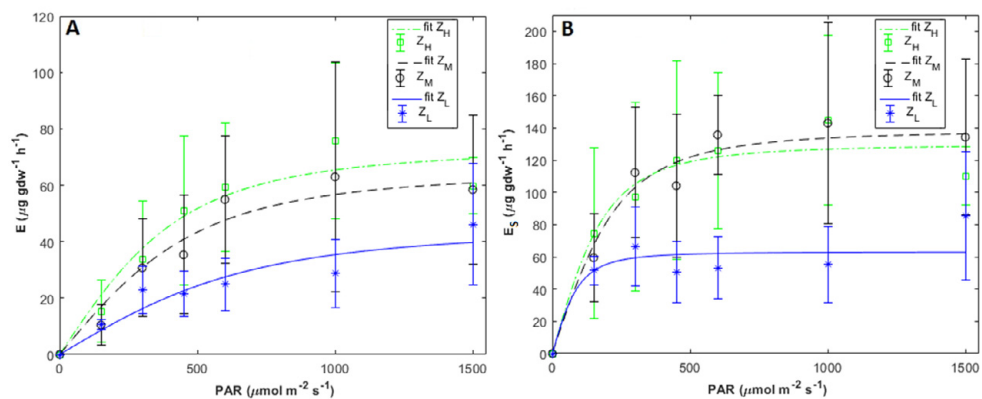


Figure 10. A) Average isoprene emissions rates ($\mu\text{g g}_{\text{dw}}^{-1} \text{h}^{-1}$, mean \pm standard deviation, $n = 3-6$) and fitted curves for different PAR values ($\mu\text{mol m}^{-2} \text{s}^{-1}$) from the different height levels, z_H (green boxes and dot-dashed line), z_M (black circles and dashed line) and z_L (blue stars and line). B). Average standardized isoprene emission rates ($\mu\text{g g}_{\text{dw}}^{-1} \text{h}^{-1}$, mean \pm standard deviation, $n = 3-6$) and fitted curves for different PAR ($\mu\text{mol m}^{-2} \text{s}^{-1}$) values from the different height levels, z_H (green boxes and dash-dotted line), z_M (black circles and dashed line) and z_L (blue stars and line).

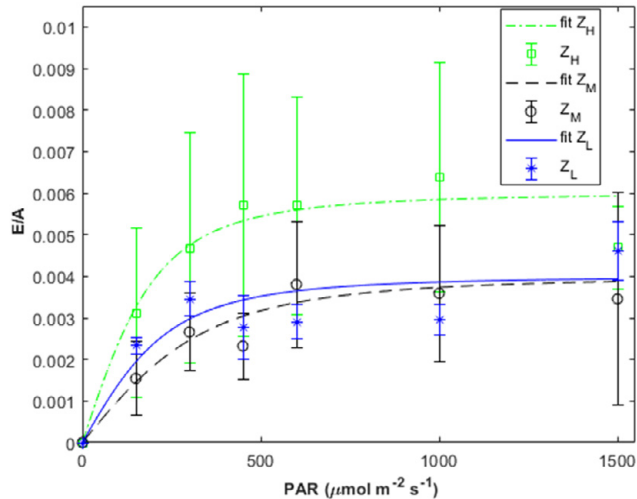


Figure 11. Ratio between isoprene emission and net assimilation (E/A , dimensionless, mean \pm standard deviation, $n = 3-5$) and fitted curves at different height levels, z_H (green boxes and dot-dashed line), z_M (black circles and dashed line) and z_L (blue stars and line) for the measured PAR ($\mu\text{mol m}^{-2} \text{s}^{-1}$) values.

Another strong evidence that emissions of terpenes are adapted to different light conditions was seen when comparing MT and SQT emissions between shaded and sun-adapted leaves. Shade-adapted *Salix* leaves emitted less MTs than sun-adapted leaves and only limonene was seen from the former, while α -pinene, limonene, p-cymene, ocimene and 3-carene were observed from the latter. The total average MT emission from z_H ($0.078 \pm 0.085 \mu\text{g g}_{\text{dw}}^{-1}$ or $0.004 \pm 0.005 \text{ mgC m}^{-2} \text{ h}^{-1}$) was almost twice as high than from z_L ($0.045 \pm 0.029 \mu\text{g g}_{\text{dw}}^{-1}$ or $0.002 \pm 0.002 \text{ mgC m}^{-2} \text{ h}^{-1}$). Further, no SQTs were emitted from the shaded leaves but four (α -farnesene, caryophyllene, humulene and nerolidol) were emitted from the sun-adapted leaves. Ocimene and α -farnesene showed an increasing emission trend for some of the PAR values (Figure 12), but this pattern was only observed from the sun-adapted leaves, since the shade-adapted did not emit these compounds.

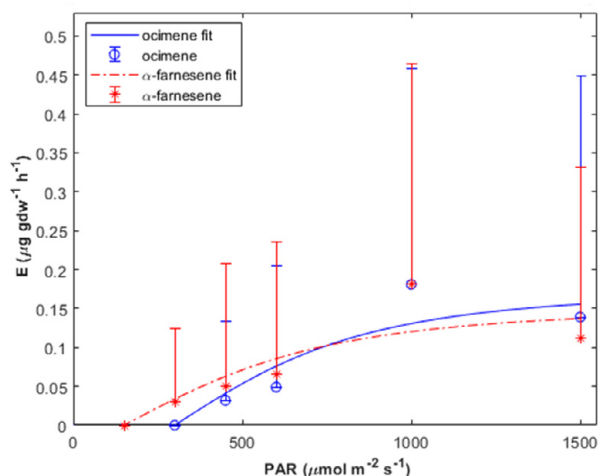


Figure 12. Average emission ($\mu\text{g g}_{\text{dw}}^{-1} \text{h}^{-1}$, mean + standard deviation, $n = 11$) and fitted curves for ocimene (blue circles and line) and α -farnesene (red stars and dot-dashed line) for the sun-adapted leaves (Z_M and Z_H) and different PAR ($\mu\text{mol m}^{-2} \text{s}^{-1}$) values.

When grouping non-terpenes together, higher emissions were observed from the lower height (Z_M) compared to the higher (Z_H), despite the similar light conditions for these locations. This result indicates that the difference is not a result to light adaption.

The height comparison for the BVOC emission from spruce showed that there was a significant difference for the emissions of camphene and limonene in Taastrup. The reason why other compounds (e.g., ocimene and isoprene) did not differ could be due to the wide spacing and consequently similar irradiation conditions for all heights (2 m, 5.5 m and 12.5 m). In Norunda, all the emissions for isoprene, MTs and SQTs differed when comparing the lowest (3 m) and the highest (20 m) height. Emissions of isoprene and MTs were even higher at 3 m compared to 20 m. Different explanations were found, e.g., the lower height had in periods higher irradiance than at 20 m (Wang, 2018), and the needles at 3 m were older with a low percentage of newly produced shoots, which can influence the concentrations of terpenes in needles (Merk et al., 1988).

Impact of the surrounding area (e.g., dense or sparse forest), shape of the canopy, phenological stages of the leaves and needles add complexity to acquire reliable height emission factors on an ecosystem-scale.

Impact of age on BVOC emissions (Paper I and II)

A comparison between the first and second growing year trees showed that all varieties in their first growing season emitted a substantially higher average emission of other VOCs ($15.70\text{--}46.74 \mu\text{g g}_{\text{dw}}^{-1} \text{h}^{-1}$) than during the second growing

season ($2.46\text{--}4.70 \mu\text{g g}_{\text{dw}}^{-1} \text{h}^{-1}$). The average emissions of some of the most emitted other VOCs from the first growing year trees were hexanal ($0.826\text{--}4.920 \mu\text{g g}_{\text{dw}}^{-1} \text{h}^{-1}$), benzaldehyde ($0.436\text{--}3.204 \mu\text{g g}_{\text{dw}}^{-1} \text{h}^{-1}$), octanal ($0.354\text{--}3.149 \mu\text{g g}_{\text{dw}}^{-1} \text{h}^{-1}$), furfural ($0.148\text{--}3.069 \mu\text{g g}_{\text{dw}}^{-1} \text{h}^{-1}$) and acetophenone ($0\text{--}2.462 \mu\text{g g}_{\text{dw}}^{-1} \text{h}^{-1}$). Many of these were less common for the one year older trees. One explanation for this difference could be that the saplings need a stronger defense before they have reached a growing stage, which provides a better prerequisite for establishment and survival. Mature trees might be less affected by damage than young trees and more capable to survive (Palo, 1984). The average emission of other VOCs from Tora on P2 in 2016 (fourth growing season) was also three times lower than the average emission from first growing season Tora on P2. Compounds other than terpenes (e.g., GLVs) have usually been studied when considering stress. Even if non-terpenes serve as protection for the plants, they can also contribute to formation of aerosols (Pandis et al., 1992 and references therein; Misztal et al., 2015; Palm et al., 2018).

The STD isoprene emission results from fourth growing season Tora at P2 in 2016 ($95.0 \pm 63.2 \mu\text{g g}_{\text{dw}}^{-1} \text{h}^{-1}$) and the first growing season Tora at P2 in 2017 ($20.9 \pm 33.5 \mu\text{g g}_{\text{dw}}^{-1} \text{h}^{-1}$), showed that the former emitted around five times more isoprene and that the older trees reached almost the same rate ($66.4 \mu\text{g g}_{\text{dw}}^{-1} \text{h}^{-1}$) at $150 \mu\text{mol m}^2 \text{s}^{-1}$ as the younger ($55.1 \mu\text{g g}_{\text{dw}}^{-1} \text{h}^{-1}$) did at $1500 \mu\text{mol m}^2 \text{s}^{-1}$ (Figure 13). Comparing STD MT emissions from Tora between the first and the fourth growing season showed that the emission rates from the younger trees ($5.240 \pm 2.272 \mu\text{g g}_{\text{dw}}^{-1} \text{h}^{-1}$) were several times higher than the older trees ($0.359 \pm 0.184 \mu\text{g g}_{\text{dw}}^{-1} \text{h}^{-1}$). More MTs were emitted from the younger trees (9 MTs: α -pinene β -pinene, d-phellandrene, eucalyptol, limonene, linalool, ocimene, p-cymene and 3-carene) compared to the older (5 MTs: α -pinene, limonene, ocimene, p-cymene and 3-carene). The STD SQT emissions for Tora differed as well and the younger trees emitted approx. 2.5 times higher average emission rate compared to the fourth growing season trees. The response to light also showed that linalool increased with PAR but only for the younger trees, whereas α -farnesene increased with PAR but only for the older trees.

From the literature, it is not clear how the age influences the emission rates. Although studies including age when measuring BVOC emissions are limited, some have reported that the age can influence the emission rates. For instance, Kim et al. (2005) and Lim et al. (2008) showed that the age had a significant impact on the MT emission rates from conifers. Nuñez and Pio (2001) reported that isoprene emission differed between young and adult eucalyptus trees. But it is likely that the impact of age is species-dependent and for some plants it might not change the BVOC emissions considerably.

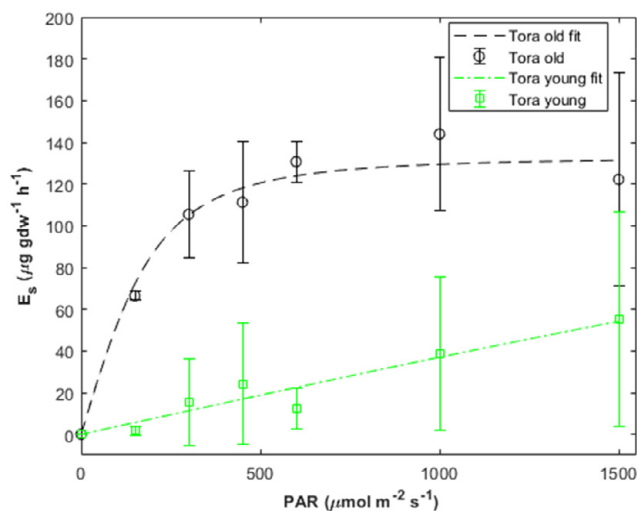


Figure 13. Standardized isoprene emission rates ($\mu\text{g gdw}^{-1} \text{h}^{-1}$, mean \pm standard deviation, $n = 7\text{--}16$) and fitted curves for first growing season (green boxes and dash-dotted line) and fourth growing season (black circles and dashed line) trees belonging to Tora on P2 at different PAR ($\mu\text{mol m}^{-2} \text{s}^{-1}$) values.

LUCC and impact on air quality from *Salix* (Paper I–IV)

The measurements performed from July 2015 to September 2017, showed a high contribution of isoprene to the atmosphere from *Salix* trees even if the rates differed among varieties. Higher emissions of isoprene were observed from late spring to early autumn. Emissions of other compounds were in general minor compared to isoprene with some exceptions, e.g., for saplings and during early season. The landcover is crucial for what kind of BVOC that will be emitted to the atmosphere. The Swedish landcover is dominated by boreal forest (68.8%), containing approx. 40.3% Norway spruce, 39.3% Scots pine, 12.4% birch and minor fractions of some others species (Skogsdata, 2020). Norway spruce trees are known to emit terpenes and particularly MTs, but they can also emit isoprene up to about the same rates as MTs (Kesselmeier and Staudt, 1999). Studies conducted in boreal forest have shown that the major part of the emitted terpenoids is made up by MTs (Rinne et al., 2000; Tarvainen et al., 2007; Rinne et al., 2009). The contribution to this MT emission is essentially from spruce and pine, although deciduous trees can contribute to the emission and especially depending on the season (Tarvainen et al., 2007; Rinne et al., 2009). The latitudinal study of Norway spruce in Sweden and Europe (Paper IV), showed that emission rates were similar but with some emission profile variability, regardless of the adaption to different environmental growing conditions at each location. However, comparing compounds separately resulted in different results. For example, limonene was a major emitted MT from the trees on all sites except in Skogaryd. Contribution from 3-carene was minor in Norunda, but in

Piikkiö it was significant, despite the similar latitude at these sites. The genetical influence among the different studied spruce trees was more important to the emission profile than climatic adaptation. Compared to *Salix* trees, all spruce sites had considerably lower emissions of isoprene and the average STD isoprene emission for the spruce sites was $<1 \mu\text{g g}_{\text{dw}}^{-1} \text{h}^{-1}$. Different species of pine have been reported as negligible isoprene emitters as well (Kesselmeier and Staudt, 1999). A LUCC, where coniferous forest such as spruce or pine is converted into SRC fields with *Salix* would drastically change the atmospheric concentrations of isoprene. This LUCC would in turn increase the risk of production of regional pollutions, e.g., O_3 and PAN, if anthropogenic sources of NO_x are sufficiently close to the plantation (Wang and Shallcross, 2000; Ryerson et al., 2001; Atkinson and Arey, 2003; Folberth et al., 2005). On the other hand, the spruce trees emitted more MTs than the older *Salix* trees and especially α -pinene, β -pinene and limonene were some of the most abundant MTs emitted by spruce. The average emission of α -pinene was approx. 4–60 times higher from spruce compared to the *Salix* trees studied 2015–2017. Spruce trees in Norunda have shown to be able to emit both α -pinene and β -pinene up to approx. $60 \mu\text{g g}_{\text{dw}}^{-1} \text{h}^{-1}$ (Wang et al., 2017), which is about the same magnitude as isoprene emitted from *Salix*. Monoterpenes are able to foster SOA production and in particular α -pinene, β -pinene and limonene have been reported to act as precursors for aerosol formation (Paulson et al., 1990; Pandis et al., 1992; Zhang et al., 1992; Ehn et al., 2014; Mutzel et al., 2016). Therefore, replacing spruce forest with *Salix* trees could reduce the number of particles and diminish the albedo in the atmosphere, which might lead to a reinforced effect on global warming (Boucher et al., 2013).

The measurements executed with the PAM reactor was unable to produce any aerosols at P1 during the summer 2015 (Paper III). The simulated aging in the reactor could neither increase the mass nor the number concentration significantly. The explanation for this was the lack of precursors, such as MTs. Ecosystem scale measurements of MTs concentrations by the PTR-TOF-MS gave an average value of approx. 140 ppt and for the MTs, and the sum of benzene, toluene and xylenes (BTX) was even lower (96 ppt). The concentration of MTs and BTX would have needed to be around one order of magnitude higher to result in a visible mass increase in the reactor. Manual measurements during daytime from the ambient air close to the inlet of the PAM reactor also confirmed the low MT concentration, which was 28 ppt (not published data). Since no measurements with the PAM reactor was made in spring, it is not possible to exclude any particle formation during this time of the year, because higher MTs emission during early growing season might increase the precursors needed for generating SOAs. Also, since the young *Salix* trees were able to emit higher rates of MTs and other VOCs, it is more likely to find increased production of aerosols from saplings or during the first growing season than from older trees.

No measurements of O_3 were performed between 2015 and 2017 but a study done about 15 km away from P1, measured isoprene from a willow coppice plantation

and their measurements could not reproduce any O₃ in their chemistry model that they used (Olofsson et al., 2005). Nevertheless, *Salix* trees exceed by far the terpene emissions from crops and grassland. Many studies have presented substantially lower emission rates of isoprene (0–0.5 μg g_{dw}⁻¹ h⁻¹) from, e.g., grassland, wheat, oat, rape, sugar beet and potato, compared to *Salix* (Winer et al., 1992; König et al., 1995; Karl et al., 2009; Morrison et al., 2016). Due to the low isoprene from traditional crops, O₃ formation is considerably higher in areas where both pollutions and isoprene are abundant (Ryerson et al., 2001). An expansion of SRPs with fast-growing plants, like *Salix* or other species with high isoprene emission (e.g., *Populus*), have to be strategically located to assure that the prerequisites for O₃ production are minimized. If not, large upscaling of SRPs could result in an increase of photochemical smog pollutions, which in turn could lead to reduced biomass production, additional premature deaths and economical costs (Fumigalli et al., 2001; Ryerson et al., 2001; Van Dingenen et al. 2009; Ashworth et al., 2012; Wagg et al., 2012; Ashworth et al., 2013; Beltman et al., 2013; Calvete-Sogo et al., 2014; Fann et al., 2015).

Conclusions and outlook

The aim of the work presented in this thesis was to study BVOC emissions from *Salix* trees that are commercially used for producing renewable energy. The influence by different factors such as seasonality, genetic diversity, height and age were studied in order to investigate the variability in the emissions. All the manual BVOC measurements were done on a leaf scale by using leaf and branch chambers combined with GC-MS analysis. Measurements of particle formation near the *Salix* SRP, and BVOCs measurements from spruce, were a part of the thesis work to assess how an expansion of *Salix* plantations could influence the air quality locally.

The measurements in 2015, 2016 and 2017 showed that isoprene was the major compound throughout the most of the growing season (Papers I and II), in accordance to what have been found in previous studies. Isoprene emissions peaked between June and August. High emissions were observed already in the beginning of May and until September, but in October the emissions were negligible. The driving factors for the isoprene emissions were mainly temperature and PAR but the phenological related changes in the leaves was also believed to influence the emissions. The seasonal trend for MTs seemed to decline from spring to autumn. Ocimene was normally the dominant MT compound emitted but was not observed in October. Caryophyllene dominated among the SQTs but this group contributed with the lowest amount to the total BVOC emission. Emissions of SQTs peaked in August and enhanced emissions of caryophyllene during summer was likely a response to biotic stress caused by *Melampsora*. No SQTs were observed in May and October 2016, which indicated that the season for these compounds were shorter than for isoprene and MTs. Non-terpenes did not show any clear seasonal pattern but there was a substantially increase for some of the other VOCs in August 2015, which was explained by the rust infestation (*Melampsora*). Compounds like nonanal, benzaldehyde and hexanal increased up to four times during this month. Stress-induced BVOC emissions are hard to predict and implement in models, since the response of the plants are probably species-specific and related to how severe the damage is. Another crucial factor that makes it difficult to estimate these impacts depends on the ability for pathogens and herbivores to adapt to the climate change. Nevertheless, it is clear that stress leads to elevated emissions and needs to be included in models to better estimate regional atmospheric BVOC budgets.

Studies have revealed that the genetical influence on the BVOC emission is important. Emission rates and blend can differ, both inter- and intraspecifically, which was also the case for the different varieties (Paper II). The variety called

Wilhelm emitted the highest rate of isoprene, which was approx. 3 times larger than for Tora. Tora, which is closer related to Wilhelm in the breeding program compared to Ester and Inger, had the lowest isoprene emission. These results emphasize the importance of making measurements. A preconception would have been that Tora and Wilhelm had similar isoprene emission rates, but they differed the most. Therefore, using emission factors from Tora to scale up isoprene emission from SRPs with Wilhelm (or vice versa), would lead to large errors. On the contrary, Ester and Inger, which were related in the breeding program, showed similar average isoprene and SQT emission rates although the terpene blend differed a bit. Interestingly, all the female varieties (Tora, Ester and Inger) seemed to have lower isoprene emission rates than the male variety (Wilhelm), but no conclusion can be made on the scarce basis from the study in 2017. Hence, more studies involving more male (and female) varieties would be needed to confirm this observation. Further, the high isoprene emission from Wilhelm makes this variety less preferable to grow in large quantities close to sources of NO_x, on account of the risk to produce photochemical pollutions such as O₃ and PAN.

Measurements at different heights for the *Salix* trees showed that sun-adapted leaves emitted higher rates of isoprene, MTs and SQTs (Paper I). Less various compounds of MTs and SQTs were also emitted by the shade-adapted leaves. In fact, no SQTs were seen from the shade-adapted leaves. The isoprene emission rate was approx. twice as high from the more sun-adapted leaves compared to the shaded leaves. Ocimene and α -farnesene, together with isoprene, increased with light intensity. However, this increase for ocimene and α -farnesene was only observed for sun-adapted leaves. None of the other VOCs had any clear correlation with light. On the other hand, emissions of these non-terpenes were higher from the lower canopy height, which indicates that there are other factors than light that influence these emissions. The sun-adapted leaves in the upper part of the canopy lost more of the photosynthesized C as isoprene compared to the shaded leaves. Even though these sun-adapted leaves showed higher net assimilation rates for most of the light levels compared to the shade-adapted leaves, they were less efficient in utilizing C from photosynthesis to primary production because they reemitted more of this C as isoprene.

To better understand how BVOC emissions are developing, stand age of plants is an adequate factor to study. To my knowledge, less focus has been on age even if there exist studies that include this factor. It might not always be easy to know the specific age (without cutting down the trees) in a study when measuring in a forest, since forest ecosystems are a mix of species with different ages. These kinds of studies are better suited for managed plants. Comparing the age and the BVOC emissions between the *Salix* trees showed that saplings and first year growing trees emitted substantially higher rates of other VOCs, probably because they need to strengthen their defense system and make them more resistance to stress. Tora was the only variety that was measured both the first growing year and before harvest (fourth growing year). The results from these measurements showed that isoprene

emission was almost five times as large from the older trees compared to the younger. Contrarily, the emissions of MTs were several times lower from the older trees compared to the younger trees. Only five MTs were seen from the older trees whilst nine were emitted from the younger. This outcome indicates that the age of the plants has an impact on the emissions and younger and mature trees can differ in both their emission rates and compound mixture.

The lack of elevated particle formation at the *Salix* site points out that these trees are not able to emit sufficiently high rates of precursors needed to produce SOAs (Paper III). The low concentration of, e.g., MTs was not enough to generate any particles in the PAM reactor. The MTs constituted only a minor fraction of the BVOC emission. However, compounds that have been reported to cause SOAs, e.g. α -pinene, β -pinene and limonene, were many times higher from the young *Salix* trees. Therefore, it is more likely to find SOAs near saplings and young trees compared to older *Salix* trees. The emission of isoprene was considerably higher from the *Salix* trees compared to the spruce trees (Paper IV). Changing from traditional spruce forest would shift the regional BVOC composition towards more isoprene and less MTs. In addition, a LUCC from annual crops or grasslands to SRPs with *Salix* would also alter the atmospheric concentrations of isoprene, since annual crops and grass are low emitters of isoprene. Consequently, an expansion of SRC fields with willow would need to be located at a sufficient distance far away from anthropogenic pollution, which could otherwise promote the production of O₃ and PAN.

The goal to counteract emissions of GHGs and preventing global warming is far away from completed. Reducing fossil fuel by renewable energy from SRCs could be one part of the solution. However, to estimate the environmental impact on the climate, long-term studies where measurement of CO₂, CH₄, N₂O and aerosols during a complete life span of the plantation (20–25 years) would be needed. Although the results presented in this thesis suggest that BVOC emissions from *Salix* plantation is not jeopardizing air quality, measurements of O₃ near a *Salix* site should also be done since studies mostly model the production of O₃ based on BVOC emission factors. Life cycle assessments of SRPs usually exclude air quality and subsequent health effects, which could be included if there existed representative measurements of, e.g., O₃. Combining leaf scale measurements with PTR-TOF-MS ecosystem scale measurements is needed as well, since these would be an appropriate method to evaluate and improve the emission models, and to investigate the impact from BVOCs if there was a substantial expansion of *Salix* plantations. The outcome from this thesis also highlights that upscaling emissions by modelling is difficult since many factors affect the emission, such as variety, height, age, season and stress. Currently, all these are not represented in the models but may be possible to incorporate in the future.

Acknowledgments

There are many people that I would like to thank and I apologize if I forget anyone.

First of all, the person responsible (a.k.a. partner in crime) for making this to come true is my SUPERvisor, **Thomas Holst**. Thank you so much for believing in me (especially when I did not believe in myself). You have an unprecedented skill in flipping disasters into something constructive and useful, this is a super-skill in particular since I managed to screw up all the time (the big question is, did I ever learn how to pack a truck safely). Without you it would not be possible to finish this.

Ylva van Meeningen and **Min Wang**, thank you very much for all the help, especially with introducing me to the methods. But even more, to welcome me to the BVOC group and taking care of this lost soul. I never had to worry when you were around. Better colleagues are hard to find.

Patrik Vestin, you have always been like a mentor to me. With your guidance, I always got back on the right track and you have probably (unofficially) supervised more people in our department than anyone else.

Leif Klemedtsson and **Paul Miller**, the positive attitude you conveyed is beyond what is possible to measure. I always looked forward to meet you since I knew I became a completely new optimistic person.

Riikka Rinnan, thanks for all the help with organizing the lab analysis. It was always nice to visit you and your team in Copenhagen. Seems like the sun is always shining in that city as long as you are there.

Adam Kristensson, Erik Ahlberg, Stina Ausmeel and Birgitta Svenningsson (a.k.a. the aerosol group), the site never became the same after you left. I really enjoy meeting you and I wished we could have done more collaboration. But I'm still wrestling with the conundrum, who wrote "I need to be washed" in the dirt on the rear window on my mother's car?

David Allbrand, working together with you was like a party. All the problems disappeared. I hope that we can do it again and meeting your family (including the dogs) was an honor.

Geert Hensgens, Olive Niyomubyeyi, Pearl Mzobe, Klas Lucander, Altaaf Mechiche-Alami, Yanzi Yan, Enass Said Al-Kharusi, Sofia Junttila, Joel White, Ehsan Abdolmajidi, Cecilia Olsson, Jalisha Theanutti, Erica Jaakkola and Yun Liu, thank you for all nice memories and activities we did, and for making this department a fun place to work in.

Majia Marushchak, to share the office with you was a lot of fun. Despite your Finish genes, you had a good sense of humor.

Johan Wallerstein, you have always inspired me and you are a true role model.

I also would like to thank **Zhanzhang Cai, Adrian Gustafson, Tetiana Svystun, Fabien Rizinjirabake, Norbert Pirk, Ana Soares, Nitin Chaudhary, Jeppe Ågård Kristensen, Augustus Aturinde, Finn Hedefalk, Oskar Löfgren, George Oriangi, Zhendong Wu, Wilhelm Dubber, Jan Blanke, Niklas Boke-Olén, Abdulhakim M. Abdi, Balathandayuthabani Panneer Selvam, Christian Stiegler, Jing Tang, Ross Petersen** and all the other PhD students that supported me.

Big thanks to **Paul Hedberg, Margareta Hellström, Meelis Mölder, Michal Heliasz, Tobias Biermann, Sachin Patade, Cecilia Akselsson, Jonas Ardö, Mats Lindeskog, Harry Lankreijer, Jonathan Seaquist, Petter Pilesjö, Maj-Lena Linderson, Anna-Maria Jönsson, Stefan Olin, Sadegh Jamali, Jörgen Olofsson, Britta Smångs, Janne Rinne, Abdulghani Hasan, Roger Groth, Per-Erik Fahlén, Oleg Mirzov, Jutta Holst, Rafael Przybyszewski, Ricardo Guillén, Marcin Jackowicz-Korczynski, Jonathan Thiry** and all the rest in the department. One never knows what kind of interesting discussions that pops up when bumping into each other.

Anders Jonsson, Stig Larsson, Sven-Elof Andersson, Sten Segerlätt and Per-Olof Andersson, thank you for all the support and help at the sites, which really facilitated doing the measurements.

Oscar Möllerström and Andreas Petersson, you are the persons that followed me through this journey (read: had to hear me whine all the time). You have been priceless and helped me to focus in a positive manner.

Niclas Arnesen and Malin Persson, thanks for hosting me during my courses in Gothenburg. It was a great memory to spend the time with you.

Lars Axelsson, Enar Karlsson and Trollhättan FIK, thank you for helping me to dispel my thoughts during fieldwork.

Lastly, I thank my family for all their support. Working and training retreats in the forest where you live, helped a lot to cross the finish line.

References

- Alexandersson, H. and Eggertsson Karlström, C., 2001. Temperaturen och nederbörden i Sverige 1961–90: Referensnormaler—utgåva 2 (in Swedish). Meteorologi 99, Swedish Meteorological and Hydrological Institute, Norrköping.
- Ameye, M., Allmann, S., Verwaeren, J., Smaghe, G., Haesaert, G., Schuurink, R. C. and Audenaert, K., 2018. Green leaf volatile production by plants: a meta-analysis. *New Phytol.*, 220, 666–683.
- Ammann, C., Spirig, C., Neftel, A., Steinbacher, M., Komenda, M. and Schaub, A., 2004. Application of PTR-MS for Measurements of Biogenic VOC in a Deciduous Forest. *Int. J. Mass Spectrom.*, 239, 87–101.
- Andersen, R.A., Hamilton-Kemp, T.R., Hildebrand, D.F., McCracken, C.T., Collins, R.W. and Fleming, P.D., 1994. Structure-Antifungal Activity Relationships among Volatile C6 and C9 Aliphatic Aldehydes, Ketones, and Alcohols. *J. Agric. Food Chem.*, 42, 1563–1568.
- Arneth, A., Monson, R. K., Schurgers, G., Niinemets, Ü. and Palmer, P. I., 2008. Why are estimates of global terrestrial isoprene emissions so similar (and why is this not so for monoterpenes)? *Atmos. Chem. Phys.*, 8, 4605–4620.
- Ashmore, M. R., 2005. Assessing the future global impacts of ozone on vegetation. *Plant, Cell and Environ.*, 28, 949–964.
- Ashworth, K., Folberth, G., Hewitt, C. N., and Wild, O., 2012. Impacts of near-future cultivation of biofuel feedstocks on atmospheric composition and local air quality. *Atmos. Chem. Phys.*, 12, 919–939.
- Ashworth, K., Wild, O. and Hewitt, C., 2013. Impacts of biofuel cultivation on mortality and crop yields. *Nature Clim. Change*, 3, 492–496.
- Atkinson, R., 1997. Gas-phase tropospheric reactions of volatile organic compounds: 1. Alkanes and alkenes. *J. Phys. Chem. Ref. Data*, 26, 215–290.
- Atkinson, R. and Arey, J., 2003. Gas-phase tropospheric chemistry of biogenic volatile organic compounds: A review. *Atmos. Environ.*, 37, 197–219.
- Baum, C., Leinweber, P., Weih, M., Lamersdorf, N. and Dimitriou, I., 2009. Effects of short rotation coppice with willows and poplar on soil ecology. *Landbauforschung Volkenrode*, 59, 183–196.
- Beauchamp, J., Wisthaler, A., Hansel, A., Kleist, E., Miebach, M., Niinemets, Ü., Schurr, U. and Wildt, J., 2005. Ozone induced emissions of biogenic VOC from tobacco: relations between ozone uptake and emission of LOX products. *Plant Cell Environ.*, 28, 1334–1343.
- Beltman, J. B., Hendriks, C., Tum, M. and Schaap, M., 2013. The impact of large scale biomass production on ozone air pollution in Europe. *Atmos. Environ.*, 71, 352–363.

- Bonde, I., Kuylenstierna, J., Bäckstrand, K., Eckerberg, K., Kåberger, T., Löfgren, Å., Rummukainen, M. and Sörlin, S., 2020. Report of the Swedish Climate Policy Council. Rapport nr 3, ISBN 978-91-984671-4-7.
- Boucher, O., D. Randall, P. Artaxo, C. Bretherton, G. Feingold, P. Forster, V.-M. Kerminen, Y. Kondo, H. Liao, U. Lohmann, P. Rasch, S.K. Satheesh, S. Sherwood, B. Stevens and X.Y. Zhang, 2013: Clouds and Aerosols. In: *Climate Change 2013: The Physical Science Basis. Contribution of Working Group I to the Fifth Assessment Report of the Intergovernmental Panel on Climate Change* [Stocker, T.F., D. Qin, G.-K. Plattner, M. Tignor, S.K. Allen, J. Boschung, A. Nauels, Y. Xia, V. Bex and P.M. Midgley (eds.)]. Cambridge University Press, Cambridge, United Kingdom and New York, NY, USA.
- Bracho-Nunez, A., Knothe, N.M., Welter, S., Staudt, M., Costa, W.R., Liberato, M.A.R., Piedade, M.T.F. and Kesselmeier, J., 2013. Leaf level emissions of volatile organic compounds (VOC) from some Amazonian and Mediterranean plants. *Biogeosciences*, 10, 5855–5873.
- Brilli, F., Hörtnagl, L., Bamberger, I., Schnitzhofer, R., Ruuskanen, T.M., Hansel, A., Loreto, F. and Wohlfahrt, G., 2012. Qualitative and quantitative characterization of volatile organic compound emissions from cut grass. *Environ. Sci. Technol.*, 46, 3859–3865.
- Bruns, E.A., El Haddad, I., Keller, A., Klein, F., Kumar, N.K., Pieber, S.M., Corbin, J.C., Slowik, J.G., Brune, W.H, Baltensperger, U., et al., 2015. Inter-comparison of laboratory smog chamber and flow reactor systems on organic aerosol yield and composition. *Atmos. Meas. Tech.*, 8, 2315–2332.
- Calfapietra, C., Fares, S., Manes, F., Morani, A., Sgrigna, G. and Loreto, F., 2013. Role of biogenic volatile organic compounds (BVOC) emitted by urban trees on ozone concentration in cities: A review. *Environ. Pollut.*, 183, 71–80.
- Calvete-Sogo, H., Elvira, S., Sanz, J., Gonzalez-Fernandez, I., Garcia-Gomez, H., Sanchez-Martin, L., Alonso, R. and Bermejo-Bermejo, V., 2014. Current ozone levels threaten gross primary production and yield of Mediterranean annual pastures and nitrogen modulates the response. *Atmos. Environ.*, 95, 197–206.
- Capitani, D., Brilli, F., Mannina, L., Proietti, N. and Loreto F., 2009. In situ investigation of leaf water status by portable unilateral nuclear magnetic resonance. *Plant Physiol.*, 149, 1638–1647.
- Chmielewski, F.-M., Heider, S. and Moryson, S., 2013. International phenological observation networks: concept of IPG and GPM. In: Schwartz, M.D. (ed.), *Phenology: An Integrative Environmental Science*, 4th ed., Springer Science+Business Media B.V, 137–153.
- Claeys, M., Wang, W., Ion, A.C., Kourtchev, I., Gelencsér, A. and Maenhaut, W., 2004. Formation of secondary organic aerosols from isoprene and its gas-phase oxidation products through reaction with hydrogen peroxide. *Atmos. Environ.*, 38, 4093–4098.
- Copeland, N., Cape, J.N. and Heal, M.R., 2012. Volatile organic compound emissions from *Miscanthus* and short rotation coppice willow bioenergy crops. *Atmos. Environ.*, 60, 327–335.

- Copolovici, L., Kännaste, A., Pazouki, L. and Niinemets, Ü., 2012. Emissions of green leaf volatiles and terpenoids from *Solanum lycopersicum* are quantitatively related to the severity of cold and heat shock treatments. *J. Plant Physiol.*, 169, 664–672.
- DeCarlo, P.F., Kimmel, J.R., Trimborn, A., Northway, M.J., Jayne, J.T., Aiken, A.C., Gonin, M., Fuhrer, K., Horvath, T., Docherty, K.S., et al., 2006. Field-deployable, high-resolution, time-of-flight aerosol mass spectrometer. *Anal. Chem.*, 78, 8281–8289.
- Dicke, M. and Vet, L.E.M., 1999. Plant-carnivore interactions: evolutionary and ecological consequences for plant, herbivore and carnivore. In: Olff, H., Brown, V.K. and Drent, R.H. (eds) *Herbivores: Between Plants and Predators*. Blackwell Science Oxford, UK, 483–520.
- Dicke, M., van Poecke, R.M.P. and de Boer, J.G., 2003a. Inducible indirect defence of plants: from mechanisms to ecological functions. *Basic Appl. Ecol.*, 4, 27–42.
- Dicke, M., de Boer J.G., Höfte, M. and Rocha-Granados, M.C., 2003b. Mixed blends of herbivore-induced plant volatiles and foraging success of carnivorous arthropods. *Oikos*, 101, 38–48.
- Dombrowski, J.E., Kronmiller, B.A., Hollenbeck, V.G., et al., 2019. Transcriptome analysis of the model grass *Lolium temulentum* exposed to green leaf volatiles. *BMC Plant Biol.*, 19, 1–17.
- Emberson, L., Pleijel, H., Ainsworth, E.A., Berg, M.V.D., Ren, W., Osborne, S., Mills, G., Pandey, D., Dentener, F., Büker, P., et al., 2018. Ozone effects on crops and consideration in crop models. *Eur. J. Agron.*, 100, 19–34.
- Ehn, M., Thornton, J.A., Kleist, E., Sipilä, M., Junninen, H., Pullinen, I., Springer, M., Rubach, F., Tillmann, R., Lee, B., Lopez-Hilfiker, F., Andres, S., Acir, I.-H., Rissanen, M., Jokinen, T., Schobesberger, S., Kangasluoma, J., Kontkanen, J., Nieminen, T., Kurtén, T., Nielsen, L.B., Jørgensen, S., Kjaergaard, H.G., Canagaratna, M., Maso, M.D., Berndt, T., Petäjä, T., Wahner, A., Kerminen, V.-M., Kulmala, M., Worsnop, D.R., Wildt, J. and Mentel, T.F., 2014. A large source of low-volatility secondary organic aerosol. *Nature*, 506, 476–479.
- European Commission, 2014. A policy framework for climate and energy in the period from 2020 up to 2030. Brussels, European commission
- Evans, R.C., Tingey, D.T. and Gumpertz, M.L., 1985. Interspecies variation in terpenoid emission rates from Engelmann and Sitka Spruce seedlings. *Forest Sci.*, 13, 132–142.
- Fan, J., Wang, Y., Rosenfeld, D. and Liu, X., 2016. Review of aerosol-cloud interactions: Mechanisms, significance, and challenges. *J. Atmos. Sci.*, 73, 4221–4252.
- Fann, N., Nolte, C.G., Dolwick, P., Spero, T.L., Curry Brown, A., Phillips S. and Anenberg, S., 2015. The geographic distribution and economic value of climate change-related ozone health impacts in the United States in 2030. *J. Air Waste Manag. Assoc.*, 65, 570–580.
- Fehsenfeld, F., Calvert, J., Fall, R., Goldan, P., Guenther, A. B., Hewitt, C. N., et al., 1992. Emissions of volatile organic compounds from vegetation and the implications for atmospheric chemistry. *Global Biogeochem. Cycles*, 6, 389–430.
- Folberth, G. A., Hauglustaine, D. A., Lathièrre, J. and Brocheton, F., 2005. Impact of biogenic hydrocarbons on tropospheric chemistry: results from a global chemistry-climate model. *Atmos. Chem. Phys. Discuss.*, 5, 10517–10612.

- Folberth, G. A., Hauglustaine, D. A., Lathière, J. and Brocheton, F., 2006. Interactive chemistry in the Laboratoire de Météorologie Dynamique general circulation model: model description and impact analysis of biogenic hydrocarbons on tropospheric chemistry. *Atmos. Chem. Phys.*, 6, 2273–2319.
- Fredga, K., Danell, K., Frank, H., Hedberg, D. and Kullander, S., 2008. Bioenergy – Opportunities and constraints. Energy Committee Report, June 2008, Kungliga Vetenskapsakademin.
- Fumagalli, I., Gimeno, B.S., Velissariou, D., De Temmerman, L. and Mills, G., 2001. Evidence of ozone-induced adverse effects on crops in the Mediterranean region. *Atmos. Environ.*, 35, 2583–2587.
- Grelle, A., Aronsson, P., Weslien, P., Klemetsson, L. and Lindroth, A., 2007. Large carbon-sink potential by Kyoto forests in Sweden – a case study on willow plantations. *Tellus B Chem. Phys. Meteorol.*, 59, 910–918.
- Guenther, A.B., 1997. Seasonal and spatial variations in natural volatile organic compound emissions. *Ecol. Appl.*, 7, 34–45.
- Guenther, A.B., Monson, R.K. and Fall, R., 1991. Isoprene and monoterpene emission rate variability: Observations with eucalyptus and emission rate algorithm development. *J. Geophys. Res.*, 96, 10799–10808.
- Guenther, A.B., Zimmerman, P., Harley, P.C., Monson, R.K. and Fall, R., 1993. Isoprene and monoterpene emission rate variability: Model evaluations and sensitivity analyses. *J. Geophys. Res.*, 98, 12609–12617.
- Guenther, A., Hewitt, C.N., Erickson, D., Fall, R., Geron, C., Graedel, T., Harley, P., Klinger, L., Lerdau, M., McKay, W.A., Pierce, T., Scholes, B., Steinbrecher, R., Tallamraju, R., Taylor, J. and Zimmerman, P., 1995. A global model of natural volatile organic compound emissions. *J. Geophys. Res.*, 100, 8873–8892.
- Guenther, A., 2002. The contribution of reactive carbon emissions from vegetation to the carbon balance of terrestrial ecosystems. *Chemosphere*, 49, 837–844.
- Guenther, A. B., Karl, T., Harley, P., Wiedinmyer, C., Palmer, P. I. and Geron, C., 2006. Estimates of global terrestrial isoprene emissions using MEGAN (Model of Emissions of Gases and Aerosols from Nature). *Atmos. Chem. Phys.*, 6, 3181–3210.
- Guenther, A. B., Jiang, X., Heald, C. L., Sakulyanontvittaya, T., Duhl, T., Emmons, L. K. and Wang, X., 2012. The Model of Emissions of Gases and Aerosols from Nature version 2.1 (MEGAN2.1): an extended and updated framework for modeling biogenic emissions. *Geosci. Model Dev.*, 5, 1471–1492.
- Gupta, S., Tirpak, D.A., Burger, N., Gupta, J., Höhne, N., Boncheva, A.I., Kanoan, G.M., Kolstad, C., Kruger, J.A., Michaelowa, A., Murase, S., Pershing, J., Saijo, T. and Sari, A. 2007: Policies, Instruments and Co-operative Arrangements. In *Climate Change 2007: Mitigation. Contribution of Working Group III to the Fourth Assessment Report of the Intergovernmental Panel on Climate Change* [B. Metz, O.R. Davidson, P.R. Bosch, R. Dave, L.A. Meyer (eds)], Cambridge University Press, Cambridge, United Kingdom and New York, NY, USA.
- Haagen-Smit, A.J., 1952. Chemistry and physiology of Los-Angeles smog. *Ind. Eng. Chem. Res.*, 44, 1342–1346.

- Hakola, H., Rinne, J. and Laurila, T., 1998. The hydrocarbon emission rates of tea-leaved willow (*Salix phylicifolia*), silver birch (*Betula pendula*) and European aspen (*Populus tremula*). *Atmos. Environ.*, 32, 1825–1833.
- Hakola, H., Rinne, J. and Laurila, T., 1999. The VOC Emission Rates of Boreal Deciduous Trees. European Commission: Biogenic VOC emissions and photochemistry in the boreal regions of Europe - Biphorep, 3, 21–28.
- Hansel, A., Jordan, A., Holzinger, R., Prazeller, P., Vogel, W. and Lindinger, W., 1995. Proton transfer reaction mass spectrometry: on-line trace gas analysis at the ppb level. *Int. J. Mass Spectrom. Ion Processes*, 149/150, 605–619.
- Hatanaka, A., 1993. The biogeneration of green odour by green leaves. *Phytochemistry*, 34, 1201–1218.
- Helmig, D., Ortega, J., Duhl, T., Tanner, D., Guenther, A., Harley, P., Wiedinmyer, C., Milford, J. and Sakulyanontvittaya, T., 2007. Sesquiterpene Emissions from Pine Trees – Identifications, Emission Rates and Flux Estimates for the Contiguous United States. *Environ. Sci. Technol.*, 41, 1545–1553.
- Hildebrand, D. F., 1989. Lipoxygenases. *Physiol. Plant.*, 76, 249–253.
- Hillier, J., Whittaker, C., Dailey, A.G., Aylott, M., Casella, E., Richter, G.M., Riche, A., Murphy, R., Taylor, G. and Smith, P., 2009. Greenhouse gas emissions from four bio-energy crops in England and Wales: integrating spatial estimates of yield and soil C balance in life cycle analyses. *GCB Bioenergy*, 1, 267–281.
- Hoffmann, T., Odum, J. R., Bowman, F., Collins, D., Klockow, D., Flagan, R. C. and Seinfeld, J. H., 1997. Formation of organic aerosols from the oxidation of biogenic hydrocarbons. *J. Atmos. Chem.*, 26, 189–222.
- Hollsten, R., Arkelöv, O. and Ingelman, G., 2013. Handbok för Salixodlare (in Swedish), Jordbruksverket, 2:a utgåvan
- Holzinger, R., 2015. PTRwid: A new widget tool for processing PTR-TOF-MS data. *Atmos. Meas. Tech.*, 8, 3903–3922.
- Holzinger, R., Lee, A., Paw U, K.T. and Goldstein, A. H., 2005. Observations of oxidation products above a forest imply biogenic emissions of very reactive compounds. *Atmos. Chem. Phys.*, 5, 67–75.
- Hough, A. M. and Johnson, C. E., 1991. Modelling the role of nitrogen oxides, hydrocarbons and carbon monoxide in the global formation of tropospheric oxidants. *Atmos. Environ.*, 25A, 1819–1835.
- Humphrey, A.J. and Beale, M.H., 2006. Terpenes. In: Crozier A., Clifford M.N. and Ashihara, H. (eds). *Plant secondary metabolites, occurrence, structure and role in the human diet*. Blackwell Publishing Ltd, Oxford, 47–101.
- IPCC, 2014: *Climate Change 2014: Synthesis Report*. Contribution of Working Groups I, II and III to the Fifth Assessment Report of the Intergovernmental Panel on Climate Change [Core Writing Team, R.K. Pachauri and L.A. Meyer (eds.)]. IPCC, Geneva, Switzerland, 151 pp.

- IPCC, 2018: Summary for Policymakers. In: Global warming of 1.5°C. An IPCC Special Report on the impacts of global warming of 1.5°C above pre-industrial levels and related global greenhouse gas emission pathways, in the context of strengthening the global response to the threat of climate change, sustainable development, and efforts to eradicate poverty [V. Masson-Delmotte, P. Zhai, H. O. Pörtner, D. Roberts, J. Skea, P. R. Shukla, A. Pirani, W. Moufouma-Okia, C. Péan, R. Pidcock, S. Connors, J. B. R. Matthews, Y. Chen, X. Zhou, M. I. Gomis, E. Lonnoy, T. Maycock, M. Tignor, T. Waterfield (eds.)]. World Meteorological Organization, Geneva, Switzerland, 32 pp.
- IPCC, 2021: Summary for Policymakers. In: *Climate Change 2021: The Physical Science Basis. Contribution of Working Group I to the Sixth Assessment Report of the Intergovernmental Panel on Climate Change* [Masson-Delmotte, V., P. Zhai, A. Pirani, S. L. Connors, C. Péan, S. Berger, N. Caud, Y. Chen, L. Goldfarb, M. I. Gomis, M. Huang, K. Leitzell, E. Lonnoy, J.B.R. Matthews, T. K. Maycock, T. Waterfield, O. Yelekçi, R. Yu and B. Zhou (eds.)]. Cambridge University Press. In Press.
- Isebrands, J., Guenther, A., Harley, P., et al., 1999. Volatile organic compound emission rates from mixed deciduous and coniferous forests in Northern Wisconsin, USA. *Atmos. Environ.*, 33, 2527–2536.
- Isebrands, J.G. and Richardson, J., 2014. Introduction. In: Isebrands, J.G., Richardson, J. (eds.), *Poplars and Willow – Trees for Society and the Environment*. The Food and Agriculture Organization of United States (FAO) and CABI, ISBN (FAO): 978 92 5 107185 4, ISBN (CABI): 978 1 78064 108 9, 1–7.
- Jiang, Y., Ye, J., Linda-Liisa Veromann, L.-L. and Niinemets, Ü., 2016. Scaling of photosynthesis and constitutive and induced volatile emissions with severity of leaf infection by rust fungus (*Melampsora larici-populina*) in *Populus balsamifera* var. *suaveolens*. *Tree Physiol.*, 36, 856–872.
- Joó, É., Dewulf, J., Amelynck, C., Schoon, N., Pokorska, O., Šimpraga, M., Steppe, K., Aubinet, M. and Van Langenhove, H., 2011. Constitutive versus heat and biotic stress induced BVOC emissions in *Pseudotsuga menziesii*. *Atmos. Environ.*, 45, 3655–3662.
- Kanakidou, M., Seinfeld, J. H., Pandis, S. N., Barnes, I., Dentener, F. J., Facchini, M. C., Van Dingenen, R., Ervens, B., Nenes, A., Nielsen, C. J., Swietlicki, E., Putaud, J. P., Balkanski, Y., Fuzzi, S., Horth, J., Moortgat, G. K., Winterhalter, R., Myhre, C. E. L., Tsigaridis, K., Vignati, E., Stephanou, E. G. and Wilson, J., 2005. Organic aerosol and global climate modelling: a review. *Atmos. Chem. Phys.*, 5, 1053–1123
- Kaplan, J. O., Folberth, G. and Hauglustaine, D. A., 2006. Role of methane and biogenic volatile organic compound sources in late glacial and Holocene fluctuations of atmospheric methane concentrations. *Glob. Biogeochem. Cycles*, 20, 1–16.
- Karl, M., Guenther, A., Köble, R., Leip, A. and Seufert, G., 2009. A new European plant specific emission inventory of biogenic volatile organic compounds for use in atmospheric transport models. *Biogeosciences*, 6, 1059–1087.
- Karlsson, T., Rinnan, R. and Holst, T., 2020. Variability of BVOC Emissions from Commercially Used Willow (*Salix* spp.) Varieties. *Atmosphere-Basel*, 11, 346.

- Karp, A., Haughton, A.J., Bohan, D.A., et al., 2009. Perennial energy crops: implications and potential. In: Winter, M., Lobley, M. (eds.), *What is Land For? The Food, Fuel and Climate Change Debate*. London, UK: Earthscan. 3–71.
- Kesselmeier, Ciccioli, P., J., Kuhn, U., et al., 2002. Volatile organic compound emissions in relation to plant carbon fixation and the terrestrial carbon budget. *Global Biogeochem. Cycles*, 16, 73-1–73-9.
- Kesselmeier, J., Schäfer, L., Ciccioli, P., Brancaleoni, E., Cecinato, A., Frattoni, M., Foster, P., Jacob, V., Denis, J., Fugit, J.-L., Dutaur, L., and Torres, L., 1996. Emission of monoterpenes and isoprene from a Mediterranean oak species *Quercus ilex* L. measured within the BEMA (Biogenic Emissions in the Mediterranean Area) project. *Atmos. Environ.*, 30, 1841–1850.
- Kesselmeier, J. and Staudt, M., 1999. Biogenic volatile organic compounds (VOC): An overview on emission, physiology and ecology. *J. Atmos. Chem.*, 33, 23–88.
- Kim, J.C., Kim, K.J., Kim, D.S. and Han, J.S., 2005. Seasonal variations of monoterpene emissions from coniferous trees of different ages in Korea. *Chemosphere*, 59, 1685–1696.
- Kimming, M., Sundberg, C., Nordberg, Å., Baky, A., Bernesson, S., Norén, O. and Hansson, P.A., 2011. Biomass from agriculture in small-scale combined heat and power plants - a comparative life cycle assessment. *Biomass Bioenergy*, 35, 1572–1581.
- Kleinman, L., Daum, P.H., Imre, D., Lee, Y.-N., Nunnermacker, L.J., Springston, S., Weinstein-Lloyd, J. and Rudolph, J., 2002. Ozone production rate and hydrocarbon reactivity in 5 urban areas: A cause of high ozone concentration in Houston. *Geophys. Res. Lett.*, 29, 105-1–105-4.
- Kuehn, B.M., 2014. WHO: More Than 7 Million Air Pollution Deaths Each Year. *JAMA.*, 311, 1486.
- Kulmala, M., Suni, T., Lehtinen, K.E.J., Maso, M.D., Boy, M., Reissell, A., Rannik, Ü., Aalto, P., Keronen, P., Hakola, H., et al., 2004. A new feedback mechanism linking forests, aerosols, and climate. *Atmos. Chem. Phys. Discuss.*, 4, 557–562.
- Kuzma, J. and Fall, R., 1993. Leaf isoprene emission rate is dependent on leaf development and the level of isoprene synthase. *Plant Physiol.*, 101, 435–440.
- Kägi, T., Deimling, S., Knuchel, R. F., Gaillard, G., Hölscher, T. and Müller-Sämman, K., 2008. Environmental impacts of annual and perennial energy crops compared to a reference food crop rotation. Empowerment of the rural actors: a renewal of farming systems perspectives: 8th European IFSA Symposium, Clermont-Ferrand, France, 6–10 July 2008, 675–681.
- König, G., Brunda, M., Puxbaum, H., Hewitt, C. N., Duckham, S. C. and Rudolph, J., 1995. Relative contribution of oxygenated hydrocarbons to the total biogenic VOC emissions of selected mid-European agricultural and natural plant species. *Atmos. Environ.*, 29, 861–874.
- Landberg, T. and Greger, M., 1996. Differences in uptake and tolerance to heavy metals in *Salix* from unpolluted and polluted areas. *Appl. Geochem.*, 11, 175–180.
- Landrigan, P.J., Fuller, R., Acosta, N.J.R., Adeyi, O., Arnold, R., Basu, N., B., et al., 2017. *The Lancet Commission on pollution and health*. 1–51.

- Lange, B.M., Rujan, T., Martin, W. and Croteau, R., 2000. Isoprenoid biosynthesis: the evolution of two ancient and distinct pathways across genomes. *Proc. Natl. Acad. Sci. USA*, 97, 13172–13177.
- Laothawornkitkul, J., Taylor, J.E., Paul, N. and Hewitt, C.N., 2009. Biogenic volatile organic compounds in the Earthsystem. *New Phytol.*, 183, 27–51.
- Lichtenthaler, H.K., 1999. The 1-deoxy-D-xylulose-5-phosphate pathway of isoprenoid biosynthesis in plants. *Annu. Rev. Plant Physiol.*, 50, 47–65.
- Lim, J.H., Kim, J.C., Kim, K.J., Son, Y.S., Sunwoo, Y. and Han, J.S., 2008. Seasonal variations of monoterpene emissions from *Pinus densiflora* in East Asia. *Chemosphere*, 73, 470–478.
- Lindinger, W., Hansel, A. and Jordan, A., 1998. On-line monitoring of volatile organic compounds at pptv levels by means of Proton-Transfer-Reaction Mass Spectrometry (PTR-MS) Medical applications, food control and environmental research. *Int. J. Mass Spectrom. Ion Process*, 173, 191–241.
- Lindgaard, K.N., Adams, P.W., Holley, M., Lamley, A., Henriksson, A., Larsson, S., von Engelbrechten, H.G., Esteban Lopez, G. and Pisarek, M., 2016. Short rotation plantations policy history in Europe: lessons from the past and recommendations for the future. *Food and energy security*, 5, 125–152.
- Loreto, F., Pinelli, P., Brancaleoni, E. and Ciccioli, P., 2004. ¹³C labelling reveals chloroplastic and extrachloroplastic pools of dimethylallyl pyrophosphate and their contribution to isoprene formation. *Plant Physiol.*, 135, 1903–1907.
- Loreto, F., et al., 2006. On the induction of volatile organic compound emissions by plants as consequence of wounding or fluctuations of light and temperature. *Plant Cell Environ.*, 29, 1820–1828.
- Loreto, F. and Schnitzler J-P., 2010. Abiotic stresses and induced BVOCs. *Trends Plant Sci.*, 15, 154–166.
- Lovelock, J.E., 1977. PAN in the natural environment, its possible significance in the epidemiology of skin cancer. *Ambio*, 6, 131–133.
- Llusià, J. and Peñuelas, J., 1998. Changes in terpene content and emission in potted Mediterranean Woody plants under severe drought. *Can. J. Bot.*, 76, 1366–1373.
- Llusià, J. and Peñuelas, J., 2001. Emission of volatile organic compounds by apple trees in response to spider mite attack and attraction of predatory mites. *Experimental and Applied Acarology*, 25, 65–77.
- van Meeningen, Y., et al., 2017. Isoprenoid emission variation of Norway spruce across a European latitudinal transect. *Atmos. Environ.*, 170, 45–57.
- McCracken, A.R. and Johnston, C.R., 2015. Potential for wastewater management using energy crops. *Sci. Papers, Ser. Manag. Econom. Eng. Agric. Rural Dev.*, 15, 275–284.
- Meers, E., Vandecasteele, B., Ruttens, A., Vangronsveld, J. and Tack, F.M.G., 2007. Potential of five willow species (*Salix* spp.) for phytoextraction of heavy metals. *Environ. Exp. Bot.*, 60, 57–68.
- Merk, L., Kloos, M., Schönwitz, R. and Ziegler, H., 1988. Influence of various factors on quantitative composition of leaf monoterpenes of *Picea abies* (L.) Karst. *Trees*, 2, 45–51.

- Misztal, P.K., Hewitt, C.N., Wildt, J., Blande, J.D., Eller, A., Fares, S., Gentner, D., Gilman, J., Graus, M., Greenberg, J., et al., 2015. Atmospheric benzenoid emissions from plants rival those from fossil fuels. *Sci. Rep.*, 5, 12064.
- Mleczek, M., Rutkowski, P., Rissmann, I., Kaczmarek, Z., Golinski, P., Szentner, K., Strażyńska, K. and Stachowiak, A., 2010. Biomass productivity and phytoremediation potential of *Salix alba* and *Salix viminalis*. *Biomass Bioenergy*, 34, 1410–1418.
- Monks, P. S., Granier, C., Fuzzi, S., Stohl, A., Williams, M. L., et al., 2010. Atmospheric composition change - global and regional air quality. *Atmos. Environ.*, 43, 5268–5350.
- Monson, R.K. and Fall, R., 1989. Isoprene emission from aspen leaves. *Plant Physiol.*, 90, 267–274.
- Monson, R.K., Harley, P.C., Litvak, M.E., Wildermuth, M., Guenther, A.B., Zimmerman, P.R. and Fall, R., 1994. Environmental and developmental controls over the seasonal pattern of isoprene emission from aspen leaves. *Oecologia*, 99, 260–270.
- Monson, R.K., Jaeger, C.H., Adams, W., Driggers, E., Silver, G. and Fall, R., 1992. Relationships among isoprene emission rate, photosynthesis rate, and isoprene synthase activity, as influenced by temperature. *Plant Physiol.*, 92, 1175–1180.
- Morrison, E. C., Drewer, J. and Heal, M.R., 2016. A comparison of isoprene and monoterpene emission rates from the perennial bioenergy crops short-rotation coppice willow and *Miscanthus* and the annual arable crops wheat and oilseed rape. *GCB. Bioenergy*, 8, 211–225.
- Mutzel, A., Rodigast, M., Iinuma, Y., Böge, O. and Herrmann, H. 2016. Monoterpene SOA – Contribution of first-generation oxidation products to formation and chemical composition, *Atmos. Environ.* 130, 136–144.
- Müller, J. F., 1992. Geographical distribution and seasonal variation of surface emissions and deposition velocities of atmospheric trace gases. *J. Geophys. Res.*, 97, 3787–3804.
- Müller, M., Graus, M., Ruuskanen, T. M., Schnitzhofer, R., Bamberger, I., Kaser, L., Titzmann, T., Hörtnagl, L., Wohlfahrt, G., Karl, T. and Hansel, A., 2010. First eddy covariance flux measurements by PTR-TOF. *Atmos. Meas. Tech.*, 3, 387–395.
- Niinemets, Ü., Loreto F. and Reichstein, M., 2004. Physiological and physico-chemical controls on foliar volatile organic compound emissions. *Trends Plant Sci.*, 9, 180–186.
- Niinemets, Ü., Copolovici, L. and Hüve, K., 2010. High within-canopy variation in isoprene emission potentials in temperate trees: implications for predicting canopy-scale isoprene fluxes. *J. Geophys. Res.-Biogeo.*, 115, G04029
- Niinemets, Ü. and Monson, R. K., 2013. Carbon Utilization and Dry Matter Production. In: *Biology, Controls and Models of Tree Volatile Organic Compound Emissions*, volume 5, *Tree Physiol.*, Springer Dordrecht Heidelberg New York London, ISBN 978-94-007-6605-121–46.
- Nuñez, T. and Pio, C., 2001. Emission of volatile organic compounds from Portuguese eucalyptus forests. *Chemosphere – Global Change Science*, 3, 239–248.

- O'Dowd, C. D., Jimenez, J. L., Bahreini, R., Flagan, R. C., Seinfeld, J. H., Hämeri, K., Pirjola, L., Kulmala, M., Jennings, S. G. and Hoffmann, T., 2002. Marine aerosol formation from biogenic iodine emissions. *Nature*, 417, 497–501.
- Olofsson, M., Ek-Olausson, B., Ljungström, E. and Langer, S., 2003. Flux of organic compounds from grass measured by relaxed eddy accumulation technique. *J. Environ. Monitor.*, 5, 963–970.
- Olofsson, M., Ek-Olausson, B., Jensen, N.O., Langer, S. and Ljungström, E., 2005. The flux of isoprene from a willow plantation and the effect on local air quality. *Atmos. Environ.*, 39, 2061–2070.
- Ortega, J. and Helmig, D., 2008. Approaches for quantifying reactive and low-volatility biogenic organic compound emissions by vegetation enclosure techniques – Part A. *Chemosphere*, 72, 343–364.
- Owen, S. M. and Hewitt, C. N., 2000. Extrapolating branch enclosure measurements to estimates of regional scale biogenic VOC fluxes in the north-western Mediterranean basin. *J. Geophys. Res.*, 105, 11573–11583.
- Paasonen, P., Asmi, A., Petäjä, T., Kajos, M.K., Äijälä, M., Junninen, H., Holst, T., Abbatt, J.P.D., Arneth, A., Birmili, W., van der Gon, H.D., Hamed, A., Hoffer, A., Laakso, L., Laaksonen, A., Leaitch, W.R., Plass-Dülmer, C., Pryor, S.C., Räisänen, P., Swietlicki, E., Wiedensohler, A., Worsnop, D.R., Kerminen, V.-M. and Kulmala, M., 2013. Warming-induced increase in aerosol number concentration likely to moderate climate change. *Nat. Geosci.*, 6, 438–442.
- Paiva, N.L., 2000. An introduction to the biosynthesis of chemicals used in plant-microbe communication. *J. Plant Growth Regul.*, 19, 131–143.
- Palm, B.B., Sá, S.S.D., Day, D.A., Campuzano-Jost, P., Hu, W., Seco, R., Sjostedt, S.J., Park, J.H., Guenther, A.B., Kim, S., et al., 2018. Secondary organic aerosol formation from ambient air in an oxidation flow reactor in central Amazonia. *Atmos. Chem. Phys. Discuss.*, 18, 467–493.
- Palo, T., 1984. Distribution of birch (*Betula* SPP.), willow (*Salix* SPP.), and poplar (*Populus* SPP.) secondary metabolites and their potential role as chemical defense against herbivores. *J. Chem. Ecol.*, 10, 499–520.
- Pandis, S.N., Harley, R.A., Cass, G.R. and Seinfeld, J.H., 1992. Secondary organic aerosol formation and transport. *Atmos. Environ.*, 26A, 2269–2282.
- Pandis, S.N., Paulson, S.E., Seinfeld, J.H., and Flagan, R.C., 1991. Aerosol formation in the photooxidation of isoprene and β -pinene. *Atmos. Environ.*, 25A, 997–1008.
- Paulson, S.E., Pandis, S.N., Baltensperger, U., Seinfeld, J.H., Flagan, R.C., Palen, E.J., Allen, D.T., Schaffner, C., Giger, W. and Protmann, A., 1990. Characterization of photochemical aerosols from biogenic hydrocarbons. *J. Aerosol Sci.*, 21, 245–248.
- Paulson, S. E., and Orlando, J. J., 1996. The reactions of ozone with alkenes: An important source of HO_x in the boundary layer. *Geophys. Res. Lett.*, 23, 3727–3730.
- Peñuelas, J. and Filella, I., 2001. Phenology: responses to a warming world. *Science*, 294, 793–795.
- Peñuelas, J. and Llusià, J., 2003. BVOCs: plant defence against climate warming?. *Trends Plant Sci.* 8, 105–109.
- Peñuelas, J., et al., 2009. Phenology feedbacks on climate change. *Science*, 324, 887–888.

- Peñuelas, J. and Staudt, M., 2010. BVOCs and global change. *Trends Plant Sci.*, 15, 133–144.
- Pétron, G., Harley, P., Greenberg, J. and Guenther, A., 2001. Seasonal temperature variations influence isoprene emission. *Geophys. Res. Lett.*, 28, 1707–1710.
- Pike, R. C. and Young, P. J., 2009. How plants can influence tropospheric chemistry: the role of isoprene emissions from the biosphere. *Weather*, 64, 12, 332–336.
- Pio, C., Nunes T. and Brito, S., 1993. Volatile hydrocarbon emissions from common and native species of vegetation in Portugal. In: Slanina, J., Angeletti G., Beilke, S. (eds.), *General Assessment of Biogenic Emissions and Deposition of Nitrogen Compounds, Sulphur compounds and Oxidants in Europe*, CEC Air Pollution Research Report 47, Brussels, Belgium, Guyot SA, 291–298.
- Pope, C. A., and Dockery, D. W., 2006. Health effects of fine particulate air pollution: Lines that connect. *J. Air Waste Manag. Assoc.*, 56, 709–742.
- Possell, M. and Loreto, F., 2013. The role of volatile organic compounds in plant resistance to abiotic stresses: responses and mechanisms. In: Niinemets Ü. and Monson R.K. (eds), *Biology, Controls and Models of Tree Volatile Organic Compound Emissions, Tree physiology 5*, Springer, Dordrecht Heidelberg New York London, 209–235.
- Ragauskas, A.J., Williams, C.K., Davison B.H., Britovsek, G., Cairney, J., Eckert, C.A, Frederick, W.J., Hallett, J.P., Leak, D.J., Liotta, C.L., Mielenz, J.R., Murphy, R., Templer, R. and Tschaplinski, T., 2006. The path forward for biofuels and biomaterials. *Science*, 311, 484–489.
- Rinne J., Tuovinen, J.P., Laurila, T., Hakola, H., Aurela, M. and Hypén, H., 2000. Measurements of isoprene and monoterpene fluxes by a gradient method above a northern boreal forest. *Agric. For. Meteorol.*, 102, 25–37.
- Rinne, J., Bäck, J. and Hakola, H., 2009. Biogenic volatile organic compound emissions from the Eurasian taiga: current knowledge and future directions. *Boreal Environ. Res.*, 14, 807–826.
- Rohmer, M., 1999. The discovery of a mevalonate-independent pathway for isoprenoid biosynthesis in bacteria, algae and higher plants. *Nat. Prod. Rep.*, 16, 565–574.
- Roselle, S. J., Pierce, T. E. and Schere, K. L., 1991. The sensitivity of regional ozone modeling to biogenic hydrocarbons. *J. Geophys. Res.*, 96, 7371–7394.
- Rosenfeld, D., Sherwood, S., Wood, R. and Donner, L., 2014. Climate effects of aerosol-cloud interactions. *Science*, 343, 379–380.
- Ruuskanen, T. M., Müller, M., Schnitzhofer, R., Karl, T., Graus, M., Bamberger, et al., 2011. Eddy covariance VOC emission and deposition fluxes above grassland using PTR-TOF. *Atmos. Chem. Phys.*, 11, 611–625.
- Ryerson, T.B., Trainer, M., Holloway, J.S., Parrish, D.D., Huey, L.G., Sueper, D.T., Frost, G.J., Donnelly, S.G., Schauffler, S., Atlas, E., et al., 2001. Observations of Ozone Formation in Power Plant Plumes and Implications for Ozone Control Strategies. *Science*, 292, 719–723.
- Sakaki T., 1998. Photochemical oxidants: toxicity. In: De Kok LJ, Stulen I, eds. *Responses of plant metabolism to air pollution and global change*. Leiden, The Netherlands: Backhuys Publishers, 117–129.

- Sanadze, G.A., 1956. Emission of gaseous organic substance from plants. *Repertuar Akademiia Nauk Gruzinskoi SSR*, 17, 429–433.
- Schnitzler, J-P., Graus, M., Kreuzwieser, J., Heizmann, U., Rennenberg, H., Wisthaler, A. and Hansel, A. 2004. Contribution of different carbon sources to isoprene biosynthesis in poplar leaves. *Plant Physiol.*, 135, 152–160.
- Seinfeld, J.H., Bretherton, C., Carslaw, K.S., et al., 2016. Improving our fundamental understanding of the role of aerosol-cloud interactions in the climate system. *Proc. Natl. Acad. Sci. USA*, 113, 5781–5790.
- Sharkey, T.D., Loreto, F. and Delwiche, C.F., 1991. High carbon dioxide and sun/shade effects on isoprene emission from oak and aspen tree leaves. *Plant Cell Environ.*, 14, 333–338.
- Sharkey, T. D. and F. Loreto., 1993. Water stress, temperature, and light effects on the capacity for isoprene emission and photosynthesis of kudzu leaves. *Oecologia*, 95, 328–333.
- Sharkey, T.D., Singsaas, E.L., Vanderveer, P.J. and Geron, C.D., 1996. Field measurements of isoprene emission from trees in response to temperature and light. *Tree Physiol.* 16, 649–654.
- Sitch S., Cox P.M., Collins W.J. and Huntingford C., 2007. Indirect radiative forcing of climate change through ozone effects on the land-carbon sink. *Nature*, 448, 791–794.
- Skogsdata, 2020. Skogsdata 2020 – Aktuella uppgifter om de svenska skogarna från SLU Riksskogstaxering, Tema: Den döda veden (in Swedish). Institutionen för skoglig underhållning, SLU Umeå, ISSN 0280-0543.
- SOU 2007:36. Bioenergi från Jordbruket–en Växande Resurs; Statens Offentliga Utredningar; Edita Sverige AB, Stockholm, Sweden, 2007. ISBN 978-91-38-22751-0
- Spracklen, D.V., Bonn, B. and Carslaw, K.S., 2008. Boreal forests, aerosols and the impacts on clouds and climate. *Phil. Trans. R. Soc. A.*, 366, 4613–4626.
- Staudt, M., Mir, C., Joffre, R., Rambal, S., Bonin, A., Landais, D. and Lumaret, R., 2004. Isoprenoid emissions of *Quercus* spp. (*Q. suber* and *Q. ilex*) in mixed stands contrasting in interspecific genetic introgression. *New Phytol.*, 163, 573–584.
- Staudt, M., et al., 2008. Do volatile organic compound emissions of Tunisian cork oak populations originating from contrasting climatic conditions differ in their responses to summer drought?. *Can. J. For. Res.* 38, 2965–2975.
- Steinbrecher, R., Schfirmann, W., Schreiner, A. M. and Ziegler, H., 1993. Terpenoid emissions from common oak (*Quercus robur* L.) and Norway spruce (*Picea abies* L. Karst.). In *General Assessment of Biogenic Emissions and Deposition of Nitrogen Compounds, Sulphur Compounds and Oxidants in Europe*, CEC Air Pollution Research Report 47 (edited by Slanina J., Angeletti G. and Beilke S.), ISBN 2-87263-095-3, E. Guyot SA, Brussels, 251–259.
- Stettler, R.F., 2009. The farers tree. In: Stettler, R.F., *Cottonwood and the River of Time: On Trees, Evolution and Society*. University of Washington Press, Seattle, Washington; London, 161–172.

- Stocker, T.F., D. Qin, G.-K. Plattner, L.V. Alexander, S.K. Allen, N.L. Bindoff, F.-M. Bréon, J.A. Church, U. Cubasch, S. Emori, P. Forster, P. Friedlingstein, N. Gillett, J.M. Gregory, D.L. Hartmann, E. Jansen, B. Kirtman, R. Knutti, K. Krishna Kumar, P. Lemke, J. Marotzke, V. Masson-Delmotte, G.A. Meehl, I.I. Mokhov, S. Piao, V. Ramaswamy, D. Randall, M. Rhein, M. Rojas, C. Sabine, D. Shindell, L.D. Talley, D.G. Vaughan and S.-P. Xie, 2013. Technical Summary. In: *Climate Change 2013: The Physical Science Basis. Contribution of Working Group I to the Fifth Assessment Report of the Intergovernmental Panel on Climate Change* [Stocker, T.F., D. Qin, G.-K. Plattner, M. Tignor, S.K. Allen, J. Boschung, A. Nauels, Y. Xia, V. Bex and P.M. Midgley (eds.)]. Cambridge University Press, Cambridge, United Kingdom and New York, NY, USA.
- Sun, J., Feng, Z. and Ort, D.R., 2014. Impacts of rising tropospheric ozone on photosynthesis and metabolite levels on field grown soybean. *Plant Sci.* 226, 147–161.
- Swedish EPA, 2019. Underlag till regeringens klimatpolitiska handlingsplan - Redovisning av Naturvårdsverkets regeringsuppdrag (in Swedish). Rapport 6879, ISBN 978-91-620-6879-0, ISSN 0282-7298.
- Tarvainen, V., Hakola, H., Hellén, H., Bäck, J., Hari, P. and Kulmala, M., 2005. Temperature and light dependence of the VOC emissions of Scots pine. *Atmos. Chem. Phys.* 5, 989–998.
- Tarvainen, V., Hakola, H., Rinne, J., Hellén, H. and Haapanala, S., 2007. Towards a comprehensive emission inventory of terpenoids from boreal ecosystems. *Tellus*, 59B, 526–534.
- Taylor, G., Tallis, M.J., Giardina, C.P., Percy, K.E., Miglietta, F., Gupta, P.S., Gioli, B., Calfapietra, C., Gielen, B., Kubiske, M.E., Scarascia-Mugnozza, G.E., Kets, K., Long, S.P. and Karnosky, D.F., 2008. Future atmospheric CO₂ leads to delayed autumnal senescence. *Global Change Biol.*, 14, 264–275.
- Temple, P. and Taylor, O., 1983. World-wide ambient measurements of peroxyacetyl nitrate (PAN) and implications for plant injury. *Atmos. Environ.*, 17, 1583–1587.
- Therasme, O., Volk, T.A., Eisenbies, M.H., et al., 2021. Life cycle greenhouse gas emissions of ethanol produced via fermentation of sugars derived from shrub willow (*Salix* spp.) hot water extraction in the Northeast United States. *Biotechnol. Biofuels*, 14, 52.
- Tingey, D.T., Manning, M., Grothaus, L.C. and Burns, W. F., 1980. Influence of light and temperature on monoterpene emissions from slash pine. *Plant Physiol.*, 65, 797–801.
- Toome, M., Randjärv, P., Copolovici, L., Niinemets, Ü., Heinsoo, K., Luik, A. and Noe, S.M., 2010. Leaf rust induced volatile organic compounds signalling in willow during the infection. *Planta*, 232, 235–243.
- Van Dingenen, R., et al., 2009. The global impact of ozone on agricultural crop yields under current and future air quality legislation. *Atmos. Environ.*, 43, 604–618.
- VanReken, T. M., Greenberg, J. P., Harley, P. C., Guenther, A. B. and Smith, J. N., 2006. Direct measurement of particle formation and growth from the oxidation of biogenic emissions. *Atmos. Chem. Phys.*, 6, 4403–4413
- Vickers, C.E., Gershenzon, J., Lerdau, M.T. and Loreto, F., 2009. A unified mechanism of action for volatile isoprenoids in plant abiotic stress. *Nat. Chem. Biol.*, 5, 283–291.

- Vyskocil, A., Viau, C. and Lamy, S., 1998. Peroxyacetyl nitrate: Review of toxicity. *Hum. Exp. Toxicol.*, 17, 212–220.
- Wagg, S., Mills, G., Hayes, F., Wilkinson, S., Cooper, D. and Davies, W.J., 2012. Reduced soil water availability did not protect two competing grassland species from the negative effects of increasing background ozone. *Environ. Pollut.*, 165, 91–99.
- Walling L.L., 2000. The myriad plant responses to herbivores. *J. Plant Growth Regul.*, 19, 195–216.
- Wang, K.-Y. and Shallcross, D.E., 2000. Modelling terrestrial biogenic isoprene fluxes and their potential impact on global chemical species using a coupled LSM–CTM model. *Atmos. Environ.*, 34, 2909–2925.
- Wang, M., 2018. Characteristics of BVOC emissions from a Swedish boreal forest: Using chambers to capture biogenic volatile organic compounds (BVOCs) from trees and forest floor. Thesis, Department of Physical Geography and Ecosystemscience, Lund University.
- Wang, M., Schurgers, G., Arneth, A., Ekberg, A. and Holst, T., 2017. Seasonal variation in biogenic volatile organic compound (BVOC) emissions from Norway spruce in a Swedish boreal forest. *Boreal Environ. Res.*, 22, 353–367.
- Watkins, E., Gianfagna, T.J., Sun, R. and Meyer, W.A., 2006. Volatile compounds of tufted hairgrass. *Crop Sci.*, 46, 2575–2580.
- Watson, L.A., Wang, K.-Y., Paul, H. and Shallcross, D.E., 2006. The potential impact of biogenic emissions of isoprene on urban chemistry in the United Kingdom. *Atmos. Sci. Lett.*, 7, 96–100.
- Went, F.W., 1960. Blue hazes in the atmosphere. *Nature*, 187, 641–643.
- Wiedensohler, A., Birmili, W., Nowak, A., Sonntag, A., Weinhold, K., Merkel, M., Wehner, B., Tuch, T., Pfeifer, S., Fiebig, M., et al., 2012. Mobility particle size spectrometers: Harmonization of technical standards and data structure to facilitate high quality long-term observations of atmospheric particle number size distributions. *Atmos. Meas. Tech.*, 5, 657–685.
- Wildt, J., Kobel, K., Schuh-Thomas, G., et al., 2003. Emissions of Oxygenated Volatile Organic Compounds from Plants Part II: Emissions of Saturated Aldehydes. *J. Atmos. Chem.*, 45, 173–196.
- Williams, J. and Koppmann, R., 2007. Introduction. In: Koppmann, R. (ed.), *Volatile Organic Compounds in the Atmosphere*, Blackwell Publishing Ltd, Oxford, UK, ISBN: 978-1-4051-3115-5, 1–32.
- Winer, A.M., Arey, J., Atkinson, R., Aschmann, S.M., Long, W.D., Morrison, C.L. and Olszyk, D.M., 1992. Emission rates of organics from vegetation in California's central valley. *Atmos. Environ.*, 26A, 2647–2659.
- Wittig, V.E., Ainsworth, E.A., Naidu, S.L., Karnoski, D.F. and Long, S.P., 2009. Quantifying the impact of current and future tropospheric ozone on tree biomass, growth, physiology and biochemistry: a quantitative meta-analysis. *Global Change Biol.*, 15, 396–424.
- Xie, X., Kirby, J. and Keasling, J.D., 2012. Functional characterization of four sesquiterpene synthases from *Ricinus communis* (castor bean). *Phytochemistry*, 78, 20–28.

- Yuan, J.S., Himanen, S.J., Holopainen, J.K., Chen, F. and Stewart Jr., C.N., 2009. Smelling global climate change: mitigation of function for plant volatile organic compounds. *Trends Ecol. Evol.*, 24, 323–331.
- Zenone, T., Zona, D., Gelfand, I., Gielen, B., Camino-Serrano, M. and Ceulemans, R., 2016. CO₂ uptake is offset by CH₄ and N₂O emissions in a poplar short-rotation coppice. *GCB Bioenergy*, 8, 524–538.
- Zhang, S.H., Shaw, M., Seinfeld, J.H. and Flagan, R.C., 1992. Photochemical aerosol formation from alpha-pinene and beta-pinene. *J. Geophys. Res.*, 97, 20717–20729.
- Åhman, I. and Larsson, S., 1999. Breeding for resistance in willow for energy production (in Swedish). *Växtnotiser*, 63, 17–19.

Web references

- Paris Agreement, 2015 <https://unfccc.int/process-and-meetings/the-paris-agreement/the-paris-agreement> (last accessed 2021-07-20)
- Lantmäteriet (<https://minkarta.lantmateriet.se/> (accessed 2021-03-30)).

Paper I



Article

Leaf-Scale Study of Biogenic Volatile Organic Compound Emissions from Willow (*Salix* spp.) Short Rotation Coppices Covering Two Growing Seasons

Tomas Karlsson ^{1,*}, Leif Klemedtsson ², Riikka Rinnan ³ and Thomas Holst ¹

¹ Department of Physical Geography and Ecosystem Science, Lund University, Sölvegatan 12, 223 62 Lund, Sweden; thomas.holst@nateko.lu.se

² Department of Earth Sciences, University of Gothenburg, Guldhedsgatan 5a, 405 30 Gothenburg, Sweden; leif.klemedtsson@gvc.gu.se

³ Terrestrial Ecology Section, Department of Biology, University of Copenhagen, Universitetsparken 15, DK-2100 Copenhagen Ø, Denmark; riikka@bio.ku.dk

* Correspondence: tomas.karlsson@nateko.lu.se

Citation: Karlsson, T.; Klemedtsson, L.; Rinnan, R.; Holst, T. Leaf-Scale Study of Biogenic Volatile Organic Compound Emissions from Willow (*Salix* spp.) Short Rotation Coppices Covering Two Growing Seasons. *Atmosphere* **2021**, *12*, x. <https://doi.org/10.3390/xxxxx>

Academic Editor: Anthony R. Lupo

Received: 14 September 2021

Accepted: 16 October 2021

Published:

Publisher's Note: MDPI stays neutral with regard to jurisdictional claims in published maps and institutional affiliations.



Copyright: © 2021 by the authors. Submitted for possible open access publication under the terms and conditions of the Creative Commons Attribution (CC BY) license (<https://creativecommons.org/licenses/by/4.0/>).

Abstract: In Europe, willow (*Salix* spp.) trees have been used commercially since the 1980s at a large scale to produce renewable energy. While reducing fossil fuel needs, growing short rotation coppices (SRCs), such as poplar or willow, may have a high impact on local air quality as these species are known to produce high amounts of isoprene, which can lead to the production of tropospheric ozone (O₃). Here, we present a long-term leaf-scale study of biogenic volatile organic compound (BVOC) emissions from a Swedish managed willow site with the aim of providing information on the seasonal variability in BVOC emissions during two growing seasons, 2015–2016. Total BVOC emissions during these two seasons were dominated by isoprene (>96% by mass) and the monoterpene (MT) ocimene. The average standardized (STD, temperature of 30 °C and photosynthetically active radiation of 1000 μmol m⁻² s⁻¹) emission rate for isoprene was 45.2 (±42.9, standard deviation) μg g_{dw}⁻¹ h⁻¹. Isoprene varied through the season, mainly depending on the prevailing temperature and light, where the measured emissions peaked in July 2015 and August 2016. The average STD emission for MTs was 0.301 (±0.201) μg g_{dw}⁻¹ h⁻¹ and the MT emissions decreased from spring to autumn. The average STD emission for sesquiterpenes (SQTs) was 0.103 (±0.249) μg g_{dw}⁻¹ h⁻¹, where caryophyllene was the most abundant SQT. The measured emissions of SQTs peaked in August both in 2015 and 2016. Non-terpenoid compounds were grouped as other VOCs (0.751 ± 0.159 μg g_{dw}⁻¹ h⁻¹), containing alkanes, aldehydes, ketones, and other compounds. Emissions from all the BVOC groups decreased towards the end of the growing season. The more sun-adapted leaves in the upper part of the plantation canopy emitted higher rates of isoprene, MTs, and SQTs compared with more shade-adapted leaves in the lower canopy. On the other hand, emissions of other VOCs were lower from the upper part of the canopy compared with the lower part. Light response curves showed that ocimene and α-farnesene increased with light but only for the sun-adapted leaves, since the shade-adapted leaves did not emit ocimene and α-farnesene. An infestation with *Melampsora* spp. likely induced high emissions of, e.g., hexanal and nonanal in August 2015. The results from this study imply that upscaling BVOC emissions with model approaches should account for seasonality and also include the canopy position of leaves as a parameter to allow for better estimates for the regional and global budgets of ecosystem emissions.

Keywords: *Salix* plantation; willow; leaf rust; terpenoids; non-terpenoids; BVOCs; leaf-scale; GC-MS

1. Introduction

The increase in greenhouse gases (GHGs) and the global temperature during the last few decades have resulted in mitigation strategies and climate targets, where the main goal is to keep the average global temperature increase within 1.5–2°C [1,2] compared with pre-industrial levels. Together with these climate targets, as declared by the European Union, Sweden also has the goal to have no net emission of GHGs into the atmosphere by 2045 [3]. One option to decrease the use of and dependency on fossil fuel is to use fast-growing biofuel crops, also known as short rotation coppices (SRCs) [4].

Perennial crops are well suited for this purpose and, in particular, willow trees (*Salix* spp.) have been used to produce energy in district heating plants since the 1980s [5]. By using life cycle assessment (LCA), willow as biomass-based energy can reduce the GHG emissions considerably compared with fossil fuel [6]. One of the advantages with willow is the possibility of hybridization and propagation, which makes it easy to develop new varieties for better biomass yield [7]. After initial establishment, the trees grow for between 3 and 5 years before their aboveground biomass is harvested, and plants continue to regrow from their root system for the next harvest cycle. Compared with annual crops, *Salix* trees do not need as much management and fertilization [8]. Current land use of SRC plantations in Sweden is just below 10,000 ha but it has been estimated that this area could expand to 200,000–300,000 ha [9]. Besides the climate change mitigation effects, *Salix* has some other environmental benefits. The plant takes up heavy metals, such as cadmium, from soil [10,11], and can also be used to clean the soil after application of sludge and wastewater [9,12].

However, *Salix* trees emit high amounts of biogenic volatile organic compounds (BVOCs) [13]. BVOCs are used by plants for signaling, to attract pollinators, and to protect the plants against biotic stress (e.g., herbivory and pathogens) and abiotic stress (e.g., extreme temperatures or pollutants such as ozone (O_3)) [14–19]. However, BVOCs are also important for atmospheric chemistry as they reduce the amount of hydroxyl radicals and thus increase the lifetime of CH_4 [20,21]. The production of O_3 is influenced by the prevailing ratio between VOCs and NO_x [22]. BVOCs could therefore efficiently contribute to the production of tropospheric O_3 in non- NO_x -limited situations [23–25]. Tropospheric O_3 is hazardous as it damages the leaf tissue when entering the stomata, leading to a lower photosynthetic capacity [26,27], but the sink strength of O_3 depends also on the stomatal conductance and thus on the ambient environmental conditions [28,29]. Since O_3 is a GHG, and also could reduce the ability of plants to absorb CO_2 , an increase in O_3 might lead to an enhancement in radiative forcing and global warming [30,31]. In addition, BVOCs act as precursors for secondary organic aerosols (SOAs) and enhance cloud condensation nuclei (CCN) production [32–39]. Depending on the properties of the aerosols and the environmental conditions, they can either decrease or enhance global warming [38], but the overall impact of CCN and SOAs is believed to cool the earth [40].

To our knowledge, few studies have investigated the whole emission spectrum of BVOCs from *Salix* [41,42] since the focus has mostly been on isoprene [43,44]. Some studies (e.g., [45]) have investigated emissions from *Salix* at different heights within the canopy. The BVOC emissions from the leaves within the canopy are expected to vary due to the different microclimatic conditions (e.g., temperature and radiation) [45,46], but the difference might be less pronounced for the standardized (STD) emissions.

This study aims to characterize BVOC emissions from *Salix* trees growing in their last year before harvest during the major part of the growing season. Our objectives were to determine seasonal trends in emission rates and spectra, and to assess for differences between leaves growing at different heights within the canopy.

2. Methods

2.1. Site Description

Measurements were done on two plantations in Skrehalla (P1, 58°16'55" N 12°46'20" E and P2, 58°17'09" N 12°45'31" E), which were located in the southwestern part of Sweden and about 80 km northeast of Gothenburg (Figure S1). The area is flat and the site was mainly surrounded by arable fields. The long-term mean annual temperature was 6.1 °C (1961–1990 in Gendalen, located 16 km from the site) and the annual precipitation was 683 mm (1961–1990 in Grästorps, 7 km from the site) [47]. The soil in the area contained clay or a silty clay loam with 34%–36% clay content, 45%–46% silt content, and no organic content (Table 1). Willow trees growing on P1 originated from the species *S. viminalis*. This plantation was established in 1994 and the last time the trees were harvested was in the beginning of 2013, which means measurements were done during their third growing season in 2015. In total, P1 covered approximately 6 ha. The variety growing on P2 is called Tora and P2 was established in 2003 on an area of approximately 5 ha. The trees on P2 were harvested in spring 2013, which means they were in their fourth growing season in 2016. At both sites, all trees were planted in double rows, separated by 0.75 m and 1.25 m between each double row. The distance between the trees in the row was 0.4 m.

Table 1. Information about the two plantations (P1 and P2) in the study. Size (ha), previous land use, year of establishment, canopy height (m), leaf area index (LAI, m² m⁻²), soil type and content, treatments, varieties, and yield (m³ ha⁻¹).

	P1	P2
Size	6 ha	5 ha
Formerly used for	cereals	<i>Salix</i>
Established	1994	2003
Canopy height ¹	4.5 m	7 m
LAI ²	5.5	4.9
Soil type ³	silty clay loam	clay loam
Clay content ³	36%	34%
Silt content ³	46%	45%
Organic content ³	0%	0%
Treatments ⁴	Fertilized (ca 2 × 100 kg N ha ⁻¹)	Fertilized (ca 1 × 100 kg N ha ⁻¹)
Varieties	unknown <i>S. viminalis</i>	Tora
Last harvest	2013	2013
Yield ⁵	ca 200 m ³ ha ⁻¹	ca 200 m ³ ha ⁻¹

¹P1: Estimated average canopy height after the growing season in 2015. P2: Estimated average canopy height after the growing season in 2016.

²P1: Simulated maximum LAI in 2013 based on measured height and diameter. P2: Measured maximum LAI in 2016.

³Taken from SGU [48].

⁴Total number of treatments during the rotation cycle.

⁵Yield after four growing years.

2.2. Experimental Setup

Measurements were done with two different setups. First, we used a branch chamber (volume ca 13 L) during repeated campaigns throughout the growing seasons 2015 and 2016. The aim of this setup was to follow the seasonal pattern of BVOC emissions during the two growing seasons.

Second, a photosynthesis system with a leaf chamber (6 cm² leaf area) was used to provide photosynthesis information in parallel to BVOC measurements focusing on the light response.

2.2.1. Branch Chamber Setup

The branch chamber used was a cylindrical construction made of PFA and stainless steel covered with a thin transparent PFA film [49–51]. At the beginning of each campaign, the tip (ca 30 cm long) of a shoot from one *Salix* tree was carefully inserted into the chamber the day before measurements started, avoiding any disturbance of the leaves. The chamber was left open on one end when not in use (i.e., during night). Every day before the measurements started, the chamber lid was closed, and the chamber was flushed with purge air for one hour. After this procedure, the branch chamber was used as a dynamic chamber with a continuous purge flow of 3–4 l min⁻¹, leading to a residence time of ca 4 min for the air within the chamber.

In 2015, only one branch chamber was used. Starting in June 2016, two identical sets of branch chambers were used in parallel at different canopy heights. Each campaign, two trees standing next to each other were chosen for the branch chamber measurements. Prevailing conditions of temperature (T, °C) and relative humidity (RH) were measured both inside and outside the branch chamber (CS215, Campbell Scientific, UT, USA). Photosynthetically active radiation (PAR, $\mu\text{mol m}^{-2} \text{s}^{-1}$) was measured close to the chamber and at canopy level (LI-190, LI-COR, NE, USA). The data were recorded on a data logger (CR1000, Campbell Scientific, UT, USA) every 10 sec and stored as 1 min averages.

2.2.2. Light Response Curves and Photosynthesis Rates

Besides the branch chamber, a portable photosynthesis system (LI-6400XT, LI-COR, NE, USA) was used in 2016 to provide photosynthesis information in parallel with BVOC measurements from individual *Salix* leaves [42,46,50,52]. The leaf chamber has a capacity to measure leaves with an area up to 6 cm² (2 × 3 cm²) and the measurements were done on the middle part of the leaves to obtain the maximum area of the leaves. The flow rate into the leaf chamber was set to 500 $\mu\text{mol s}^{-1}$ (ca 0.71 min⁻¹). The leaf chamber was equipped with a LED source (6400-02B). This photosynthesis system made it possible to control the PAR, T, RH, and carbon dioxide (CO₂) concentration within the leaf chamber. Temperature and CO₂ were set to ambient conditions (20–25 °C and 400 ppm), while PAR was set to increase between 0 and 1500 $\mu\text{mol m}^{-2} \text{s}^{-1}$ in six steps (0, 150, 300, 450, 600, 1000, and 1500 $\mu\text{mol m}^{-2} \text{s}^{-1}$) to obtain light response curves. Relative humidity was regulated to match ambient values and ranged mainly from 30% to 70%. Net assimilation rate (A, $\mu\text{mol CO}_2 \text{ m}^{-2} \text{s}^{-1}$), transpiration (Tr, mmol H₂O m⁻² s⁻¹), and stomatal conductance (g_s, mol H₂O m⁻² s⁻¹) were measured with the Li-6400XT, and water use efficiency (WUE, mmol CO₂ mol⁻¹ H₂O) was then calculated by dividing A by Tr.

2.3. BVOC Sampling

BVOC sampling was based on adsorbent cartridges containing Tenax TA (a porous organic polymer) and Carbograph 1TD (graphitized black carbon (C)) (Markes International Ltd., Mid Glamorgan, UK). Prior to sampling, all cartridges were conditioned. In this process, N₂ is used as a carrier gas while the cartridges are heated up to 300 °C, which empties the cartridges from possible contamination.

Air from the dynamic chamber was pulled through an adsorbent cartridge for 20 min per sample at a flow rate of 200 mL min⁻¹ using a flow-controlled pump (Pocket Pump, SKC Ltd., Dorset, UK), leading to a total sample volume of 4 L. In the case of the leaf chamber, the photosynthesis system had been modified with a trace-gas tube connection after the outlet of the leaf chamber [42,46,50,52]. This way, BVOC samples could be taken in parallel to the on-going photosynthesis measurements.

To provide VOC-free and O₃-free air into the branch chamber, air entering the branch chamber was passed through a hydrocarbon trap (Alltech, Associates Inc., US), which contained activated C and a MnO₂-coated copper mesh. The hydrocarbon trap was also attached to the intake of the photosynthesis system. For the branch chamber, background samples of the purge air entering the chamber were taken every day, while blank samples

from the empty leaf chamber were taken after the last light intensity ($1500 \mu\text{mol m}^{-2} \text{s}^{-1}$) measurement.

During the campaigns, BVOC samples were taken during day time (8:00–18:00). In the case of the leaf chamber, measurements started one hour after the leaf was inserted to avoid potential stress-induced BVOCs from physical handling [42,52]. When a new light level was set, 30 min passed before the BVOC sampling started so the leaf had time to adapt to the new condition [52]. After sampling, the cartridges were sealed with Teflon-coated brass caps and stored at $3 \text{ }^\circ\text{C}$ until analysis. After each campaign was finished, the sampled leaves were harvested and dried at $75 \text{ }^\circ\text{C}$ for two days to measure the dry weight.

In total, 754 samples were taken on 35 trees during 15 campaigns between July 2015 and October 2016, and the campaigns were in general 2–5 days (Table 2). Due to setup and instrumental failure, 26 samples were missing in 2015 and 65 in 2016. Campaigns performed in 2015 were all on P1 except the last one in September, where the first day was on P1 (P1* in Table 2, the star means another variety) and the last two days were on P2. This change was due to a rust outbreak of a fungi (*Melampsora* spp.). Signs of the infestation were seen in July, and by mid-September most of the trees had shed their leaves (Figure S2). Leaves with the least damage were chosen, but more or less all trees were equally affected. All the campaigns performed in 2016 were done at P2. No signs of *Melampsora* were observed on Tora but leaf-feeding beetles (*Phratora vulgatissima*) damaged the leaves, especially higher up in the canopy. On account of *P. vulgatissima*, undamaged leaves were hard to find, at least in the uppermost part of the canopy, from July onward (Figure S3).

The heights of the measurements were divided into three categories. The lower height (z_L) included leaves that were below or in the lower part of canopy (up to ca 70% of the total canopy height (TCH)) and growing within the plantation. The higher height (z_H) included leaves above z_L (>70% of TCH) and growing in a more sun-adapted environment compared with the shade-adapted leaves in z_L . Trees growing at the edge that were <70% of the TCH were classified as middle (z_M) because they were expected to be more sunlit than if they grew within the plantation. The canopy height (H) was measured as the average height for the trees that were growing just next to the leaves, which the BVOC emissions were measured from, as these trees were responsible for the light conditions at the measured leaves. All measurements during 2015 were done on z_H except for the last campaign. Measurements with the branch chambers in 2016 were done at the edge of P2, while the measurements with the leaf chamber were done both on the edge and within P2.

Table 2. All campaigns done in 2015 and 2016 with branch and leaf chambers. Two different plantations (P1 and P2) were studied and new trees were studied each campaign. The star (P1*) means that another variety was measured at this site compared with the rest of the campaigns on P1. Height levels were z_L (up to ca 70% of the total canopy height (TCH)), z_M (up to ca 70% of the TCH but growing at the edge of the plantation), and z_H (heights above z_L). z/H means the ratio between the measured leaves (z) and the canopy height (H).

Branch Chamber						
Campaign No.	Time	Relative Canopy Height (z/H)	Height Group	Samples	Trees	Plantation
1	2015: 16–17 July	1.00	z_H	8	1	P1
2	2015: 28–31 July	1.00	z_H	30	1	P1
3	2015: 4–7 Aug.	1.00	z_H	28	1	P1
4	2015: 18–21 Aug.	1.00	z_H	31	1	P1
5	2015: 1–4 Sep.	0.85	z_H	31	1	P1
6	2015: 8 and 10–11 Sep.	0.35; 0.80	$z_M; z_H$	4; 10	2	P1* & P2
				Tot: 142	Tot: 7	
Branch Chamber						
Campaign No.	Time	Relative Canopy Height (z/H)	Height Group	Samples	Trees	Plantation
1	2016: 4–5 May	0.40	z_M	14	1	P2

2	2016: 24 May	0.75	ZH	6	1	P2
3	2016: 6–10 June	0.30; 0.75	ZM; ZH	39; 10	2	P2
4	2016: 19–23 June	0.30; 0.75	ZM; ZH	39; 40	2	P2
5	2016: 11–15 July	0.30; 0.80	ZM; ZH	36; 36	2	P2
6	2016: 26–29 July	0.70; 0.90	ZM; ZH	32; 30	2	P2
7	2016: 15–17 Aug.	0.55; 0.90	ZM; ZH	20; 12	2	P2
8	2016: 6–9 Sep.	0.65; 0.90	ZM; ZH	30; 28	2	P2
9	2016: 10–13 Oct.	0.50; 0.95	ZM; ZH	29; 26	2	P2
				Tot: 427	Tot: 16	
Leaf Chamber						
Campaign No.	Time	Relative Canopy Height (z/H)	Height Group	Samples	Trees	Plantation
5	2016: 11–15 July	0.15; 0.15; 0.40	ZM; ZM; ZM	7; 7; 4	3	P2
6	2016: 26–29 July	0.15; 0.60; 0.80; 0.80	ZM; ZL; ZH; ZH	7; 7; 7; 7	3	P2
7	2016: 15–17 Aug.	0.20; 0.65; 0.90	ZM; ZL; ZH	6; 7; 7	3	P2
8	2016: 6–9 Sep.	0.65; 0.20; 0.95; 0.95	ZL; ZM; ZH; ZH	7; 7; 7; 7	3	P2
				Tot: 94	Tot: 12	

2.4. Gas Chromatography–Mass Spectrometry and Data Processing

All samples were analyzed by thermal desorption (UNITY2 thermal desorber, Markes International Ltd., Mid Glamorgan, UK) in combination with an ULTRA autosampler and gas chromatograph–mass spectrometer (GC-MS) (7890A Series GC coupled with a 5975C inert MSD/DS Performance Turbo EI System, Agilent, CA, USA) [42,53]. Separation of BVOCs was done by a HP-5 capillary column (50 m × 0.2 mm, film thickness 0.33 μm) and helium was used as a carrier gas. The oven temperature started at 40 °C for 1 min, was first raised to 210 °C with a rate of 5 °C min⁻¹, and was then raised to 250 °C with a rate of 20 °C min⁻¹. The compounds were analyzed in the program Enhanced ChemStation (MSD ChemStation E.02.01.1177, Copyright 1989–2010 Agilent Technologies, Inc.) and identified by injected external standards (Table S4) or according to mass spectra in the NIST 8.0 database. To quantify BVOCs for which no specific standard was available, α-pinene was used for monoterpenes (MTs), humulene for sesquiterpenes (SQTs), and toluene for other VOCs. Only sample peaks that had at least twice as strong a signal as the corresponding peaks in background samples were chosen for further analysis.

Two compounds, toluene and butylated hydroxytoluene, were removed from all measurements done by LI-6400XT because they had approximately the same concentration in the background samples as the measurements from the leaves and were therefore assumed to be emitted by this instrument.

The emission rates for the BVOCs were calculated by Equation (1), according to Ortega and Helmig [54]

$$E = (C_2 - C_1) \times Q \times m^{-1} \quad (1)$$

where E (μg g_{dwt}⁻¹ h⁻¹) is the emission rate, C_2 (μg l⁻¹) is the BVOC concentration taken from the chamber, C_1 (μg l⁻¹) is the BVOC concentration entering the branch chamber or the BVOC concentration inside the empty leaf chamber, Q (l h⁻¹) is the flow rate of the purge air, and m (g_{dwt}) is the dried mass of the leaves contained in the chamber.

A standardization for BVOCs that were both light and temperature dependent was done by Equation (2) according to Guenther et al. [55]. The reason for this standardization was to allow for comparison with other studies, regardless of prevailing environmental conditions. The STD values for T and PAR were 303.15 K and 1000 μmol m⁻² s⁻¹, respectively. The compounds that were STD with Equation 2 were isoprene, ocimene, and α-farnesene.

$$E = E_s \times C_T \times C_L \quad (2)$$

where E ($\mu\text{g g}_{\text{dw}}^{-1} \text{h}^{-1}$) is the actual emission at the measured chamber temperature T (K) and PAR ($\mu\text{mol m}^{-2} \text{s}^{-1}$), E_s is the STD emission, and C_T and C_L are dimensionless correction factors for temperature and light defined by Equations (3) and (4).

$$C_L = \frac{\alpha C_{L1} PAR}{\sqrt{1 + \alpha^2 PAR^2}} \quad (3)$$

where α ($=0.0027$) and C_{L1} ($=1.066$) are empirical coefficients taken from Guenther et al. [55]

$$C_T = \frac{\exp\left(\frac{C_{T1}(T - T_s)}{RT_s T}\right)}{1 + \exp\left(\frac{C_{T2}(T - T_M)}{RT_s T}\right)} \quad (4)$$

where C_{T1} ($=95\,000 \text{ J mol}^{-1}$), C_{T2} ($=230\,000 \text{ J mol}^{-1}$), and T_M ($=314 \text{ K}$) are empirical coefficients [55]. R ($=8.314 \text{ J K}^{-1} \text{ mol}^{-1}$) is the universal gas constant and T_s ($=303.15 \text{ K}$) is the standard temperature.

For compounds that are temperature, but not light, dependent, the STD emission can be calculated with the temperature-dependent Equation (5), which was used on all terpenoids except isoprene, ocimene, and α -farnesene.

$$E = E_s \times e^{\beta(T - T_s)} \quad (5)$$

where E is the actual emission rate ($\mu\text{g g}_{\text{dw}}^{-1} \text{h}^{-1}$) at temperature T (K), E_s ($\mu\text{g g}_{\text{dw}}^{-1} \text{h}^{-1}$) is the STD emission rate at the standard temperature T_s ($=303.15 \text{ K}$), and β ($=0.09 \text{ K}^{-1}$ for MTs and 0.17 K^{-1} for SQTs) is an empirical constant [55,56].

Fitted net assimilation curves were done by using Smith's equation, Equation (6) [57]

$$A = \frac{\alpha_A PAR}{\sqrt{1 + \frac{\alpha_A^2 PAR^2}{A_{max}^2}}} - A_d \quad (6)$$

where A is net assimilation ($\mu\text{mol CO}_2 \text{ m}^{-2} \text{ s}^{-1}$), α_A is the initial quantum yield (mol mol^{-1}), A_d is dark respiration ($\mu\text{mol CO}_2 \text{ m}^{-2} \text{ s}^{-1}$), and A_{max} is net assimilation at the maximum PAR ($1500 \mu\text{mol m}^{-2} \text{ s}^{-1}$).

The statistical tests were performed with a Kruskal–Wallis test at a significance level of 0.05 when comparing emissions between different heights since the data did not have a Gaussian distribution. The optimized parameters for the fitted light response curves were determined by minimizing the difference between measured and simulated emissions according to a root mean square procedure.

3. Results

3.1. BVOC Emissions from Salix

The total number of detected peaks found during GC–MS analysis was 39 (Table S5), whereof 37 could be identified and the remaining were named as unknown. The average total BVOC emission from all measurements in 2015 and 2016 was 24.4 (± 5.8 , standard deviation) $\mu\text{g g}_{\text{dw}}^{-1} \text{h}^{-1}$. Isoprene made up more than 96% of the total emission and had an average emission rate of 23.5 (± 28.1) $\mu\text{g g}_{\text{dw}}^{-1} \text{h}^{-1}$ (Table 3). The corresponding STD isoprene emission rate was 45.2 (± 42.9) $\mu\text{g g}_{\text{dw}}^{-1} \text{h}^{-1}$.

The average MT emission rate was 0.163 (± 0.117) $\mu\text{g g}_{\text{dw}}^{-1} \text{h}^{-1}$, which was 0.7% of the total BVOC emission. Nine MTs were detected: allo-ocimene, α -pinene, eucalyptol, limonene, linalool, myrcene, ocimene, p-cymene, and 3-carene. Except in October, ocimene was the dominant MT ($0.137 \pm 0.321 \mu\text{g g}_{\text{dw}}^{-1} \text{h}^{-1}$) and more than 17 times higher than the second most emitted MT, which was limonene ($0.008 \pm 0.042 \mu\text{g g}_{\text{dw}}^{-1} \text{h}^{-1}$). The total STD MT emission rate was 0.301 (± 0.201) $\mu\text{g g}_{\text{dw}}^{-1} \text{h}^{-1}$. The group with the lowest emission rate

among the terpenoids was SQTs with an average emission of $0.035 (\pm 0.062) \mu\text{g g}_{\text{dw}}^{-1} \text{h}^{-1}$, which resulted in a contribution of ca 0.1% to the total average BVOC emission. Four SQTs were observed: α -farnesene, caryophyllene, humulene, and nerolidol. The highest average emission rates were seen for caryophyllene ($0.011 \pm 0.031 \mu\text{g g}_{\text{dw}}^{-1} \text{h}^{-1}$) and humulene ($0.010 \pm 0.090 \mu\text{g g}_{\text{dw}}^{-1} \text{h}^{-1}$). The average STD emission of SQTs was $0.103 (\pm 0.249) \mu\text{g g}_{\text{dw}}^{-1} \text{h}^{-1}$.

Non-terpenoid compounds were grouped as other VOCs and their classification can be seen in Table 3 and Table S5. The most abundant among the identified other VOCs were cyclopentenyl acetylene ($0.083 \pm 0.205 \mu\text{g g}_{\text{dw}}^{-1} \text{h}^{-1}$), benzaldehyde ($0.065 \pm 0.163 \mu\text{g g}_{\text{dw}}^{-1} \text{h}^{-1}$), hexanal ($0.064 \pm 0.320 \mu\text{g g}_{\text{dw}}^{-1} \text{h}^{-1}$), nonanal ($0.061 \pm 0.147 \mu\text{g g}_{\text{dw}}^{-1} \text{h}^{-1}$), and 2-ethylhexanoic acid ($0.059 \pm 0.252 \mu\text{g g}_{\text{dw}}^{-1} \text{h}^{-1}$).

Table 3. Measured (E) and standardized (Es) emission rates ($\mu\text{g g}_{\text{dw}}^{-1} \text{h}^{-1}$, $n = 663$) from all measurements for the most abundant compounds in each group. Numbers in parentheses are standard deviation (SD, $\mu\text{g g}_{\text{dw}}^{-1} \text{h}^{-1}$). No standardization was made for other VOCs (-).

BVOC	E \pm SD ($\mu\text{g g}_{\text{dw}}^{-1} \text{h}^{-1}$)	Es \pm SD ($\mu\text{g g}_{\text{dw}}^{-1} \text{h}^{-1}$)
isoprene	23.5 (28.1)	45.2 (42.9)
Total MTs	0.163 (0.117)	0.301 (0.201)
ocimene	0.137 (0.321)	0.255 (0.540)
limonene *	0.008 (0.042)	0.014 (0.081)
p-cymene	0.006 (0.042)	0.011 (0.069)
linalool	0.006 (0.017)	0.010 (0.035)
α -pinene	0.003 (0.021)	0.005 (0.034)
3-carene *	0.002 (0.019)	0.004 (0.040)
Total SQTs	0.035 (0.062)	0.103 (0.249)
caryophellene †	0.011 (0.031)	0.024 (0.080)
humulene	0.010 (0.090)	0.040 (0.409)
α -farnesene †	0.009 (0.062)	0.017 (0.125)
Total other VOCs	0.751 (0.159)	-
cyclopentyl acetylene §	0.083 (0.205)	-
benzaldehyde (benzenoid)	0.065 (0.163)	-
hexanal (aldehyde)	0.064 (0.320)	-
nonanal (aldehyde)	0.061 (0.147)	-
2-ethylhexanoic acid § (carboxylic acid)	0.059 (0.252)	-
pentanal § (aldehyde)	0.037 (0.226)	-
decanal § (aldehyde)	0.036 (0.148)	-
octanal (aldehyde)	0.030 (0.105)	-
2-methylbutane § (alkane)	0.027 (0.105)	-
2-pentanone § (ketone)	0.026 (0.208)	-

* These MTs were quantified with α -pinene as the injected standard in GC-MS.

† These SQTs were quantified with humulene as the injected standard in GC-MS.

§ These other VOCs were quantified with toluene as the injected standard in GC-MS.

3.2. Seasonality of BVOC Emissions Measured with Branch Chambers

3.2.1. Isoprene

The emission rates for isoprene changed mostly according to prevailing T and PAR values. The average STD isoprene emission from P1 in 2015 was $59.3 (\pm 44.5) \mu\text{g g}_{\text{dw}}^{-1} \text{h}^{-1}$, where the corresponding average chamber T (T_c) and chamber PAR (PAR_c) were $24.9 (\pm 5.4) ^\circ\text{C}$ and $462 (\pm 296) \mu\text{mol m}^{-2} \text{s}^{-1}$, respectively. Most of the measured isoprene emissions that varied between 92.0 and $153.2 \mu\text{g g}_{\text{dw}}^{-1} \text{h}^{-1}$ during 2015 occurred in the middle of July and during the second half of August. The chamber T was high ($>27.5 ^\circ\text{C}$) and PAR_c varied

from 304 to 1654 $\mu\text{mol m}^{-2} \text{s}^{-1}$ for these isoprene emissions (Figure 1 A–C). The measured emission peaked ($153.2 \mu\text{g g}_{\text{dw}}^{-1} \text{h}^{-1}$) in July and the STD emission peaked ($177.6 \mu\text{g g}_{\text{dw}}^{-1} \text{h}^{-1}$) in August 2015.

With more unsteady weather conditions and under cloudy conditions and even rain, low emissions of isoprene ($1.6\text{--}7.0 \mu\text{g g}_{\text{dw}}^{-1} \text{h}^{-1}$) were observed even during the peak growing season in July and August 2015 due to low PARc values ($<200 \mu\text{mol m}^{-2} \text{s}^{-1}$). In particular, in the beginning of September when Tc was $<15 \text{ }^{\circ}\text{C}$ and PARc was $<160 \mu\text{mol m}^{-2} \text{s}^{-1}$, the emission rates only reached up to $0.1 \mu\text{g g}_{\text{dw}}^{-1} \text{h}^{-1}$. In addition, the leaves were damaged in September due to the infestation of *Melampsora* on P1.

The seasonal trend for measured and STD isoprene emissions in 2016 showed an increase from spring to summer; thereafter, it decreased from late summer to mid-autumn. The average STD isoprene emission in 2016 was $30.6 (\pm 26.7) \mu\text{g g}_{\text{dw}}^{-1} \text{h}^{-1}$ and the average Tc and PARc were $23.2 (\pm 7.6) \text{ }^{\circ}\text{C}$ and $521 (\pm 444) \mu\text{mol m}^{-2} \text{s}^{-1}$. The measured isoprene emission varied from 50.1 to $143.7 \mu\text{g g}_{\text{dw}}^{-1} \text{h}^{-1}$ between June and August but emissions up to $46.5 \mu\text{g g}_{\text{dw}}^{-1} \text{h}^{-1}$ were already observed in May (Figure 2C). All measured isoprene emission rates $>50 \mu\text{g g}_{\text{dw}}^{-1} \text{h}^{-1}$ in 2016 had corresponding Tc and PARc ranging from 26.8 to $39.9 \text{ }^{\circ}\text{C}$ and from 365 to $1518 \mu\text{mol m}^{-2} \text{s}^{-1}$. The STD isoprene emission peaked ($150.0 \mu\text{g g}_{\text{dw}}^{-1} \text{h}^{-1}$) in late July 2016, while the measured isoprene emission peaked ($143.7 \mu\text{g g}_{\text{dw}}^{-1} \text{h}^{-1}$) in August. Isoprene emissions were negligible during the last campaign in October, when Tc and PARc were low (less than $11 \text{ }^{\circ}\text{C}$ and $110 \mu\text{mol m}^{-2} \text{s}^{-1}$, respectively).

The influence of Tc on the isoprene emission rates showed a stronger exponential increase for the variety on P1 than for Tora on P2 (Figure 3). In particular, when Tc reached above $23 \text{ }^{\circ}\text{C}$, the average emission in 2015 increased faster than during 2016. The steeper response in 2015 was possibly due to the fact that this variety was a stronger emitter of isoprene, but the unexpected lower average emission when Tc varied from 30 to $36 \text{ }^{\circ}\text{C}$ in 2016 also reduced the slope of the fitted curve this year.

3.2.2. Monoterpenes

The emitted MTs from P1 in 2015 were α -pinene, eucalyptol, linalool, and ocimene. The average STD MT emission was $0.365 (\pm 0.151) \mu\text{g g}_{\text{dw}}^{-1} \text{h}^{-1}$. Ocimene was emitted during all campaigns and the highest measured emissions were seen during the first campaign in mid-July ($0.409\text{--}1.648 \mu\text{g g}_{\text{dw}}^{-1} \text{h}^{-1}$) and the fourth campaign in mid-August ($0\text{--}0.932 \mu\text{g g}_{\text{dw}}^{-1} \text{h}^{-1}$). Ocimene contributed with $90\text{--}100\%$ to the average STD MT emission rate during all campaigns in 2015 (Table S6), and STD emissions of ocimene peaked ($1.631 \mu\text{g g}_{\text{dw}}^{-1} \text{h}^{-1}$) in July. α -pinene was the second most abundant MT in 2015, with the STD emission ranging from 0 to $0.076 \mu\text{g g}_{\text{dw}}^{-1} \text{h}^{-1}$, but α -pinene was not observed in September 2015. The total average STD MT emission decreased from $0.580 (\pm 0.292) \mu\text{g g}_{\text{dw}}^{-1} \text{h}^{-1}$ in July to $0.286 (\pm 0.182) \mu\text{g g}_{\text{dw}}^{-1} \text{h}^{-1}$ in September and a similar trend was seen for the measured average total MT emission.

More MTs were emitted from P2 in 2016. Except for the MTs mentioned above, allo-ocimene, limonene, myrcene, p-cymene, and 3-carene were also observed. The average STD emission of MTs was $0.281 (\pm 0.222) \mu\text{g g}_{\text{dw}}^{-1} \text{h}^{-1}$. Like in 2015, ocimene dominated over the other MTs in 2016 but with higher measured ($0\text{--}2.930 \mu\text{g g}_{\text{dw}}^{-1} \text{h}^{-1}$) and STD emission rates ($0\text{--}4.277 \mu\text{g g}_{\text{dw}}^{-1} \text{h}^{-1}$). The measured emission peaked in June and the STD emission peaked in July. Instead of α -pinene, linalool was the second most abundant MT in 2016. The highest measured ($0\text{--}0.206 \mu\text{g g}_{\text{dw}}^{-1} \text{h}^{-1}$) and STD ($0\text{--}0.335 \mu\text{g g}_{\text{dw}}^{-1} \text{h}^{-1}$) emissions of linalool occurred in May, and together with ocimene they contributed with $>97\%$ to the STD MT emission in May. Throughout the rest of the season in 2016 and until September, they contributed with $95\text{--}99\%$ to the average STD MT emission. Myrcene and allo-ocimene were only seen in June. The STD MT emission during 2016 was highest in May ($0.590 \pm 0.306 \mu\text{g g}_{\text{dw}}^{-1} \text{h}^{-1}$) followed by June ($0.488 \pm 0.330 \mu\text{g g}_{\text{dw}}^{-1} \text{h}^{-1}$), and lowest in October ($0.022 \pm 0.028 \mu\text{g g}_{\text{dw}}^{-1} \text{h}^{-1}$). This pattern was also observed for the measured average total MT emission, which is in line with the MT emission trend in 2015.

3.2.3. Sesquiterpenes

The average STD emission of SQTs from P1 in 2015 was $0.082 (\pm 0.060) \mu\text{g g}_{\text{dw}}^{-1} \text{h}^{-1}$. Caryophyllene had the highest emission rate among the SQTs in 2015 and the STD emission varied between 0 and $0.478 \mu\text{g g}_{\text{dw}}^{-1} \text{h}^{-1}$. The highest STD emissions occurred in September and caryophyllene was the only emitted SQT this month (Figure 1E and Table S6). The measured SQT emission peaked in the second half of August. α -farnesene had the second highest average emission rate among the SQTs during 2015 and was emitted in July and August. Measured emissions of α -farnesene ($0\text{--}0.242 \mu\text{g g}_{\text{dw}}^{-1} \text{h}^{-1}$) were highest in August but STD emissions ($0\text{--}0.193 \mu\text{g g}_{\text{dw}}^{-1} \text{h}^{-1}$) peaked already in late July.

The average STD SQT emission from P2 in 2016 was $0.012 (\pm 0.018) \mu\text{g g}_{\text{dw}}^{-1} \text{h}^{-1}$ and the same SQTs were observed this year as during 2015. August was the month where both the STD emission ($0.054 \pm 0.046 \mu\text{g g}_{\text{dw}}^{-1} \text{h}^{-1}$) and the measured emission ($0.084 \pm 0.057 \mu\text{g g}_{\text{dw}}^{-1} \text{h}^{-1}$) peaked during 2016. Caryophyllene dominated between June and August and the STD emission varied from 0 to $0.215 \mu\text{g g}_{\text{dw}}^{-1} \text{h}^{-1}$. It contributed with 64%–96% to the STD SQT emission during these months. α -farnesene was emitted from July to September with STD emissions between 0 and $0.345 \mu\text{g g}_{\text{dw}}^{-1} \text{h}^{-1}$. It was the only SQT observed in September. Humulene was seen from June to July, where the STD emission ranged from 0 to $0.043 \mu\text{g g}_{\text{dw}}^{-1} \text{h}^{-1}$. No SQTs were emitted in May and October.

3.2.4. Other VOCs

The average emission of other VOCs at P1 in 2015 was $0.937 (\pm 0.105) \mu\text{g g}_{\text{dw}}^{-1} \text{h}^{-1}$. The highest emissions occurred in the beginning of August and the average emission for this campaign was $2.766 (\pm 0.186) \mu\text{g g}_{\text{dw}}^{-1} \text{h}^{-1}$, which was several times higher compared with the other campaigns in 2015 and 2016 (Figures 1F and 2F). The compounds that contributed most in August were nonanal ($0\text{--}1.570 \mu\text{g g}_{\text{dw}}^{-1} \text{h}^{-1}$), benzoic acid ($0\text{--}1.330 \mu\text{g g}_{\text{dw}}^{-1} \text{h}^{-1}$), benzaldehyde ($0\text{--}0.896 \mu\text{g g}_{\text{dw}}^{-1} \text{h}^{-1}$), decanal ($0\text{--}0.800 \mu\text{g g}_{\text{dw}}^{-1} \text{h}^{-1}$), octanal ($0\text{--}0.634 \mu\text{g g}_{\text{dw}}^{-1} \text{h}^{-1}$), and hexanal ($0\text{--}0.607 \mu\text{g g}_{\text{dw}}^{-1} \text{h}^{-1}$). The emissions of many compounds increased during the August campaign compared with the rest in 2015. Compounds such as nonanal and hexanal increased 4-fold, while benzoic acid increased almost 17-fold. The lowest emissions during 2015 were observed in September.

The average emission of other VOCs in 2016 was $0.279 (\pm 0.049) \mu\text{g g}_{\text{dw}}^{-1} \text{h}^{-1}$. The majority of the highest other VOC emissions were observed during July and especially during mid-July. The emissions of nonanal and benzaldehyde varied from 0 to $1.060 \mu\text{g g}_{\text{dw}}^{-1} \text{h}^{-1}$ and 0 to $0.701 \mu\text{g g}_{\text{dw}}^{-1} \text{h}^{-1}$ in July, respectively, but during the other months they were usually less than $0.200 \mu\text{g g}_{\text{dw}}^{-1} \text{h}^{-1}$. Emissions of 2-ethylhexanol also peaked in July ($0.974 \mu\text{g g}_{\text{dw}}^{-1} \text{h}^{-1}$). Octanal peaked in July but higher emissions were seen in both May and July ($0\text{--}0.441 \mu\text{g g}_{\text{dw}}^{-1} \text{h}^{-1}$) compared with the other months ($0\text{--}0.089 \mu\text{g g}_{\text{dw}}^{-1} \text{h}^{-1}$). Tetradecane was only observed in July and August ($0\text{--}0.034 \mu\text{g g}_{\text{dw}}^{-1} \text{h}^{-1}$), where it peaked in August, and pentadecane was seen in July, August, and September ($0\text{--}0.072 \mu\text{g g}_{\text{dw}}^{-1} \text{h}^{-1}$).

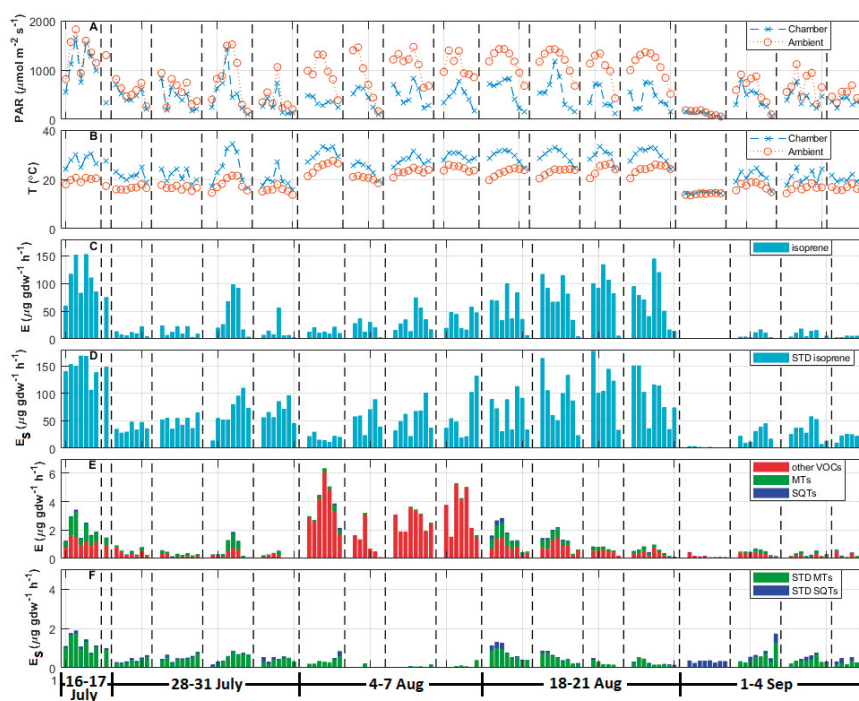


Figure 1. Measurements from P1 in 2015. (A) PAR ($\mu\text{mol m}^{-2} \text{s}^{-1}$) values for chamber condition (PARc, blue cross and dashed line) and ambient condition (red circle and dotted line). (B) Temperature ($^{\circ}\text{C}$) values for chamber condition (T_c , blue cross and dashed line) and ambient condition (red circle and dotted line). (C) Emission rates ($\mu\text{g g}_{\text{dw}}^{-1} \text{h}^{-1}$) for isoprene (cyan). (D) Standardized (STD) emission rates ($\mu\text{g g}_{\text{dw}}^{-1} \text{h}^{-1}$) for isoprene (cyan). (E) Emission rates ($\mu\text{g g}_{\text{dw}}^{-1} \text{h}^{-1}$) of other VOCs (red), monoterpenes (MTs, green), and sesquiterpenes (SQTs, blue). (F) STD emission rates ($\mu\text{g g}_{\text{dw}}^{-1} \text{h}^{-1}$) for monoterpenes (MTs, green) and sesquiterpenes (SQTs, blue). Vertical dashed lines separate the different days. Each bar represents individual measurements.

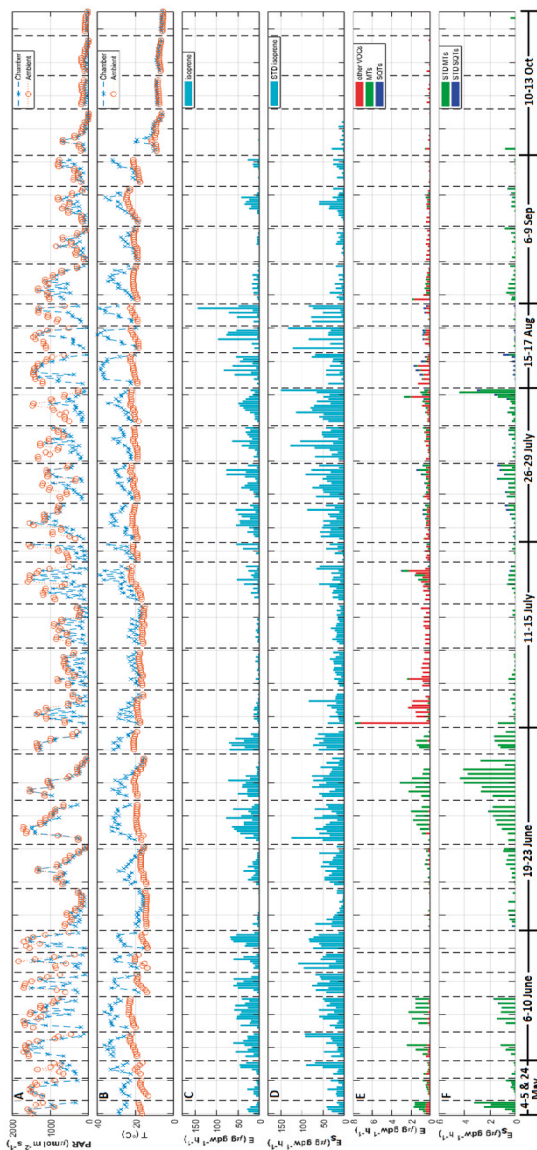


Figure 2. Measurements with branch chambers in 2016. (A) PAR ($\mu\text{mol m}^{-2} \text{s}^{-1}$) values for chamber condition (PAR_C, blue cross and dashed line) and ambient condition (red circle and dotted line). (B) Temperature ($^{\circ}\text{C}$) values for chamber condition (T_C, blue cross and dashed line) and ambient condition (red circle and dotted line). (C) Emission rates ($\mu\text{g g}_{\text{dw}}^{-1} \text{h}^{-1}$) for isoprene (cyan). (D) Standardized (STD) emission rates ($\mu\text{g g}_{\text{dw}}^{-1} \text{h}^{-1}$) for isoprene (cyan). (E) Emission rates ($\mu\text{g g}_{\text{dw}}^{-1} \text{h}^{-1}$) of other VOCs (red), monoterpenes (MTs, green), and sesquiterpenes (SQTs, blue). (F) STD emission rates ($\mu\text{g g}_{\text{dw}}^{-1} \text{h}^{-1}$) for monoterpenes (MTs, green) and sesquiterpenes (SQTs, blue). Vertical dashed lines separate the different days. Each bar represents individual measurements.

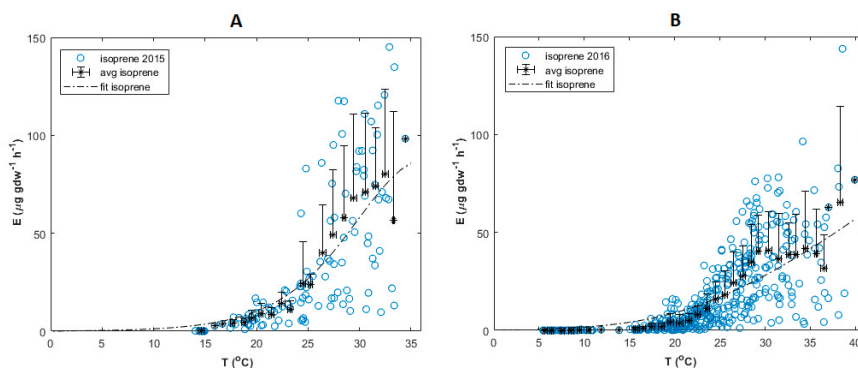


Figure 3. Measured isoprene emissions (blue circles, $\mu\text{g g}_{\text{dw}}^{-1} \text{h}^{-1}$), calculated mean emissions + standard deviation (black stars, $\mu\text{g g}_{\text{dw}}^{-1} \text{h}^{-1}$), and fitted isoprene emission curves according to Equation (2) versus chamber temperature (T_c , °C) from (A) P1 in 2015 and (B) P2 in 2016. Values for the parameters can be found in Table S7.

3.3. Height Comparison with Branch Chamber Measurements in 2016

The average STD isoprene emission from the middle canopy height Z_M ($33.6 \pm 28.2 \mu\text{g g}_{\text{dw}}^{-1} \text{h}^{-1}$) did not significantly differ from the upper canopy height Z_H ($26.7 \pm 24.1 \mu\text{g g}_{\text{dw}}^{-1} \text{h}^{-1}$). The largest difference between Z_M and Z_H for the STD isoprene emission was observed in August (Tables 4 and 5). Due to *P. vulgatissima*, leaves at Z_H were more damaged than at Z_M in August, which could be one explanation for the different STD isoprene emissions.

Comparing MT emissions between the heights showed that Z_H emitted higher rates of MTs than Z_M . The average STD MT emission from Z_H was $0.509 (\pm 0.294) \mu\text{g g}_{\text{dw}}^{-1} \text{h}^{-1}$ and ca 5 times higher compared with Z_M ($0.102 \pm 0.137 \mu\text{g g}_{\text{dw}}^{-1} \text{h}^{-1}$; $p < 0.05$). The only time when the average STD MT emission from Z_M exceeded that from Z_H was in May and October (Tables 4 and 5). In October, it was difficult to find any intact leaves at Z_H (Figure S3). Consequently, the leaves at Z_H were not able to emit any observable MTs in October. The number of emitted MT compounds from Z_H was also larger compared with Z_M , which did not have emissions of myrcene and allo-ocimene. Ocimene was the dominantly emitted MT from both Z_M (0%–91.9%) and Z_H (0%–96.8%), and linalool also contributed substantially to the MT emission for Z_H (0%–81.7%). Limonene (0%–50.0%), p-cymene (0%–33.3%) and 3-carene (0%–25.0%) only had a significant contribution for Z_M . The only MTs that were observed in October (α -pinene, 3-carene, and limonene) were emitted from Z_M .

The STD SQT emission from Z_H ($0.019 \pm 0.023 \mu\text{g g}_{\text{dw}}^{-1} \text{h}^{-1}$) was almost three times larger than from Z_M ($0.007 \pm 0.018 \mu\text{g g}_{\text{dw}}^{-1} \text{h}^{-1}$; $p < 0.05$). The same SQTs were observed at both heights (α -farnesene, caryophellene, and humulene). Sesquiterpenes were seen from Z_H in June, July, and September, but only in August from Z_M (Tables 4 and 5). Caryophyllene was the dominantly emitted SQT for Z_H (0%–90.0%) and Z_M (0%–65.0%).

The number of other VOCs from Z_H (20) was almost the same as from Z_M (22) but the average emission from Z_M ($0.347 \pm 0.061 \mu\text{g g}_{\text{dw}}^{-1} \text{h}^{-1}$) was more than twice as high compared with Z_H ($0.159 \pm 0.030 \mu\text{g g}_{\text{dw}}^{-1} \text{h}^{-1}$; $p < 0.05$). The highest average emission of other VOCs from Z_M occurred during July. The compounds that contributed most to this emission in July were benzaldehyde, cyclopentenyl acetylene, 2-ethylhexanol, nonanal, hexanal, and octanal. The average other VOC emission from Z_H was highest in May followed by July. Nonanal, hexanal, octanal, and acetophenone were the dominant other VOCs from Z_H during May. The average emission of 2-ethylhexanol was 16 times higher from Z_M compared with Z_H . Hexanal, benzaldehyde, and octanal were 3–4 times higher from Z_M compared with Z_H . The other VOC emission from Z_H was considerably lower at the end of

the growing season whereas z_M still emitted higher amounts during September and October.

Table 4. Emission rates (STD for isoprene, MTs, and SQTs, $\mu\text{g g}_{\text{dw}}^{-1} \text{h}^{-1}$) and fraction (%) of the total BVOC emission or within the BVOC group (MTs and SQTs) from z_H in 2016. Bottom: average T_c ($^{\circ}\text{C}$), PAR_c ($\mu\text{mol m}^{-2} \text{s}^{-1}$), and the corresponding standard deviation for each month.

2016 z_H	May	June	July	Aug	Sep	Oct
isoprene	44.8 (99.1%)	32.6 (95.8%)	37.5 (98.3%)	11.1 (97.8%)	18.2 (98.1%)	0.2 (87.3%)
MTs (tot)	0.127 (0.3%)	1.240 (3.6%)	0.371 (1.0%)	0.071 (0.6%)	0.275 (1.5%)	0
α -pinene	0	<0.001 (<0.1%)	0.001 (0.3%)	0.001 (1.4%)	0.001 (0.4%)	0
myrcene	0	<0.001 (<0.1%)	0	0	0	0
3-carene	0.008 (6.3%)	0	<0.001 (0.1%)	0.001 (1.4%)	0	0
ocimene	0.004 (3.2%)	1.200 (96.8%)	0.358 (96.4%)	0.038 (53.6%)	0.257 (93.4%)	0
limonene	0.004 (3.2%)	<0.001 (<0.1%)	0.003 (0.8%)	0	0	0
linalool	0.104 (81.7%)	0.033 (2.7%)	0.007 (1.9%)	0.028 (39.4%)	0.016 (5.8%)	0
p-cymene	0.003 (2.4%)	<0.001 (<0.1%)	<0.001 (0.2%)	0.001 (1.4%)	0	0
allo-ocimene	0	<0.001 (<0.1%)	0	0	0	0
eucalyptol	0.004 (3.2%)	0.004 (0.3%)	0.001 (0.3%)	0.002 (2.8%)	0.001 (0.4%)	0
SQTs (tot)	0	0.010 (<0.1%)	0.043 (0.1%)	0	0.007 (<0.1%)	0
α -farnesene	0	0	0.002 (4.7%)	0	0.007 (100%)	0
humulene	0	<0.001 (10.0%)	0.005 (11.6%)	0	0	0
caryophyllene	0	0.009 (90.0%)	0.036 (83.7%)	0	0	0
other VOCs (tot)	0.262 (0.6%)	0.172 (0.5%)	0.228 (0.6%)	0.176 (1.6%)	0.067 (0.4%)	0.029 (12.7%)
BVOCs (tot)	45.189 (100%)	34.021 (100%)	38.140 (100%)	11.347 (100%)	18.549 (100%)	0.229 (100%)
T_c	26.9 (3.5)	24.5 (6.0)	25.5 (4.8)	31.1 (6.4)	25.7 (4.4)	8.8 (2.9)
PAR_c	521 (149)	727 (494)	629 (365)	833 (445)	313 (235)	96 (126)

Table 5. Emission rates (STD for isoprene, MTs, and SQTs, $\mu\text{g g}_{\text{dw}}^{-1} \text{h}^{-1}$) and fraction (%) of the total BVOC emission or within the BVOC group (MTs and SQTs) from z_M in 2016. Bottom: average T_c ($^{\circ}\text{C}$), PAR_c ($\mu\text{mol m}^{-2} \text{s}^{-1}$), and the corresponding standard deviation for each month.

2016 z_M	May	June	July	Aug	Sep	Oct
isoprene	23.5 (95.3%)	48.7 (99.8%)	34.0 (97.4%)	60.5 (98.9%)	9.6 (96.0%)	2.8 (93.6%)
MTs (tot)	0.788 (3.2%)	0.005 (<0.1%)	0.147 (0.4%)	0.062 (0.1%)	0.012 (0.1%)	0.042 (1.4%)
α -pinene	0	<0.001 (15.9%)	0.004 (2.7%)	0	0	0.007 (16.7%)
myrcene	0	0	0	0	0	0
3-carene	0.002 (0.3%)	<0.001 (6.2%)	0.005 (3.4%)	0	0.003 (25.0%)	0.014 (33.3%)
ocimene	0.701 (89.0%)	0.003 (55.9%)	0.121 (82.3%)	0.057 (91.9%)	0	0
limonene	0	0	0.001 (0.7%)	0	0.003 (25.0%)	0.021 (50%)
linalool	0.071 (9.0%)	0	<0.001 (<0.1%)	0.005 (8.1%)	0	0
p-cymene	0.001 (0.1%)	0.001 (22.0%)	0.006 (4.1%)	0	0.004 (33.3%)	0
allo-ocimene	0	0	0	0	0	0
eucalyptol	0.013 (1.6%)	0	0.010 (6.8%)	0	0.002 (16.7%)	0
SQTs (tot)	0	0	0	0.086 (0.1%)	0	0
α -farnesene	0	0	0	0.021 (24.4%)	0	0
humulene	0	0	0	0.009 (10.5%)	0	0
caryophyllene	0	0	0	0.056 (65.1%)	0	0
other VOCs (tot)	0.359 (1.5%)	0.077 (0.2%)	0.761 (2.2%)	0.531 (0.9%)	0.386 (3.9%)	0.149 (5.0%)
BVOCs (tot)	24.647 (100%)	48.782 (100%)	34.908 (100%)	61.179 (100%)	9.998 (100%)	2.991 (100%)
T_c	25.7 (1.7)	25.4 (5.6)	23.1 (3.9)	31.1 (7.0)	24.3 (4.7)	8.6 (2.5)
PAR_c	1135 (406)	699 (469)	298 (254)	627 (450)	486 (342)	83 (123)

3.4. Light Response Curves with Leaf Chamber

Starting in the middle of July 2016 and ending in September, light response curves were measured with a leaf chamber at different heights (Table 2). The average emission of isoprene from z_H was $42.2 (\pm 31.6) \mu\text{g g}_{\text{dw}}^{-1} \text{h}^{-1}$ (or $2.42 \pm 1.69 \text{ mgC m}^{-2} \text{h}^{-1}$) and almost twice as high as z_L ($22.1 \pm 17.3 \mu\text{g g}_{\text{dw}}^{-1} \text{h}^{-1}$ or $1.22 \pm 0.84 \text{ mgC m}^{-2} \text{h}^{-1}$). The isoprene emission from z_M ($33.6 \pm 30.9 \mu\text{g g}_{\text{dw}}^{-1} \text{h}^{-1}$ or $1.58 \pm 1.54 \text{ mgC m}^{-2} \text{h}^{-1}$) was in between z_H and z_L but the average T_c and PAR_c for z_M ($22.7 \pm 2.4 ^{\circ}\text{C}$ and $497 \pm 451 \mu\text{mol m}^{-2} \text{s}^{-1}$, respectively) were lower than for z_H ($24.9 \pm 0.1 ^{\circ}\text{C}$ and $571 \pm 484 \mu\text{mol m}^{-2} \text{s}^{-1}$, respectively) and z_L (24.8 ± 0.1

$^{\circ}\text{C}$ and $571 \pm 484 \mu\text{mol m}^{-2} \text{s}^{-1}$, respectively). The corresponding STD emissions for these height levels were $96.1 (\pm 64.6) \mu\text{g g}_{\text{dw}}^{-1} \text{h}^{-1}$ (or $5.47 \pm 0.26 \text{ mgC m}^{-2} \text{h}^{-1}$) (Z_{H}), $94.1 (\pm 61.9) \mu\text{g g}_{\text{dw}}^{-1} \text{h}^{-1}$ (or $4.55 \pm 3.17 \text{ mgC m}^{-2} \text{h}^{-1}$) (Z_{M}), and $51.8 (\pm 32.9) \mu\text{g g}_{\text{dw}}^{-1} \text{h}^{-1}$ ($2.88 \pm 1.57 \text{ mgC m}^{-2} \text{h}^{-1}$) (Z_{L}). Both the measured and the STD isoprene emission for Z_{H} and Z_{L} were significantly different.

In particular, the response to PAR differed between the height levels under low-light conditions for measured isoprene emissions (Figure 4A). For instance, the slope between 0 and $150 \mu\text{mol m}^{-2} \text{s}^{-1}$ for Z_{H} was $0.140 \mu\text{g g}_{\text{dw}}^{-1} \text{h}^{-1}/(\mu\text{mol m}^{-2} \text{s}^{-1})$, while it was $0.058 \mu\text{g g}_{\text{dw}}^{-1} \text{h}^{-1}/(\mu\text{mol m}^{-2} \text{s}^{-1})$ for Z_{L} (Table S8). This fast response resulted in isoprene comprising more than 90% of the total BVOC emission already at $150 \mu\text{mol m}^{-2} \text{s}^{-1}$ for Z_{H} (Figure 5B). When comparing the STD isoprene emissions between Z_{L} and Z_{H} , then the slope of the fitted curves differed less for low PAR values (Figure S9 and Table S10).

The ratio between isoprene emission and net assimilation (E/A, dimensionless) showed that Z_{H} emitted more of the synthesized C as isoprene relative to the assimilated C, compared with Z_{M} and Z_{L} (Figure 4B). In particular, Z_{H} had the highest E/A ratio when PAR was $1000 \mu\text{mol m}^{-2} \text{s}^{-1}$ and more than 0.6% of the C was emitted as isoprene. For Z_{M} and Z_{L} , this value was less than 0.4% and 0.3%, respectively. Z_{L} was the only height level that increased the E/A ratio from $1000 \mu\text{mol m}^{-2} \text{s}^{-1}$ (ca 0.3%) to $1500 \mu\text{mol m}^{-2} \text{s}^{-1}$ (ca 0.46%).

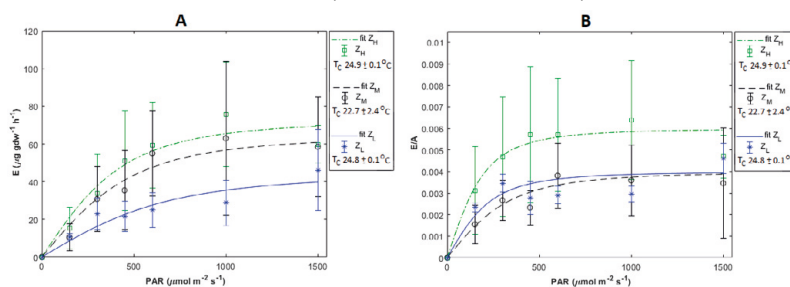


Figure 4. (A) Average isoprene emissions rates ($\mu\text{g g}_{\text{dw}}^{-1} \text{h}^{-1}$, mean \pm standard deviation, $n = 3-6$) and fitted curves for different PAR values ($\mu\text{mol m}^{-2} \text{s}^{-1}$) at different heights using Equation (2). The chamber temperature (T_{c} , mean \pm standard deviation, $n = 3-6$) for each height level is included in the legend. Parameter values can be seen in Table S8. (B) Ratio between isoprene and net assimilation (unitless, $n = 3-6$) for different PAR values at different heights. The chamber temperature (T_{c} , mean \pm standard deviation, $n = 3-6$) for each height level is included in the legend. The fitted curves are based on Equation (8) (see Supplementary) and the parameter values can be found in Table S11.

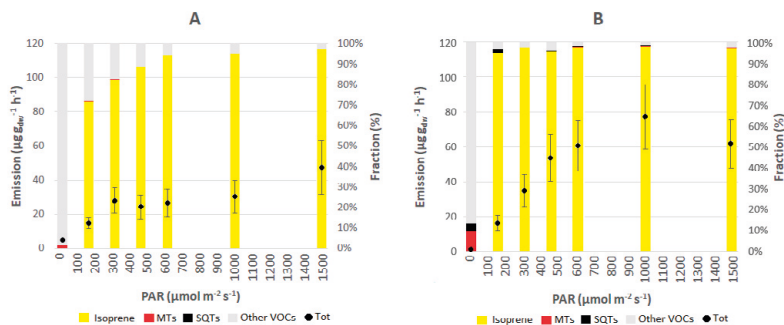


Figure 5. Total average emission rates ($\mu\text{g g}_{\text{dw}}^{-1} \text{h}^{-1} \pm$ standard deviation, black circles and left y -axis), and the percentages (stacked bars and right y -axis) for the different BVOC groups at different light levels ($\mu\text{mol m}^{-2} \text{s}^{-1}$). (A) Lower height (Z_{L} , $n = 3$). (B) Higher height (Z_{H} , $n = 5$).

One MT was seen at Z_L (limonene), four at Z_H (α -pinene, limonene, p-cymene, and ocimene), and five at Z_M (3-carene, α -pinene, limonene, p-cymene, and ocimene). Only ocimene seemed to be influenced by PAR and the average emission of ocimene increased when PAR varied from 300 to 1000 $\mu\text{mol m}^{-2} \text{s}^{-1}$ (Figure 6A). The MT emission from Z_H ($0.078 \pm 0.085 \mu\text{g g}_{\text{dw}}^{-1} \text{h}^{-1}$ or $0.004 \pm 0.005 \text{mgC m}^{-2} \text{h}^{-1}$) was almost twice as high as Z_L ($0.045 \pm 0.029 \mu\text{g g}_{\text{dw}}^{-1} \text{h}^{-1}$ or $0.002 \pm 0.002 \text{mgC m}^{-2} \text{h}^{-1}$). The MT fraction was in general lower than 1% for all heights and light levels, except when there was no light, due to no isoprene emission (Figure 5A,B and Figure S12).

No SQTs were emitted from Z_L . Three SQTs were observed at Z_H (α -farnesene, humulene, and nerolidol) and four at Z_M (α -farnesene, caryophyllene, humulene, and nerolidol). Average emissions of α -farnesene increased when PAR varied from 150 to 1000 $\mu\text{mol m}^{-2} \text{s}^{-1}$ (Figure 6A).

None of the observed other VOCs from the leaf chamber measurements showed a clear relationship with light. However, the emissions of a few compounds seemed to increase or decrease for certain PAR values. The average emission of 2-methylbutane increased from $0.145 (\pm 0.148) \mu\text{g g}_{\text{dw}}^{-1} \text{h}^{-1}$ to $0.226 (\pm 0.239) \mu\text{g g}_{\text{dw}}^{-1} \text{h}^{-1}$ when PAR varied between 0 and 300 $\mu\text{mol m}^{-2} \text{s}^{-1}$ and decreased thereafter (Figure 6B). The average emission of 2-ethylhexanoic acid ranged between 0.293 and $0.641 \mu\text{g g}_{\text{dw}}^{-1} \text{h}^{-1}$ for the PAR values 0–450 $\mu\text{mol m}^{-2} \text{s}^{-1}$, but the opposite trend was seen for 2-pentanone, the average emission of which decreased from 0.330 to $0 \mu\text{g g}_{\text{dw}}^{-1} \text{h}^{-1}$ when PAR increased from 150 to 1000 $\mu\text{mol m}^{-2} \text{s}^{-1}$.

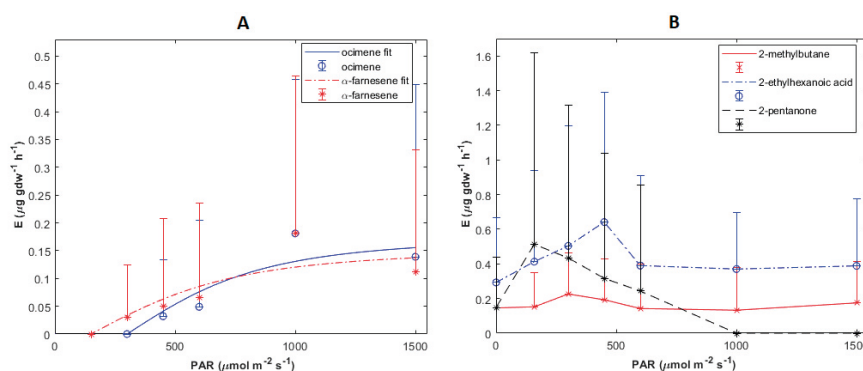


Figure 6. (A) Average emission ($\mu\text{g g}_{\text{dw}}^{-1} \text{h}^{-1}$, mean + standard deviation, $n = 11$) for ocimene (blue circles) and α -farnesene (red stars) from height levels Z_M and Z_H at different light levels. Fitted curves have been done by a modified Equation (2), where C_L has been replaced with Equation (9) for ocimene and Equation (10) for α -farnesene (see Supplementary for Equations (9) and (10) and Table S13 for values). (B) Average emission ($\mu\text{g g}_{\text{dw}}^{-1} \text{h}^{-1}$, mean + standard deviation, $n = 7-14$) for 2-methylbutane, (red cross), 2-ethylhexanoic acid, (blue circles), and 2-pentanone (black stars) from height levels Z_L and Z_M .

The average net assimilation at the maximum light intensity (1500 $\mu\text{mol m}^{-2} \text{s}^{-1}$) at Z_M ($21.30 \pm 2.92 \mu\text{mol CO}_2 \text{m}^{-2} \text{s}^{-1}$) and Z_H ($18.10 \pm 4.89 \mu\text{mol CO}_2 \text{m}^{-2} \text{s}^{-1}$) was higher than at Z_L ($12.05 \pm 3.01 \mu\text{mol CO}_2 \text{m}^{-2} \text{s}^{-1}$) (Figure 7A and Table 6). The average A values for each light step for Z_M and Z_H increased all the way up to 1500 $\mu\text{mol m}^{-2} \text{s}^{-1}$, while the average A for Z_L leveled out when PAR exceeded 600 $\mu\text{mol m}^{-2} \text{s}^{-1}$. (Figure 7A and Table S14).

Transpiration at Z_H was higher than at Z_M and Z_L when there was light (Figure 7B). Stomatal conductance at Z_H exceeded g_s at Z_M and Z_L at light intensities above 600 $\mu\text{mol m}^{-2} \text{s}^{-1}$ (Figure 7C). The lower height had the lowest g_s response to PAR but was mainly in between Z_H and Z_M for Tr. Water use efficiency was similar for Z_H and Z_L when PAR varied between 0 and 450 $\mu\text{mol m}^{-2} \text{s}^{-1}$; thereafter, Z_H increased to ca $6 \text{mmol CO}_2 \text{mol}^{-1} \text{H}_2\text{O}$ while

z_L was more or less constant and remained below $5 \text{ mmol CO}_2 \text{ mol}^{-1} \text{ H}_2\text{O}$ (Figure 7D). On the other hand, WUE for z_M was approximately twice as high as for z_H and z_L for $450\text{--}1500 \text{ } \mu\text{mol m}^{-2} \text{ s}^{-1}$.

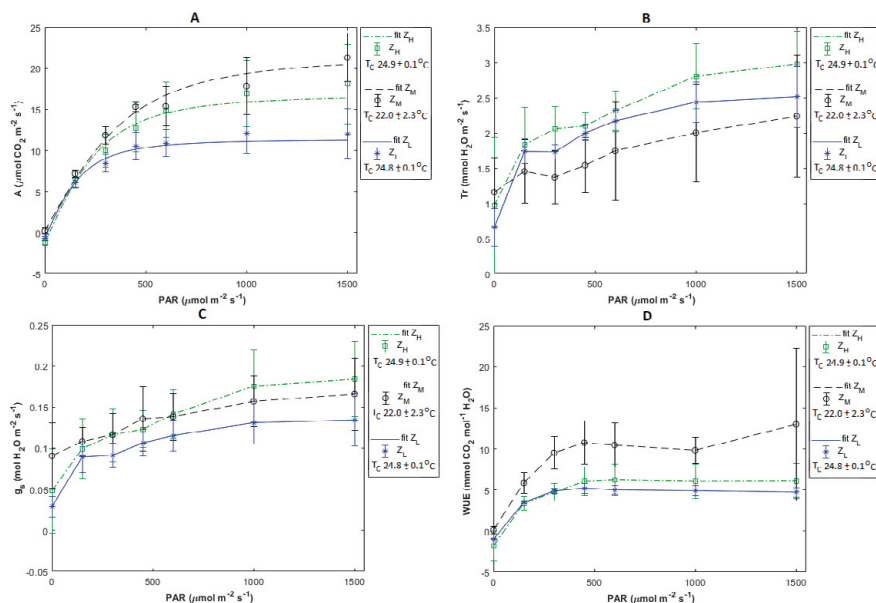


Figure 7. (A) Net assimilation (A , mean \pm SD, $\mu\text{mol CO}_2 \text{ m}^{-2} \text{ s}^{-1}$, $n = 2\text{--}6$) and fitted curves by using Equation (6) (values of parameters can be seen in Table S15), (B) transpiration (Tr , mean \pm SD, $\text{mmol H}_2\text{O m}^{-2} \text{ s}^{-1}$, $n = 2\text{--}6$), (C) stomatal conductance (g_s , mean \pm SD, $\text{mol H}_2\text{O m}^{-2} \text{ s}^{-1}$, $n = 2\text{--}6$), and (D) water use efficiency (WUE, mean \pm standard deviation, $\text{mmol CO}_2 \text{ mol}^{-1} \text{ H}_2\text{O}$, $n = 2\text{--}6$) for different PAR ($\mu\text{mol m}^{-2} \text{ s}^{-1}$) and height levels. The chamber temperature (T_c , mean \pm standard deviation, $n = 3\text{--}6$) for each height level is included in all legends.

Table 6. Net assimilation (A , mean \pm SD, $\mu\text{mol CO}_2 \text{ m}^{-2} \text{ s}^{-1}$, $n = 3\text{--}6$), transpiration (Tr , $\text{mmol H}_2\text{O m}^{-2} \text{ s}^{-1}$, $n = 3\text{--}6$), water use efficiency (WUE, mean \pm standard deviation, $\text{mmol CO}_2 \text{ mol}^{-1} \text{ H}_2\text{O}$, $n = 3\text{--}6$), and stomatal conductance (g_s , $\text{mol H}_2\text{O m}^{-2} \text{ s}^{-1}$, $n = 3\text{--}6$) at $1500 \text{ } \mu\text{mol m}^{-2} \text{ s}^{-1}$ for different height levels.

PAR = $1500 \text{ } \mu\text{mol m}^{-2} \text{ s}^{-1}$	Lower (z_L)	Middle (z_M)	Higher (z_H)
A ($\mu\text{mol CO}_2 \text{ m}^{-2} \text{ s}^{-1}$)	12.05 (3.01)	21.30 (2.92)	18.10 (4.89)
Tr ($\text{mmol H}_2\text{O m}^{-2} \text{ s}^{-1}$)	2.51 (0.43)	2.24 (0.97)	2.98 (0.47)
WUE ($\text{mmol CO}_2 \text{ mol}^{-1} \text{ H}_2\text{O}$)	4.73 (0.55)	12.99 (9.28)	6.10 (2.13)
g_s ($\text{mol H}_2\text{O m}^{-2} \text{ s}^{-1}$)	0.13 (0.03)	0.17 (0.04)	0.18 (0.05)

4. Discussion

4.1. Isoprene Emissions, Net Assimilation, and Water Use Efficiency

As expected, isoprene was the dominant compound throughout the growing season and made up 90%–99% of the total BVOC emission, with measured emission rates reaching up to $150 \text{ } \mu\text{g g}_{\text{dw}}^{-1} \text{ h}^{-1}$. The STD isoprene emission rate averaged over the whole study ($45.2 \text{ } \mu\text{g g}_{\text{dw}}^{-1} \text{ h}^{-1}$) is comparable to what has been shown in other studies [13,58,59]. However, the reported range of STD isoprene emission rates is wide [13,59]. In Morrison et al. [59], the STD isoprene emission for unknown *Salix* spp. varieties varied from 0.1 to $15.9 \text{ } \mu\text{g g}_{\text{dw}}^{-1} \text{ h}^{-1}$ for three different sites in the United Kingdom. In their study, a similar method was used as in this study but since they included the whole year, a lower emission can be

expected on account of the low temperature and PAR during the non-peak season. Moreover, the age of the measured trees was not the same in their study (first, second, and third growing season) as in this study (third and fourth growing season). Another study done close to our site reported a ca 6 times lower STD isoprene emission from clones that originated from the same species (*S. viminalis*) as was measured in this study, during peak summer [44]. In their study, a relaxed eddy accumulation technique scaled by foliar mass density was used, which is a different method compared with the methods used in this study and could therefore explain the disparity. In particular, this method includes measurements from the whole canopy, i.e., both sun-exposed and shaded leaves, whereas most leaves in this study were adapted to sunlit conditions. Additionally, emission rates vary within the same species [13], which can explain why the average STD isoprene emission in 2015 was twice as high as in 2016, despite similar T_c and PAR_c , since the plantations contained different varieties. According to Karlsson et al. [42], it has been shown that *Salix* varieties growing on SRC fields emit various amounts of isoprene and that the Tora-variety growing on P2 is a low emitter.

The seasonal patterns for isoprene emissions in the two *Salix* varieties we measured in 2015 and 2016 were similar. The highest emission rates typically occurred when weather was warm and sunny. The measurements in 2016 showed that the trees were able to emit high rates of isoprene already in the beginning of May. At this point, the weather had started to become warmer, which resulted in the trees developing small leaves with a light green color. It is well known that isoprene emission is influenced by temperature because of the linkage to the enzyme isoprene synthase [60,61]. In September, measured and STD isoprene emissions during 2015 and 2016 started to decline compared with the former months. In October 2016, isoprene emissions were negligible. The reason for the declining trend is mostly explained by changing weather (2015), and the approaching fall and leaf senescence [62,63]. In particular, all isoprene emissions were $<3.0 \mu\text{g g}_{\text{dw}}^{-1} \text{h}^{-1}$ and most of the samples contained no isoprene during October. Zero emissions of isoprene occurred when T_c was ca 11°C or lower, and $PAR_c < 110 \mu\text{mol m}^{-2} \text{s}^{-1}$, indicating that these values could be a threshold for isoprene emission during late season for this location and variety. These growing conditions in combination with the leaf damage caused by *P. vulgatisissima* explain why the isoprene emissions from z_H were exceptionally low in October since many leaves at z_H were almost gone and more or less only the midrib was left (Figure S3).

The *Melampsora* infestation on P1 likely affected the emission rates. Toome et al. [64] showed that willow trees infected with *Melampsora* reduced their isoprene emission rates by almost 30% and a similar result was observed for *Populus* [65]. Perhaps, the isoprene emissions would have been even higher in 2015 if no *Melampsora* outbreak had occurred.

Measured and STD isoprene emissions from the more sunlit leaves (z_H) exceeded emission rates from shaded leaves (z_L) as expected [45,66,67]. Previous studies have reported a hyperbolic curve for isoprene when PAR increases [55,68,69], which can be linked to the photosynthetic electron transport [69,70], and a similar behavior was observed in this study. Isoprene emissions from sun-adapted leaves at z_H responded faster to increased light, and reached twice as high maximum emission rates. This result is in line with Sharkey et al. [66], who studied isoprene emissions from oak and aspen, and it also points out that large errors can be expected if up-scaled emissions are based on data from only one canopy height [45].

The isoprene emission increased exponentially with temperature but it is hard to state if the optimum temperature was reached in our study. In a subarctic *Salix myrsinites*, isoprene emission increased exponentially across the temperature range of $10\text{--}38^\circ\text{C}$ without reaching a maximum [71]. According to Niinemets et al. [72], the optimum often occurs around 40°C , suggesting that this could be the same for the varieties in this study. Nevertheless, measurements at higher temperatures are needed to confirm this.

The net assimilation was higher for z_H compared with z_L , but lower than for z_M . An increasing A pattern with canopy height has been reported previously [73,74]. Since also

Tr from z_M was below the others, this resulted in a higher WUE for z_M , making these leaves more efficient in their water use than the leaves at z_L and z_H . The E/A ratio at z_H exceeded that at z_L , which means that the light-adapted leaves in the upper part of the canopy lose more C as isoprene than less light-adapted leaves. However, despite the lower isoprene emission rates from the shaded leaves at z_L , they showed a strong increase (ca 50%) in their E/A ratio when PAR increased from 1000 to 1500 $\mu\text{mol m}^{-2} \text{s}^{-1}$. So, even for leaves less acclimatized to sunlight, isoprene serves as a strongly induced compound when the leaves are light-stressed. The leaves that were more sun-adapted (z_H and z_M) did not show this pattern.

Measurements of A and simultaneously emitted BVOCs showed that the trees only use a minor fraction (0.4%) of photosynthetic C for BVOC emission, although compounds with less than five carbon units (i.e., methanol, acetone) were not detectable with the methods used in this study. This ratio is comparable with the results from a study conducted during summer on a spruce forest, where the assimilated C loss on average was approximately 0.3% [75]. For isoprene, the ratio between emitted C and A was similar to what had been found for some species of poplar [76], which are also known to be high isoprene emitters. Only a small percentage of the net carbon assimilation is in general released as BVOCs [77–80] but under stressed conditions, carbon loss can be 7%–8% due to increased isoprene emissions [68,81].

The maximum A for the sunlit leaves is in line with results in other studies, which suggest that A for *Salix* trees can vary between 10 to 35 $\mu\text{mol CO}_2 \text{m}^{-2} \text{s}^{-1}$ [42,82]. The WUE values for z_L and z_H were comparable with the values for Tora reported in Karlsson et al. [42].

The variety Tora in Karlsson et al. [42] had a ca 80% lower STD isoprene emission compared with Tora on P2 when comparing the leaf chamber measurements for sun-adapted leaves. This difference is probably due to the fact that the trees were younger (first and second growing season) in Karlsson et al. [42].

Changing from traditional crops, e.g., wheat, rye, oat, or oilseed rape, which are low emitters of isoprene [59,83–85] to a SRC (e.g., willow) would drastically alter the regional concentration of isoprene and increase the risk of O_3 production near polluted areas [86–88].

4.2. Emissions of Monoterpenes, Sesquiterpenes, and Other Volatile Organic Compounds

The second most emitted compound was ocimene and together with α -pinene, they contributed with more than 95% to the MT emission throughout 2015. In 2016, ocimene dominated over the other MTs, followed by limonene, p-cymene, and linalool. Even if the emission rates of the compounds varied individually during the season, both 2015 and 2016 showed the same trend, where the measured average total emission of MTs decreased across the measurement periods, but occasional higher emissions were still possible in late summer and autumn. Emissions of MTs can be dependent on the season and willow leaves have shown a stronger capacity to emit MTs in the beginning of the growing season close to bud break [59,89]. However, we cannot verify this suggestion as we did not measure in early spring. The most abundant SQTs were caryophyllene, humulene, and α -farnesene. The emissions of these compounds peaked in the second part of the growing season between July and September. No SQTs could be observed during May and October.

Ocimene and α -farnesene were the only terpenes, besides isoprene, that were influenced by PAR. Ocimene was also found to increase with light by Karlsson et al. [42]. Many studies have shown a correlation between terpenes and light [42,90–92]. This similarity with isoprene shows that emissions of some MTs and SQTs could be described by a similar light- and temperature-dependent algorithm developed by Guenther et al. [55] for short-term emissions.

Shade-adapted leaves at z_L emitted less MTs and had lower emission rates than the sun-adapted leaves at z_H but the emissions from z_M were higher than z_H in May and

October. The only month when the SQT emission from the lower height (z_M) exceeded that from the higher height level (z_H) was in August. Neither ocimene nor α -farnesene were emitted from z_L , which suggests that the leaves require an adaptation to an environment with sufficient sunlight to be able to emit these terpenes. Monoterpenes and SQTs are very reactive and protect the plant against different abiotic and biotic stresses [49,93–100].

Several times higher emissions of other VOCs were observed in August 2015 compared with the other months this year. The compounds responsible for these emission rates (e.g., benzaldehyde, nonanal, octanal, decanal, and hexanal) have been reported to be induced during abiotic and biotic stresses [65,101–104]. Jiang et al. [65] reported induced emissions of nonanal and decanal from *Populus* leaves infested by *Melampsora*. Toome et al. [64] also studied the impact of *Melampsora* and showed that an infection on willow trees resulted in increased emission of some GLVs (e.g., (Z)-3-hexenol and (E)-2-hexenal), as well as (Z)- β -ocimene and (E,E)- α -farnesene. Moreover, Arimura et al. [105] observed stress-induced emissions of (E)- β -ocimene, linalool, and (E,E)- α -farnesene from poplar leaves eaten by caterpillar. The higher emissions of α -farnesene and caryophyllene might have been a consequence of the *Melampsora* infestation (2015) and herbivore insects (2016).

Emissions of other VOCs were larger from the lower canopy height compared with the higher canopy height, but it is difficult to pinpoint the underlying reason. If the leaves were more attractive to leaf-eating insects at the upper canopy, one would expect higher emission rates from this level as a self-defending mechanism [94,106]. On the other hand, the higher emission rates from the lower canopy could be the reason why these beetles strike the upper part. However, one explanation for the difference might be related to how the leaves looked. In July and August, the leaves at the lower height were smaller with a brighter green color compared with the higher height. Further, the damage by *P. vulgatis-sima* is believed to have reduced the emission from the upper part of the canopy, especially in October.

Most studies have only focused on isoprene and a few other compounds, which usually are most abundant [43,59,107,108]. Even if isoprene is dominant and crucial for air chemistry processes, other compounds might also be of importance. Monoterpenes constitute a group responsible for particle formation and generation of SOAs [38,109]. Additionally, stress-induced compounds are usually not included (yet) in modeling processes, but biogenic non-terpenoids can contribute with the same magnitude as anthropogenic sources of non-terpenoids to SOA formation and should not be discarded [104].

5. Summary and Conclusions

We studied seasonal trends and canopy height differences for BVOC emissions of willow varieties growing as bio-energy crops on SRC fields. The majority of the measurements in 2015 were done on an unknown variety belonging to *S. viminalis*, while all measurements in 2016 were on the variety Tora. The results from this study confirm that isoprene was the most dominant BVOC during the major part of the growing season. Emissions of MTs, SQTs, and other VOCs were in general only a minor fraction of the total BVOC emission. The prevailing infestation of *Melampsora* (2015) was probably responsible for increased emissions of, e.g., nonanal, hexanal, and caryophyllene.

The emissions of isoprene peaked during summer (in July 2015 and in August 2016) but the leaves had high emissions already in May. The seasonal pattern for SQTs showed that these peaked during summer as well. Emissions of MTs showed a decreasing trend from May to October and the overall terpenoid emission seemed to be substantially lower by the end of the growing season as a consequence of colder weather and proceeding leaf senescence.

Our study suggests that Tora is a better choice when it comes to having a reduced risk for impaired air quality since it emitted ca 50% less isoprene, which can be a source for O₃ and peroxyacetyl nitrate. Nevertheless, *Salix* trees are high emitters of isoprene

compared with commercial crops, and an expansion of *Salix* plantations would need to be strategically planned and placed at a sufficiently long distance away from pollution sources to avoid elevated photochemical production of O₃ under high NO_x conditions.

Leaves higher up in the canopy and acclimatized to more sunlight emitted higher rates of isoprene than the leaves growing in the lower and more shaded parts of the canopy. Emissions of MTs were also lower for the leaves in the shaded conditions and no SQT emissions were observed from the shade-adapted leaves. On the contrary, emissions of non-terpenoids were higher from the lower part of the canopy. These results point out that the location within the canopy is one important factor when it comes to emissions of different compounds, particularly those compounds that are dependent on PAR. Hence, to make better estimations of the regional and global BVOC fluxes, models need to adjust for, e.g., the vertical distribution of leaf area within the canopy layer.

Ocimene and α -farnesene were the only compounds, except isoprene, that were influenced by light, suggesting that they can be modeled with a similar algorithm as isoprene.

This study highlights that scaling-up BVOC emissions and basing models on one simplified emission potential for the whole canopy could lead to large errors.

Supplementary Materials: Figure S1: Photos of the two plots. Figure S2: Photos of *Melampsora*-infested leaves. Figure S3: Photos of leaves in October. Table S4: Injected standards in GC-MS. Table S5: Average emission values for all detected compounds. Table S6: Average emission, T_c and PAR_c for each month of 2015. Table S7: Parameter values for fitted isoprene curves in Figure 3. Table S8: Slope and parameter values for fitted curves in Figure 4A. Figure S9: STD isoprene emission vs. PAR. Table S10: Parameter values for fitted isoprene curves in Figure S9. Table S11: Parameter values for fitted E/A curves in Figure 4B. Figure S12: Total average BVOC emission and fraction vs. PAR at z_m. Table S13: Parameter values for fitted emission curves in Figure 6A,B. Table S14: Slope values for A in Figure 7A. Table S15: Parameter values for fitted A curves in Figure 7A.

Author Contributions: Conceptualization, T.H. and T.K.; methodology, T.H.; software, T.H.; validation, T.K. and T.H.; formal analysis, T.K.; investigation, T.K.; data curation, T.K. T.H., and R.R.; resources, T.H., R.R., and L.K.; writing—original draft preparation, T.K.; writing—review and editing, T.K., R.R., L.K., and T.H.; supervision T.H.; project administration, T.K. and T.H.; funding acquisition, T.H. All authors have read and agreed to the published version of the manuscript.

Funding: This study was partly financed by the Swedish Research Council for Sustainable Development (FORMAS) under grant 2012-727.

Institutional Review Board Statement: Not applicable

Informed Consent Statement: Not applicable

Data Availability Statement: Data from this study is available from the corresponding author upon reasonable request.

Acknowledgments: We thank Swedish Infrastructure for Ecosystem Science (SITES) for the logistic support. Additionally, we thank Anders Jonsson and Per-Olof Andersson in Gråstorp for their permission to conduct measurements and helping out at the site.

Conflicts of Interest: The authors declare no conflicts of interest. The funders had no role in the design of the study; in the collection, analyses, or interpretation of data; in the writing of the manuscript; or in the decision to publish the results.

References

1. *A Policy Framework for Climate and Energy in the Period from 2020 up to 2030*; European Commission: Brussels, Belgium, 2014.
2. IPCC. 2021: Summary for Policymakers. In *Climate Change 2021: The Physical Science Basis. Contribution of Working Group I to the Sixth Assessment Report of the Intergovernmental Panel on Climate Change*; Masson-Delmotte, V., Zhai, P., Pirani, A., Connors, S.L., Péan, C., Berger, S., Caud, N., Chen, Y., Goldfarb, L., Gomis, M.I., et al., Eds.; Cambridge University Press, Cambridge, United Kingdom, 2021; In Press.
3. Bonde, I.; Kuylenstierna, J.; Bäckstrand, K.; Eckerberg, K.; Käberger, T.; Löfgren, Å.; Rummukainen, M.; Sörlin, S. *2020-Report of the Swedish Climate Policy Council*; Rapport nr 3: Swedish Climate Policy Council, Stockholm, Sweden, 2020, ISBN 978-91-984671-4-7.

4. Don, A.; Osborne, B.; Hastings, A.; Skiba, U.; Carter, M.S.; Drewer, J.; Flessa, H.; Freibauer, A.; Hyvönen, N.; Jones, M.B.; et al. Land-use change to bioenergy production in Europe: Implications for the greenhouse gas balance and soil carbon. *Glob. Chang. Biol. Bioenergy* **2011**, *4*, 372–391.
5. Lindgaard, K.N.; Adams, P.W.; Holley, M.; Lamley, A.; Henriksson, A.; Larsson, S.; von Engelbrechten, H.G.; Esteban Lopez, G.; Pisarek, M. Short rotation plantations policy history in Europe: Lessons from the past and recommendations for the future. *Food Energy Secur.* **2016**, *5*, 125–152.
6. Kimming, M.; Sundberg, C.; Nordberg, Å.; Baky, A.; Bernesson, S.; Norén, O.; Hansson, P.A. Biomass from agriculture in small-scale combined heat and power plants—A comparative life cycle assessment. *Biomass Bioenerg.* **2011**, *35*, 1572–1581.
7. Åhman, I.; Larsson, S. *Resistensförädling i Salix för Energiproduktion, SLU*; Institutionen för entomologi, Nr/avsnitt: 2; SLU: Alnarp, Sweden, 1999.
8. Kägi, T.; Deimling, S.; Knuchel, R.F.; Gaillard, G.; Hölscher, T.; Müller-Sämann, K. Environmental impacts of annual and perennial energy crops compared to a reference crop rotation. In Proceedings of the Empowerment of the Rural Actors: A Renewal of Farming Systems Perspectives 8th European IFSA Symposium, Clermont-Ferrand, France, 6–10 July 2008; pp. 675–681.
9. Fredga, K.; Danell, K.; Frank, H.; Hedberg, D.; Kullander, S. Bioenergy—Opportunities and constraints. In *Energy Committee Report*; Kungliga Vetenskapsakademien: Stockholm, Sweden, 2008.
10. Landberg, T.; Greger, M. Differences in uptake and tolerance to heavy metals in Salix from unpolluted and polluted areas. *Appl. Geochem.* **1996**, *11*, 175–180.
11. Meers, E.; Vandecasteele, B.; Ruttens, A.; Vangronsveld, J.; Tack, F. Potential of five willow species (*Salix* spp.) for phytoextraction of heavy metals. *Environ. Exp. Bot.* **2007**, *60*, 57–68.
12. SOU 2007:36. *Bioenergi från jordbruket—en Växande Resurs*; Statens Offentliga Utredningar; Edita Sverige AB: Stockholm, Sweden, 2007, ISBN 978-91-38-22751-0.
13. Kesselmeier, J.; Staudt, M. Biogenic volatile organic compounds (VOC): An overview on emission, physiology and ecology. *J. Atmos. Chem.* **1999**, *33*, 23–88.
14. Dicke, M.; Vet, L.E.M. Plant-carnivore interactions: Evolutionary and ecological consequences for plant, herbivore and carnivore. In *Herbivores: Between Plants and Predators*; Olff, H., Brown, V.K., Drent, R.H., Eds.; Blackwell Science: Oxford, UK, 1999; pp. 483–520.
15. Llusà, J.; Peñuelas, J. Emission of volatile organic compounds by apple trees in response to spider mite attack and attraction of predatory mites. *Exp. Appl. Acarol.* **2001**, *25*, 65–77.
16. Dicke, M.; van Poecke, R.M.P.; de Boer, J.G. Inducible indirect defence of plants: From mechanisms to ecological functions. *Basic Appl. Ecol.* **2003**, *4*, 27–42.
17. Dudareva, N.; Pichersky, E. Metabolic engineering of plant volatiles. *Curr. Opin. Biotech.* **2008**, *19*, 1–9.
18. Laothawornkitkul, J.; Taylor, J.; Paul, N.; Hewitt, C. Biogenic volatile organic compounds in the Earth system. *New Phytol.* **2009**, *183*, 27–51.
19. Possell, M.; Loreto, F. The role of volatile organic compounds in plant resistance to abiotic stresses: Responses and mechanisms. In *Biology, Controls and Models of Tree Volatile Organic Compound Emissions*; Tree Physiology; Niinemets, Ü., Monson, R.K., Eds.; Springer: Berlin/Heidelberg, Germany, **2013**; Volume 5, pp. 209–235.
20. Folberth, G.A.; Hauglustaine, D.A.; Lathière, J.; and Brocheton, F. Interactive chemistry in the Laboratoire de Météorologie Dynamique general circulation model: Model description and impact analysis of biogenic hydrocarbons on tropospheric chemistry. *Atmos. Chem. Phys.* **2006**, *6*, 2273–2319.
21. Arneth, A.; Monson, R.K.; Schurgers, G.; Niinemets, Ü.; Palmer, P.I. Why are estimates of global terrestrial isoprene emissions so similar (and why is this not so for monoterpenes)? *Atmos. Chem. Phys.* **2008**, *8*, 4605–4620.
22. Calfapietra, C.; Fares, S.; Manes, F.; Morani, A.; Sgrigna, G.; Loreto, F. Role of biogenic volatile organic compounds (BVOC) emitted by urban trees on ozone concentration in cities: A review. *Environ. Pollut.* **2013**, *183*, 71–80.
23. Chameides, W.L.; Lindsay, R.W.; Richardson, J. The Role of Biogenic Hydrocarbons in Urban Photochemical Smog: Atlanta as a Case Study. *Science* **1988**, *241*, 1473–1475.
24. Ryerson, T.B.; Trainer, M.; Holloway, J.S.; Parrish, D.D.; Huey, L.G.; Sueper, D.T.; Frost, G.J.; Donnelly, S.G.; Schaufli, S.; Atlas, E.L.; et al. Observations of Ozone Formation in Power Plant Plumes and Implications for Ozone Control Strategies. *Science* **2001**, *292*, 719.
25. Kleinman, L.I.; Daum, P.H.; Imre, D.; Lee, Y.-N.; Nunnermacker, L.J.; Springston, S.R.; Weinstein-Lloyd, J.; Rudolph, J. Ozone production rate and hydrocarbon reactivity in 5 urban areas: A cause of high ozone concentration in Houston. *Geophys. Res. Lett.* **2002**, *29*, 105-1–105-4.
26. Fares, S.; Barta, C.; Ederli, L.; Ferranti, F.; Pasqualini, S.; Reale, L.; Brilli, F.; Tricoli, D.; Loreto, F. Impact of high ozone on isoprene emission and some anatomical and physiological parameters of developing *Populus alba* leaves directly or indirectly exposed to the pollutant. *Physiol. Plant.* **2006**, *128*, 456–465.
27. Wittig, V.E.; Ainsworth, E.A.; Naidu, S.L.; Karnoski, D.F.; Long, S.P. Quantifying the impact of current and future tropospheric ozone on tree biomass, growth, physiology and biochemistry: A quantitative meta-analysis. *Glob. Chang. Biol.* **2009**, *15*, 396–424.
28. Kurpius, M.R.; Goldstein, A.H. Gas-phase chemistry dominates O₃ loss to a forest, implying a source of aerosols and hydroxyl radicals to the atmosphere. *Geophys. Res. Lett.* **2003**, *30*, 1371.

29. Agyei, T.; Juráň, S.; Kwakye, K.O.; Šigut, L.; Urban, O.; Marek, M.V. The impact of drought on total ozone flux in a mountain Norway spruce forest. *J. For. Sci.* **2020**, *66*, 280–287.
30. Ashmore, M.R. Assessing the future global impacts of ozone on vegetation. *Plant Cell Environ.* **2005**, *28*, 949–964.
31. Sitch, S.; Cox, P.M.; Collins, W.J.; Huntingford, C. Indirect radiative forcing of climate change through ozone effects on the land-carbon sink. *Nature* **2007**, *448*, 791–794.
32. Hoffmann, T.; Odum, J.R.; Bowman, F.; Collins, D.; Klockow, D.; Flagan, R.C.; Seinfeld, J.H. Formation of organic aerosols from the oxidation of biogenic hydrocarbons. *J. Atmos. Chem.* **1997**, *26*, 189–222.
33. O’Dowd, C.D.; Jimenez, J.L.; Bahreini, R.; Flagan, R.C.; Seinfeld, J.H.; Hämeri, K.; Pirjola, L.; Kulmala, M.; Jennings, S.G.; Hoffmann, T. Marine aerosol formation from biogenic iodine emissions. *Nature* **2002**, *417*, 497–501.
34. Claeys, M.; Graham, B.; Vas, G.; Wang, W.; Vermeylen, R.; Pashynska, V.; Cafmeyer, J.; Guyon, P.; Andreae, M.O.; Artaxo, P.; et al. Formation of secondary organic aerosols through photooxidation of isoprene. *Science* **2004**, *303*, 1173–1176.
35. Kulmala, M.; Suni, T.; Lehtinen, K.E.J.; Dal Maso, M.; Boy, M.; Reissell, A.; Rannik, Ü.; Aalto, P.; Keronen, P.; Hakola, H.; Bäck, J.; et al. A new feedback mechanism linking forests, aerosols, and climate. *Atmos. Chem. Phys.* **2004**, *4*, 557–562.
36. VanReken, T.M.; Greenberg, J.P.; Harley, P.C.; Guenther, A.B.; Smith, J.N. Direct measurement of particle formation and growth from the oxidation of biogenic emissions. *Atmos. Chem. Phys.* **2006**, *6*, 4403–4413.
37. Spracklen, D.V.; Bonn, B.; Carslaw, K.S. Boreal forests, aerosols and the impacts on clouds and climate. *Phil. Trans. R. Soc. A* **2008**, *366*, 4613–4626.
38. Paasonen, P.; Asmi, A.; Petäjä, T.; Kajos, M.K.; Äijälä, M.; Junninen, H.; Holst, T.; Abbatt, J.P.D.; Arneth, A.; Birmili, W.; et al. Warming-induced increase in aerosol number concentration likely to moderate climate change. *Nat. Geosci.* **2013**, *6*, 438–442.
39. Ehn, M.; Thornton, J.A.; Kleist, E.; Sipilä, M.; Junninen, H.; Pullinen, I.; Springer, M.; Rubach, F.; Tillmann, R.; Lee, B.; et al. A large source of low-volatility secondary organic aerosol. *Nature* **2014**, *506*, 476–479.
40. Boucher, O.; Randall, P.D.; Artaxo, C.; Bretherton, G.; Feingold, P.; Forster, V.-M.; Kerminen, Y.; Kondo, H.; Liao, U.; Lohmann, P.; et al. 2013: Clouds and Aerosols. In *Climate Change 2013: The Physical Science Basis. Contribution of Working Group I to the Fifth Assessment Report of the Intergovernmental Panel on Climate Change*; Stocker, T.F., Qin, D., Plattner, G.-K., Tignor, M., Allen, S.K., Boschung, J., Nauels, A., Xia, Y., Bex, V., Midgley, P.M., Eds.; Cambridge University Press: Cambridge, UK; New York, NY, USA, 2013.
41. Vedel-Petersen, I.; Schollert, M.; Nymand, J.; Rinnan, R. Volatile organic compound emission profiles of four common arctic plants. *Atmos. Environ.* **2015**, *120*, 117–126.
42. Karlsson, T.; Rinnan, R.; Holst, T. Variability of BVOC Emissions from Commercially Used Willow (*Salix* spp.) Varieties. *Atmosphere* **2020**, *11*, 356.
43. Owen, S.M.; Boissard, C.; Hewitt, C.N. Volatile organic compounds (VOCs) emitted from 40 Mediterranean plant species: VOC speciation and extrapolation to habitat scale. *Atmos. Environ.* **2001**, *35*, 5393–5409.
44. Olofsson, M.; Ekolausson, B.; Jensen, N.; Langer, S.; Ljungström, E. The flux of isoprene from a willow coppice plantation and the effect on local air quality. *Atmos. Environ.* **2005**, *39*, 2061–2070.
45. Niinemets, Ü.; Copolovici, L.; Hüve, K. High within-canopy variation in isoprene emission potentials in temperate trees: Implications for predicting canopy-scale isoprene fluxes. *J. Geophys. Res.* **2010**, *115*, G04029.
46. Persson, Y.; Schurgers, G.; Ekberg, A.; Holst, T. Effects of intra-genotypic variation, variance with height and time of season on BVOC emissions. *Meteorol. Z.* **2016**, *25*, 377–388.
47. Alexandersson, H.; Eggertsson Karlström, C. *Temperaturer och nederbörden i Sverige 1961–90: Referensnormaler—utgåva 2. Meteorologi 99*; Swedish Meteorological and Hydrological Institute: Norrköping, Sweden, 2001. (In Swedish)
48. SGU, Geology Survey of Sweden. Available online: <http://maps-test.sgu.se:8080/TestSguMapView2/kartvisare-lerhaltskarta-sv.html> (accessed on 7 March 2019).
49. Haapanala, S.; Ekberg, A.; Hakola, A.; Tarvainen, V.; Rinne, J.; Hellén, H.; Arneth, A. Mountain birch—Potentially large source of sesquiterpenes into high latitude atmosphere. *Biogeosciences* **2009**, *6*, 2709–2718.
50. van Meeningen, Y.; Wang, M.; Karlsson, T.; Seifert, A.; Schurgers, G.; Rinnan, R.; Holst, T. Isoprenoid emission variation of Norway spruce across a European latitudinal transect. *Atmos. Environ.* **2017**, *170*, 45–57.
51. Wang, M.; Schurgers, G.; Arneth, A.; Ekberg, A.; Holst, T. Seasonal variation in biogenic volatile organic compound (BVOC) emissions from Norway spruce in a Swedish boreal forest. *Boreal Environ. Res.* **2017**, *22*, 353–367.
52. van Meeningen, Y.; Schurgers, G.; Rinnan, R.; Holst, T. Isoprenoid emission response to changing light conditions of English oak, European beech and Norway spruce. *Biogeosciences* **2017**, *14*, 4045–4060.
53. Lindwall, F.; Svendsen, S.S.; Nielsen, C.S.; Michelsen, A.; Rinnan, R. Warming in-creases isoprene emissions from an arctic fen. *Sci. Total Environ.* **2016**, *553*, 297–304.
54. Ortega, J.; Helmig, D. Approaches for quantifying reactive and low-volatility biogenic organic compound emissions by vegetation enclosure techniques—Part A. *Chemosphere* **2008**, *72*, 343–364.
55. Guenther, A.B.; Zimmerman, P.; Harley, P.C.; Monson, R.K.; Fall, R. Isoprene and monoterpene emission rate variability: Model evaluations and sensitivity analyses. *J. Geophys. Res.* **1993**, *98*, 12609–12617.
56. Helmig, D.; Ortega, J.; Duhl, T.; Tanner, D.; Guenther, A.; Harley, P.; Wiedinmyer, C.; Milford, J.; Sakulyanontvittaya, T. Sesquiterpene Emissions from Pine Trees – Identifications, Emission Rates and Flux Estimates for the Contiguous United States. *Environ. Sci. Technol.* **2007**, *41*, 1545–1553.

57. Niinemets, Ü.; Sun, Z.; Talts, E. Controls of the quantum yield and saturation light of isoprene emission in different-aged aspen leaves. *Plant Cell Environ.* **2015**, *38*, 2707–2720.
58. Owen, S.M.; Hewitt, C.N. Extrapolating branch enclosure measurements to estimates of regional scale biogenic VOC fluxes in the north-western Mediterranean basin. *J. Geophys. Res.* **2000**, *105*, 11573–11583.
59. Morrison, E.C.; Drewer, J.; Heal, M.R. A comparison of isoprene and monoterpene emission rates from the perennial bioenergy crops short-rotation coppice willow and *Miscanthus* and the annual arable crops wheat and oilseed rape. *GCB Bioenergy* **2016**, *8*, 211–225.
60. Monson, R.K.; Jaeger, C.H.; Adams, W.; Driggers, E.; Silver, G.; Fall, R. Relationships among isoprene emission rate, photosynthesis rate, and isoprene synthase activity, as influenced by temperature. *Plant Physiol.* **1992**, *92*, 1175–1180.
61. Kuzma, J.; Fall, R. Leaf isoprene emission rate is dependent on leaf development and the level of isoprene synthase. *Plant Physiol.* **1993**, *101*, 435–440.
62. Monson, R.K.; Harley, P.C.; Litvak, M.E.; Wildermuth, M.; Guenther, A.B.; Zimmerman, P.R.; Fall, R. Environmental and developmental controls over the seasonal pattern of isoprene emission from aspen leaves. *Oecologia* **1994**, *99*, 260–270.
63. Schnitzler, J.-P.; Lehning, A.; Steinbrecher, R. Seasonal Pattern of Isoprene Synthase Activity in *Quercus robur* Leaves and its Significance or Modeling Isoprene Emission Rates. *Bot. Acta* **1997**, *110*, 240–243.
64. Toome, M.; Randjäär, P.; Copolovici, L.; Niinemets, Ü.; Heinsoo, K.; Luik, A.; Noe, S.M. Leaf rust induced volatile organic compounds signalling in willow during the infection. *Planta* **2010**, *232*, 235–243.
65. Jiang, Y.; Ye, J.; Veromann, L.-L.; Niinemets, Ü. Scaling of photosynthesis and constitutive and induced volatile emissions with severity of leaf infection by rust fungus (*Melampsora larici-populina*) in *Populus balsamifera* var. *suaveolens*. *Tree Physiol.* **2016**, *36*, 856–872.
66. Sharkey, T.D.; Loreto, F.; Delwiche, C.F. High carbon dioxide and sun/shade effects on isoprene emission from oak and aspen tree leaves. *Plant Cell Environ.* **1991**, *14*, 333–338.
67. Lerdau, M.; Throop, H.L. Sources of variability in isoprene emission and photosynthesis in two species of tropical wet forest trees. *Biotropica* **2000**, *32*, 670–676.
68. Monson, R.K.; Fall, R. Isoprene emission from aspen leaves. *Plant Physiol.* **1989**, *90*, 267–274.
69. Guenther, A.B.; Monson, R.K.; Fall, R. Isoprene and monoterpene emission rate variability: Observations with eucalyptus and emission rate algorithm development. *J. Geophys. Res.* **1991**, *96*, 10799–10808.
70. Sharkey, T.D.; Monson, R.K. Isoprene research—60 years later, the biology is still enigmatic. *Plant Cell Environ.* **2017**, *40*, 1671–1678.
71. Simin, T.; Tang, J.; Holst, T.; Rinnan, R. Volatile organic compound emission in tundra shrubs—Dependence on species characteristics and the near-surface environment. *Environ. Exp. Bot.* **2021**, *184*, 104387.
72. Niinemets, Ü.; Tenhunen, J.D.; Harley, P.C.; Steinbrecher, R. A model of isoprene emission based on energetic requirements for isoprene synthesis and leaf photosynthetic properties for Liquidambar and *Quercus*. *Plant Cell Environ.* **1999**, *22*, 1319–1335.
73. Kenzo, T.; Ichie, T.; Watanabe, Y.; Yoneda, R.; Ninomiya, I.; Koike, T. Changes in photosynthesis and leaf characteristics with tree height in five dipterocarp species in a tropical rain forest. *Tree Physiol.* **2006**, *26*, 865–873.
74. Kosugi, Y.; Takanashi, S.; Yokoyama, N.; Philip, E.; Kamakura, M. Vertical variation in leaf gas exchange parameters for a Southeast Asian tropical rainforest in Peninsular Malaysia. *J. Plant. Res.* **2012**, *125*, 735–748.
75. Juraň, S.; Pallozzi, E.; Guidolotti, G.; Fares, S.; Šigut, L.; Calfapietra, C.; Alivernini, A.; Savi, F.; Večeřová, K.; Křůmal, K.; et al. Fluxes of biogenic volatile organic compounds above temperate Norway spruce forest of the Czech Republic. *Agr. For. Meteorol.* **2017**, *232*, 500–513.
76. Guidolotti, G.; Calfapietra, C.; Loreto, F. The relationship between isoprene emission, CO₂ assimilation and water use efficiency across a range of poplar genotypes. *Physiol. Plant.* **2011**, *142*, 297–304.
77. Tingey, D.T.; Manning, M.; Grothaus, L.C.; Burns, W.F. The influence of light and temperature on isoprene emission rates from live oak. *Physiol. Plant.* **1979**, *47*, 112–118.
78. Llusà, J.; Peñuelas, J. Seasonal patterns of terpene content and emission from seven Mediterranean woody species in field conditions. *Am. J. Bot.* **2000**, *87*, 133–140.
79. Kesselmeier, J.; Ciccioli, P.; Kuhn, U.; Stefani, P.; Biesenthal, T.; Rottenberger, S.; Wolf, A.; Vitullo, M.; Valentini, R.; Nobre, A.; et al. Volatile organic compound emissions in relation to plant carbon fixation and the terrestrial carbon budget. *Glob. Biogeochem. Cycles* **2002**, *16*, 1126.
80. Bracho-Nunez, A.; Knothe, N.M.; Welter, S.; Staudt, M.; Costa, W.R.; Liberato, M.A.R.; Piedade, M.T.F.; Kesselmeier, J. et al. Leaf level emissions of volatile organic compounds (VOC) from some Amazonian and Mediterranean plants. *Biogeosciences* **2013**, *10*, 5855–5873.
81. Loreto, F.; Sharkey, T.D. A gas-exchange study of photosynthesis and isoprene emission in *Quercus rubra* L. *Planta* **1990**, *182*, 523–531.
82. Larcher, W. Carbon Utilization and Dry Matter Production. In *Physiological Plant Ecology: Ecophysiology and Stress Physiology of Functional Groups*, 4th ed.; Springer: Berlin/Heidelberg, Germany; New York, NY, USA, 2003; pp. 69–184.
83. Winer, A.M.; Arey, J.; Atkinson, R.; Aschmann, S.M.; Long, W.D.; Morrison, C.L.; Olszyk, D.M. Emission rates of organics from vegetation in California's central valley. *Atmos. Environ.* **1992**, *26*, 2647–2659.

84. König, G.; Brunda, M.; Puxbaum, H.; Hewitt, C.N.; Duckham, S.C.; Rudolph, J. Relative contribution of oxygenated hydrocarbons to the total biogenic VOC emissions of selected mid-European agricultural and natural plant species. *Atmos. Environ.* **1995**, *29*, 861–874.
85. Karl, M.; Guenther, A.; Köble, R.; Leip, A.; Seufert, G. A new European plantspecific emission inventory of biogenic volatile organic compounds for use in atmospheric transport models. *Biogeosciences* **2009**, *6*, 1059–1087.
86. Roberts, J.M.; Williams, J.; Baumann, K.; Buhr, M.P.; Goldan, P.D.; Holloway, J.; Hubler, G.; Kuster, W.C.; McKeen, S.A.; Ryerson, T.B.; et al. Measurements of PAN, PPN, MPAN made during the 1994 and 1995 Nashville Intensives of the Southern Oxidant Study: Implications for regional ozone production from biogenic hydrocarbons. *J. Geophys. Res.* **1998**, *103*, 22473–22490.
87. Wang, K.-Y.; Shallcross, D.E. Modelling terrestrial biogenic isoprene fluxes and their potential impact on global chemical species using a coupled LSM–CTM model. *Atmos. Environ.* **2000**, *34*, 2909–2925.
88. Watson, L.A.; Wang, K.-Y.; Paul, H.; Shallcross, D.E. The potential impact of biogenic emissions of isoprene on urban chemistry in the United Kingdom. *Atmos. Sci. Lett.* **2006**, *7*, 96–100.
89. Hakola, H.; Rinne, J.; Laurila, T. The VOC emission rates of boreal deciduous trees. In *Biogenic VOC Emissions and Photochemistry in the Boreal Regions of Europe–Biphorep*; European Commission: Brussels, Belgium, 1999.
90. Staudt, M.; Seufert, G. Light-dependent emission of monoterpenes by Holm oak (*Quercus ibex* L.). *Naturwissenschaften* **1995**, *82*, 89–92.
91. Kesselmeier, J.; Schäfer, L.; Ciccioli, P.; Brancaleoni, E.; Cecinato, A.; Frattoni, M.; Foster, P.; Jacob, V.; Denis, J.; Fugit, J.-L.; et al. Emission of monoterpenes and isoprene from a Mediterranean oak species *Quercus ilex* L. measured within the BEMA (Biogenic Emissions in the Mediterranean Area) project. *Atmos. Environ.* **1996**, *30*, 1841–1850.
92. Peñuelas, J.; Llusà, J. Short-term responses of terpene emission rates to experimental changes of PFD in *Pinus halepensis* and *Quercus ilex* in summer field conditions. *Environ. Exp. Bot.* **1999**, *42*, 61–68.
93. Loreto, F.; Forster, A.; Durr, M.; Csiky, O.; Seufert, G. On the monoterpene emission under heat stress and on the increased thermotolerance of leaves of *Quercus ilex* L. fumigated with selected monoterpenes. *Plant Cell Environ.* **1998**, *21*, 101–107.
94. Paré, P.W.; Tumlinson, J.H. Plant volatiles as a defense against insect herbivores. *Plant Physiol.* **1999**, *121*, 325–332.
95. Delfine, S.; Csiky, O.; Seufert, G.; Loreto, F. Fumigation with exogenous monoterpenes of a non-isoprenoid-emitting oak (*Quercus suber*): Monoterpene acquisition, translocation, and effect on the photosynthetic properties at high temperatures. *New Phytol.* **2000**, *146*, 27–36.
96. Peñuelas, J.; Llusà, J. Linking photorespiration, monoterpenes and thermotolerance in *Quercus*. *New Phytol.* **2002**, *155*, 227–237.
97. Copolovici, L.; Kännaste, A.; Pazouki, L.; Niinemets, Ü. Emissions of green leaf volatiles and terpenoids from *Solanum lycopersicum* are quantitatively related to the severity of cold and heat shock treatments. *J. Plant. Physiol.* **2012**, *169*, 664–672.
98. Palmer-Young, E.C.; Veit, D.; Gershenzon, J.; Schuman, M.C. The Sesquiterpenes (E)- β -Farnesene and (E)- α -Bergamotene Quench Ozone but Fail to Protect the Wild Tobacco *Nicotiana attenuata* from Ozone, UVB, and Drought Stresses. *PLoS ONE* **2015**, *10*, e0127296.
99. Pazouki, L.; Kanagendran, A.; Li, S.; Kännaste, A.; Memari, H.R.; Bichele, R.; Niinemets, Ü. Mono- and sesquiterpene release from tomato (*Solanum lycopersicum*) leaves upon mild and severe heat stress and through recovery: From gene expression to emission responses. *Environ. Exp. Bot.* **2016**, *132*, 1–15.
100. Tiiva, P.; Häikiö, E.; Kasurinen, A. Impact of warming, moderate nitrogen addition and bark herbivory on BVOC emissions and growth of Scots pine (*Pinus sylvestris* L.) seedlings. *Tree Physiol.* **2018**, *38*, 1461–1475.
101. Hildebrand, D.F. Lipoxigenases. *Physiol. Plant.* **1989**, *76*, 249–253.
102. Andersen, R.A.; Hamilton-Kemp, T.R.; Hildebrand, D.F.; McCracken, C.T.; Collins, R.W.; Fleming, P.D. Structure-Antifungal Activity Relationships among Volatile C6 and C9 Aliphatic Aldehydes, Ketones, and Alcohols. *J. Agric. Food Chem.* **1994**, *42*, 1563–1568.
103. Wildt, J.; Kobel, K.; Schuh-Thomas, G.; Heiden, A. Emissions of Oxygenated Volatile Organic Compounds from Plants Part II: Emissions of Saturated Aldehydes. *J. Atmos. Chem.* **2003**, *45*, 173–196.
104. Misztal, P.K.; Hewitt, C.N.; Wildt, J.; Blande, J.D.; Eller, A.; Fares, S.; Gentner, D.; Gilman, J.; Graus, M.; Greenberg, J.; et al. Atmospheric benzenoid emissions from plants rival those from fossil fuels. *Sci. Rep.* **2015**, *5*, 12064.
105. Arimura, G.; Huber, D.P.; Bohlmann, J. Forest tent caterpillars (*Malacosoma disstria*) induce local and systemic diurnal emissions of terpenoid volatiles in hybrid poplar (*Populus trichocarpa* \times *deltoides*): cDNA cloning, functional characterization, and patterns of gene expression of (–)-germacrene D synthase, PtdTPS1. *Plant J.* **2004**, *37*, 603–616.
106. Kleist, E.; Mentel, T.F.; Andres, S.; Bohne, A.; Folkers, A.; Kiendler-Scharr, A.; Rudich, Y.; Springer, M.; Tillmann, R.; Wildt, J. Irreversible impacts of heat on the emissions of monoterpenes, sesquiterpenes, phenolic BVOC and green leaf volatiles from several tree species. *Biogeosciences* **2012**, *9*, 5111–5123.
107. Hakola, H.; Rinne, J.; Laurila, T. The hydrocarbon emission rates of tea-leafed willow (*Salix phylicifolia*), silver birch (*Betula pendula*) and European aspen (*Populus tremula*). *Atmos. Environ.* **1998**, *32*, 1825–1833.
108. Copeland, N.; Cape, J.N.; Heal, M.R. Volatile organic compound emissions from *Miscanthus* and short rotation coppice willow bioenergy crops. *Atmos. Environ.* **2012**, *60*, 327–335.
109. Peräkylä, O.; Vogt, M.; Tikkanen, O.P.; Laurila, T.; Kajos, M.K.; Rantala, P.A.; Patokoski, J.; Aalto, J.; Yli-Juuti, T.; Ehn, M.; et al. Monoterpenes oxidation capacity and rate over a boreal forest: Temporal variation and connection to growth of newly formed particles. *Boreal Environ. Res.* **2014**, *19*, 293–310.

Supplement to:
**Leaf-scale Study of Biogenic Volatile Organic
Compound Emissions from Willow (*Salix* spp.) Short
Rotation Coppices Covering Two Growing Seasons**

T. Karlsson^{1,*}, L. Klemedtsson², R. Rinnan³, T. Holst¹

¹Lund University, Department of Physical Geography and Ecosystem Science, Sölvegatan 12, 223 62 Lund, Sweden

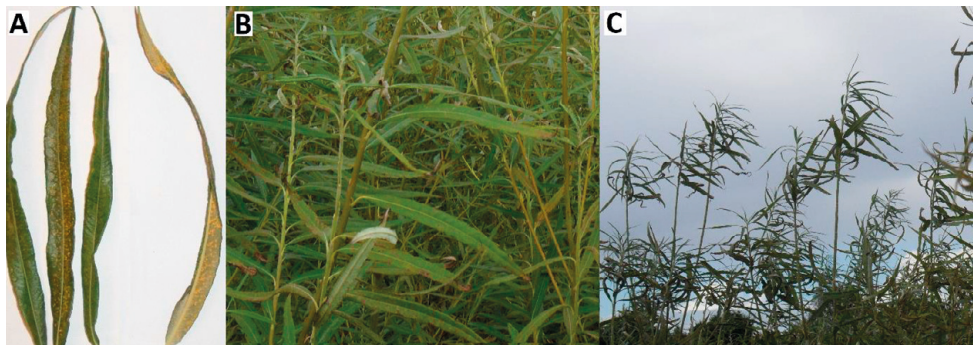
²Department of Earth Sciences, University of Gothenburg, Guldhedsgatan 5a, 405 30 Gothenburg, Sweden

³University of Copenhagen, Terrestrial Ecology Section, Department of Biology, Universitetsparken 15, DK-2100 Copenhagen Ø, Denmark

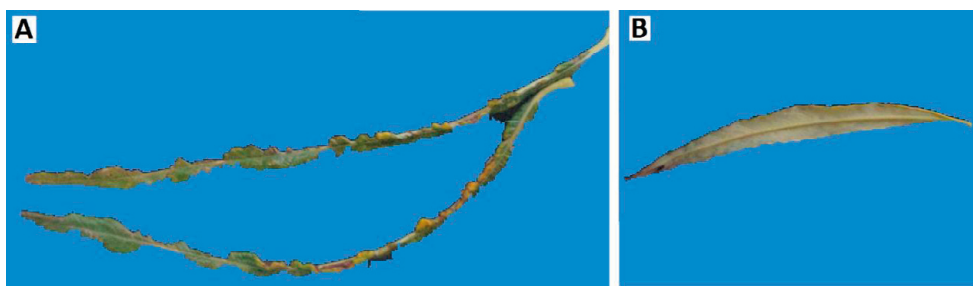
* Correspondence to: T. Karlsson (tomas.karlsson@nateko.lu.se)



S1. The two sites where the measurements were performed. A) P1 (58°16'55" N 12°46'20" E) and B) P2 (58°17'09" N 12°45'31" E). Black marks are the locations of the measurements. Maps are taken and modified from Karlsson et al. (2020).



S2. Impact of rust (*Melampsora* spp.) infestation on P1. A) Visible yellow dots in late July. B) Lower part of the trees in September where some parts of leaves have changed the color to red/brown (necrotic lesions) and started to fold. C) Top of the trees in September. Many leaves were shed or folded.



S3. A) Leaves from the higher part (z_H) of the canopy that were measured with the branch chamber in October showing damage from leaf beetles (*Phratora vulgatissima*). B) Leaves from the lower part (z_M) of the canopy in October measured with the branch chamber.

S4. Pure injected standards in the GC-MS analysis. Numbers in the parentheses are CAS-number.

Hemiterpenes	Monoterpenes	Sesquiterpenes	other VOCs
isoprene* (78-79-5)	α -pinene [§] (80-56-8)	aromadendrene* (109119-91-7)	2-methylfuran* (534-22-5)
	camphene* (79-92-5)	humulene* (6753-98-6)	toluene [§] (108-88-3)
	β -pinene [§] (127-91-3)	nerolidol [§] (142-50-7)	1-octene [§] (111-66-0)
	myrcene [§] (123-35-3)		hexanal* (66-25-1)
	α -phellandrene [§] (99-83-2)		furfural* (98-01-1)
	p-cymene (99-87-6)		2-hexenal* (505-57-7)
	eucalyptol [§] (470-82-6)		p-xylene [§] (106-42-3)
	γ -terpinene [§] (99-85-4)		o-xylene [§] (95-47-6)
	ocimene [§] (502-99-8)		benzaldehyde [§] (100-52-7)
	terpinolene* (586-62-9)		1-octen-3-ol [§] (3391-86-4)
	linalool [§] (78-70-6)		octanal* (124-13-0)
			cis-3-hexenyl acetate [§] (3681-71-8)
			nonanal [§] (124-19-6)
			cis-3-hexenyl butyrate [§] (16491-36-4)

*These standards were produced by Sigma-Aldrich. [§]These standards were produced by Supelco.

S5. Measured (E) and standardized (Es) emission rates ($\mu\text{g g}_{\text{dw}}^{-1} \text{h}^{-1}$, $n = 663$) for all compounds and all measurements. Numbers in parentheses are standard deviation (SD, $\mu\text{g g}_{\text{dw}}^{-1} \text{h}^{-1}$). No standardization is made for OVOCs (-).

BVOC	E \pm SD ($\mu\text{g g}_{\text{dw}}^{-1} \text{h}^{-1}$)	Es \pm SD ($\mu\text{g g}_{\text{dw}}^{-1} \text{h}^{-1}$)
------	---	--

isoprene	23.5 (28.1)	45.2 (42.9)
Tot MTs	0.163 (0.117)	0.301 (0.201)
ocimene	0.137 (0.321)	0.255 (0.540)
limonene*	0.008 (0.042)	0.014 (0.081)
p-cymene	0.006 (0.042)	0.011 (0.069)
linalool	0.006 (0.017)	0.010 (0.035)
α -pinene	0.003 (0.021)	0.005 (0.034)
3-carene*	0.002 (0.019)	0.004 (0.040)
eucalyptol	0.001 (0.010)	0.002 (0.024)
myrcene	<0.001 (<0.001)	<0.001 (<0.001)
allo-ocimene*	<0.001 (<0.001)	<0.001 (<0.001)
Tot SQTs	0.035 (0.062)	0.103 (0.249)
caryophellene ⁺	0.011 (0.031)	0.024 (0.080)
humulene	0.010 (0.090)	0.040 (0.409)
α -farnesene ⁺	0.009 (0.062)	0.017 (0.125)
nerolidol	0.004 (0.049)	0.022 (0.243)
Tot other VOCs	0.751 (0.159)	-
cyclopentyl acetylene [§]	0.083 (0.205)	-
benzaldehyde (benzenoid)	0.065 (0.163)	-
hexanal (aldehyde)	0.064 (0.320)	-
nonanal (aldehyde)	0.061 (0.147)	-
2-ethylhexanoic acid [§] (carboxylic acid)	0.059 (0.252)	-
pentanal [§] (aldehyde)	0.037 (0.226)	-
decanal [§] (aldehyde)	0.036 (0.148)	-
octanal (aldehyde)	0.030 (0.105)	-
2-methylbutane [§] (alkane)	0.027 (0.105)	-
2-pentanone [§] (ketone)	0.026 (0.208)	-
2-ethylhexanol [§] (alcohol)	0.024 (0.082)	-
2-hexanone [§] (ketone)	0.023 (0.146)	-
benzoic acid [§] (carboxylic acid)	0.023 (0.116)	-
1-dodecene [§] (alkene)	0.022 (0.205)	-
unknown 1 [§]	0.021 (0.150)	-
pentadecane [§] (alkane)	0.020 (0.078)	-
heptanal [§] (aldehyde)	0.019 (0.083)	-
furfural (aldehyde)	0.018 (0.149)	-
toluene (benzenoid)	0.018 (0.051)	-
phenol [§] (phenol)	0.016 (0.098)	-
cyclopropane, ethylidene- ⁻ (hemiterpene)	0.013 (0.033)	-
acetophenone [§] (ketone)	0.012 (0.049)	-
unknown 2 [§]	0.012 (0.234)	-
3-methylhexane [§] (alkane)	0.011 (0.081)	-
tetradecane [§] (alkane)	0.011 (0.074)	-

*These MTs were quantified with α -pinene as injected standard in GC-MS.

⁺These SQTs were quantified with humulene as injected standard in GC-MS.

[§]These other VOCs were quantified with toluene as injected standard in GC-MS.

[§]This compound was quantified with isoprene as injected standard in GC-MS.

S6. Emission rates (STD for isoprene, MTs and SQTs, $\mu\text{g g}_{\text{dw}}^{-1} \text{h}^{-1}$) and fraction (%) of the total BVOC emission or within the BVOC group (MTs and SQTs) from z_{H} in 2015. Bottom: average T_{c} ($^{\circ}\text{C}$, mean and standard deviation) and PAR_{c} ($\mu\text{mol m}^{-2} \text{s}^{-1}$, mean and standard deviation) for each month.

2015 z_{H}	July	Aug	Sep
isoprene	74.8 (98.5%)	70.4 (97.3%)	19.2 (96.7%)
MTs (tot)	0.580 (0.8%)	0.268 (0.4%)	0.286 (1.4%)
α -pinene	0.036 (6.2 %)	0.007 (2.6%)	0
ocimene	0.540 (93.1 %)	0.256 (95.6%)	0.286 (100%)
linalool	0	0.004 (1.9%)	0
eucalyptol	0.004 (0.7 %)	0.001 (0.4%)	0
SQTs (tot)	0.076 (0.1%)	0.040 (<0.1%)	0.171 (0.9%)
α -farnesene	0.022 (29.3%)	0.014 (35.0%)	0
humulene	<0.001 (0.2%)	0.001 (2.5%)	0
caryophyllene	0.053 (70.5%)	0.025 (62.5%)	0.171 (100%)
OVOCs (tot)	0.441 (0.6%)	1.640 (2.3%)	0.207 (1.0%)
BVOCs (tot)	75.896 (100%)	72.348 (100 %)	19.864 (100%)
T_{c}	23.2 (4.7)	28.9 (2.9)	19.3 (3.4)
PAR_{c}	562 (397)	467 (230)	329 (192)

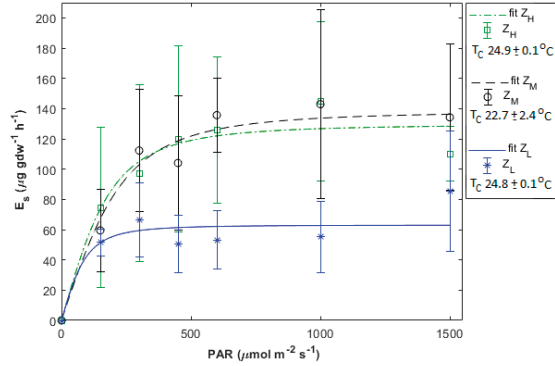
S7. Values used for the fitted curves in Figure 3. E_{s} is the emission factor ($\mu\text{g g}_{\text{dw}}^{-1} \text{h}^{-1}$), C_{L} is the correction factor for light (calculated by using mean PAR_{c} for the whole season and year, and α , T_{s} and C_{L1} adopted from Guenther et al. (1993)). C_{T1} (J mol^{-1}), C_{T2} (J mol^{-1}) and T_{m} (K) are empirical constants.

	2015	2016
E_{s} ($\mu\text{g g}_{\text{dw}}^{-1} \text{h}^{-1}$)	93.8	97.1
C_{L}	0.8317	0.8688
C_{T1}	148700	135300
C_{T2}	211000	103000
T_{m} (K)	307	298

S8. Slope (E/PAR , $\mu\text{g g}_{\text{dw}}^{-1} \mu\text{mol}^{-1} \text{m}^2 \text{s}$, $n = 3-6$) between different PAR values at different height levels for the fitted curves in Figure 4A.

Bottom: values for the fitted parameters in Figure 4A.

PAR	Lower (z_{L})	Middle (z_{M})	Higher (z_{H})
0–150 $\mu\text{mol m}^{-2} \text{s}^{-1}$	0.058	0.112	0.140
150–300 $\mu\text{mol m}^{-2} \text{s}^{-1}$	0.051	0.093	0.111
300–450 $\mu\text{mol m}^{-2} \text{s}^{-1}$	0.042	0.067	0.075
450–600 $\mu\text{mol m}^{-2} \text{s}^{-1}$	0.033	0.045	0.048
600–1000 $\mu\text{mol m}^{-2} \text{s}^{-1}$	0.020	0.023	0.023
1000–1500 $\mu\text{mol m}^{-2} \text{s}^{-1}$	0.009	0.008	0.008
I_{s} ($\mu\text{g g}_{\text{dw}}^{-1} \text{h}^{-1}$)	30.7	147.9	242.1
C_{T}	0.5142	0.3880	0.5207
α	0.0013	0.0018	0.002
C_{L1}	2.83	1.13	0.58



S9. Standardized isoprene emissions rates ($\mu\text{g g}_{\text{dw}}^{-1} \text{h}^{-1}$, mean \pm standard deviation, $n = 3-6$) and fitted curves for different PAR values ($\mu\text{mol m}^{-2} \text{s}^{-1}$) using Equation (7) below at different heights. Values for the parameters can be seen in Table S10 below.

$$E_S = E_S^P \times C_T \times C_L \quad (7)$$

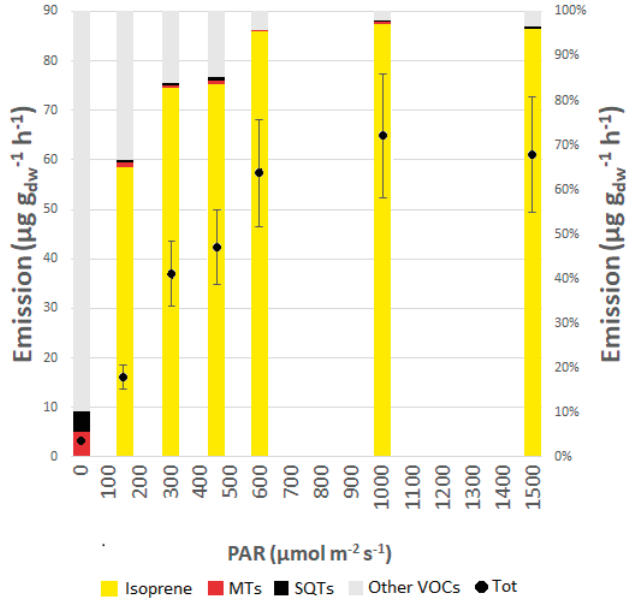
S10. Values for the fitted STD isoprene curves in Figure S9. E_S^P is a STD potential emission factor ($\mu\text{g g}_{\text{dw}}^{-1} \text{h}^{-1}$). C_T was calculated by using mean T_C for the whole season and year, and C_{T1} , C_{T2} , T_S and T_M were adopted from Guenther et al. (1993).

	Lower (z _L)	Middle (z _M)	Higher (z _H)
E_S^P ($\mu\text{g g}_{\text{dw}}^{-1} \text{h}^{-1}$)	27.2	118.6	89.6
C_T	0.5142	0.3880	0.5207
α	0.0093	0.0038	0.0046
C_{L1}	4.51	2.92	2.78

$$R_{E/A} = C_{E/A} \frac{\alpha_{E/A} PAR}{\sqrt{1 + \alpha_{E/A}^2 PAR_{E/A}^2}} \quad (8)$$

S11. Values for the fitted E/A ratio curves in Figure 4B. The light-dependent part of isoprene (Equation 2) has been adopted and modified. $C_{E/A}$ (dimensionless) and $\alpha_{E/A}$ ($\mu\text{mol}^{-1} \text{m}^2 \text{s}^{-1}$) are constants.

	Lower (z _L)	Middle (z _M)	Higher (z _H)
$C_{E/A}$	0.004	0.004	0.006
$\alpha_{E/A}$	0.0037	0.0026	0.0043



S12. Total average emission rates ($\mu\text{g g}_{\text{dw}}^{-1} \pm$ standard deviation, black circles and left y-axis), and the percentages (stacked bars and right y-axis) for the different BVOC groups at different light levels ($\mu\text{mol m}^{-2} \text{s}^{-1}$) at z_M ($n = 6$).

$$C_{L,300} = \frac{\alpha C_{L1}(\text{PAR} - 300)}{\sqrt{1 + \alpha^2(\text{PAR} - 300)^2}} \quad (9)$$

$$C_{L,150} = \frac{\alpha C_{L1}(\text{PAR} - 150)}{\sqrt{1 + \alpha^2(\text{PAR} - 150)^2}} \quad (10)$$

S13. Values for the fitted curves in Figure 6A,B using Equation (9) for ocimene and Equation (10) for α -farnesene instead of Equation (3) in Equation (2).

	ocimene	α -farnesene
E_s ($\mu\text{g g}_{\text{dw}}^{-1} \text{h}^{-1}$)	0.10	0.29
C_r	0.4471	0.4471
α	0.0016	0.0015
C_{L1}	3.92	1.18

S14. Slope (A/PAR, $\mu\text{mol CO}_2 \text{m}^{-2} \text{s}^{-1} \mu\text{mol}^{-1} \text{m}^2 \text{s}$, $n = 3-6$) between different PAR values at different height levels in Figure 7A.

PAR	Lower (z_L)	Middle (z_M)	Higher (z_H)
0–150 $\mu\text{mol m}^{-2} \text{s}^{-1}$	0.0449	0.0465	0.0525
150–300 $\mu\text{mol m}^{-2} \text{s}^{-1}$	0.0159	0.0313	0.0224
300–450 $\mu\text{mol m}^{-2} \text{s}^{-1}$	0.0135	0.0230	0.0183
450–600 $\mu\text{mol m}^{-2} \text{s}^{-1}$	0.0028	0.0004	0.0147
600–1000 $\mu\text{mol m}^{-2} \text{s}^{-1}$	0.0029	0.0061	0.0049
1000–1500 $\mu\text{mol m}^{-2} \text{s}^{-1}$	-0.0001	0.0069	0.0024

S15. Values for the parameters of the fitted curves in Figure 7A using Equation (6). A_d and A_{max} are mean values ($n = 2-6$) at 0 and 1500 $\mu\text{mol m}^{-2} \text{s}^{-1}$, respectively.

	Lower (z_L)	Middle (z_M)	Higher (z_H)
A_d ($\mu\text{mol CO}_2 \text{ m}^{-2} \text{ s}^{-1}$)	0.66 (0.28)	-0.21 (0.36)	1.27 (0.21)
A_{max} ($\mu\text{mol CO}_2 \text{ m}^{-2} \text{ s}^{-1}$)	12.05 (3.01)	21.30 (2.92)	18.10 (4.89)
α_A ($\mu\text{mol CO}_2 \text{ m}^{-2} \text{ s}^{-1}$)	0.0541	0.0437	0.0538

Paper II





Article

Variability of BVOC Emissions from Commercially Used Willow (*Salix* spp.) Varieties

Tomas Karlsson ^{1,*}, Riikka Rinnan ² and Thomas Holst ^{1,2}

¹ Department of Physical Geography and Ecosystem Science, Lund University, Sölvegatan 12, SE-223 62 Lund, Sweden; thomas.holst@nateko.lu.se

² Terrestrial Ecology Section, Department of Biology, University of Copenhagen, Universitetsparken 15, DK-2100 Copenhagen Ø, Denmark; riikkar@bio.ku.dk

* Correspondence: tomas.karlsson@nateko.lu.se

Received: 5 February 2020; Accepted: 3 April 2020; Published: 7 April 2020



Abstract: Willow (*Salix* spp.) trees are commonly used in short rotation coppices (SRC) to produce renewable energy. However, these plants are also known to emit high concentrations of biogenic volatile organic compounds (BVOCs), which have a large influence on air quality. Many different clones of commercially used *Salix* varieties exist today, but only a few studies have focused on BVOC emissions from these newer varieties. In this study, four varieties commercially propagated for biofuel production have been studied on a leaf-scale in the southern part of Sweden. The trees had either their first or second growing season, and measurements on BVOC emissions were done during the growing season in 2017 from the end of May to the beginning of September. Isoprene was the dominant emitted compound for all varieties but the average emission amongst varieties varied from 4.00 to 12.66 $\mu\text{g g}_{\text{dw}}^{-1} \text{h}^{-1}$. Average monoterpene (MT) (0.78–1.87 $\mu\text{g g}_{\text{dw}}^{-1} \text{h}^{-1}$) and sesquiterpene (SQT) emission rates (0.22–0.57 $\mu\text{g g}_{\text{dw}}^{-1} \text{h}^{-1}$) differed as well among the varieties. Besides isoprene, other compounds like ocimene, linalool and caryophyllene also showed a response to light but not for all varieties. Younger plants had several times higher emissions of non-isoprenoids (other VOCs) than the corresponding 1-year-old trees. The conclusions from this study show that the choice of variety can have a large impact on the regional BVOC emission budget. Genetics, together with stand age, should be taken into account when modelling BVOC emissions on a regional scale, for example, for air quality assessments.

Keywords: *Salix*; biofuel plantation; terpenoid emissions; BVOC

1. Introduction

The extended use of biofuels is widely promoted to decrease the carbon (C) emissions from fossil fuels, i.e., to fulfil the requirements of the EU directive (2009/28/EC) on renewable energies and to achieve zero net emissions of greenhouse gases in Sweden by the year 2045 [1,2]. In 2017, biofuels alone contributed 25% [3] of Sweden's total energy supply. Most of the energy supply from biofuels are based on 'classical' forest products (pulp industry fuels, wood fuel and sawmill by-products) but logging residues and tree stumps have also been used [4]. However, the contribution to energy production based on agroforestry (i.e., energy crops) is expected to increase to meet the requirements of the EU directive. Besides 'classical' biofuel crops like rapeseed, sugar beets or oil seeds, fast-growing tree species (willow (*Salix* spp.), poplar and hybrid aspen) are increasingly used as energy crops [5], either for direct combustion or for the production of liquid fuels by 'second generation' bioethanol from lignocellulose. Energy crops are currently using 3% of arable land in Sweden [5]. *Salix* trees have been reported to grow on 12,000 ha in Sweden in 2014 [6] but the potential use is estimated at 300,000 ha [5]. The advantages of willow are the high energy content (more than twice that of oat), the ability to clean

up from soils waste water treatment products and cadmium, and the greater increase in the C stock in soil and mulch compared to with annual crops, as willow is grown for 4 years before cutting [7,8].

Willow has been used intensively as energy crop since the 1990s, and varieties have been propagated to increase both biomass production and resistance against weeds and pests [9]. Depending on the climate conditions, different varieties are suitable. For instance, at higher latitudes, such as in the middle and northern parts of Sweden, varieties need to be more resistant to frost, whereas at southern latitudes, trees can suffer from heat damage. There exist no official data on the distribution of the varieties, but studies have shown that Tora has been successfully grown in Sweden, as it gives 40–50% higher yield and has a better resistance to rust compared to older varieties such as L 78183, Orm and Rapp [9]. Other varieties, e.g., Sven and Inger, are suitable to be grown in Sweden, and Inger is also suitable for soils with a low soil water capacity [10]. As *Salix* is easy to propagate, new varieties are continuously propagated by commercial companies that aim at increasing biomass yield and tolerance against insects, plant pests and weeds. Additionally, a change of growing conditions due to climate change might imply that older varieties should be replaced with newer ones, which have been specifically propagated to cope better with drought.

While *Salix* plantations may be a good option for energy crop production, a large-scale land-use change towards *Salix* might have severe impacts on atmospheric chemistry and local air quality. Areas used for short-rotation coppices (SRC) to increase the production of biofuels are most converted from traditional agricultural crops. In contrast to agricultural crops, *Salix* species are regarded as high-emitters of biogenic volatile organic compounds (BVOCs) [11] that are very reactive and can contribute to the production of ozone (O₃) and secondary organic aerosols (SOAs) [12–17]. *Salix* species have been shown to emit large amounts of isoprene, with standardized emission rates ranging from 12.5 to 115.0 $\mu\text{g g}_{\text{dw}}^{-1} \text{h}^{-1}$ [11,18–22]. Monoterpene (MT) emissions from some *Salix* spp. have also been reported [11,18,23], but data for the quantification of compounds other than isoprene and monoterpenes (MTs) are scarce [22].

The large variation of published standardized emission rates for *Salix* spp. indicates an influence of genetic disposition on the BVOC production and emission [24], which has been observed for other species as well [25,26]. Consequently, commercial propagation methods to find better varieties that provide higher biomass yields, increased resistance against plant pests and enhanced competitiveness against weeds might also affect the production and emission of BVOCs.

Here, we analyze leaf-scale BVOC emissions from several varieties of willow that were growing either in field trails or commercially on SRC plantations. We aim to identify the compound spectrum emitted by these varieties, and provide standardized emission rates that can be used in emission inventories and distributed vegetation models to assess the impact of willow plantations on regional air quality.

2. Material and Methods

2.1. Experimental Sites

Four plots in southern Sweden were used in this study. Two of them (plot 1, 55°52′32.9″ N 13°1′18.2″ E and plot 2, 55°52′11.7″ N 13°1′33.3″ E, Figure 1A,B) were field trial areas for a commercial company (European Willow Breeding AB) outside Billeberga and stocked with 12–15 different varieties of willow. Two other plots (plot 3, 58°17′09″ N 12°45′31″ E and plot 4, 58°16′55″ N 12°46′20″ E, Figure 1C,D) were located outside Grästorps ca 300 km north of plots 1 and 2 and used for the commercial production of biomass for energy purposes. The varieties measured on plot 1 were planted in 2014, but were cut down before the growing season in 2016 (Table 1). The land on plot 1 had previously been used for growing other *Salix* varieties before the new establishment of the varieties in 2014 (Table S1). Plot 2 consisted of almost the same varieties as plot 1, but these trees were planted in 2017. Plot 2 had not been used for growing *Salix* before; instead, crops such as cereals, beets and rapeseeds had been growing here until 2016.

Table 1. The plot type, size (ha), canopy height (m), varieties, establishment, last harvest and age (months) for the trees.

	Plot 1	Plot 2	Plot 3	Plot 4
Type	field trial	field trial	biofuel plantation	biofuel plantation
Plot size	0.07 ha	0.07 ha	5 ha	9 ha
Canopy height ¹	4.5 m	1.5 m	2.5 m	1–1.5 m
Varieties	Tora, Wilhelm, Ester and Inger	Tora, Wilhelm, Ester and Inger	Tora	Wilhelm
Established	2013	2017	2003	2017
Last harvest	2016	-	2017	-
Age of the trees ¹	16 months	5 months	9 months	5 months

¹ Average canopy height and age for the varieties at the last campaign at each plot.

Each variety on plots 1 and 2 was grown on 5 rows that were a few meters long. The rows were separated by ca 0.7 m and the trees had been planted at 0.5 m intervals. The distance between the two plots was approximately 700 m. The mean annual temperature (T) was 7.7 °C (1961–1990 in Svalöv, located 6 km from the plots) and the accumulated annual precipitation was 687 mm (1961–1990 in Svalöv) [27]. The surrounding area was used for growing traditional crops. Only one variety was growing on plot 3 and another one on plot 4. Plot 3 was established in 2003 and harvested before spring 2017. Plot 4 was replanted during spring 2017, since the older variety, established in 1994, was exterminated after harvest in 2016. The trees on plots 3 and 4 were planted in double rows, with 0.75 cm between the rows in the double row. Each double row was separated with 1.25 m and the space between the trees in a row was 0.4 m. The distance between plots 3 and 4 was approximately 1 km. Mean annual T and precipitation for plots 3 and 4 were 6.1 °C (1961–1990 in Gendalen, located 16 km from the plots) and 683 mm (1961–1990 in Grästorps, located 7 km from the plots), respectively [27]. No watering or fertilization were done on any of the plots.



Figure 1. The different plantations where the measurements were done. (A) Plot 1, the field trial of second year growing varieties established in 2014. (B) Plot 2, the field trial of first year growing varieties established in 2017. (C) Plot 3, the biofuel plantation of first year growing trees established in 2017. (D) Plot 4, the biofuel plantation of first year growing trees established in 2003. The black rectangles indicate the positions of the leaf scale measurement. The photos are modified from Lantmäteriet [28].

2.2. *Salix* Varieties

Near plots 1 and 2, a company (European Willow Breeding AB) has been growing *Salix* trees since 2011. The 4 species chosen are briefly described below and the information was provided by the breeding company. All species have been propagated for commercial use to produce renewable energy. Between 1994 and 2007, regular yield tests were done for new commercial varieties where variety L 78183 was used as a reference with a yield of 100 kg dry weight per plot ($\text{kg}_{\text{dw}} \text{plot}^{-1}$) [9]. This system was discontinued in 2009, and the yield for varieties produced thereafter has been based only on rough estimates.

S. Tora

Tora is a female hybrid and a cross between the clone L 79069 (*S. schwerinii*) and the variety Orm. The cross was made in 1989 and has shown to be one of the most suitable species for growing in the northern part of Europe, with a yield of $150.5 \text{ kg}_{\text{dw}} \text{plot}^{-1}$ and almost no rust infestation or insect attacks. The estimated growing area in Europe is 5000 ha. Because of the resistance to frost and rust, Tora is one of the most appropriate varieties to grow at northern latitudes, e.g., in Sweden.

S. Inger

Inger is a female hybrid cross between the clone SW 930887 (*S. triandra* from Siberia) and the variety Jorr. The cross was made in 1994 and gives a high yield in mild or warm climates with a normal water supply. The estimated growing area in Europe is 2000 ha. The yield is $140.5 \text{ kg}_{\text{dw}} \text{plot}^{-1}$.

S. Wilhelm

Wilhelm is a male hybrid from a cross between the varieties Sherwood and Björn. It was made in 2011 and the biomass productivity from this variety is in between the values for Tora and Inger. The estimated growing area in Europe is 400 ha.

S. Ester

Ester is a female hybrid and a cross between the variety Linnéa and a clone of “Shrubby willow” (*S. miyabeana*). The cross was made in 2012. The yield from this variety is similar to Inger. Ester is suited for dry and hot climates. Compared to the other species, Ester is almost completely free of leaf beetle attacks but is tasty for game, e.g., roe deer and elk. The estimated growing area in Europe is 200 ha.

2.3. BVOC Measurements

All measurements on plots 1 and 2 were executed during 4 campaigns throughout the growing season in 2017. Two species were measured each day, and the length of the campaigns was 4 days each (Table 2). Measurements on plots 3 and 4 were divided into 5 campaigns, and the length varied from 1 to 3 days. In total, 319 sample cartridges were taken, but 20 out of these were lost during GC-MS analyses. Toluene and butylated hydroxytoluene had to be removed from the measurements done by LI-6400XT, and toluene from LI-6400, since huge peaks were seen in the background samples, indicating that they were emitted from the instruments. One of the two unknown sesquiterpene (SQT) compounds could not be completely determined by NIST 8.0 database, and 2 options were suggested, copaene or α -cubebene; copaene was chosen.

Table 2. All of the campaigns in 2017 and the number of samples taken for each variety. The abbreviations in the parentheses indicate what age the varieties were (e.g., T1 means the first growing season for Tora).

Plot 1	29 & 31 May, 2 & 5 June	5–6 & 9–10 July	22, 25–26 & 28 July	28–31 August	
Tora (T2)	7	7	7	6	
Wilhelm (W2)	7	7	7	6	
Ester (E2)	7	7	7	6	
Inger (I2)	7	7	7	7	
Plot 2					
Tora (T1)	7	7	7	7	
Wilhelm (W1)	7	7	7	6	
Ester (E1)	7	7	7	5	
Inger (I1)	7	7	7	3	
Plot 3	15 June	15 July	1 August	7 September	
Tora (T1)	7	14	7	7	
Plot 4	13 June	28 June	12–14 July	2 August	5 September
Wilhelm (W1)	7	14	18	4	7

2.4. Experimental Setup

Fully expanded sun-exposed leaves were chosen from the upper part of the canopy. Two portable photosynthesis systems (LI-6400/LI-6400XT, LI-COR, Lincoln, NE, USA) with $2 \times 3 \text{ cm}^2$ LED source leaf chambers (6400-02B) were used. The middle part of a *Salix* leaf was inserted into the chamber so that the maximum area of the leaf was used in the chamber. Air was continuously entering the chamber with a flow rate of $500 \mu\text{mol s}^{-1}$ (approximately 0.7 l min^{-1}). This purge air passed through a hydrocarbon trap filter (Alltech, Associates Inc., USA) that contained active carbon and MnO_2 -coated copper nets to clean the air of BVOCs and O_3 before it entered the chamber. The temperature inside the chamber was set to match the expected ambient temperature taken from the weather forecast, and the reference CO_2 within the chamber was set to 400 ppm. Relative humidity (RH) inside the chamber was regulated to be close to ambient RH and mostly varied between 40% and 70%. The photosynthesis systems were modified for BVOC measurements on adsorbent cartridges by adding a flow divider at the leaf chamber outlet, which lead one part of the sample air towards the built-in gas analyzer (CO_2 , H_2O) of the photosynthesis system. A second sub-sample of 200 mL min^{-1} was pulled through a sample cartridge (Markes International Limited, Llantrisant, UK) by a battery-operated pump (Pocket Pump, SKC Ltd., Dorset, UK). The sample cartridges were filled in a 2-bed configuration with Tenax TA (porous organic polymer) and Carbograph 1TD (graphitized carbon black) adsorbents. Similar set-ups had been used in other studies before [26,29–31].

Samples were collected at seven light levels (0, 150, 300, 450, 600, 1000 and $1500 \mu\text{mol m}^{-2} \text{ s}^{-1}$) in order to generate a light response curve for the BVOC emissions. Measurements started 1 h after enclosing the leaf by the chamber to prevent stress-induced BVOC emissions from affecting the samples [29], and the air from the chamber was sampled for 20 min at 200 mL min^{-1} (total sample volume of 4 L). After switching the light conditions for the next step, 30 min was allowed to pass to allow for the leaf to adapt to the new light conditions before BVOC sampling was continued at the new light level. During the measurements, the net assimilation rates (A , $\mu\text{mol CO}_2 \text{ m}^{-2} \text{ s}^{-1}$) and transpiration (Tr , $\text{mmol H}_2\text{O m}^{-2} \text{ s}^{-1}$) were measured. By taking the ratio between A and Tr , water use efficiency (WUE , $\text{mmol CO}_2 \text{ mol}^{-1} \text{ H}_2\text{O}$) was calculated. Because of problems with matching the concentrations of CO_2 and H_2O in the sample cell to those in the reference cell in the leaf chamber, the number of measurements included in the A and WUE calculations had to be reduced to 226. At the end of each light response curve, a background sample was taken from an empty chamber to determine the background concentration of the purge air. Ambient T and RH at canopy level were recorded during

the measurement (CS215, Campbell Scientific, USA). Photosynthetically active radiation (PAR, $\mu\text{mol m}^{-2} \text{s}^{-1}$) above the canopy was also measured (LI-190, LI-COR, USA) and together with ambient T and RH, these data were recorded by a logger (CR1000, Campbell Scientific, USA). When sampling was completed, the leaves were harvested and dried for two days at 75 °C to determine the dry weights.

After sampling, the cartridges were sealed with long-term storage caps and stored at 3 °C before being analyzed by TD-GC-MS in the laboratory [32]. Compounds were analyzed in the Enhanced ChemStation (MSD ChemStation E.02.01.1177, Copyright 1989–2010 Agilent Technologies, Inc.) and identified by pure standards (isoprene, 2-methylfuran, toluene, 1-octene, hexanal, furfural, 2-hexanal, p-xylene, o-xylene, α -pinene, camphene, benzaldehyde, β -pinene, myrcene, octanal, cis-3-hexenyl acetate, d-phellandrene, p-cymene, eucalyptol, ocimene, terpinolene, linalool, nonanal, cis-3-hexenyl butyrate, aromadendrene, humulene and nerolidol) or using the NIST 8.0 database. Standard mixtures were prepared in methanol at a concentration of 20 $\mu\text{g mL}^{-1}$ and injected into cartridges under a steady stream of helium (100 mL min^{-1}). The standards were run at the beginning and at the end of every batch of samples. The sample concentrations were calculated by using the ratios between the sample peak areas and standard peak areas. To check the linearity of responses for the compounds, calibration curves were generated periodically by serial dilutions of the standard mixture to six concentrations (0–25 $\mu\text{g mL}^{-1}$). The detection limit was based on the background samples. Only sample peaks that had an area twice as large (or more) as the corresponding peaks in the background sample were included in the analysis. To be able to quantify BVOCs for which no standard was available, α -pinene was used for MTs, humulene was used for SQTs and toluene was used for other VOCs (compounds not belonging to terpenoids).

2.5. BVOC Emissions and Standardization

The emission rates (E) of BVOCs were calculated by using Equation (1), shown below (see e.g., [33])

$$E = (C_2 - C_1) \times F \times m^{-1} \quad (1)$$

where E ($\mu\text{g g}_{\text{dw}}^{-1} \text{h}^{-1}$) is the emission rate, C_2 ($\mu\text{g l}^{-1}$) is BVOC concentration in the samples, C_1 ($\mu\text{g l}^{-1}$) is the BVOC concentration in the purge air, F (l h^{-1}) is the flow rate of the purge air and m (g) is the dried mass of the leaves. Only compounds that had at least twice as high a concentration in the sample air C_2 as in the VOC-filtered purge air, C_1 , were included in the analysis.

To be able to compare emission rates with other studies, they needed to be standardized, because prevailing environmental factors (T, PAR) govern some of the compounds. This normalization can be done in two ways. For compounds that are light and temperature dependent (e.g., isoprene), Equation (2) was used according to Guenther et al. [34]. The standard values for T and PAR are 303.15 K and 1000 $\mu\text{mol m}^{-2} \text{s}^{-1}$.

$$E = E_s \times C_T \times C_L \quad (2)$$

E ($\mu\text{g g}_{\text{dw}}^{-1} \text{h}^{-1}$) is the actual (measured) emission at the chamber temperature T (K) and PAR ($\mu\text{mol m}^{-2} \text{s}^{-1}$). E_s ($\mu\text{g g}_{\text{dw}}^{-1} \text{h}^{-1}$) is the standardized emission, and C_T and C_L are correction factors for temperature and light as defined by Equations (3) and (4).

$$C_L = \frac{\alpha C_{L1} \text{PAR}}{\sqrt{1 + \alpha^2 \text{PAR}^2}} \quad (3)$$

where α (=0.0027) and C_{L1} (=1.066) are empirical coefficients [34].

$$C_T = \frac{\exp \frac{C_{T1}(T-T_s)}{RT_s T}}{1 + \exp \frac{C_{T2}(T-T_M)}{RT_s T}} \quad (4)$$

where C_{T1} ($=95,000 \text{ J mol}^{-1}$), C_{T2} ($=230,000 \text{ J mol}^{-1}$) and T_M ($=314 \text{ K}$) are empirical coefficients, R ($=8.314 \text{ J K}^{-1} \text{ mol}^{-1}$) is the universal gas constant and T_s ($=303.15 \text{ K}$) is the standard temperature [34]. For the compounds that showed light dependence, a curve was fitted by optimizing the parameters on the right-hand side of Equation (2) to the measured emission values. In this procedure, C_T was kept as a constant and determined by the average T for each variety.

For compounds where emissions are dependent on T alone, Equation (5) can be used.

$$E = E_s \times e^{\beta(T-T_s)} \quad (5)$$

where E ($\mu\text{g g}_{\text{dw}}^{-1} \text{ h}^{-1}$) is the actual emission rate at temperature T (K), E_s ($\mu\text{g g}_{\text{dw}}^{-1} \text{ h}^{-1}$) is the standard emission rate at the standard temperature T_s ($=303.15 \text{ K}$) and β ($=0.09 \text{ K}^{-1}$ for MTs and 0.17 K^{-1} for SQTs) is an empirical constant [34,35].

2.6. Statistical Analysis

The significance of the differences between the emissions from the varieties were analyzed by a Kruskal-Wallis test, which compared all varieties within a BVOC group. If this test resulted in a significant p -value ($p < 0.05$), then a Mann-Whitney U-test with a Bonferroni correction to account for multiple comparisons was used on each pair of varieties. Differences in the light responses for isoprene, ocimene and caryophyllene among the varieties were analyzed by multiple linear regression.

3. Results

3.1. Climate Data

The long-term climate data were taken from the Swedish Meteorological and Hydrological Institute (SMHI). The closest weather station for plots 1 and 2 that records T is located in Lund (circa 19 km from plots 1 and 2) and for precipitation is Landskrona (circa 11 km from plots 1 and 2). The T for plots 3 and 4 was recorded in Gendalen and precipitation was measured in Trökörna (circa 9 km from plots 3 and 4). To be able to compare the phenological status between the two sites, growing degree days (GDDs, $^{\circ}\text{C}$) was calculated as $\Sigma[(T_{\text{max}} + T_{\text{min}})/2 - T_{\text{base}}]$ for each day where $T_{\text{base}} = 5 \text{ }^{\circ}\text{C}$. If the GDD value was $<0 \text{ }^{\circ}\text{C}$ for a specific day, then it was set as $0 \text{ }^{\circ}\text{C}$. The long-term GDD means between 1987 and 2016 were calculated (Table 3). Comparing the GDDs in 2017 with the long-term means showed that 2017 was similar to previous years, with a maximum GDD difference $< 30 \text{ }^{\circ}\text{C}$. Furthermore, all months had higher GDDs at plots 1 and 2 than at plots 3 and 4, especially May to September. This result indicates that the trees at plots 1 and 2 started to grow before the trees at plots 3 and 4. On the other hand, since the campaigns were not done at the same time for the different plots, the phenological status was not necessarily higher for plots 1 and 2. For example, when the first campaign at plots 1 and 2 was done in May, the GDD value was $335.6 \text{ }^{\circ}\text{C}$ at this location. Two weeks later in June, when the first campaign was done at plots 3 and 4, the GDD had risen to $365.8 \text{ }^{\circ}\text{C}$ for these plots (Table S2).

Table 3. The average ambient T (°C), average precipitation (mm) and mean values of growing degree days (GDDs, °C) for each month in 2017. The long-term means for T and GDD were calculated between 1987 and 2016 for all plots. The long-term precipitation for plots 1 and 2 was calculated between 1987 and 2016, but between 1992 and 2016 for plots 3 and 4. The temperature was recorded in Lund, and the precipitation in Landskrona, for plots 1 and 2. For plots 3 and 4, the T from Gendalen and precipitation from Trökörna have been used.

2017 plots 1 & 2	January	February	March	April	May	June	July	August	September
T (°C)	0.6	1.5	4.8	6.8	13.1	16.2	16.8	17.4	13.8
Precipitation (mm)	13.7	39.6	36.8	31.9	14.5	77.0	58.6	57.3	61.4
GDDs ¹ (°C)	1.3	6.8	36.1	112.2	370.9	715.2	1082.7	1478.6	1754.5
Long-term plots 1 & 2									
T (°C)	0.7	1.1	3.0	7.6	12.3	15.5	18.1	17.6	13.8
Precipitation (mm)	44.9	34.5	32.7	30.3	43.2	59.2	65.7	74.8	60.3
GDDs ¹ (°C)	7.7	10.9	31.2	130.0	365.3	686.9	1101.0	1502.9	1779.8
2017 plots 3 & 4									
T (°C)	-0.3	0.1	3.1	5.3	11.7	14.9	15.9	15.1	12.0
Precipitation (mm)	30.6	38.7	61.5	36.7	39.5	78	36.2	92.4	68.7
GDDs ¹ (°C)	0.5	0.8	13.6	55.1	258.6	560.8	896.4	1215.8	1433.4
Long-term plots 3 & 4									
T (°C)	-1.3	-1.0	1.4	6.2	11.1	14.4	16.8	15.7	11.8
Precipitation (mm)	59.4	47.7	37.8	49.7	55.3	83.4	83.5	83.9	69.9
GDD ¹ (°C)	1.9	4.3	13.9	73.2	255.6	532.4	893.8	1229.0	1436.8

¹ GDD was calculated as $\sum[(T_{\max} + T_{\min})/2 - T_{\text{base}}]$ for each day between 1987 and 2016. $T_{\text{base}} = 5\text{ }^{\circ}\text{C}$, and if $(T_{\max} + T_{\min})/2 < 0$, then $(T_{\max} + T_{\min})/2 - T_{\text{base}} = 0$.

More precipitation fell throughout the growing season on plots 3 and 4 compared to on plots 1 and 2, and the only months between January and September that had less rain at plots 3 and 4 were February and July (Table 3). The temperature and precipitation for each month in 2017 differed somewhat compared to the long-term means at the sites, which were calculated between 1987 and 2016 (T plots 1–4 and precipitation plots 1 and 2) and between 1992 and 2016 (precipitation plots 3 and 4). For instance, February, March, May and June were circa 0.4–1.8 °C warmer in 2017 than the long-term means at plots 1 and 2 (Table 3 and Figure S4A). February, March and June in 2017 received circa 13–30% more precipitation than the corresponding months between 1987 and 2016 at plots 1 and 2, whilst May got 66% less rain. For plots 3 and 4, April, July and August were colder (circa 0.6–0.9 °C) and January–March, May, June and September were warmer (circa 0.2–1.7 °C) than the long-term means (Table 3 and Figure S4B). March received more rain (>60%) and January, February, April, May and July had less precipitation (circa 19–57%) compared to the means calculated between 1992 and 2016. The lower T and the drier conditions in April 2017 might have slowed down the growing process for the trees on plots 3 and 4 at the beginning of the growing season.

The absolute difference between the average leaf T within the chamber and the average ambient T during the measurements varied from 0.3 to 2.3 °C at plot 1, 0.2 to 2.4 °C at plot 2, 0.7 to 2.3 °C at plot 3 and 0.1 to 2.1 °C at plot 4 (Table S2). The temperature differences between the chamber and ambient air are small and are considered to cause no or little stress to the trees, since the leaf T is close to the prevailing T that the rest of the tree experienced during the measurement.

3.2. BVOC Emission

From all campaigns, in total, 193 different peaks could be detected during GC-MS analysis, but only 87 compounds could be identified. The unidentified peaks were named as unknown. The average measured BVOC emission from all varieties and plots for the whole season in 2017 was 26.33 (± 1.54) $\mu\text{g g}_{\text{dw}}^{-1} \text{h}^{-1}$. The average measured BVOC emission varied campaign-wise from 3.17 to 55.34 $\mu\text{g g}_{\text{dw}}^{-1} \text{h}^{-1}$, where the highest emission rate was seen during the first campaign (29 May–5 June) and the lowest during the last (5–7 September) (Figure 2). The dominant compound from the trees was isoprene, with an average emission rate of 8.08 (± 14.67) $\mu\text{g g}_{\text{dw}}^{-1} \text{h}^{-1}$ (Table 4). Isoprene

contributed almost 30% of the total BVOC emissions. The average measured isoprene emission rate for each campaign varied between 0 and $21.61 \mu\text{g g}_{\text{dw}}^{-1} \text{h}^{-1}$, where no emissions could be seen during the second campaign (13–15 June) from plots 3 and 4. The highest average measured emission rate was observed during the third campaign (28 June). Except for in the third campaign, the fraction of isoprene was higher in the second part of the season, where it varied from 40% to 70% of the total BVOC emissions.

Fourteen different MTs were emitted, whereof 13 were identified (α -pinene, α -thujene, β -pinene, camphene, d-phellandrene, eucalyptol, γ -terpinene, limonene, linalool, ocimene, p-cymene, terpinolene and 3-carene). Ocimene was the dominant MT and the average rate was $0.54 (\pm 1.21) \mu\text{g g}_{\text{dw}}^{-1} \text{h}^{-1}$. The average MT emission rate for each campaign ranged from 0.10 to $2.59 \mu\text{g g}_{\text{dw}}^{-1} \text{h}^{-1}$. The highest rate was emitted during the first campaign (28 May–5 June) and lowest during the last (5–7 September) (Figure 2). The MT fraction reached up to 11% of the total average BVOC emissions at the end of August but was 8% or less during the rest of the campaigns.

Six SQTs were observed, whereof five could be identified (α -farnesene, caryophyllene, copaene, humulene and nerolidol). Nerolidol had the highest emission rate ($0.26 \pm 0.61 \mu\text{g g}_{\text{dw}}^{-1} \text{h}^{-1}$) among all SQTs, which was more than three times higher than that of the second most emitted SQT, which was humulene ($0.08 \pm 0.28 \mu\text{g g}_{\text{dw}}^{-1} \text{h}^{-1}$). The average rates from the group of SQTs were lower than for MTs and varied between 0.007 and $0.74 \mu\text{g g}_{\text{dw}}^{-1} \text{h}^{-1}$, where the peaks and the lowest values occurred at same campaigns as for the group of MTs. The contribution from the SQTs to the total BVOC emissions varied from 0.1% to 3.4%. The highest SQT fraction was seen during the seventh campaign (1–2 August) and lowest during the third (28 June).

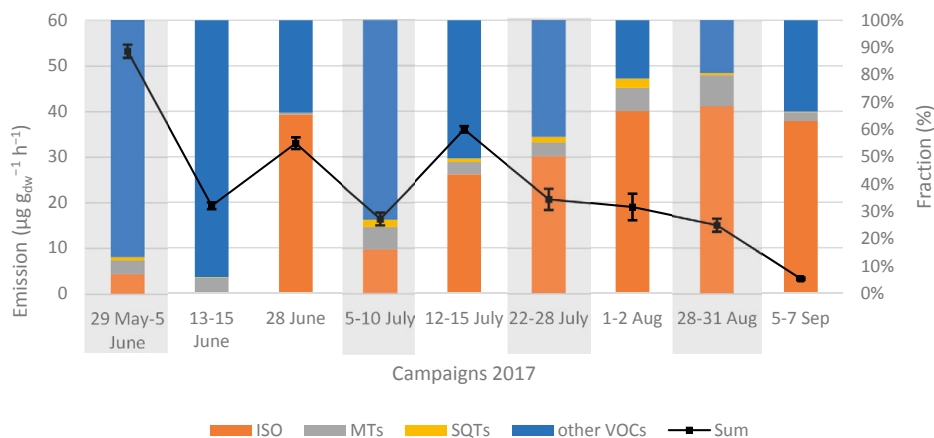


Figure 2. Total biogenic volatile organic compound (BVOC) emissions (black square, mean \pm standard deviation, $\mu\text{g g}_{\text{dw}}^{-1} \text{h}^{-1}$, $n = 11\text{--}56$), and the fractions of isoprene (ISO), monoterpenes (MTs), sesquiterpenes (SQTs) and other volatile organic compounds (other VOCs) throughout the season for each campaign. Campaigns performed on plots 1 and 2 (grey boxes) were done from 29 May to 5 June, 5 to 10 July, 22 to 28 July and 28 to 31 August. Campaigns performed on plots 3 and/or 4 were done from 13 to 15 June, on 28 June, from 12 to 15 July, from 1 to 2 August and from 5 to 7 September.

Table 4. The measured (M , $\mu\text{g g}_{\text{dw}}^{-1} \text{h}^{-1}$) and standardized emissions (STD , $\mu\text{g g}_{\text{dw}}^{-1} \text{h}^{-1}$, $n = 299$) of the BVOC groups and some of the most abundant identified compounds in each group. The numbers in the parentheses are standard deviations (SD , $\mu\text{g g}_{\text{dw}}^{-1} \text{h}^{-1}$). No standardization has been done on other VOCs (–).

BVOC	$M \pm SD$ ($\mu\text{g g}_{\text{dw}}^{-1} \text{h}^{-1}$)	$STD \pm SD$ ($\mu\text{g g}_{\text{dw}}^{-1} \text{h}^{-1}$)
isoprene	8.08 (14.67)	33.21 (53.43)
MTs	1.30 (0.68)	4.40 (2.05)
ocimene	0.54 (1.21)	2.15 (4.50)
limonene	0.30 (1.74)	0.84 (4.52)
linalool	0.10 (0.22)	0.46 (0.86)
camphene	0.07 (1.19)	0.20 (3.22)
β -pinene	0.07 (0.24)	0.20 (0.74)
SQTs	0.40 (0.29)	2.51 (2.03)
nerolidol	0.26 (0.61)	1.67 (4.22)
humulene	0.08 (0.28)	0.48 (2.08)
α -farnesene	0.02 (0.08)	0.10 (0.43)
other VOCs	16.55 (1.01)	–
hexanal	1.86 (9.61)	–
octanal	1.08 (5.11)	–
acetophenone	0.77 (2.51)	–
benzaldehyde	0.69 (1.87)	–
furfural	0.46 (1.65)	–
nonanal	0.40 (1.38)	–
1-hexanol, 2-ethyl-	0.40 (0.83)	–
phenol	0.37 (0.67)	–
p-xylene	0.30 (0.82)	–
decanal	0.30 (0.65)	–

The average emissions from other VOCs during each campaign ranged from 1.06 to 45.99 $\mu\text{g g}_{\text{dw}}^{-1} \text{h}^{-1}$, and the average emissions of all other VOCs were $16.55 \pm 1.01 \mu\text{g g}_{\text{dw}}^{-1} \text{h}^{-1}$. The highest average rate ($45.99 \pm 1.36 \mu\text{g g}_{\text{dw}}^{-1} \text{h}^{-1}$) was seen during the first campaign and was more than twice as high as the second highest ($18.25 \pm 2.21 \mu\text{g g}_{\text{dw}}^{-1} \text{h}^{-1}$) in the middle of July. The lowest other VOC emission rate was observed during the last campaign. The other VOC fraction varied between 19% and 94%, where the two highest values were observed during the first (86%) and the second (94%) campaigns, while the lowest fraction occurred during the eighth campaign at the end of August (Figure 2). Among the other VOCs, hexanal was the most emitted compound ($1.86 \pm 9.61 \mu\text{g g}_{\text{dw}}^{-1} \text{h}^{-1}$), followed by octanal ($1.08 \pm 5.11 \mu\text{g g}_{\text{dw}}^{-1} \text{h}^{-1}$) and acetophenone ($0.77 \pm 2.51 \mu\text{g g}_{\text{dw}}^{-1} \text{h}^{-1}$) (Table 4). The contribution from these compounds varied between the campaigns. Hexanal contributed almost 53% of the total other VOC emissions in the middle of the season (12–15 July) but <17% during the rest of the campaigns. The emissions of octanal and acetophenone were higher in the beginning of the season, where they contributed circa 3–11% and 4–29% to the total average other VOC emissions, respectively.

3.2.1. Terpenoid Emission Differences between the Varieties

The highest total terpenoid emission rate was from Wilhelm ($13.68 \pm 5.84 \mu\text{g g}_{\text{dw}}^{-1} \text{h}^{-1}$) followed by those from Inger ($10.02 \pm 3.32 \mu\text{g g}_{\text{dw}}^{-1} \text{h}^{-1}$), Ester ($7.93 \pm 2.73 \mu\text{g g}_{\text{dw}}^{-1} \text{h}^{-1}$) and Tora ($5.96 \pm 2.06 \mu\text{g g}_{\text{dw}}^{-1} \text{h}^{-1}$) (Table 5). Both average values of T and PAR were similar for all varieties and varied between 18.9 and 19.0 $^{\circ}\text{C}$, and 551 and 573 $\mu\text{mol m}^{-2} \text{s}^{-1}$, respectively. Isoprene emission was highest for Wilhelm ($12.66 \pm 20.63 \mu\text{g g}_{\text{dw}}^{-1} \text{h}^{-1}$) with a corresponding standardized emission (STD) rate of $50.33 (\pm 72.63) \mu\text{g g}_{\text{dw}}^{-1} \text{h}^{-1}$, but there were no significant differences between the varieties and the measured isoprene emissions (Table 6). However, STD isoprene emission was significantly higher for

Wilhelm compared to for Tora. Isoprene emission exceeded the emissions of both MTs and SQTs for all varieties. Inger emitted the highest amount of MTs, but with high variance. Tora had significantly higher MT emissions than Ester and Wilhelm (Table 6). The average MT emission rate among the varieties varied between 0.80 and 1.87 $\mu\text{g g}_{\text{dw}}^{-1} \text{h}^{-1}$, which corresponds to the average STD range 3.09–6.00 $\mu\text{g g}_{\text{dw}}^{-1} \text{h}^{-1}$. Sesquiterpene emissions were significantly higher for Ester, which had twice as high emissions as Wilhelm ($0.57 \pm 0.44 \mu\text{g g}_{\text{dw}}^{-1} \text{h}^{-1}$ vs. $0.22 \pm 0.24 \mu\text{g g}_{\text{dw}}^{-1} \text{h}^{-1}$). Ester and Inger had a similar average SQT emission rate.

Table 5. Upper part: Isoprene, monoterpene (MT), sesquiterpene (SQT) and total terpenoid emissions ($\mu\text{g g}_{\text{dw}}^{-1} \text{h}^{-1}$, mean \pm standard deviation) for the different *Salix* varieties. Middle part: Standardized (STD) emission rates ($\mu\text{g g}_{\text{dw}}^{-1} \text{h}^{-1}$, mean \pm standard deviation). Lower part: Average T ($^{\circ}\text{C}$), photosynthetically active radiation (PAR, $\mu\text{mol m}^{-2} \text{s}^{-1}$) and relative humidity (RH) (%) in the measurement cuvette.

	Tora, n = 90	Wilhelm, n = 104	Ester, n = 53	Inger, n = 52
isoprene ($\mu\text{g g}_{\text{dw}}^{-1} \text{h}^{-1}$)	4.00 (7.05)	12.66 (20.63)	6.11 (9.06)	7.77 (11.65)
MTs ($\mu\text{g g}_{\text{dw}}^{-1} \text{h}^{-1}$)	1.56 (0.62)	0.80 (0.28)	1.25 (1.01)	1.87 (1.24)
SQTs ($\mu\text{g g}_{\text{dw}}^{-1} \text{h}^{-1}$)	0.40 (0.28)	0.22 (0.24)	0.57 (0.44)	0.56 (0.26)
Sum ($\mu\text{g g}_{\text{dw}}^{-1} \text{h}^{-1}$)	5.96 (2.06)	13.68 (5.84)	7.93 (2.73)	10.02 (3.32)
STD isoprene ($\mu\text{g g}_{\text{dw}}^{-1} \text{h}^{-1}$)	17.99 (27.18)	50.53 (72.63)	25.84 (34.36)	32.75 (47.82)
STD MTs ($\mu\text{g g}_{\text{dw}}^{-1} \text{h}^{-1}$)	5.84 (1.90)	3.09 (0.99)	3.44 (2.35)	6.00 (3.21)
STD SQTs ($\mu\text{g g}_{\text{dw}}^{-1} \text{h}^{-1}$)	2.43 (1.63)	1.30 (1.53)	3.76 (3.20)	3.71 (1.91)
T ($^{\circ}\text{C}$)	19.0 (2.1)	19.0 (2.0)	18.9 (2.2)	19.0 (2.3)
PAR ($\mu\text{mol m}^{-2} \text{s}^{-1}$)	571 (487)	551 (477)	561 (477)	573 (494)
RH (%)	61.5 (13.0)	53.9 (16.9)	48.2 (9.5)	51.4 (8.9)

Table 6. The *p*-values from statistical tests for differences between varieties in measured (upper) and STD (lower) isoprene, total MT and SQT emissions. The *p*-values originate from pairwise Mann-Whitney U-tests. The significance level after applying a Bonferroni correction is circa 0.008 (0.05/6 \approx 0.008). All *p*-values written in bold indicate significant differences.

isoprene				STD isoprene			
Variety	Wilhelm	Ester	Inger	Variety	Wilhelm	Ester	Inger
Tora	0.015	0.768	0.330	Tora	0.007	0.802	0.343
Wilhelm		0.033	0.299	Wilhelm		0.024	0.217
Ester			0.218	Ester			0.254
MTs				STD MTs			
Variety	Wilhelm	Ester	Inger	Variety	Wilhelm	Ester	Inger
Tora	0.006	<0.001	0.108	Tora	0.005	<0.001	0.064
Wilhelm		0.107	0.632	Wilhelm		0.030	0.685
Ester			0.045	Ester			0.026
SQTs				STD SQTs			
Variety	Wilhelm	Ester	Inger	Variety	Wilhelm	Ester	Inger
Tora	0.006	0.892	<0.001	Tora	0.003	0.652	<0.001
Wilhelm		0.051	<0.001	Wilhelm		0.070	<0.001
Ester			0.001	Ester			<0.001

Ocimene was the dominant MT emitted among all *Salix* varieties (0.03–1.08 $\mu\text{g g}_{\text{dw}}^{-1} \text{h}^{-1}$) and made up almost 70% and 50% of the total MT emissions from Tora and Wilhelm, respectively (Figure 3). Ocimene was emitted less by Ester, from which the contribution was lower than 3%. Instead, camphene (31%) contributed most of the MTs from Ester, followed by limonene (29%). On the other hand, the emissions of camphene were negligible for the other varieties. Limonene was the second most

abundant MT ($0.14\text{--}0.78 \mu\text{g g}_{\text{dw}}^{-1} \text{h}^{-1}$) and contributed 11–41% of the total MT rate among the varieties. The lowest MT emission rate was seen from Wilhelm, and the highest from Inger. Inger was the only variety that emitted α -thujene, and Tora was the only variety that did not emit terpinolene.

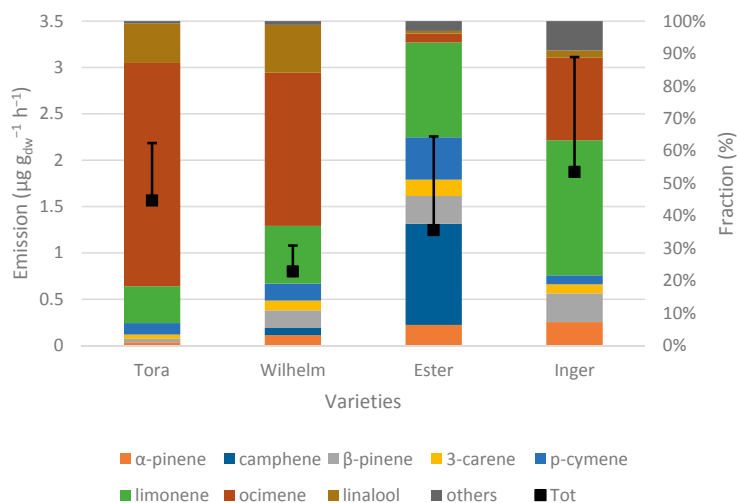


Figure 3. Total MT emissions (black square, $\mu\text{g g}_{\text{dw}}^{-1} \text{h}^{-1}$, mean + standard deviation, $n = 52\text{--}104$) and the contribution from each MT for the different varieties. Others includes d-phellandrene, terpinolene, γ -terpinene and one unknown compound.

Nerolidol was the most prominent SQT and the average emission rate varied from 0.12 to $0.47 \mu\text{g g}_{\text{dw}}^{-1} \text{h}^{-1}$ (Figure 4). The contribution from nerolidol was higher than 45% for all varieties and exceeded the contribution from each of the other SQTs. Humulene was the second most emitted SQT ($0.04\text{--}0.17 \mu\text{g g}_{\text{dw}}^{-1} \text{h}^{-1}$) and contributed 7–30% of the total SQT rate. All SQTs observed in this study were seen in emissions from all varieties, except for one unknown, which was not emitted by Tora, and caryophyllene, which was not emitted by Wilhelm.

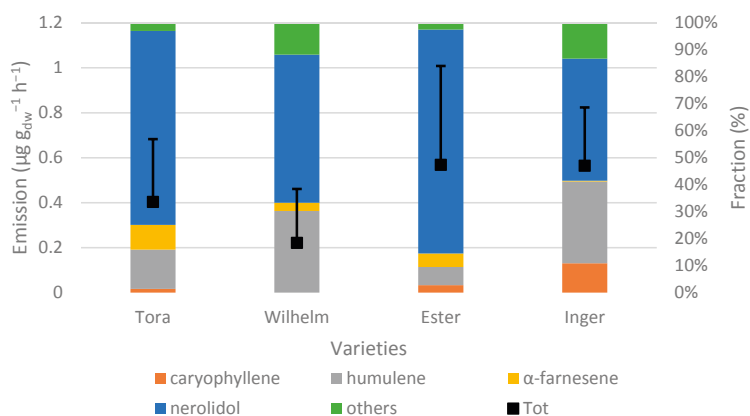


Figure 4. Total SQT emissions (black square, $\mu\text{g g}_{\text{dw}}^{-1} \text{h}^{-1}$, mean + standard deviation, $n = 52\text{--}104$) and the contribution from each SQT for the different varieties. Others includes copaene and one unknown compound.

3.2.2. The Responses of Terpenoid Emission, Net Assimilation and Water Use Efficiency to Different Light Levels

The average total terpenoid emission rate increased, in general, with increasing PAR until the highest PAR level of the tested light response curves, $1500 \mu\text{mol m}^{-2} \text{s}^{-1}$, which is explained by the increase in isoprene emission, but this pattern was not completely consistent for Ester and Inger. Terpenoid emissions from Ester had already peaked at a light level of $450 \mu\text{mol m}^{-2} \text{s}^{-1}$ ($12.94 \pm 3.42 \mu\text{g g}_{\text{dw}}^{-1} \text{h}^{-1}$), partly due to high emissions of MTs (Figure 5C). Wilhelm emitted higher average terpenoid emissions when PAR varied between 300 and $1500 \mu\text{mol m}^{-2} \text{s}^{-1}$ compared to the other varieties, and the average total terpenoid values for Wilhelm ranged from 0.74 to $34.02 \mu\text{g g}_{\text{dw}}^{-1} \text{h}^{-1}$, when PAR ranged from 0 to $1500 \mu\text{mol m}^{-2} \text{s}^{-1}$ (Figure 5B). The corresponding emissions from the other three varieties varied between 0.63 and $19.56 \mu\text{g g}_{\text{dw}}^{-1} \text{h}^{-1}$. Thus, Wilhelm had an average terpenoid emission rate almost twice as high as the second highest (Inger) when PAR peaked. Tora had lower terpenoid emissions ($0.68\text{--}13.88 \mu\text{g g}_{\text{dw}}^{-1} \text{h}^{-1}$) than the rest of the varieties at all PAR levels, except at $1500 \mu\text{mol m}^{-2} \text{s}^{-1}$, where Ester had the lowest emission rate ($11.34 \pm 3.85 \mu\text{mol m}^{-2} \text{s}^{-1}$).

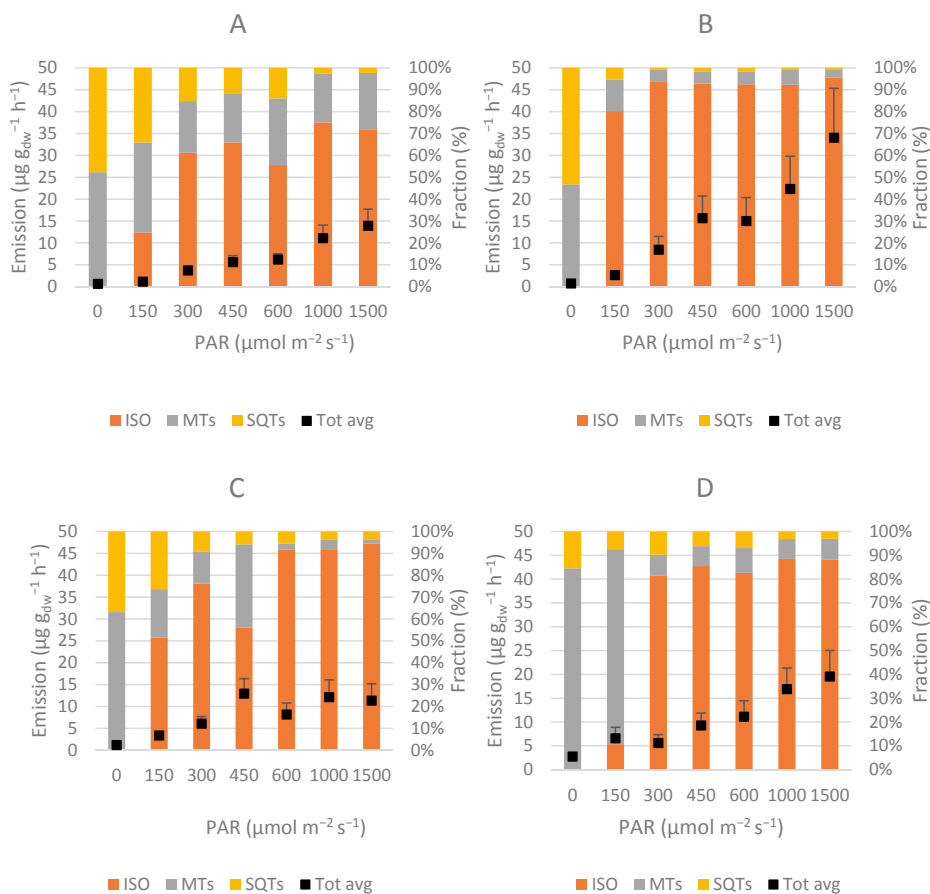


Figure 5. Total terpenoid emissions (black squares, $\mu\text{g g}_{\text{dw}}^{-1} \text{h}^{-1}$, mean + standard deviation, $n = 7\text{--}16$) and the fraction of isoprene (ISO), MTs and SQTs for different PAR values ($\mu\text{mol m}^{-2} \text{s}^{-1}$). (A) Tora, (B) Wilhelm, (C) Ester and (D) Inger.

Isoprene

Isoprene dominated over the other terpenoids and contributed > 50% of the total terpenoid emissions for all varieties when PAR was equal to 300 $\mu\text{mol m}^{-2} \text{s}^{-1}$ or more. Isoprene responded faster to the increasing light levels for Wilhelm compared to the other varieties, and the response was significantly higher compared to all the other varieties (Figure 6). Isoprene reached >75% of the total terpenoid emission rate, already at 150 $\mu\text{mol m}^{-2} \text{s}^{-1}$, for Wilhelm, and increased to >90% when PAR varied between 300 and 1500 $\mu\text{mol m}^{-2} \text{s}^{-1}$ (Figure 5B). The isoprene fraction for Inger did not change between 300 and 1500 $\mu\text{mol m}^{-2} \text{s}^{-1}$, and contributed 80–90% of the total terpenoid emissions. Isoprene emission peaked at 1500 $\mu\text{mol m}^{-2} \text{s}^{-1}$ for all varieties except Ester, where the average isoprene emission rate reached a maximum at 1000 $\mu\text{mol m}^{-2} \text{s}^{-1}$ (Figure 6). At a PAR level of 1500 $\mu\text{mol m}^{-2} \text{s}^{-1}$, the highest average isoprene emissions were observed for Wilhelm ($32.52 \pm 33.81 \mu\text{g g}_{\text{dw}}^{-1} \text{h}^{-1}$), which was more than three times higher than those for Tora. The fitted curves showed that Ester and Inger responded in the same way up to circa 450 $\mu\text{mol m}^{-2} \text{s}^{-1}$. Thereafter, the emission rates from Ester leveled out faster than the others and approached the isoprene emission rates from Tora. Values related to the fitted curves can be seen in Table S3.

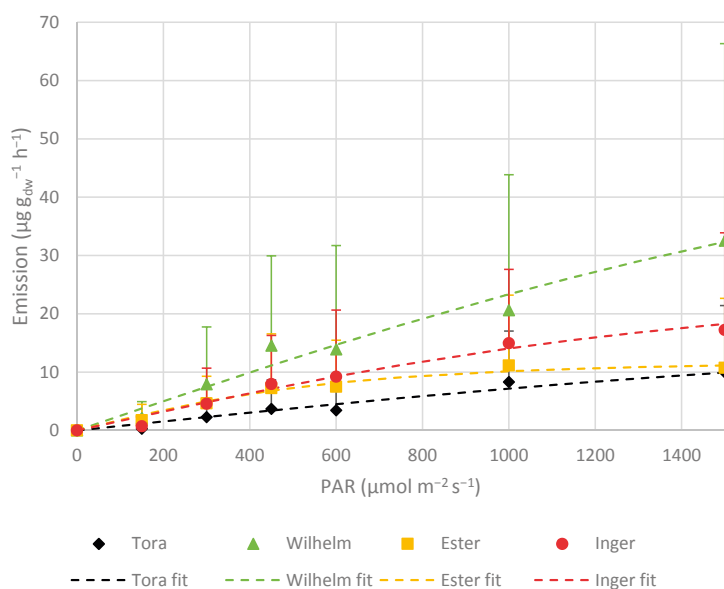


Figure 6. Isoprene emission rates ($\mu\text{g g}_{\text{dw}}^{-1} \text{h}^{-1}$, mean + standard deviation, $n = 7\text{--}16$) and fitted curves according to Equation (2) for the *Salix* varieties at different PAR values ($\mu\text{mol m}^{-2} \text{s}^{-1}$).

Monoterpenes

Tora was the only variety that constantly had increased MT emissions with increasing PAR (Figure 5A). This trend is mainly due to the light-response for ocimene and linalool, which were the only MTs that showed light dependence. This light dependence was observed for Tora, Wilhelm and Inger, but not for Ester (Figure 7). The average emission of ocimene increased at all PAR steps for Tora ($0\text{--}2.90 \mu\text{g g}_{\text{dw}}^{-1} \text{h}^{-1}$) and Inger ($0\text{--}1.32 \mu\text{g g}_{\text{dw}}^{-1} \text{h}^{-1}$), whereas it reached $0.75 \mu\text{g g}_{\text{dw}}^{-1} \text{h}^{-1}$ at 1000 $\mu\text{mol m}^{-2} \text{s}^{-1}$ for Wilhelm and leveled out thereafter. The light response of ocimene for Tora was significantly higher compared to for the other varieties. The fitted curves showed that emissions of ocimene from Wilhelm and Inger responded in the same way up to 450 $\mu\text{mol m}^{-2} \text{s}^{-1}$, but afterwards, Inger had a steeper response with PAR than Wilhelm. The average emission of linalool from Tora varied from 0 to $0.41 \mu\text{g g}_{\text{dw}}^{-1} \text{h}^{-1}$, and the light response was significantly higher compared to that for the

others (Figure 8). The trend for Inger was less clear, even if the average emission rates seemed to level out when PAR exceeded 1000 $\mu\text{mol m}^{-2} \text{s}^{-1}$. The MT fraction of the terpenoid emissions had a similar pattern for the four varieties. As expected, a substantial contribution to the total terpenoid emissions came from MTs (47–85%) when PAR was equal to 0 $\mu\text{mol m}^{-2} \text{s}^{-1}$ for all varieties (Figure 5A–D). When PAR increased to 150 $\mu\text{mol m}^{-2} \text{s}^{-1}$, Tora and Inger still had a considerable contribution of MT emissions (41% and 82% respectively), whilst the fractions for Wilhelm and Ester were 14% and 22%, respectively. At the higher light levels, the MT fraction was mainly <10% due to the light-induced isoprene emissions, except for Ester at 450 $\mu\text{mol m}^{-2} \text{s}^{-1}$, and for Tora.

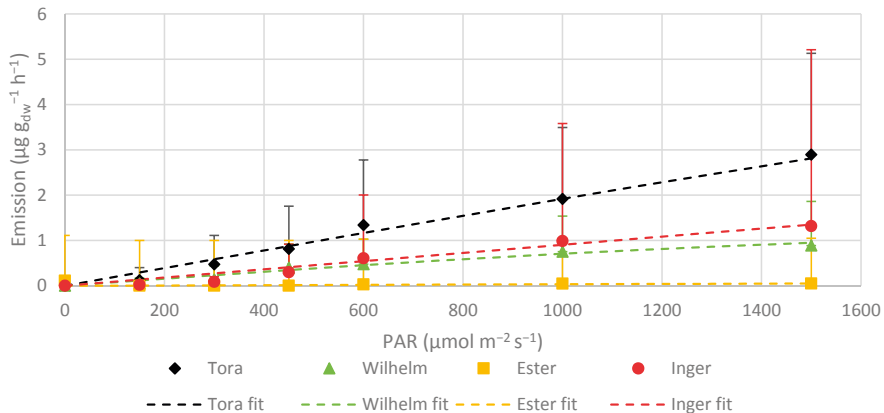


Figure 7. The light response of ocimene emissions ($\mu\text{g g}_{\text{dw}}^{-1} \text{h}^{-1}$, mean + standard deviation, $n = 7\text{--}16$) to different PAR values ($\mu\text{mol m}^{-2} \text{s}^{-1}$) for the *Salix* varieties.

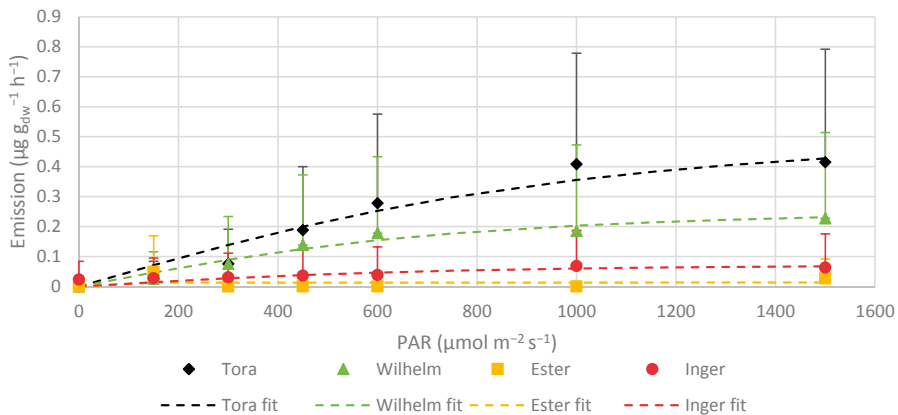


Figure 8. The light response of linalool emissions ($\mu\text{g g}_{\text{dw}}^{-1} \text{h}^{-1}$, mean + standard deviation, $n = 7\text{--}16$) to different PAR values ($\mu\text{mol m}^{-2} \text{s}^{-1}$) for the *Salix* varieties.

Sesquiterpenes

The emissions of SQTs peaked at both low PAR values (e.g., darkness) and at higher PAR (e.g., 600 $\mu\text{mol m}^{-2} \text{s}^{-1}$) among the varieties. Caryophyllene seemed to be influenced by light, but this was only clear for Inger (Figure 9), as its light response for caryophyllene differed significantly to that for the other varieties, and the average emissions increased from 0 to 0.14 $\mu\text{g g}_{\text{dw}}^{-1} \text{h}^{-1}$ when PAR varied between 0 and 1500 $\mu\text{mol m}^{-2} \text{s}^{-1}$. The SQT fractions were in general larger for light levels up to 300 $\mu\text{mol m}^{-2} \text{s}^{-1}$ (Figure 5A–D). When PAR was equal to 0, SQTs contributed 15–53% of the terpenoid

emission rate. At 150 $\mu\text{mol m}^{-2} \text{s}^{-1}$, only Tora and Ester showed a significant contribution of SQTs (34% and 26% respectively) of the total terpenoid emission rate. The contribution from SQTs did not reach above 16% when PAR values were $>150 \mu\text{mol m}^{-2} \text{s}^{-1}$. The SQT fraction seemed to decrease with higher PAR values because of increasing isoprene rates. The highest average emissions of SQTs for the different light levels reached up to $0.89 (\pm 0.49) \mu\text{g g}_{\text{dw}}^{-1} \text{h}^{-1}$, which was emitted by Ester when PAR was $150 \mu\text{mol m}^{-2} \text{s}^{-1}$. Even the third highest SQT rate ($0.76 \pm 0.57 \mu\text{g g}_{\text{dw}}^{-1} \text{h}^{-1}$ at $450 \mu\text{mol m}^{-2} \text{s}^{-1}$) was observed from Ester. Wilhelm emitted lower SQT rates at all light levels, except at zero $\mu\text{mol m}^{-2} \text{s}^{-1}$.

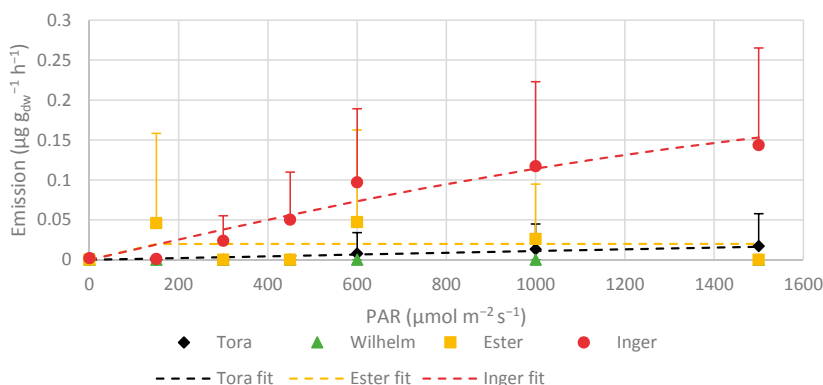


Figure 9. The light response of caryophyllene ($\mu\text{g g}_{\text{dw}}^{-1} \text{h}^{-1}$, mean + standard deviation, $n = 8$) to different PAR values ($\mu\text{mol m}^{-2} \text{s}^{-1}$) for the *Salix* varieties.

Net Assimilation (A) and Water Use Efficiency (WUE)

Tora ($7.10\text{--}17.80 \mu\text{mol CO}_2 \text{m}^{-2} \text{s}^{-1}$), Wilhelm ($7.46\text{--}17.15 \mu\text{mol CO}_2 \text{m}^{-2} \text{s}^{-1}$) and Inger ($7.84\text{--}17.29 \mu\text{mol CO}_2 \text{m}^{-2} \text{s}^{-1}$) had a similar A when they were exposed to light (Table 7). The lowest A was observed for Ester, which varied from 5.36 to $12.19 \mu\text{mol CO}_2 \text{m}^{-2} \text{s}^{-1}$. The WUE was higher for Ester ($10.15\text{--}15.08 \text{mmol CO}_2 \text{mol}^{-1} \text{H}_2\text{O}$) at all light levels compared to for the other varieties ($5.55\text{--}9.53 \text{mmol CO}_2 \text{mol}^{-1} \text{H}_2\text{O}$) and almost twice as high for some PAR values than for the other varieties. For the highest PAR values, Tora was the variety that had lowest WUE. Thus, the water loss due to transpiration was larger for Tora compared to for the others when PAR reached $1000 \mu\text{mol m}^{-2} \text{s}^{-1}$ or more. In contrast, the water loss from Ester was only 35–60% of the loss from the other varieties.

Table 7. Upper part: Net assimilation rate (A, $\mu\text{mol CO}_2 \text{m}^{-2} \text{s}^{-1}$, mean \pm standard deviation, $n = 6\text{--}14$) at different PAR values ($\mu\text{mol m}^{-2} \text{s}^{-1}$) for the varieties. Lower part: Water use efficiency (WUE, $\text{mmol CO}_2 \text{mol}^{-1} \text{H}_2\text{O}$, mean \pm standard deviation, $n = 6\text{--}14$) at different PAR values.

PAR ($\mu\text{mol m}^{-2} \text{s}^{-1}$)	150	300	450	600	1000	1500
Tora ($\mu\text{mol CO}_2 \text{m}^{-2} \text{s}^{-1}$)	7.10 (1.65)	10.87 (3.12)	13.31 (2.70)	15.00 (3.33)	16.96 (3.34)	17.80 (3.58)
Wilhelm ($\mu\text{mol CO}_2 \text{m}^{-2} \text{s}^{-1}$)	7.46 (1.31)	11.24 (1.87)	13.75 (2.84)	14.31 (3.16)	16.98 (4.48)	17.15 (5.71)
Ester ($\mu\text{mol CO}_2 \text{m}^{-2} \text{s}^{-1}$)	5.36 (1.02)	8.65 (1.17)	9.84 (1.23)	10.48 (1.66)	12.12 (2.29)	12.19 (3.53)
Inger ($\mu\text{mol CO}_2 \text{m}^{-2} \text{s}^{-1}$)	7.84 (2.22)	11.53 (2.93)	13.53 (3.69)	14.49 (3.75)	16.20 (5.33)	17.29 (5.42)
Tora ($\text{mmol CO}_2 \text{mol}^{-1} \text{H}_2\text{O}$)	6.67 (5.42)	6.57 (3.30)	6.57 (2.36)	7.69 (4.28)	7.12 (2.68)	6.56 (2.32)
Wilhelm ($\text{mmol CO}_2 \text{mol}^{-1} \text{H}_2\text{O}$)	6.81 (4.73)	6.65 (1.67)	8.38 (4.49)	7.45 (1.75)	9.53 (3.89)	8.00 (2.27)
Ester ($\text{mmol CO}_2 \text{mol}^{-1} \text{H}_2\text{O}$)	10.15 (8.42)	12.57 (12.64)	11.85 (11.81)	15.08 (11.32)	11.33 (11.49)	12.80 (13.58)
Inger ($\text{mmol CO}_2 \text{mol}^{-1} \text{H}_2\text{O}$)	5.55 (2.51)	7.47 (2.89)	8.32 (4.03)	8.45 (3.38)	8.32 (3.72)	8.49 (3.19)

3.2.3. Comparison between Ages

All the younger individuals (T1, W1, E1 and I1) showed higher emission rates of other VOCs compared to the 1-year-old trees (T2, W2, E2 and I2). Especially, the saplings of variety Ester (E0,

$46.74 \pm 1.18 \mu\text{g g}_{\text{dw}}^{-1} \text{h}^{-1}$) emitted 19 times more other VOCs than the older trees of variety Ester (E1, $2.46 \pm 0.07 \mu\text{g g}_{\text{dw}}^{-1} \text{h}^{-1}$) (Table 8). The high emission rate of other VOCs for E0 is due to a large contribution from hexanal ($4.92 \pm 6.53 \mu\text{g g}_{\text{dw}}^{-1} \text{h}^{-1}$), furfural ($3.07 \pm 3.93 \mu\text{g g}_{\text{dw}}^{-1} \text{h}^{-1}$), benzaldehyde ($3.20 \pm 4.56 \mu\text{g g}_{\text{dw}}^{-1} \text{h}^{-1}$), octanal ($3.00 \pm 4.79 \mu\text{g g}_{\text{dw}}^{-1} \text{h}^{-1}$) and acetophenone ($2.46 \pm 3.97 \mu\text{g g}_{\text{dw}}^{-1} \text{h}^{-1}$) (Table S4). Hexanal contributed substantially for W0 ($4.23 \pm 17.80 \mu\text{g g}_{\text{dw}}^{-1} \text{h}^{-1}$), but less for T0 ($1.03 \pm 4.88 \mu\text{g g}_{\text{dw}}^{-1} \text{h}^{-1}$) and I0 ($0.86 \pm 1.72 \mu\text{g g}_{\text{dw}}^{-1} \text{h}^{-1}$), to the other VOC emissions. The contribution of octanal to the other VOC emissions was high for T0 ($3.15 \pm 10.16 \mu\text{g g}_{\text{dw}}^{-1} \text{h}^{-1}$) but less than $0.50 \mu\text{g g}_{\text{dw}}^{-1} \text{h}^{-1}$ for W0 and I0. All the measured and the STD emission rates for MTs and SQTs were higher for the younger than for the older trees, except for Wilhelm (Table 8). Additionally, for MTs and SQTs, Ester was the variety with largest differences between the ages. The emissions for E0 were 10–11 times higher compared to E1. Camphene ($0.79 \pm 3.96 \mu\text{g g}_{\text{dw}}^{-1} \text{h}^{-1}$) and limonene ($0.60 \pm 1.58 \mu\text{g g}_{\text{dw}}^{-1} \text{h}^{-1}$) were the dominant MTs for E0, whereas nerolidol ($0.86 \pm 1.27 \mu\text{g g}_{\text{dw}}^{-1} \text{h}^{-1}$) was the dominant SQT.

Table 8. Upper part: Measured emission rates ($\mu\text{g g}_{\text{dw}}^{-1} \text{h}^{-1}$, mean \pm standard deviation, $n = 24\text{--}77$) for isoprene, MTs, SQTs and other VOCs for the different *Salix* varieties and ages. Lower part: The standardized (STD) emission rate ($\mu\text{g g}_{\text{dw}}^{-1} \text{h}^{-1}$, mean \pm standard deviation, $n = 26\text{--}77$) for isoprene, MTs, and SQTs for the different varieties and ages.

Variety	Tora		Wilhelm		Ester		Inger	
	1	2	1	2	1	2	1	2
Age of trees								
isoprene	4.21 (7.72)	3.65 (4.93)	14.11 (22.13)	8.53 (14.85)	5.48 (8.36)	6.97 (9.74)	6.61 (9.29)	8.77 (13.26)
MTs	1.80 (0.69)	1.02 (0.39)	0.74 (0.26)	0.95 (0.34)	2.33 (1.43)	0.22 (0.18)	2.52 (1.69)	1.32 (0.64)
SQTs	0.52 (0.33)	0.14 (0.09)	0.16 (0.18)	0.40 (0.37)	1.03 (0.62)	0.09 (0.08)	0.79 (0.35)	0.38 (0.12)
other VOCs	20.91 (1.05)	3.88 (0.14)	20.95 (1.50)	5.87 (0.27)	46.74 (1.18)	2.46 (0.07)	15.70 (0.94)	4.70 (0.13)
STD isoprene	17.22 (27.74)	19.76 (25.75)	52.74 (76.08)	38.38 (57.38)	27.47 (37.64)	24.27 (30.79)	32.27 (44.84)	33.16 (50.22)
STD MTs	5.82 (2.05)	4.50 (1.52)	2.57 (0.81)	4.31 (1.38)	6.36 (3.29)	0.72 (0.05)	6.81 (3.96)	5.30 (0.74)
STD SQTs	3.04 (1.90)	1.10 (0.62)	0.78 (0.79)	2.82 (0.47)	7.37 (4.49)	0.28 (0.05)	5.55 (2.68)	2.17 (0.36)

4. Discussion

Wilhelm was the variety that emitted the highest rate of terpenoids. Most of this emission (circa 90%) came from isoprene. In fact, Wilhelm emitted over three times more isoprene than Tora and almost twice as much as Ester and Inger. However, when comparing MTs and SQTs, Wilhelm had the lowest emissions. The average emissions of isoprene and SQTs were almost the same for Ester and Inger. The pathways of producing BVOCs have been studied and disentangled to a certain extent. Even if it is not fully understood, studies have shown that there is some linkage between the productions of these compounds [36,37]. The originating substrates responsible for the end products (e.g., isoprene, MTs and SQTs) are shared and divided into the separate pathways, which could be one of the explanations why Wilhelm emits lower amounts of MTs and SQTs, but more isoprene. The average T and PAR values within the chambers were almost the same for the varieties, indicating that the different emission rates among the varieties are related to other differences in the environment, or genetic variation. Genetic diversity was concluded by van Meeningen et al. [30] to be more important than, e.g., local growing conditions, when studying spruce BVOC emissions. Hence, for one specific species, the BVOC emission rates can differ among the varieties or clones. This difference is not always accounted for in models and should not be discarded when improving modelling for upscaling BVOC emissions.

The A was similar for Tora, Wilhelm and Inger (circa $13.5 \mu\text{mol CO}_2 \text{ m}^{-2} \text{ s}^{-1}$), reflecting that they are equally good at biomass production in the prevailing conditions in this study. Ester had circa 25% lower A, showing less productivity than the others. Despite the lower A, Ester showed a better ability to utilize water for producing biomass when photosynthesis occurred. The values of WUE related to Ester were up to twice as large compared to the others for some PAR values, which means that Ester lost less than 40% of the water. Therefore, Ester is more suitable for hot and dry climates and it outcompetes the other varieties in regions warmer and drier than southern Sweden. The maximum A for *Salix* trees has been reported to range from 20 to $30 \mu\text{mol CO}_2 \text{ m}^{-2} \text{ s}^{-1}$ [38]. The varieties in this

study had, in general, lower A, but they were able to assimilate more than $20 \mu\text{mol CO}_2 \text{ m}^{-2} \text{ s}^{-1}$ when PAR reached 1000 or $1500 \mu\text{mol m}^{-2} \text{ s}^{-1}$.

As expected [31,34,39–41], isoprene increased with increasing PAR levels. Studies have also shown that the emission rates of isoprene have a hyperbolic relationship with PAR [34,40,42,43]. Tora, Ester and Inger showed a similar trend, where the emission rates levelled out for the higher light levels. Ester was the only variety that peaked at $1000 \mu\text{mol m}^{-2} \text{ s}^{-1}$. Since no obvious damages could be seen on the leaves, this result indicates that the leaves belonging to Ester were saturated at lower light levels and could not utilize and respond to the highest PAR level like the other varieties. On the other hand, isoprene emission from Wilhelm continued to increase and showed no trend towards levelling out. Even though Wilhelm and Tora share similar ancestors from the breeding program, Tora is closer to Ester and Inger when it comes to isoprene emission. The photolysis of BVOCs and NO_x can lead to the production of O_3 and PAN [44,45], which are harmful for humans and vegetation at high concentrations [46–49]. Isoprene has been shown to be able to increase O_3 and PAN [44,50], which makes Wilhelm less preferable in high- NO_x environments compared to the other varieties. A major part of land cover in Sweden is boreal forest, whereof most is spruce (*Picea abies*) and pine (*Pinus sylvestris*). Isoprene emission from these species is much lower compared to that from *Salix* [11,30]. In the Southern part of Sweden, the common land cover is farmland. Commercial crops growing on agricultural areas in Sweden, such as wheat, also emit significantly lower rates of isoprene [11,23]. Hence, a land cover change from the traditional species to *Salix* plantations could alter the regional atmospheric chemistry leading to, e.g., increased levels of O_3 . However, isoprene-emitting plants seem to tolerate O_3 better than other non-isoprene emitting plants, and in this sense, varieties such as Wilhelm may be more resistant if growing in areas with high prevailing O_3 concentrations [51–53].

The monoterpene ocimene was emitted by all varieties, but at different rates. For Tora, Wilhelm and Inger, ocimene contributed circa 25–69% of the total MT emissions, whilst it was a minor compound for Ester. Ocimene and linalool were the only MTs which showed light dependency in Tora, Wilhelm and Inger, but not in Ester, likely due to being emitted only in very low amounts. In Tora and Inger, ocimene emission did not show any clear indication of leveling out, even at the highest measured PAR values. Wilhelm, on the other hand, did not increase the emission of ocimene much after $1000 \mu\text{mol m}^{-2} \text{ s}^{-1}$, and linalool seemed to level out for Tora and Wilhelm when PAR was above $1000 \mu\text{mol m}^{-2} \text{ s}^{-1}$. To date, no study has reported a light dependent relationship for MT emissions from willow trees, because the focus of most studies has been on isoprene. Monoterpenes can be important for generating secondary organic aerosols [54–57]. Since Ester was the only variety that did not increase MT emissions with increasing light, this variety might be more suitable near urban regions with more solar irradiance to avoid impaired air quality.

Nerolidol was the most dominant SQT and, together with humulene, constituted 75% or more of the total SQT emissions. Ester and Inger emitted approximately the same amounts of SQTs. Both of these varieties are female hybrids suitable for warm climates, and Ester also originates from Inger, which probably explains the similarities. However, the fractions of the emitted BVOCs differed. For example, no camphene was emitted by Inger, while camphene contributed almost one third of the MT emissions of Ester. In addition, Inger was the only variety that had a clearly increased emission rate of caryophyllene when light availability increased.

Saplings emitted approximately 3–19 times more other VOCs than the trees that were 1-year-old. Younger plants are more vulnerable than mature ones, and one way to strengthen their survival could be to emit more BVOCs [58]. Tora, on plot 3, which had the same growing season as the saplings, emitted lower rates of other VOCs than the one year old Tora on plot 1, but higher than the saplings belonging to Tora on plot 2. The root system on plot 3 was established in 2003, which can be one reason why they differed in comparison to the saplings, since they had already a developed root system and trunk. The ratio between other VOCs and isoprene emission changed according to the aging of the trees. At the beginning of the season, the fraction of other VOCs exceeded the fraction of isoprene, but at the end of the season, the opposite was seen.

Compounds other than isoprene and MTs are rarely reported in studies on *Salix* trees, and only low emission rates have been observed for these compounds in the few studies that have [22]. However, the results of this study show that they should not be discarded, at least not for saplings. Hexanal, which was the most emitted other VOC, has been reported as an important compound in abiotic and biotic stress [59–61]. Irrespectively, the reason why leaf beetles attacked all of the other varieties but not Ester is unclear. No unique compound emitted by Ester was found. Benzaldehyde and xylenes have been reported as stress-induced compounds in trees [62]. Even though the emissions of compounds such as benzaldehyde, furfural, p-cymene, camphene and nerolidol were higher from Ester compared to from the other varieties, the major contributions to these emission rates were observed from the saplings belonging to Ester and not from the 1-year-old trees. Therefore, one suggestion why the insects avoid Ester could be that this variety has compounds or other substances stored within their leaves that are not emitted unless the surface layer is broken, making Ester less attractive for leaf beetles.

The average standardized isoprene emission for the whole season ($33.21 \pm 53.43 \mu\text{g g}_{\text{dw}}^{-1} \text{h}^{-1}$) is in line with other studies that have measured emissions from *Salix* trees [11,23]. It is hard to make a straightforward comparison since the methods, soil, adaptation to local growing conditions, age and different clones are likely to affect the emissions, and all these pieces of information are seldom presented in studies. Wild growing *Salix* species will also probably have different emission rates compared to commercial managed species. According to Morrison et al. [23], standardized isoprene emission from *Salix* trees can be more than $100 \mu\text{g g}_{\text{dw}}^{-1} \text{h}^{-1}$ but many emission rates range from 20 to $50 \mu\text{g g}_{\text{dw}}^{-1} \text{h}^{-1}$.

The standardized average MT emission rate was $4.40 \pm 2.05 \mu\text{g g}_{\text{dw}}^{-1} \text{h}^{-1}$. The time of the year has been shown to influence the emission rate, and other studies have reported that *Salix* trees are prone to emit higher concentrations of MTs when they recently have had their bud break [23,63]. The study done by Ghelardini et al. [64] showed that the day of bud burst for *Salix* can vary between seasons, and differ for different varieties [65]. For the trees studied in Ghelardini et al. [64], it took up to 260 degree days of $T > 0 \text{ }^\circ\text{C}$ since the first of March to have a bud burst. This value was reached by the middle of April for plots 1 and 2, and by the end of April for plots 3 and 4, when counting degree days in the same way as in their study. The first campaign in this study was started by the end of May for plots 1 and 2, and in the middle of June for plots 3 and 4, which makes it unlikely that the observed emissions included any enhanced emissions of MTs close to the bud break. Besides, saplings planted on plots 2 and 3 had developed their leaves before they were put in the ground, and therefore, no elevated MT emissions were expected from them due to the changing processes during bud break and leaf development.

The sesquiterpenes were the group that contributed least to the total BVOC emissions. The standardized emissions were $2.51 \pm 2.03 \mu\text{g g}_{\text{dw}}^{-1} \text{h}^{-1}$. Sesquiterpenes are, in general, less studied when measuring emissions from *Salix*. Toome et al. [66] observed emissions of α -copaene, (E,E)- α -farnesene and α -murolene from rust-infected leaves, but not from control leaves. Emissions of α -copaene and α -farnesene have also been seen for wild growing *Salix* species [67]. α -farnesene was emitted from all varieties in this study, but no visible sign of rust was seen from the measured leaves.

5. Conclusions

In this study, four different *Salix* varieties (Tora, Wilhelm, Ester and Inger) were studied in southern Sweden. The emissions of BVOC, net assimilation rates and water use efficiency were compared. The varieties were exposed to similar light levels in the leaf chambers to be able to focus on the variation between the varieties.

The measured isoprene emissions from Wilhelm were three times higher than those from Tora, a genetically related species, but this difference was not statistically significant. This outcome emphasizes the complexity behind BVOC emissions, and plants that are more closely related do not necessarily respond in the same way. To be able to fully understand emissions of BVOCs, factors as production pathways, the environment and stress factors need to be taken into account. These

parameters are preferably studied in laboratory experiments rather than out in the field. The results from this study show that Tora is a low emitter of isoprene, and it is suggested to be the best candidate near polluted areas, where the potential for, e.g., O₃ formation is higher. Tora, Wilhelm and Inger had equally good A, and are consequently all suitable for growing as SRC in southern Sweden or similar climatic environments. Ester, which had lower A but higher WUE than the others, might be more appropriate in warm and dry areas. A clear difference was observed for the non-terpenoid emissions when comparing tree ages. Saplings emitted rates several times higher than those from the one year old trees. Particularly, the average emissions of hexanal were high, but benzaldehyde and octanal also showed higher rates for some of the young varieties, which may strengthen the defense system for the more sensitive younger trees [58–60].

Even if the outcomes from this study are related to local environmental issues, they need to be considered from a broader perspective. These kinds of biofuel plantation exist in many places in Europe, which could affect the environment for many people if the plantations are close to polluted areas. In addition, since BVOCs also act as precursors to SOA and cloud formation, they will likely have a regional impact as well [54,68,69]. Finally, the results from this study point out that both variety and age should be considered in modelling when scaling up BVOC emissions to better estimate regional budgets.

Supplementary Materials: The following are available online at <http://www.mdpi.com/2073-4433/11/4/356/s1>, Figure S1: Experimental setup in the field. Figure S2: Chromatogram of a sample in GS-MS. Figure S3: Chromatogram of a background sample in GS-MS. Figure S4: Thermopluviograms for plot 1–4. Table S1: Information about the different plots. Table S2: Average T, PAR and GDDs for all campaigns. Table S3: Values used for the fitted curves in Figures 6–9. Table S5: Emissions of BVOCs for first growing season trees.

Author Contributions: Conceptualization, T.H. and T.K.; methodology, T.H.; software, T.H.; validation, T.K. and T.H.; formal analysis, T.K.; investigation, T.K.; data curation, T.K. T.H. and R.R.; resources, T.H. and R.R.; writing—original draft preparation, T.K.; writing—review and editing, T.K., R.R. and T.H.; supervision T.H.; project administration, T.K. and T.H.; funding acquisition, T.H. All authors have read and agreed to the published version of the manuscript.

Funding: The project was funded by FORMAS (2012-727).

Acknowledgments: We thank Sten Segerslätt and Stig Larsson at European Willow Breeding AB for supporting and the permission to do the measurements at the two plots in Billeberga. We also thank Anders Jonsson and Per-Olof Andersson in Gråstorp for their support and to make it possible for doing the measurements here. Finally, we thank Ida Vedel-Petersen for performing the GC-MS analysis.

Conflicts of Interest: The authors declare no conflict of interest. The funders had no role in the design of the study; in the collection, analyses, or interpretation of data; in the writing of the manuscript, or in the decision to publish the results.

References

1. *Agenda: Handlingsplan Agenda 2030 2018–2020*; Artikelnr.: Fi 2018:3; Regeringskansliet: Stockholm, Sweden, 2018.
2. Naturvårdsverket. *Underlag till Regeringens Klimatpolitiska Handlingsplan Redovisning av Naturvårdsverkets Regeringsuppdrag*; Rapport 6879; Naturvårdsverket: Stockholm, Sweden, 2019; ISBN 978-91-620-6879-0. ISSN 0282-7298.
3. *Energiläget: ET 2017:12*; Statens Energimyndighet: Bromma, Sweden, 2017; ISSN 1404-3343.
4. *Skogsstyrelsen: Skogsstatistisk årsbok 2014 Swedish Statistical Yearbook of Forestry*; Redaktör Linn Christiansen; Skogsstyrelsen: Jönköping, Sweden, 2014; ISBN 978-91-87535-05-5. ISSN 0491-7847.
5. Fredga, K.; Danell, K.; Frank, H.; Hedberg, D.; Kullander, S. Bioenergy—Opportunities and constraints. In *Energy Committee Report*; Kungliga Vetenskapsakademien: Stockholm, Sweden, 2008.
6. Statistics Sweden. *Agricultural Statistics: Jordbruksstatistisk Sammanställning*; Statistics Sweden, Agricultural Statistics Unit: Örebro, Sweden, 2015.
7. Grelle, A.; Aronsson, P.; Weslien, P.; Klemedtsson, L.; Lindroth, A. Large carbon-sink potential by Kyoto forests in Sweden—a case study on willow plantations. *Tellus B Chem. Phys. Meteorol.* **2007**, *59*, 910–918. [[CrossRef](#)]

8. SOU 2007:36. *Bioenergi från Jordbruket—en Växande Resurs*; Statens Offentliga Utredningar; Edita Sverige AB: Stockholm, Sweden, 2007; ISBN 978-91-38-22751-0.
9. Åhman, I.; Larsson, S. *Resistensförädling i Salix för Energiproduktion*, SLU; Institutionen för entomologi, Nr/avsnitt: 2; SLU: Alnarp, Sweden, 1999.
10. Hollsten, R.; Arkelöv, O.; Ingelman, G. *Handbok för Salixodlare*; 2:a utgåvan; Jordbruksverket: Jönköping, Sweden, 2013.
11. Kesselmeier, J.; Staudt, M. Biogenic Volatile Organic Compounds (VOC): An Overview on Emission, Physiology and Ecology. *J. Atmos. Chem.* **1999**, *33*, 23–88. [[CrossRef](#)]
12. Hoffmann, T.; Odum, J.R.; Bowman, F.; Collins, D.; Klockow, D.; Flagan, R.C.; Seinfeld, J.H. Formation of Organic Aerosols from the Oxidation of Biogenic Hydrocarbons. *J. Atmos. Chem.* **1997**, *26*, 189–222. [[CrossRef](#)]
13. Ryerson, T.B.; Trainer, M.; Holloway, J.S.; Parrish, D.D.; Huey, L.G.; Sueper, D.T.; Frost, G.J.; Donnelly, S.G.; Schaubler, S.; Atlas, E.; et al. Observations of Ozone Formation in Power Plant Plumes and Implications for Ozone Control Strategies. *Science* **2001**, *292*, 719–723. [[CrossRef](#)] [[PubMed](#)]
14. Kleinman, L.; Daum, P.H.; Imre, D.; Lee, Y.-N.; Nunnermacker, L.J.; Springston, S.; Weinstein-Lloyd, J.; Rudolph, J. Ozone production rate and hydrocarbon reactivity in 5 urban areas: A cause of high ozone concentration in Houston. *Geophys. Res. Lett.* **2002**, *29*, 105–1–105–4. [[CrossRef](#)]
15. O'Dowd, C.; Jimenez, J.-L.; Bahreini, R.; Flagan, R.C.; Seinfeld, J.H.; Hämeri, K.; Pirjola, L.; Kulmala, M.; Jennings, S.G.; Hoffmann, T. Marine aerosol formation from biogenic iodine emissions. *Nature* **2002**, *417*, 632–636. [[CrossRef](#)]
16. Kulmala, M.; Suni, T.; Lehtinen, K.E.J.; Maso, M.D.; Boy, M.; Reissell, A.; Rannik, Ü.; Aalto, P.; Keronen, P.; Hakola, H.; et al. A new feedback mechanism linking forests, aerosols, and climate. *Atmos. Chem. Phys. Discuss.* **2004**, *4*, 557–562. [[CrossRef](#)]
17. Penuelas, J.; Staudt, M. BVOCs and global change. *Trends Plant Sci.* **2010**, *15*, 133–144. [[CrossRef](#)]
18. Hakola, H.; Rinne, J.; Laurila, T. The hydrocarbon emission rates of tea-leaved willow (*Salix phylicifolia*), silver birch (*Betula pendula*) and European aspen (*Populus tremula*). *Atmos. Environ.* **1998**, *32*, 1825–1833. [[CrossRef](#)]
19. Owen, S.M.; Hewitt, C.N. Extrapolating branch enclosure measurements to estimates of regional scale biogenic VOC fluxes in the northwestern Mediterranean basin. *J. Geophys. Res. Space Phys.* **2000**, *105*, 11573–11583. [[CrossRef](#)]
20. Owen, S.M.; Mackenzie, A.R.; Stewart, H.; Donovan, R.; Hewitt, C.N. Biogenic volatile organic compound flux from the UK West Midlands urban tree canopy. *Ecol. Appl.* **2003**, *13*, 927–938. [[CrossRef](#)]
21. Olofsson, M.; Ekolausson, B.; Jensen, N.; Langer, S.; Ljungström, E. The flux of isoprene from a willow coppice plantation and the effect on local air quality. *Atmos. Environ.* **2005**, *39*, 2061–2070. [[CrossRef](#)]
22. Copeland, N.; Cape, J.; Heal, M.R. Volatile organic compound emissions from Miscanthus and short rotation coppice willow bioenergy crops. *Atmos. Environ.* **2012**, *60*, 327–335. [[CrossRef](#)]
23. Morrison, E.C.; Drewer, J.; Heal, M.R. A comparison of isoprene and monoterpene emission rates from the perennial bioenergy crops short-rotation coppice willow and Miscanthus and the annual arable crops wheat and oilseed rape. *GCB Bioenergy* **2015**, *8*, 211–225. [[CrossRef](#)]
24. Isebrands, J. Volatile organic compound emission rates from mixed deciduous and coniferous forests in Northern Wisconsin, USA. *Atmos. Environ.* **1999**, *33*, 2527–2536. [[CrossRef](#)]
25. Bäck, J.; Aalto, J.; Henriksson, M.; Hakola, H.; He, Q.; Boy, M. Chemodiversity of a Scots pine stand and implications for terpene air concentrations. *Biogeosciences* **2012**, *9*, 689–702. [[CrossRef](#)]
26. Persson, Y.; Schurgers, G.; Ekberg, A.; Holst, T. Effects of intra-genotypic variation, variance with height and time of season on BVOC emissions. *Meteorol. Z.* **2016**, *25*, 377–388. [[CrossRef](#)]
27. Alexandersson, H.; Eggertsson Karlström, C. *Temperaturen och nederbörden i Sverige 1961–90: Referensnormaler—utgåva 2*. *Meteorologi* 99; Swedish Meteorological and Hydrological Institute: Norrköping, Swedish, 2001. (In Swedish)
28. Lantmäteriet. Available online: <https://kso.etjanster.lantmateriet.se/#> (accessed on 17 September 2019).
29. Van Meeningen, Y.; Schurgers, G.; Rinnan, R.; Holst, T. BVOC emissions from English oak (*Quercus robur*) and European beech (*Fagus sylvatica*) along a latitudinal gradient. *Biogeosciences* **2016**, *13*, 6067–6080. [[CrossRef](#)]

30. Van Meeningen, Y.; Wang, M.; Karlsson, T.; Seifert, A.; Schurgers, G.; Rinnan, R.; Holst, T. Isoprenoid emission variation of Norway spruce across a European latitudinal transect. *Atmos. Environ.* **2017**, *170*, 45–57. [[CrossRef](#)]
31. Van Meeningen, Y.; Schurgers, G.; Rinnan, R.; Holst, T. Isoprenoid emission response to changing light conditions of English oak, European beech and Norway spruce. *Biogeosciences* **2017**, *14*, 4045–4060. [[CrossRef](#)]
32. Lindwall, F.; Faubert, P.; Rinnan, R. Diel Variation of Biogenic Volatile Organic Compound Emissions- A field Study in the Sub, Low and High Arctic on the Effect of Temperature and Light. *PLoS ONE* **2015**, *10*, e0123610. [[CrossRef](#)] [[PubMed](#)]
33. Hakola, H.; Tarvainen, V.; Laurila, T.; Hiltunen, V.; Hellén, H.; Keronen, P. Seasonal variation of VOC concentrations above a boreal coniferous forest. *Atmos. Environ.* **2003**, *37*, 1623–1634. [[CrossRef](#)]
34. Guenther, A.; Zimmerman, P.R.; Harley, P.; Monson, R.K.; Fall, R. Isoprene and monoterpene emission rate variability: Model evaluations and sensitivity analyses. *J. Geophys. Res. Space Phys.* **1993**, *98*, 12609. [[CrossRef](#)]
35. Helmig, D.; Ortega, J.; Duhl, T.; Tanner, D.; Guenther, A.; Harley, P.; Wiedinmyer, C.; Milford, J.; Sakulyanontvittaya, T. Sesquiterpene Emissions from Pine Trees—Identifications, Emission Rates and Flux Estimates for the Contiguous United States. *Environ. Sci. Technol.* **2007**, *41*, 1545–1553. [[CrossRef](#)] [[PubMed](#)]
36. Laothawornkitkul, J.; Taylor, J.E.; Paul, N.; Hewitt, C.N. Biogenic volatile organic compounds in the Earth system. *New Phytol.* **2009**, *183*, 27–51. [[CrossRef](#)]
37. Biology, Controls and Models of Tree Volatile Organic Compound Emissions. *Tree Physiol.* **2013**, *5*, 153–178.
38. Larcher, W. Carbon Utilization and Dry Matter Production. In *Physiological Plant Ecology: Ecophysiology and Stress Physiology of Functional Groups*, 4th ed.; Springer: Berlin/Heidelberg, Germany; New York, NY, USA, 2003; pp. 69–184.
39. Monson, R.K.; Fall, R. Isoprene Emission from Aspen Leaves. *Plant Physiol.* **1989**, *90*, 267–274. [[CrossRef](#)]
40. Guenther, A.B.; Monson, R.K.; Fall, R. Isoprene and monoterpene emission rate variability: Observations with eucalyptus and emission rate algorithm development. *J. Geophys. Res. Space Phys.* **1991**, *96*, 10799. [[CrossRef](#)]
41. Monson, R.K.; Jaeger, C.H.; Adams, W.W.; Driggers, E.M.; Silver, G.M.; Fall, R. Relationships among Isoprene Emission Rate, Photosynthesis, and Isoprene Synthase Activity as Influenced by Temperature. *Plant Physiol.* **1992**, *98*, 1175–1180. [[CrossRef](#)]
42. Tingey, D.T.; Evans, R.C.; Bates, E.H.; Gumpertz, M.L. Isoprene emissions and photosynthesis in three fens—The influence of light and temperature. *Physiol. Plantarum* **1987**, *69*, 609–616. [[CrossRef](#)]
43. Niinemets, Ü.; Tenhunen, J.D.; Harley, P.C.; Steinbrecher, R. A model of isoprene emission based on energetic requirements for isoprene synthesis and leaf photosynthetic properties for Liquidambar and Quercus. *Plant Cell Environ.* **1999**, *22*, 1319–1335. [[CrossRef](#)]
44. Wang, K.-Y.; Shallcross, D.E. Modelling terrestrial biogenic isoprene fluxes and their potential impact on global chemical species using a coupled LSM–CTM model. *Atmos. Environ.* **2000**, *34*, 2909–2925. [[CrossRef](#)]
45. Atkinson, R.; Arey, J. Gas-phase tropospheric chemistry of biogenic volatile organic compounds: A review. *Atmos. Environ.* **2003**, *37*, 197–219. [[CrossRef](#)]
46. Lovelock, J.E. PAN in the natural environment, its possible significance in the epidemiology of skin cancer. *Ambio* **1977**, *6*, 131–133.
47. Temple, P.; Taylor, O. World-wide ambient measurements of peroxyacetyl nitrate (PAN) and implications for plant injury. *Atmos. Environ. (1967)* **1983**, *17*, 1583–1587. [[CrossRef](#)]
48. Vyskocil, A.; Viau, C.; Lamy, S. Peroxyacetyl nitrate: Review of toxicity. *Hum. Exp. Toxicol.* **1998**, *17*, 212–220. [[CrossRef](#)]
49. Emberson, L.; Pleijel, H.; Ainsworth, E.A.; Berg, M.V.D.; Ren, W.; Osborne, S.; Mills, G.; Pandey, D.; Dentener, F.; Büker, P.; et al. Ozone effects on crops and consideration in crop models. *Eur. J. Agron.* **2018**, *100*, 19–34. [[CrossRef](#)]
50. Watson, L.A.; Wang, K.-Y.; Paul, H.; Shallcross, D.E. The potential impact of biogenic emissions of isoprene on urban chemistry in the United Kingdom. *Atmos. Sci. Lett.* **2006**, *7*, 96–100. [[CrossRef](#)]
51. Loreto, F. Ozone Quenching Properties of Isoprene and Its Antioxidant Role in Leaves. *Plant Physiol.* **2001**, *126*, 993–1000. [[CrossRef](#)]

52. Fares, S.; Barta, C.; Brilli, F.; Centritto, M.; Ederli, L.; Ferranti, F.; Pasqualini, S.; Reale, L.; Tricoli, D.; Loreto, F. Impact of high ozone on isoprene emission, photosynthesis and histology of developing *Populus alba* leaves directly or indirectly exposed to the pollutant. *Physiol. Plant.* **2006**, *128*, 456–465. [\[CrossRef\]](#)
53. Sharkey, T.D.; Wiberley, A.E.; Donohue, A.R. Isoprene Emission from Plants: Why and How. *Ann. Bot.* **2007**, *101*, 5–18. [\[CrossRef\]](#) [\[PubMed\]](#)
54. Paasonen, P.; Asmi, A.; Petäjä, T.; Kajos, M.K.; Äijälä, M.; Junninen, H.; Holst, T.; Abbatt, J.P.D.; Arneth, A.; Birmili, W.; et al. Warming-induced increase in aerosol number concentration likely to moderate climate change. *Nat. Geosci.* **2013**, *6*, 438–442. [\[CrossRef\]](#)
55. Ehn, M.; Thornton, J.A.; Kleist, E.; Sipilä, M.; Junninen, H.; Pullinen, I.; Springer, M.; Rubach, F.; Tillmann, R.; Lee, B.H.; et al. A large source of low-volatility secondary organic aerosol. *Nature* **2014**, *506*, 476–479. [\[CrossRef\]](#) [\[PubMed\]](#)
56. Peräkylä, O.; Vogt, M.; Tikkanen, O.P.; Laurila, T.; Kajos, M.K.; Rantala, P.A.; Patokoski, J.; Aalto, J.; Yli-Juuti, T.; Ehn, M.; et al. Monoterpenes' oxidation capacity and rate over a boreal forest: Temporal variation and connection to growth of newly formed particles. *Boreal Environ. Res.* **2014**, *19*, 293–310.
57. Mutzel, A.; Rodigast, M.; Iinuma, Y.; Böge, O.; Herrmann, H. Monoterpene SOA—Contribution of first-generation oxidation products to formation and chemical composition. *Atmos. Environ.* **2016**, *130*, 136–144. [\[CrossRef\]](#)
58. Palo, T. Distribution of birch (*Betula* SPP.), willow (*Salix* SPP.), and poplar (*Populus* SPP.) secondary metabolites and their potential role as chemical defense against herbivores. *J. Chem. Ecol.* **1984**, *10*, 499–520. [\[CrossRef\]](#)
59. Hildebrand, D.F. Lipoxygenases. *Physiol. Plant.* **1989**, *76*, 249–253. [\[CrossRef\]](#)
60. Andersen, R.A.; Hamilton-Kemp, T.R.; Hildebrand, D.F.; McCracken, C.T.; Collins, R.W.; Fleming, P.D. Structure-Antifungal Activity Relationships among Volatile C6 and C9 Aliphatic Aldehydes, Ketones, and Alcohols. *J. Agric. Food Chem.* **1994**, *42*, 1563–1568. [\[CrossRef\]](#)
61. Wildt, J.; Kobel, K.; Schuh-Thomas, G.; Heiden, A.C. Emissions of Oxygenated Volatile Organic Compounds from Plants Part II: Emissions of Saturated Aldehydes. *J. Atmos. Chem.* **2003**, *45*, 173–196. [\[CrossRef\]](#)
62. Misztal, P.K.; Hewitt, C.N.; Wildt, J.; Blande, J.D.; Eller, A.; Fares, S.; Gentner, D.; Gilman, J.; Graus, M.; Greenberg, J.; et al. Atmospheric benzenoid emissions from plants rival those from fossil fuels. *Sci. Rep.* **2015**, *5*, 12064. [\[CrossRef\]](#)
63. Hakola, H.; Rinne, J.; Laurila, T. The VOC emission rates of boreal deciduous trees. In *Biogenic VOC Emissions and Photochemistry in the Boreal Regions of Europe—Biphorep*; European Commission: Brussels, Belgium, 1999; pp. 21–28.
64. Ghelardini, L.; Berlin, S.; Weih, M.; Lagercrantz, U.; Gyllenstrand, N.; Rönnerberg-Wästljung, A.C. Genetic architecture of spring and autumn phenology in *Salix*. *BMC Plant Biol.* **2014**, *14*, 31. [\[CrossRef\]](#) [\[PubMed\]](#)
65. Weih, M. Genetic and environmental variation in spring and autumn phenology of biomass willows (*Salix* spp.): Effects on shoot growth and nitrogen economy. *Tree Physiol.* **2009**, *29*, 1479–1490. [\[CrossRef\]](#) [\[PubMed\]](#)
66. Toome, M.; Randjävär, P.; Copolovici, L.; Niinemets, Ü.; Heinsoo, K.; Luik, A.; Noe, S.M. Leaf rust induced volatile organic compounds signalling in willow during the infection. *Planta* **2010**, *232*, 235–243. [\[CrossRef\]](#) [\[PubMed\]](#)
67. Vedel-Petersen, I.; Schollert, M.; Nyman, J.; Rinnan, R. Volatile organic compound emission profiles of four common arctic plants. *Atmos. Environ.* **2015**, *120*, 117–126. [\[CrossRef\]](#)
68. Claeys, M.; Wang, W.; Ion, A.C.; Kourtchev, I.; Gelencsér, A.; Maenhaut, W. Formation of secondary organic aerosols from isoprene and its gas-phase oxidation products through reaction with hydrogen peroxide. *Atmos. Environ.* **2004**, *38*, 4093–4098. [\[CrossRef\]](#)
69. Carlton, A.G.; Wiedinmyer, C.; Kroll, J.H. A review of Secondary Organic Aerosol (SOA) formation from isoprene. *Atmos. Chem. Phys. Discuss.* **2009**, *9*, 4987–5005. [\[CrossRef\]](#)



Supplement to:

Variability of BVOC Emissions from Commercially Used Willow (*Salix* spp.) Varieties

T. Karlsson^{1,*}, R. Rinnan², T. Holst^{1,2}

¹Lund University, Department of Physical Geography and Ecosystem Science, Sölvegatan 12, 223 62 Lund, Sweden

²University of Copenhagen, Terrestrial Ecology Section, Department of Biology, Universitetsparken 15, DK-2100 Copenhagen Ø, Denmark

* Correspondence to: T. Karlsson (tomas.karlsson@nateko.lu.se)

Table S1. Plot type, size (ha), previous land use, canopy height (m), soil type and content, varieties, establishment, last harvest and age (months.) for the trees.

	Plot 1	Plot 2	Plot 3	Plot 4
Type	field trial	field trial	biofuel plantation	biofuel plantation
Plot size	0.07 ha	0.07 ha	5 ha	9 ha
Formerly used for	<i>Salix</i>	cereals, beets and rapes	<i>Salix</i>	<i>Salix</i>
Canopy height ¹	4.5 m	1.5 m	2.5 m	1-1.5 m
Soil type ²	loam	loam	clay loam	silty clay loam
Clay content ²	18%	24%	34%	36%
Silt content ²	34%	36%	45%	46%
Organic content ²	0%	0%	0%	0%
Varieties	Tora, Wilhelm, Ester and Inger	Tora, Wilhelm, Ester and Inger	Tora	Wilhelm
Established	2013	2017	2003	2017
Last harvest	2016	-	2017	-
Age of the trees	1 months	0 months	0 months	0 months

¹Average canopy height and age for the varieties at the last campaign at each plot.

²Taken from SGU, <http://maps-test.sgu.se:8080/TestSguMapView2/kartvisare-lerhalskarta-sv.html> (2019-03-07).



Figure S1. Experimental setup of leaf chamber system. To the right on the top of the tripod, the leaf chamber is attached and connected to the portable photosynthesis system (LI-6400) to the left. BVOC-sampling was done by taking a sub-sample of 200 ml/min of air leaving the leaf chamber using adsorbent tubes filled with Tenax TA and Carboxograph with a small flow regulated pump.

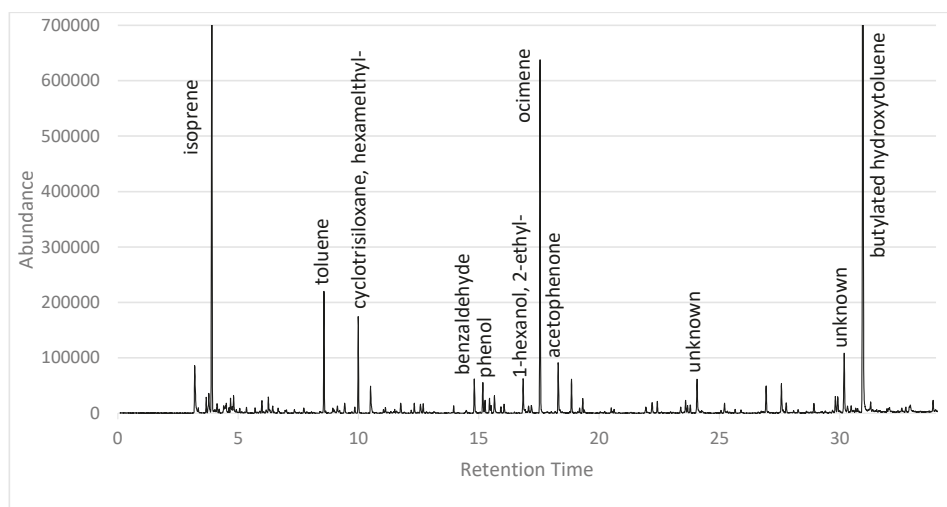


Figure S2. Total ion chromatogram sequence from a sample in GC-MS instrument where some of the most abundant peaks are identified. This measurement was taken on Inger at PAR $1500 \mu\text{mol m}^{-2} \text{s}^{-1}$ and chamber temperature 19.5°C .

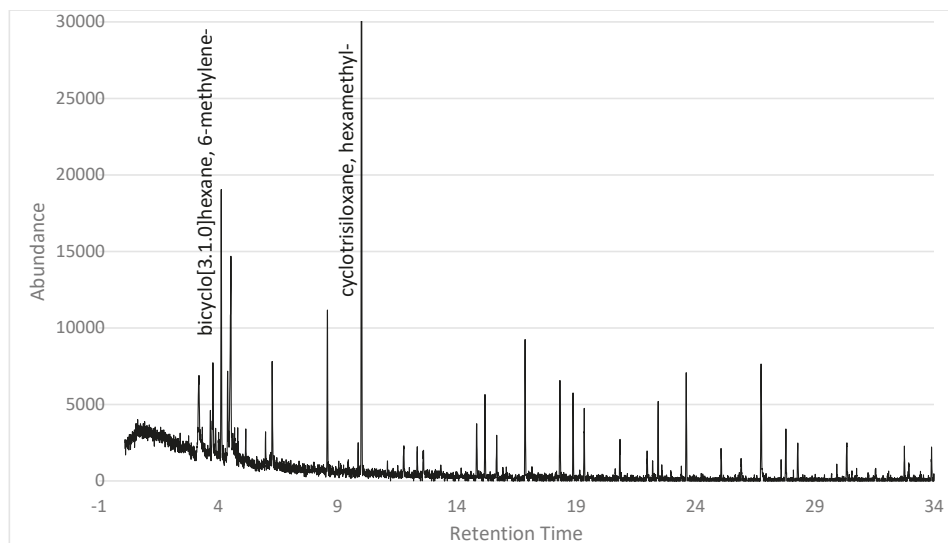


Figure S3. Total ion chromatogram sequence from a background sample in GC-MS instrument. Only bicyclo[3.1.0]hexane, 6-methylene- and cyclotrisiloxane, hexamethyl- had enough abundance to be detected in ChemStation.

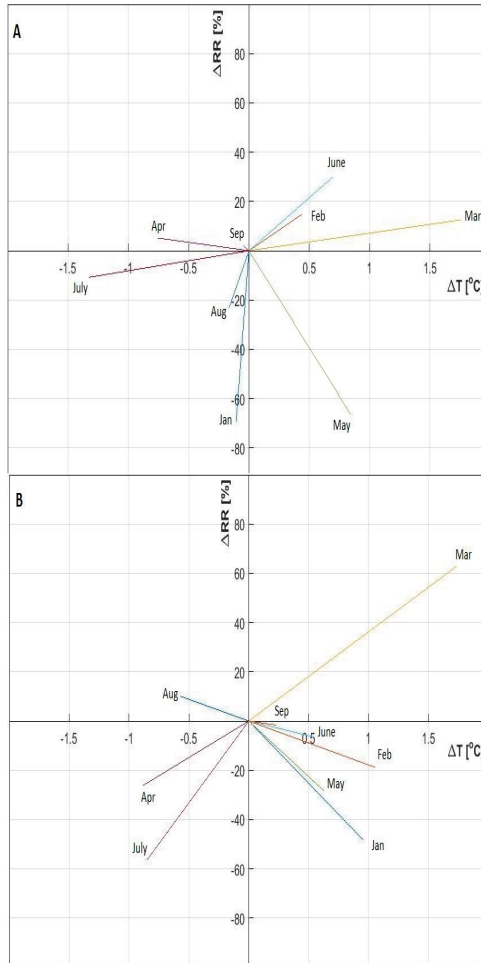


Figure S4. Thermopluviogram for plot 1 and 2 (A), and 3 and 4 (B). Values on y- and x-axis are the relative difference for precipitation, ΔRR (%), and temperature, ΔT ($^{\circ}C$), for each month (January–September) in 2017 compared to the average monthly values between 1987–2016 (for T plot 1–4 and precipitation plot 1 and 2) and 1992–2016 (for precipitation plot 3 and 4). Data is taken from SMHI.

Table S2. Average values for ambient T ($^{\circ}C$), T inside the leaf chamber, ambient PAR ($\mu mol m^{-2} s^{-1}$) during the measurements and growing degree days (GDDs, $^{\circ}C$) for each day when measurements were done. No values of ambient T and PAR could be recorded on site 1 on 29 May (x) because of battery failure. No PAR was measured on 15 June (-) on site 3.

Plot 1	29 May	31 May	5 July	6 July	22 July	25 July	28 Aug	29 Aug
Ambient T ($^{\circ}C$)	x	13.9	18.5	19.8	20.6	18.8	19.8	23.2
Chamber T ($^{\circ}C$)	16.0	15.0	17	19.0	20.0	19.5	17.5	22.9

Ambient PAR								
($\mu\text{mol m}^{-2}\text{s}^{-1}$)	x	471	1344	1474	1085	417	1019	1132
GDDs ¹ (°C)	335.6	348.3	757.9	768.9	957.1	993.9	1424.8	1437.0
Plot 2								
	2 June	5 June	9 July	10 July	26 July	28 July	30 Aug	31 Aug
Ambient T (°C)	19.0	18.6	20.1	21.0	21.7	20.9	19.9	16.6
Chamber T (°C)	18.0	18.2	18.3	20.0	19.3	20.0	20.9	16.8
Ambient PAR								
($\mu\text{mol m}^{-2}\text{s}^{-1}$)	891	1235	1393	801	1015	1281	324	206
GDDs ¹ (°C)	380.7	409.5	792.1	805.4	1005.5	1033.5	1450.2	1465.2
Plot 3								
	15 June	15 July	15 July	1 Aug	1 Aug	7 Sep		
Ambient T (°C)	20.9	22.3	22.3	21.6	22.0	16.3		
Chamber T (°C)	20.2	20.9	21.0	20.9	21.0	14.0		
Ambient PAR								
($\mu\text{mol m}^{-2}\text{s}^{-1}$)	-	1363	1350	1194	1218	801		
GDDs ¹ (°C)	386.1	708.0	708.0	896.4	896.4	1263.3		
Plot 4								
	13 June	28 June	28 June	12 July	13 July	14 July	2 Aug	5 Sep
Ambient T (°C)	19.3	22.6	22.6	21	21.6	23.0	20.6	15.7
Chamber T (°C)	19.2	21.3	20.7	19.5	21.1	20.9	19.8	15.0
Ambient PAR								
($\mu\text{mol m}^{-2}\text{s}^{-1}$)	902	1112	1100	1061	1339	1389	919	177
GDDs ¹ (°C)	365.0	526.8	526.8	677.7	688.8	697.5	908.5	1245.3

¹GDDs was calculated as $\Sigma[(T_{\text{max}}+T_{\text{min}})/2 - T_{\text{base}}]$ for each starting from 1 jan 2017. $T_{\text{base}} = 5\text{ }^{\circ}\text{C}$ and if $(T_{\text{max}}+T_{\text{min}})/2$

< 0 , then $(T_{\text{max}}+T_{\text{min}})/2 - T_{\text{base}} = 0$.

Table S3. Values used for the fitted curves in figure 6–9. E_s is STD emission rate ($\mu\text{g g}_{\text{dw}}^{-1}\text{ h}^{-1}$), C_T is correction factor for temperature described by eq. 4, α and C_{L1} are coefficient used in eq. 3 and R is Pearson's correlation coefficient for the curves. No emission of caryophyllene (-) was observed for Wilhelm.

	isoprene				ocimene			
	Tora	Wilhelm	Ester	Inger	Tora	Wilhelm	Ester	Inger
E_s	20.4	95.1	41.5	98.1	9.0	13.9	0.2	8.6
C_T	0.2416	0.2416	0.2384	0.2416	0.2416	0.2416	0.2384	0.2416
α	0.0004	0.0004	0.002	0.0006	0.0002	0.0005	0.0002	0.0001
C_{L1}	3.91	2.73	1.23	1.15	4.49	0.47	3.73	4.37
R	0.983	0.985	0.987	0.992	0.995	0.987	0.972	0.988
	linalool				caryophyllene			
	Tora	Wilhelm	Ester	Inger	Tora	Wilhelm	Ester	Inger
E_s	0.9	0.7	0.1	0.1	0.1	-	0.1	1.7
C_T	0.2416	0.2416	0.2384	0.2416	0.2416	0.2416	0.2384	0.2416
α	0.0009	0.0012	0.05	0.0013	0.0001	-	0.05	0.0005

C _{Li}	2.44	1.56	0.55	3.13	4.57	-	0.82	0.62
R	0.979	0.981	0.296	0.897	0.951	-	0.294	0.978

Table S4. The 20 most abundant identified BVOCs ($\mu\text{g g}_{\text{dw}}^{-1} \text{h}^{-1}$, mean \pm standard deviation, n = 24–50) for the different varieties and the first growing season trees.

T1 (plot 2)		T1 (plot 3)	
octanal	6.85 (14.40)	isoprene	5.02 (9.60)
isoprene	3.10 (4.55)	acetophenone	2.11 (4.76)
hexanal	2.32 (7.11)	ocimene	1.48 (2.12)
tridecane	1.44 (2.46)	benzaldehyde	0.73 (1.31)
heptanal	0.98 (2.77)	nonanal	0.42 (0.96)
ocimene	0.97 (1.04)	2-cyclopenten-1-one	0.29 (0.73)
1-hexanol, 2-ethyl-	0.89 (1.47)	nerolidol	0.24 (0.41)
benzaldehyde	0.83 (1.96)	linalool	0.22 (0.33)
decanal	0.80 (1.21)	octanal	0.19 (0.54)
2-heptanone	0.79 (1.56)	2,5-cyclohexadiene-1,4-dione, 2,6-bis(1,1-dimethylethyl)-	0.17 (0.29)
2-hexanone	0.73 (1.87)	phenol	0.16 (0.30)
furfural	0.67 (2.01)	o-xylene	0.14 (0.22)
nerolidol	0.59 (0.76)	p-xylene	0.13 (0.32)
tetradecane	0.56 (0.83)	2-pentanone	0.13 (0.33)
pentanoic acid, 2-ethylhexyl ester	0.55 (0.82)	furfural	0.13 (0.34)
o-xylene	0.51 (1.04)	2-cyclohexen-1-one	0.12 (0.28)
p-xylene	0.46 (0.47)	α -humulene	0.12 (0.28)
limonene	0.45 (0.71)	hexanoic acid, 2-ethyl-	0.12 (0.25)
acetic acid, butyl ester	0.45 (1.09)	cis-3-hexenyl	0.11 (0.23)
2-cyclopenten-1-one	0.44 (0.90)	2-heptanone	0.11 (0.30)
W1 (plot 2)		W1 (plot 4)	
isoprene	10.58 (18.47)	isoprene	16.01 (23.65)
acetophenone	2.37 (3.76)	hexanal	6.36 (21.95)
nonanal	1.78 (3.72)	2-pentanone	0.86 (3.94)
octanal	1.27 (2.38)	phenol	0.55 (0.83)
1-hexanol, 2-ethyl-	1.13 (1.68)	nonanal	0.38 (0.45)
tridecane	0.80 (1.61)	acetophenone	0.36 (0.51)
decanal	0.77 (1.28)	ocimene	0.35 (0.72)
benzaldehyde	0.66 (1.08)	benzaldehyde	0.31 (0.98)
pentanoic acid, 2-ethylhexyl ester	0.65 (1.21)	decanal	0.29 (0.38)
phenol	0.63 (0.80)	3-pentanone, 2-methyl-	0.27 (1.21)
phenylmaleic anhydride	0.45 (0.70)	tetradecane	0.27 (0.32)
2-heptanone	0.44 (0.85)	tridecane	0.22 (0.29)
hexanal	0.44 (1.05)	p-xylene	0.20 (0.55)
o-xylene	0.42 (0.67)	pentanoic acid, 2-ethylhexyl ester	0.20 (0.31)
tetradecane	0.39 (0.81)	nerolidol	0.16 (0.45)



furfural	0.39 (0.99)	bicyclo[3.1.0]hexane, 6-methylene-	0.10 (0.19)
undecane	0.34 (0.57)	linalool	0.10 (0.27)
ocimene	0.33 (0.48)	o-xylene	0.09 (0.17)
benzoic acid	0.32 (0.61)	pentadecane	0.08 (0.17)
2-cyclopenten-1-one	0.31 (0.60)	phenylmaleic anhydride	0.07 (0.33)
E1		I1	
isoprene	5.48 (8.36)	isoprene	6.60 (9.29)
hexanal	4.92 (6.53)	limonene	1.61 (5.55)
benzaldehyde	3.20 (4.56)	benzaldehyde	0.90 (1.13)
furfural	3.07 (3.93)	hexanal	0.83 (1.72)
octanal	3.01 (4.79)	pentane, 2-methyl-	0.73 (3.10)
acetophenone	2.46 (3.97)	furfural	0.70 (1.42)
2-cyclopenten-1-one	1.07 (1.56)	phenol	0.56 (0.74)
nonanal	0.95 (1.61)	1-hexanol, 2-ethyl-	0.47 (0.33)
2-hexanone	0.88 (1.22)	nerolidol	0.43 (0.69)
nerolidol	0.86 (1.27)	decanal	0.36 (0.33)
p-xylene	0.85 (1.96)	octanal	0.35 (0.56)
phenol	0.82 (1.20)	nonanal	0.33 (0.59)
heptanal	0.80 (1.11)	p-xylene	0.30 (0.62)
camphene	0.79 (3.96)	hexanoic acid, 2-ethyl-	0.27 (0.35)
o-xylene	0.75 (1.16)	propanoic acid, 3-ethoxy-, ethyl ester	0.25 (1.17)
1-hexanol, 2-ethyl-	0.73 (0.72)	β -pinene	0.23 (0.61)
2-heptanone	0.70 (0.99)	butane, 2-methyl-	0.23 (0.26)
2-pentanone	0.66 (0.95)	o-xylene	0.21 (0.42)
limonene	0.60 (1.58)	γ -terpinene	0.20 (0.75)
hexanoic acid, 2-ethyl-	0.57 (0.98)	α -humulene	0.18 (0.32)

Paper III



Article

No Particle Mass Enhancement from Induced Atmospheric Ageing at a Rural Site in Northern Europe

Erik Ahlberg ^{1,2,*}, Stina Ausmeel ², Axel Eriksson ^{2,3}, Thomas Holst ⁴, Tomas Karlsson ⁴, William H. Brune ⁵, Göran Frank ², Pontus Roldin ², Adam Kristensson ² and Birgitta Svenningsson ²

¹ Centre for Environmental and Climate Research, Lund University, Sölvegatan 37, 223 52 Lund, Sweden

² Division of Nuclear Physics, Lund University, Box 118, 221 00 Lund, Sweden

³ Ergonomics and Aerosol Technology, Lund University, Box 118, 221 00 Lund, Sweden

⁴ Department of Physical Geography and Ecosystem Science, Lund University, Sölvegatan 12, 223 62 Lund, Sweden

⁵ Department of Meteorology and Atmospheric Science, Pennsylvania State University, University Park, PA 16802, USA

* Correspondence: erik.ahlberg@nuclear.lu.se

Received: 20 June 2019; Accepted: 15 July 2019; Published: 17 July 2019



Abstract: A large portion of atmospheric aerosol particles consists of secondary material produced by oxidation reactions. The relative importance of secondary organic aerosol (SOA) can increase with improved emission regulations. A relatively simple way to study potential particle formation in the atmosphere is by using oxidation flow reactors (OFRs) which simulate atmospheric ageing. Here we report on the first ambient OFR ageing experiment in Europe, coupled with scanning mobility particle sizer (SMPS), aerosol mass spectrometer (AMS) and proton transfer reaction (PTR)-MS measurements. We found that the simulated ageing did not produce any measurable increases in particle mass or number concentrations during the two months of the campaign due to low concentrations of precursors. Losses in the reactor increased with hydroxyl radical (OH) exposure and with increasing difference between ambient and reactor temperatures, indicating fragmentation and evaporation of semivolatile material.

Keywords: oxidation flow reactor; secondary organic aerosol; ambient aerosol; PAM

1. Introduction

Submicron particle mass is often dominated by secondary material formed from atmospheric oxidation of both organic and inorganic precursors [1,2]. Despite major research advances in the fields of atmospheric organic chemistry and secondary organic aerosols (SOA) during the last decade, knowledge and understanding is far from complete [3–5]. Knowledge gaps include speciation and the chemical and physical processes governing both formation and removal of SOA mass. Organic precursors (volatile organic compounds, VOCs) are emitted from both anthropogenic and biogenic sources, while inorganic sources are mainly anthropogenic.

In recent years, several research groups have employed oxidation flow reactors (OFRs) to study secondary aerosol particle properties. The most common OFR to date is the potential aerosol mass (PAM) reactor. High oxidant concentrations and a continuous flow enables faster experiments and higher degree of oxidation. OFRs have proved valuable as an alternative or complement to the traditionally used large smog chambers [6,7]. Although mobile smog chambers exist [8], they are not portable in the same way as an OFR. By deploying OFRs at field sites, ideally with complimentary

gas phase measurements, the potential aerosol formation of the ambient atmosphere can be studied directly, thereby overriding some of the difficulties in translating simplified laboratory experiments to atmospheric implications. To date, only a handful of such field deployments target ambient air, as opposed to a specific emitter (such as vehicles or biomass burning), have been performed. Since the ambient aerosol is always aged to a certain extent, less pronounced particle production can be expected in environments far away from precursor sources. Most campaigns have seen a net mass loss at the highest OH exposures, consistent with laboratory measurements [7], which is interpreted as a shift from functionalization to fragmentation of SOA precursors. In urban areas, Ortega et al. [9] measured organic mass enhancement factors in Los Angeles of around 1.3 during days and 1.8 during night-time, while George et al. [10] saw significant oxidation but little or no mass enhancement in downtown Toronto. In a pine forest in Colorado, dominated by biogenic sources, the SOA mass enhancement scaled with measured monoterpenes, although OH induced oxidation of unmeasured semi- or intermediate volatility organic compounds was needed to explain the formed mass [11,12]. Similarly to the Los Angeles study, the enhancement was larger at night-time. Using a different reactor, Slowik et al. [13] saw significant losses of organics in a remote Canadian forest influenced by biogenic sources, which they attributed to a volatilization from an increased temperature and OH oxidation. In central Amazonia, Palm et al. [14] again saw maximum enhancement at night-time, while daytime oxidation produced much less SOA, especially during the wet season. Kang et al. [15], measuring in the Yellow Sea, saw net losses of organics but an increase in sulphate aerosol mass. With OFRs now being produced commercially, these types of measurements can be expected to become more frequent.

Here we report, to the best of our knowledge, the first ambient OFR campaign in Europe. Ambient aerosol measurements, alternating through a PAM OFR, were performed during July and August of 2015 at a willow (*Salix viminalis*) bioenergy plantation in southwestern Sweden. We aimed to study the aerosol formation potential of background air at a rural site, as well as the influence of the fast-growing energy crops. We compare the results to previous literature and discuss correlations between the (lack of) enhancement with temperature, wind and ambient aerosol levels. The sensitivity of ambient OFR measurements, expressed as required precursor concentration and yield as a function of ambient condensation sink, is also estimated.

2. Experimental Methods

2.1. Campaign Site and Set-Up

The measurement site located in Skrehalla (58°17' N, 12°46' E) is surrounded mostly by arable land. It is about 80 km north-east of Gothenburg (580 k inhabitants), 30 km to the nearest city (Trollhättan, 49 k inhabitants) and 10 km to three smaller villages (1–3 k inhabitants). A major road from Gothenburg to Stockholm is located 10 km southeast of the site, with around 10 k vehicles per day at the nearest section during summer (accessed on 22 September 2017. Available online: <http://vtf.trafikverket.se/>). The *Salix* plantation, about six hectares, was in its third growing season at the time of the campaign and more than two meters tall. Measurements took place during July–August 2015. Meteorological data was retrieved from the SMHI (Swedish Meteorological and Hydrological Institute) station in Hällum, 16 km to the east of the measurement site.

All instruments were placed in an air-conditioned laboratory container. The inlet consisted of quarter inch annealed 316(L) stainless steel tubing and a funnel installed to sample upwards, just above the *salix* canopy. The flow through the inlet was 6.3 lpm (assumed laminar flow with an approximate Reynolds number of 2100), and tubing length was about 4.5 m which gives a residence time in the inlet tubing of 0.6 s. The instruments were checked remotely, but also serviced once a week. Data from a total of 27 days were analyzed.

2.2. Instrumentation

PAM reactors have been extensively used and characterized during the last years [16–19]. The version used is a 13 l aluminum cylinder with two UV lamps (peak intensities at 185 and 254 nm) mounted inside to produce ozone and hydroxyl radicals from oxygen and water. The OH exposure was calibrated offline in a laboratory environment, using the decay of 2 ppb SO₂. OH exposure during field measurements was calculated using a parameterization from the calibration and measured absolute humidity and ozone. OH exposure during the campaign was mostly in the range 1×10^{11} – 1×10^{12} molecules cm⁻³ s. In order to scan OH exposure and potential particle formation, the voltage across the lamps was automatically changed in steps according to a programmed schedule. Flow through the reactor was 5 lpm. Sampling through the reactor during 60 min was alternated by 20 min of ambient sampling. During analysis, the first ten minutes of reactor sampling and first five minutes of ambient sampling were not considered, in order to give flows time to stabilize.

A scanning mobility particle sizer (SMPS, [20]) and a high-resolution time-of-flight aerosol mass spectrometer (AMS from here on, [21]) were used to monitor particle characteristics. The SMPS, consisting of a DMA (TSI 3071) and a CPC (TSI 3775), was used to measure the number size distribution of particles between 11–600 nm in electrical mobility diameter, while the AMS measured chemically resolved mass concentrations in the approximate range 50–1000 nm (vacuum aerodynamic diameter) with less than 100% transmission at the low and high end of the size spectrum. Although ambient number concentrations apparently approached zero at the high end of the SMPS mass spectrum (Figure S1), a small number of large particles (likely measurement artefacts) distorted the volume size distribution. The error in number concentration from this distortion is negligible and relative changes in volume are not affected, but the absolute volume measurements are likely overestimated by on average 20%. Due to the low mass concentration of Aitken mode particles, the AMS lens penetration is not believed to have been an issue. In order to measure dry aerosol particles, a Permapure drier was installed between the OFR and the SMPS and AMS. The AMS ionization efficiency was calibrated three times during the campaign. The airbeam signal and linear interpolations between these calibrations were used to correct the data.

A proton transfer reaction-time of flight-mass spectrometer (PTR-TOF-MS 8000; Ionicon Analytik GmbH, Innsbruck, Austria) was used to monitor ambient VOC concentrations during the experiment. The PTR-TOF-MS uses a soft ionization technique to protonate VOC in ambient air, and reaction products are mass-discriminated through a time-of-flight detection unit with a typical mass resolution of 4000 m/Δm [22,23]. The instrument was operated in a laboratory trailer and ambient air from above the plantation was sampled at a height of 4.7 m a.g.l. through a ca. 30 m long heated PFA inlet (1/2" OD, PFA-T8-062, Swagelok, OH, USA) with a high flow rate (20 lpm) from which the PTR-TOF took a subsample of 200 mL min⁻¹. SO₂ was measured using a UV fluorescent monitor (Environnement S.A AF22M). The concentration was, however, at all times close to or below the detection limit of the monitor with a campaign average of 0.1 ppb. This data was not analyzed further.

2.3. Analysis

Particle losses in the reactor were calculated using a three day period with the UV lamps turned off, by taking the ratio of the reactor to ambient measurements. The ambient value was calculated using an average before and after the reactor measurements. The average SMPS volume losses were $6 \pm 6\%$ (1σ) and AMS mass losses was $4 \pm 4\%$ (1σ). The losses were somewhat size-dependent (Figure S1), but given the low correction and largely similar volume size distribution during the campaign (volume geometric mean diameter 249 ± 38 nm, 1σ), the average values were used to correct the reactor output data. Particle losses in the inlet tubing and reactor bypass were assessed using the Max Planck Particle Loss Calculator [24]. The effect on total volume of this correction was relatively small and stable during the campaign ($4.4 \pm 0.6\%$, 1σ). Gas phase losses in the reactor were considered using the model first published in Palm et al. [11] (Figure S2). This model was used to calculate the fate of low-volatile organic compounds (LVOCs) by comparing four competing loss rates, walls of the reactor,

fragmentation (assumed after reacting with OH five times), condensation onto particles and exiting the reactor. Wall loss rate, coefficient of eddy diffusion and reaction rate with OH were all similar to those in the original paper (see Figure S2 caption).

A collection efficiency (CE) of 1 for the AMS was assumed after comparison with the SMPS volume concentration. The CE parameterizations of Middlebrock et al. [25] were assessed and resulted in a CE close to 0.5. Changes from the default value were mostly due to acidity effects. Since sulphate relative ionization efficiency (RIE) was not calibrated in this campaign, which can give an inaccurate ammonium ion balance, this parameterization method was deemed uncertain. The data was instead compared to the volume of the SMPS measurements. The volume was converted to mass using an organic density of 1.4 g cm^{-3} and inorganic density of 1.75 g cm^{-3} . As seen in Figure S3, the AMS and calculated SMPS mass concentrations fall roughly on a 1:1 line, except for an offset of $\sim 0.5 \mu\text{g m}^{-3}$ in the SMPS data corresponding to the measurement artefact at large diameters. Figure S3 also shows that there was no difference between OFR and ambient CE (implying that the CE only affects absolute values and not the ratio between reactor and ambient values). The SMPS was regularly checked and serviced but no comparisons to other instruments were made. Although uncommon, CE = 1 have been previously seen [11], and was not investigated further. In order to calculate organonitrates, the nitrate fragmentation pattern in the AMS was analyzed according to the procedure of Farmer et al. [26]. The elemental ratios was calculated using the “improved-ambient” parameterization [27].

The PTR-ToF-MS raw data was analyzed with the PTR-wid software [28] that provides peak detection, a mass scale calibration, and a unified mass list to analyze and convert long-term data sets into mixing ratios. While the analyzing software applies a typical mass dependent transmission function [29,30], the instrument was calibrated against a gas standard mixture (Ionicon Analytik GmbH, Innsbruck, Austria) including e.g., methanol, acetaldehyde, acetone, isoprene, benzene, toluene, o-xylene and α -pinene several times before, during and after the experiment. Thus, for those compounds used in this study the instrument was directly calibrated against those gas standards. The instrument background was measured three times per day automatically for 30 min each, and readings were corrected for this.

3. Results and Discussion

Accounting for reactor losses, OFR processing led to net losses ($1 - C_{\text{OFR}}/C_{\text{Ambient}}$) of $7.5\% \pm 7.1$ (1σ) in SMPS volume concentration and $9.8\% \pm 10.4$ (1σ) in AMS mass concentration. The ambient particle properties were relatively stable during the two months of measurements. The average number concentration was 2100 ± 850 (1σ) and AMS pm1 was 2.8 ± 1.7 (1σ) $\mu\text{g m}^{-3}$. Particles were dominated by organics ($63\% \pm 13$, 1σ) and sulphate ($26\% \pm 10$, 1σ). A time series of ambient SMPS number and volume concentrations and AMS fractional composition, covering the entire campaign, is shown in Figure S4. Winds were predominantly from the south and southwest (54% of the time). The number mode was mostly below 100 nm, while the volume geometric mean diameter was 249 ± 38 nm (1σ).

An example of a typical time series is seen in Figure 1, with reactor measurements on light blue background. As expected, the oxidizing environment lead to an increased O:C and decreased H:C ratio, with campaign averages H:C and O:C ratios of 1.47 ± 0.07 (1σ) and 0.68 ± 0.08 (1σ) ($\text{OS}_C = -0.11$) for ambient measurements and 1.39 ± 0.08 (1σ) and 0.84 ± 0.11 (1σ) ($\text{OS}_C = 0.30$) for reactor measurements. SMPS number and volume concentrations were consistently higher during ambient measurements, and the AMS shows that the losses were composition dependent (note that nitrate and ammonium was increased by a factor of five in the figure). Total losses were dominated by organics while sulphate was not substantially affected by the reactor. This indicates that the losses were due to volatilization by a temperature gradient or heterogeneous fragmentation, or both. Figure 2 shows the absolute difference between reactor and ambient AMS nominal organic mass peaks. Most fragments decrease in a proportional manner to their ambient concentration. The fragment CO_2^+ (m/z 44), and fragments related to it (m/z 28 and 18), were not lost in the same manner and played a dominant role in the difference between the two measurements. An m/z ratio of 44 is generally related to a

higher degree of oxidation, but also to a lower volatility, which again are hard to separate. However, the fact that the reactor output at times had higher concentrations of CO_2^+ points to the fact that the aerosol was oxidized and that temperature driven evaporation was not the only driving force. Although very low during the campaign, significant losses of nitrate were measured in the reactor. Ammonium nitrate is known to evaporate, but the nitrate present as organonitrates was high for both ambient and reactor measurements with campaign average fractions of 0.80 and 0.96 respectively. Similar to previous OFR field measurements, the ratio of reactor/ambient organics is dependent on OH exposure [9,11]. Figure 3 shows that the organic losses increase with OH exposure. It is however hard to quantify the relative contribution from temperature and fragmentation effects, since the temperature in the OFR can be expected to increase with higher lamp intensities, and loss of the most volatile compounds most likely affects the elemental ratios in a similar manner in both cases. However, in a lab environment, the temperature increase in the reactor was measured to be below 2°C at an OH exposure of 7×10^{11} molecules cm^{-3} s and a room temperature of 22°C . This moderate increase in reactor temperature would not evaporate much of the particle mass, but the reactor has a longer residence time than the bypass sampling line which increases the time the aerosol spends in the air conditioned room before being measured. Although there were times when enhancement in the reactor occurred (reactor/ambient ratio >1), inspection of the time series showed that most, if not all, of these points are due to ambient particle mass concentration changes and the fact that losses/enhancements are calculated by taking the average of ambient concentrations before and after the reactor measurements. The lack of a maximum reactor/ambient ratio in Figure 3 indicates that there were very few occasions when there was a net production of SOA in the reactor.

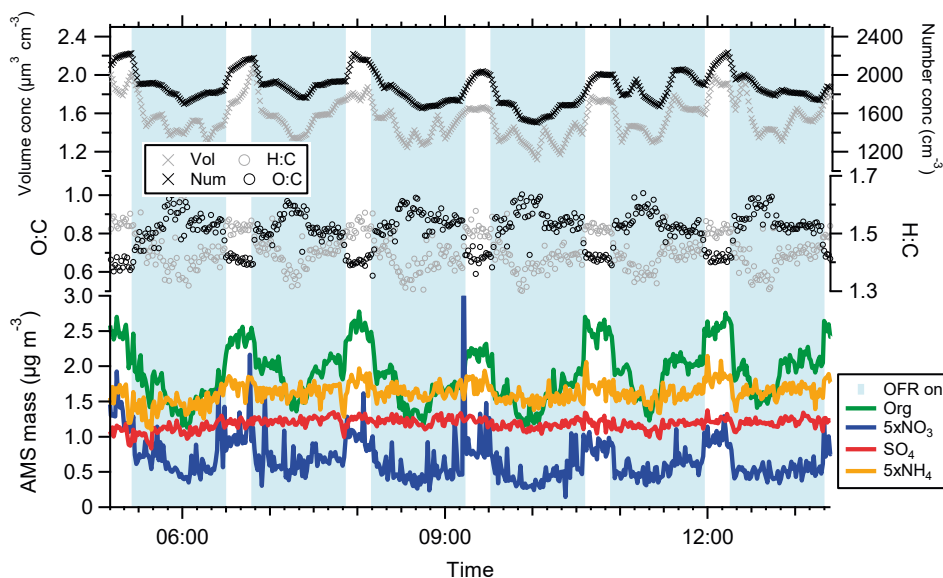


Figure 1. Typical time series from the campaign showing scanning mobility particle sizer (SMPS) volume and number concentrations, O:C and H:C elemental ratios and chemically resolved mass concentration (NO_3 and NH_4 are offset a factor 5 for clarity). Reactor measurements, highlighted in light blue gives lower volume and number concentrations, but higher O:C. Organics and nitrate is lost while sulphate is not affected.

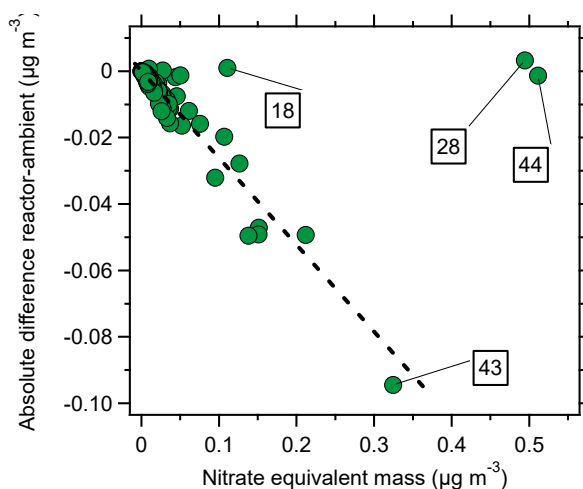


Figure 2. Aerosol mass spectrometer (AMS) mass peak difference between reactor and ambient measurements as a function of nitrate equivalent mass (signal strength). Losses due to diffusion or impaction would result in a linear decrease (given uniform particle composition). The dashed line shows the correlation between loss and signal excluding the fragments m/z 44, 28 and 18 (all belonging to the ion CO_2^+) which shows a deviation consistent with evaporation and/or oxidation.

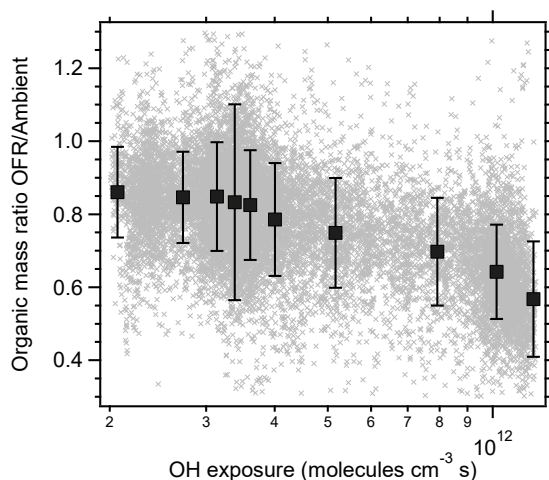


Figure 3. The ratio between reactor and ambient organic mass (with a 4% loss correction) as a function of OH exposure during the whole campaign. The 10% OH exposure quantiles with error bars corresponding to 1σ are shown for clarity. Some data included in the quantiles are outside the axis ranges.

If the losses were due to an increased temperature in the reactor, a correlation with ambient temperature should be seen, since more semi-volatile material would have been condensed at low ambient temperature. Figure 4 shows that there was a significant ($p < 0.01$) temperature effect up to $\sim 18^\circ\text{C}$, but above that value there was still a net loss in the reactor, likely due to heterogeneous oxidation. The temperature effect also gave rise to a diurnal pattern with maximum loss during night when temperatures were lower. This is in contrast to previous OFR field campaigns in which

maximum enhancement was seen during the night when ambient OH exposure and boundary layer height generally is lower. Although the particle mass concentrations during this campaign were low, which leads to lower yields in the OFR, and there was likely an effect of the temperature difference, the main reason behind the lack of net production in the OFR seen in this campaign is believed to be low production of SOA in the OFR due to low ambient VOC concentrations, as measured by the PTR-MS. The total monoterpene concentration was on average ~ 140 ppt ($0.79 \mu\text{g m}^{-3}$) with a diurnal pattern with minimum during daytime. The sum of benzene, toluene and xylenes were even lower at 96 ppt ($0.36 \mu\text{g m}^{-3}$), showing the same diurnal pattern. Further indication that little SOA formation took place in the reactor is the lack of nucleated particles. The rapid oxidation in OFRs normally produces substantial amounts of small particles, given that enough precursors are available. In this campaign, $\sim 10\%$ net loss in particle number was observed in the reactor (no correction applied).

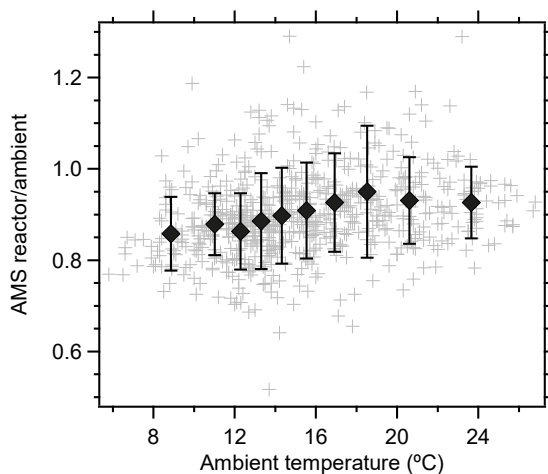


Figure 4. Ratio between reactor and ambient total AMS mass concentrations (hourly values, loss corrected) as a function of temperature. 10% temperature quantiles show a significant trend below 18°C .

The sensitivity of OFR measurements can be estimated using assumptions on particle mass yield and SOA partitioning. For example, if the minimum detectable SOA mass is $0.5 \mu\text{g m}^{-3}$ and the precursor particle mass yield is assumed to be 10%, we need to oxidize a precursor concentration of $5 \mu\text{g m}^{-3}$. Incorporating the effective condensation sink effect from the model of Palm et al. [11] increases the precursor concentration needed. In Figure 5, we calculated the SOA precursor concentration needed to see a $0.2 \mu\text{g m}^{-3}$ absolute increase, which is possible to measure with a variety of instruments, or a 5% mass based increase, which would cancel out the reactor losses in this campaign, as a function of effective condensation sink at four different yields. The approximate mass concentration is shown on the top axis (parameterized from the condensation sink of this campaign). The campaign average mass and the sum of monoterpenes and aromatics are also plotted. The α -pinene SOA mass yields from Ahlberg et al. (2017) is added as a reference. This yield was $\sim 10\%$ at the average campaign particle mass concentration. This value is an underestimation due to the condensation sink effect [31], but is far from the 50% yield needed to see a $0.2 \mu\text{g m}^{-3}$ increase. The average yield of an ambient precursor mixture is unknown, but it is not likely to be 50%. In this campaign, the concentration of monoterpenes and aromatics likely would have to be almost an order of magnitude higher to produce any visible mass in the reactor. However, many other precursors exist, some which would not be visible in the PTR-MS [11].

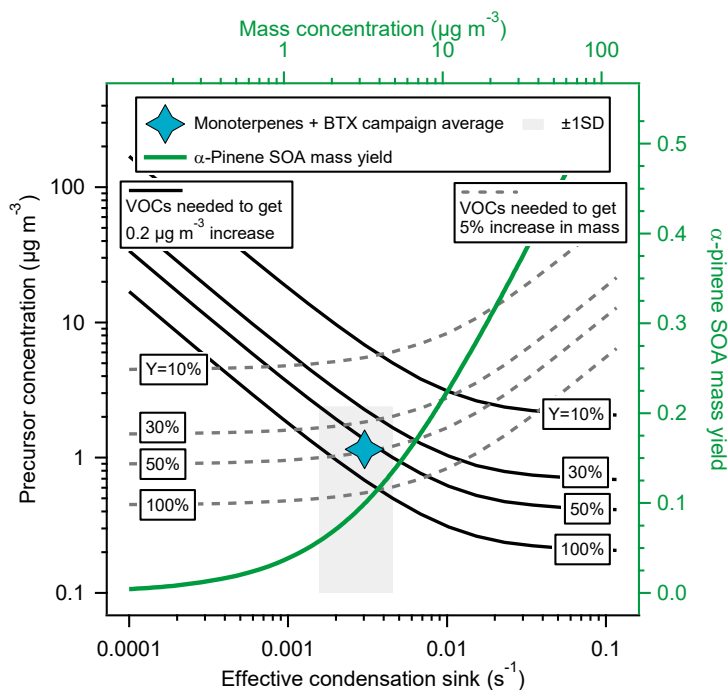


Figure 5. The precursor concentration needed to measure either a $0.2 \mu\text{g m}^{-3}$ or a 5% increase in particle mass at different effective condensation sinks and particle mass yields (boxes). The top axis shows the corresponding mass concentration at each condensation sink parameterized from the campaign data. The blue star shows the campaign average particle mass concentration and the concentration of common precursors (monoterpenes, benzene, toluene and xylenes), with $\pm 1\sigma$ in grey. For comparison, the secondary organic aerosols (SOA) mass yield of α -pinene from Ahlberg et al. (2017) as a function of organic mass is added (green axes and line).

To assess the potential losses of VOCs in the inlet, the penetration efficiency was calculated [32]. The penetration depends on the diffusion coefficient, flow rate, length of the tubing and wall accommodation coefficients. Assuming a diffusion coefficient of $7 \times 10^{-2} \text{ cm}^2 \text{ s}^{-1}$ [11] and that anything hitting the walls will stay there, the penetration would be only 3%. If the wall accommodation coefficient is 0.1 the penetration of the same molecule is 90%. Figure S5 shows the calculated penetration for diffusion coefficients between $1\text{--}10 \times 10^{-2} \text{ cm}^2 \text{ s}^{-1}$ [33,34] and mass accommodation coefficients of 0.01–1. It is clear that the uncertainty in wall accommodation had a much larger effect on penetration than the uncertainty of the diffusion coefficient. Although inlet losses may have been a factor for some species, there are compensating effects of wall loss, diffusion and particle accommodation. For example, a low volatility molecule with high wall accommodation generally also means that the diffusion is slower and the likelihood that the molecule is already bound to a particle is higher. On the other hand, a more volatile SOA precursor molecule is less likely to stick to the walls, and more likely to desorb if it does. The accommodation coefficient on Teflon is orders of magnitude lower than 0.1 [35,36], but to our knowledge, no literature data on wall accommodation coefficients on stainless steel exist. Pagonis et al. [37] investigated the effect of partitioning between gas and Teflon tubing for several VOCs, and found that significant delays due to the retention times could occur. The time-scales for equilibrium partitioning in the inlet is unknown, but the duration of the measurements, together with the PTR-MS measurements, favors the conclusion that the lack of reactor SOA production was not due to VOC losses.

4. Conclusions

We present the first ambient oxidation flow reactor measurements in Europe. The measurements took place during summer at a rural site surrounded by arable land, with 30 km to the nearest city. We saw virtually no increases in particle mass or number concentrations during the two months of the campaign. PTR-MS measurements showed that precursor concentrations were too low to form a significant amount of secondary material. A net particle mass loss of ~10%, which was correlated to ambient temperature and OH exposure, was seen. We attribute this to both evaporation of organic material in the reactor due to differences between ambient and reactor temperatures, and to fragmentation reactions. These effects are hard to separate, but it is clear that the change in elemental ratios was not only driven by evaporation, since the AMS mass fragment CO^{2+} was often increased in the reactor output. This could be due to both gas and particle phase reactions. Reactor processing led to an increase in carbon oxidation state, which is commonly linked to water uptake.

The conditions at the site are representative of many parts of northern Europe. The results are due to the relatively clean air of the site, but also because of the fast atmospheric conversion of trace gases. Net losses due to temperature driven evaporation can be limited by keeping the reactor at ambient temperatures, as has been done on other campaigns (e.g., [9,11]). However, this is not always possible at field sites and would likely not have affected the conclusions of this campaign. The sensitivity of the reactor measurements at different precursor concentrations and effective condensation sinks was calculated. It was shown that, with an ambient pm₁ concentration of ~3 $\mu\text{g m}^{-3}$, an order of magnitude higher precursor concentrations would have been needed to form significant amounts of SOA in the reactor. Sites closer to precursor emissions and with relatively high ambient aerosol mass concentrations will give much stronger responses in an OFR. These measurements show that further processing of relatively clean ambient aerosols can result in lower mass concentrations.

Supplementary Materials: The following are available online at <http://www.mdpi.com/2073-4433/10/7/408/s1>, Figure S1: Average size spectrum and reactor losses. Figure S2: Modeled fractional fate of LVOCs. Figure S3: AMS vs. SMPS mass concentrations. Figure S4: SMPS concentrations and chemical composition. Figure S5: Calculated penetration through the inlet.

Author Contributions: Conceptualization, B.S., T.H. and E.A.; methodology, B.S., T.H., A.K., G.F. and E.A.; software, B.S.; validation, E.A., T.H. and A.E.; formal analysis, E.A., T.H.; investigation, E.A., S.A., T.H., T.K., G.F., A.K. and B.S. data curation, E.A. and T.H.; writing—original draft preparation, E.A.; writing—review and editing, E.A., S.A., A.E., T.H., T.K., W.H.B., G.F., P.R., A.K. and B.S.; supervision, B.S. and A.K.; project administration, E.A. and B.S.; funding acquisition, B.S.

Funding: This work was supported by The Swedish Research Council Formas [grant number 2011-1101-19993-37] and the strategic research area MERGE at Lund University.

Acknowledgments: We thank L.C. and A.J., for providing the research infrastructure in Skrehalla.

Conflicts of Interest: The authors declare no conflict of interest.

References

1. Zhang, Q.; Jimenez, J.L.; Canagaratna, M.R.; Allan, J.D.; Coe, H.; Ulbrich, I.; Alfarra, M.R.; Takami, A.; Middlebrook, A.M.; Sun, Y.L.; et al. Ubiquity and dominance of oxygenated species in organic aerosols in anthropogenically-influenced Northern Hemisphere midlatitudes. *Geophys. Res. Lett.* **2007**, *34*. [[CrossRef](#)]
2. Pandis, S.N.; Skyllakou, K.; Florou, K.; Kostenidou, E.; Kaltsonoudis, C.; Hasa, E.; Presto, A.A. Urban particulate matter pollution: A tale of five cities. *Faraday Discuss.* **2016**, *189*, 277–290. [[CrossRef](#)] [[PubMed](#)]
3. Glasius, M.; Goldstein, A.H. Recent Discoveries and Future Challenges in Atmospheric Organic Chemistry. *Environ. Sci. Technol.* **2016**, *50*, 2754–2764. [[CrossRef](#)] [[PubMed](#)]
4. Shrivastava, M.; Cappa, C.D.; Fan, J.; Goldstein, A.H.; Guenther, A.B.; Jimenez, J.L.; Kuang, C.; Laskin, A.; Martin, S.T.; Ng, N.L.; et al. Recent advances in understanding secondary organic aerosol: Implications for global climate forcing. *Rev. Geophys.* **2017**, *55*, 509–559. [[CrossRef](#)]
5. Jimenez, J.L. Concluding remarks: Faraday Discussion on chemistry in the urban atmosphere. *Faraday Discuss.* **2016**, *189*, 661–667. [[CrossRef](#)] [[PubMed](#)]

6. Bruns, E.A.; El Haddad, I.; Keller, A.; Klein, F.; Kumar, N.K.; Pieber, S.M.; Corbin, J.C.; Slowik, J.G.; Brune, W.H.; Baltensperger, U.; et al. Inter-comparison of laboratory smog chamber and flow reactor systems on organic aerosol yield and composition. *Atmos. Meas. Tech.* **2015**, *8*, 2315–2332. [[CrossRef](#)]
7. Lambe, A.T.; Chhabra, P.S.; Onasch, T.B.; Brune, W.H.; Hunter, J.F.; Kroll, J.H.; Cummings, M.J.; Brogan, J.F.; Parmar, Y.; Worsnop, D.R.; et al. Effect of oxidant concentration, exposure time, and seed particles on secondary organic aerosol chemical composition and yield. *Atmos. Chem. Phys.* **2015**, *15*, 3063–3075. [[CrossRef](#)]
8. Platt, S.M.; Haddad, I.E.; Zardini, A.A.; Clairotte, M.; Astorga, C.; Wolf, R.; Slowik, J.G. Secondary organic aerosol formation from gasoline vehicle emissions in a new mobile environmental reaction chamber. *Atmos. Chem. Phys.* **2013**, *13*, 9141–9158. [[CrossRef](#)]
9. Ortega, A.M.; Hayes, P.L.; Peng, Z.; Palm, B.B.; Hu, W.; Day, D.A.; Li, R.; Cubison, M.J.; Brune, W.H.; Graus, M.; et al. Real-time measurements of secondary organic aerosol formation and aging from ambient air in an oxidation flow reactor in the Los Angeles area. *Atmos. Chem. Phys.* **2016**, *16*, 7411–7433. [[CrossRef](#)]
10. George, I.J.; Slowik, J.; Abbatt, J.P.D. Chemical aging of ambient organic aerosol from heterogeneous reaction with hydroxyl radicals. *Geophys. Res. Lett.* **2008**, *35*. [[CrossRef](#)]
11. Palm, B.B.; Campuzano-Jost, P.; Ortega, A.M.; Day, D.A.; Kaser, L.; Jud, W.; Karl, T.; Hansel, A.; Hunter, J.F.; Cross, E.S.; et al. In situ secondary organic aerosol formation from ambient pine forest air using an oxidation flow reactor. *Atmos. Chem. Phys.* **2016**, *16*, 2943–2970. [[CrossRef](#)]
12. Palm, B.B.; Campuzano-Jost, P.; Day, D.A.; Ortega, A.M.; Fry, J.L.; Brown, S.S.; Zarzana, K.J.; Dube, W.; Wagner, N.L.; Draper, D.C.; et al. Secondary organic aerosol formation from in situ OH, O-3, and NO₃ oxidation of ambient forest air in an oxidation flow reactor. *Atmos. Chem. Phys.* **2017**, *17*, 5331–5354. [[CrossRef](#)]
13. Slowik, J.G.; Wong, J.P.S.; Abbatt, J.P.D. Real-time, controlled OH-initiated oxidation of biogenic secondary organic aerosol. *Atmos. Chem. Phys.* **2012**, *12*, 9775–9790. [[CrossRef](#)]
14. Palm, B.B.; Sá, S.S.D.; Day, D.A.; Campuzano-Jost, P.; Hu, W.; Seco, R.; Sjøstedt, S.J.; Park, J.H.; Guenther, A.B.; Kim, S.; et al. Secondary organic aerosol formation from ambient air in an oxidation flow reactor in central Amazonia. *Atmos. Chem. Phys. Discuss.* **2018**, *18*, 467–493. [[CrossRef](#)]
15. Kang, E.; Lee, M.; Brune, W.H. Taehyung Lee Photochemical aging of organic and inorganic ambient aerosol from the Potential Aerosol Mass (PAM) reactor experiment in East Asia. *Atmos. Chem. Phys. Discuss.* **2017**. [[CrossRef](#)]
16. Kang, E.; Root, M.J.; Toohey, D.W.; Brune, W.H. Introducing the concept of Potential Aerosol Mass (PAM). *Atmos. Chem. Phys.* **2007**, *7*, 5727–5744. [[CrossRef](#)]
17. Lambe, A.T.; Ahern, A.T.; Williams, L.R.; Slowik, J.G.; Wong, J.P.S.; Abbatt, J.P.D.; Brune, W.H.; Ng, N.L.; Wright, J.P.; Croasdale, D.R.; et al. Characterization of aerosol photooxidation flow reactors: Heterogeneous oxidation, secondary organic aerosol formation and cloud condensation nuclei activity measurements. *Atmos. Meas. Tech.* **2011**, *4*, 445–461. [[CrossRef](#)]
18. Li, R.; Palm, B.B.; Ortega, A.M.; Hlywiak, J.; Hu, W.; Peng, Z.; Day, D.A.; Knote, C.; Brune, W.H.; De Gouw, J.A.; et al. Modeling the Radical Chemistry in an Oxidation Flow Reactor: Radical Formation and Recycling, Sensitivities, and the OH Exposure Estimation Equation. *J. Phys. Chem. A* **2015**, *119*, 4418–4432. [[CrossRef](#)]
19. Peng, Z.; Day, D.A.; Stark, H.; Li, R.; Lee-Taylor, J.; Palm, B.B.; Brune, W.H.; Jimenez, J.L. HO_x radical chemistry in oxidation flow reactors with low-pressure mercury lamps systematically examined by modeling. *Atmos. Meas. Tech.* **2015**, *8*, 4863–4890. [[CrossRef](#)]
20. Wiedensohler, A.; Birmili, W.; Nowak, A.; Sonntag, A.; Weinhold, K.; Merkel, M.; Wehner, B.; Tuch, T.; Pfeifer, S.; Fiebig, M.; et al. Mobility particle size spectrometers: Harmonization of technical standards and data structure to facilitate high quality long-term observations of atmospheric particle number size distributions. *Atmos. Meas. Tech.* **2012**, *5*, 657–685. [[CrossRef](#)]
21. DeCarlo, P.F.; Kimmel, J.R.; Trimborn, A.; Northway, M.J.; Jayne, J.T.; Aiken, A.C.; Gonin, M.; Fuhrer, K.; Horvath, T.; Docherty, K.S.; et al. Field-deployable, high-resolution, time-of-flight aerosol mass spectrometer. *Anal. Chem.* **2006**, *78*, 8281–8289. [[CrossRef](#)] [[PubMed](#)]
22. Graus, M.; Müller, M.; Hansel, A. High Resolution PTR-TOF: Quantification and Formula Confirmation of VOC in Real Time. *J. Am. Soc. Mass Spectrom.* **2010**, *21*, 1037–1044. [[CrossRef](#)] [[PubMed](#)]

23. Lindinger, W.; Hansel, A.; Jordan, A. On-line monitoring of volatile organic compounds at pptv levels by means of proton-transfer-reaction mass spectrometry (PTR-MS) - Medical applications, food control and environmental research. *Int. J. Mass Spectrom.* **1998**, *173*, 191–241. [[CrossRef](#)]
24. Von der Weiden, S.L.; Drewnick, F.; Borrmann, S. Particle Loss Calculator—A new software tool for the assessment of the performance of aerosol inlet systems. *Atmos. Meas. Tech.* **2009**, *2*, 479–494. [[CrossRef](#)]
25. Middlebrook, A.M.; Bahreini, R.; Jimenez, J.L.; Canagaratna, M.R. Evaluation of Composition-Dependent Collection Efficiencies for the Aerodyne Aerosol Mass Spectrometer using Field Data. *Aerosol Sci. Technol.* **2012**, *46*, 258–271. [[CrossRef](#)]
26. Farmer, D.K.; Matsunaga, A.; Docherty, K.S.; Surratt, J.D.; Seinfeld, J.H.; Ziemann, P.J.; Jimenez, J.L. Response of an aerosol mass spectrometer to organonitrates and organosulfates and implications for atmospheric chemistry. *Proc. Natl. Acad. Sci. USA* **2010**, *107*, 6670–6675. [[CrossRef](#)] [[PubMed](#)]
27. Canagaratna, M.R.; Jimenez, J.L.; Kroll, J.H.; Chen, Q.; Kessler, S.H.; Massoli, P.; Hildebrandt Ruiz, L.; Fortner, E.; Williams, L.R.; Wilson, K.R.; et al. Worsnop: Elemental ratio measurements of organic compounds using aerosol mass spectrometry: Characterization, improved calibration, and implications. *Atmos. Chem. Phys.* **2015**, *15*, 253–272. [[CrossRef](#)]
28. Holzinger, R. PTRwid: A new widget tool for processing PTR-TOF-MS data. *Atmos. Meas. Tech.* **2015**, *8*, 3903–3922. [[CrossRef](#)]
29. Holzinger, R.; Kasper-Giebl, A.; Staudinger, M.; Schauer, G.; Röckmann, T. Analysis of the chemical composition of organic aerosol at the Mt. Sonnblick observatory using a novel high mass resolution thermal-desorption proton-transfer-reaction mass-spectrometer (hr-TD-PTR-MS). *Atmos. Chem. Phys.* **2010**, *10*, 10111–10128. [[CrossRef](#)]
30. Cappellin, L.; Biasoli, F.; Schuhfried, E.; Soukoulis, C.; Märk, T.D.; Gasperi, F. Extending the dynamic range of proton transfer reaction time-of-flight mass spectrometers by a novel dead time correction. *Rapid Commun. Mass Spectrom.* **2011**, *25*, 179–183. [[CrossRef](#)]
31. Ahlberg, E.; Eriksson, A.; Brune, W.H.; Roldin, P.; Svenningsson, B. Effect of salt seed particle surface area, composition and phase on secondary organic aerosol mass yields in oxidation flow reactors. *Atmos. Chem. Phys.* **2019**, *19*, 2701–2712. [[CrossRef](#)]
32. Hinds, W.C. *Aerosol Technology: Properties, Behavior, and Measurement of Airborne Particles*; John Wiley & Sons: Hoboken, NJ, USA, 2012.
33. Lugg, G.A. Diffusion Coefficients of Some Organic and Other Vapors in Air. *Anal. Chem.* **1968**, *40*, 1072–1077. [[CrossRef](#)]
34. Tang, M.J.; Shiraiwa, M.; Pöschl, U.; Cox, R.A.; Kalberer, M. Compilation and evaluation of gas phase diffusion coefficients of reactive trace gases in the atmosphere: Volume 2. Diffusivities of organic compounds, pressure-normalised mean free paths, and average Knudsen numbers for gas uptake calculations. *Atmos. Chem. Phys.* **2015**, *15*, 5585–5598. [[CrossRef](#)]
35. McMurry, P.H.; Grosjean, D. Gas and Aerosol Wall Losses in Teflon Film Smog Chambers. *Environ. Sci. Technol.* **1985**, *19*, 1176–1182. [[CrossRef](#)] [[PubMed](#)]
36. Matsunaga, A.; Ziemann, P.J. Gas-Wall Partitioning of Organic Compounds in a Teflon Film Chamber and Potential Effects on Reaction Product and Aerosol Yield Measurements. *Aerosol Sci. Technol.* **2010**, *44*, 881–892. [[CrossRef](#)]
37. Pagonis, D.; Krechmer, J.E.; de Gouw, J.; Jimenez, J.L.; Ziemann, P.J. Effects of Gas-Wall Partitioning in Teflon Tubing and Instrumentation on Time-Resolved Measurements of Gas-Phase Organic Compounds. *Atmos. Meas. Tech. Discuss.* **2017**, *10*, 4687–4696. [[CrossRef](#)]



Supplemental Information for

No particle mass enhancement from induced atmospheric ageing at a rural site in northern Europe

Erik Ahlberg^{1,2,*}, Stina Ausmeel², Axel Eriksson^{2,3}, Thomas Holst⁴, Tomas Karlsson⁴, William H. Brune⁵, Göran Frank², Pontus Roldin², Adam Kristensson², Birgitta Svenningsson²

¹ Centre for Environmental and Climate Research, Lund University, Sölvegatan 37, 223 52 Lund, Sweden

² Division of Nuclear Physics, Lund University, Box 118, 221 00 Lund, Sweden

³ Ergonomics and Aerosol Technology, Lund University, Box 118, 221 00 Lund, Sweden

⁴ Department of Physical Geography and Ecosystem Science, Lund University, Sölvegatan 12, 223 62 Lund, Sweden

⁵ Department of Meteorology, Pennsylvania State University, University Park, PA, United States

* Correspondence: erik.ahlberg@nuclear.lu.se

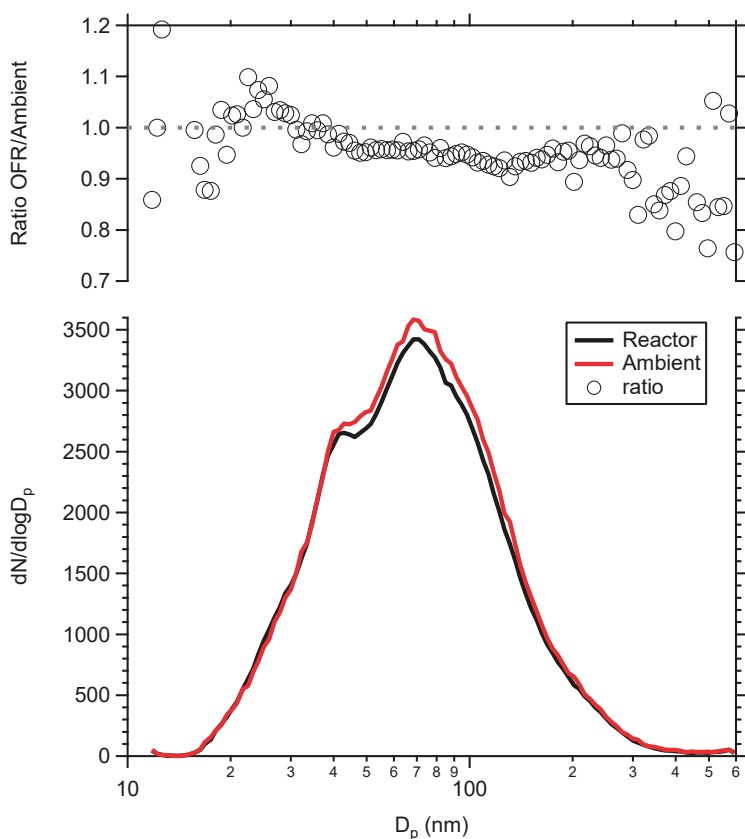


Figure S1. Average size spectrum and size resolved losses in the reactor from a period when the UV lamps were off. The ratio between OFR and ambient data shows significant noise at sizes where the number concentration is low.

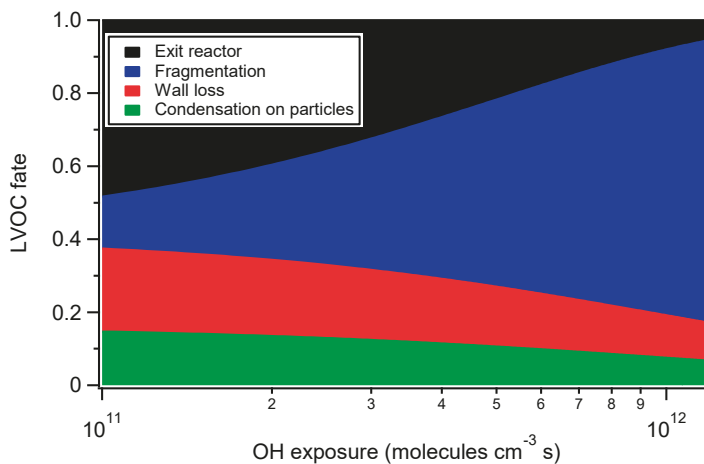


Figure S2. The modeled fractional fate of LVOCs in the reactor as a function of OH exposure. The model was constructed using the same principles as in Palm *et al.* [1]. The settings used were $k_{OH} = 1 \times 10^{-11} \text{ cm}^3 \text{ molecules}^{-1} \text{ s}^{-1}$, a residence time of 160 s, a condensation sink of $1.29 \times 10^{-3} \text{ s}^{-1}$ (campaign average, corresponding to a surface area concentration of $42 \mu\text{m}^2 \text{ cm}^{-3}$), eddy diffusion coefficient of 0.0042 and wall loss rate of 0.0020 s^{-1} . Loss to fragmentation is assumed after reaction with OH five times.

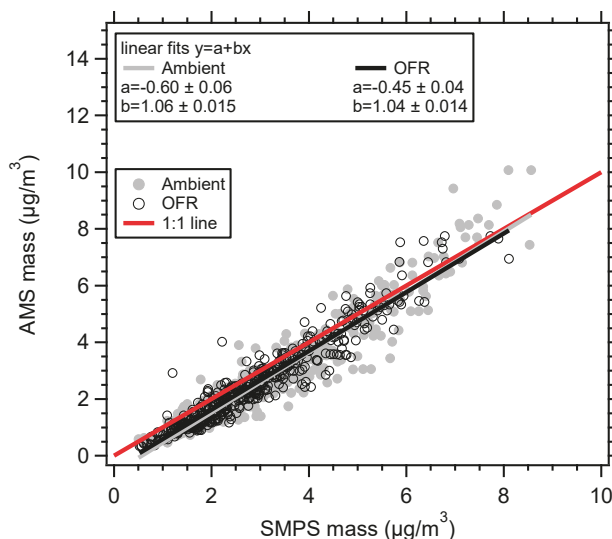


Figure S3. Total AMS and SMPS mass concentrations. The slopes of the data gives the collection efficiency of the AMS. The offset in SMPS mass (a-value) is likely from a constant error at the high end of the SMPS size spectra.

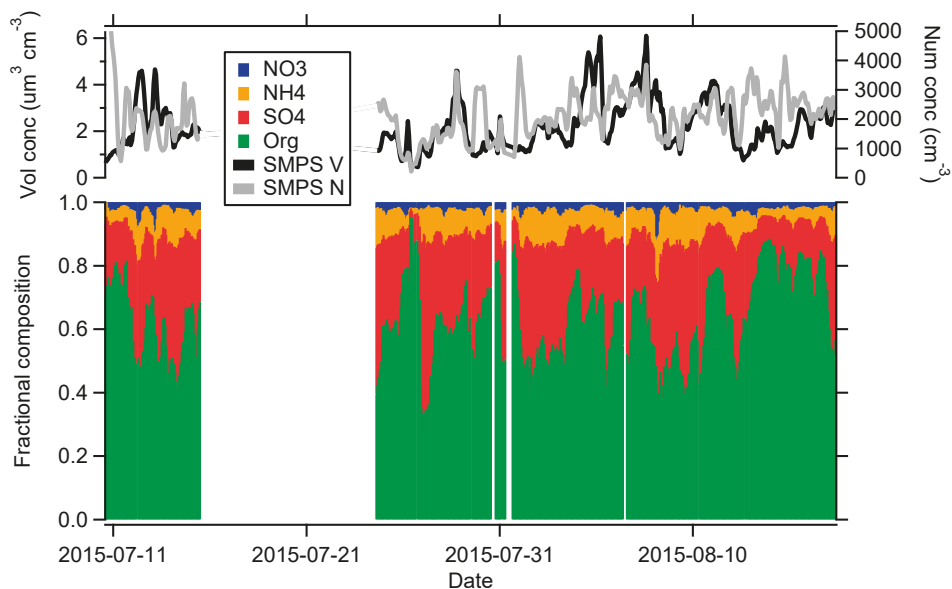


Figure S4. Overview of the campaign showing SMPS number and volume concentrations and AMS chemical composition.

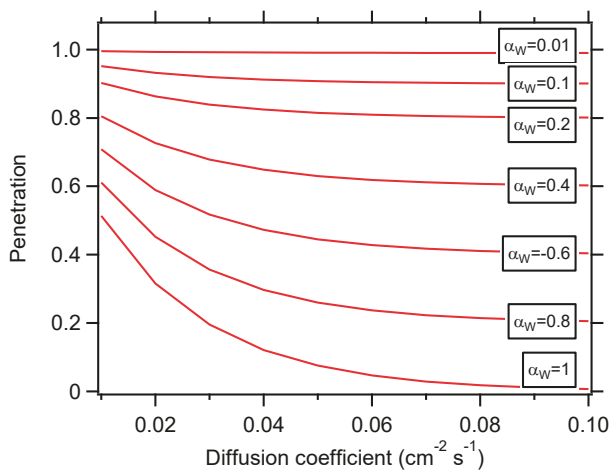


Figure S5. Calculated penetration through the inlet up to the reactor as a function of diffusion coefficients and wall mass accommodation coefficient.

1. Palm, B. B., Campuzano-Jost, P., Ortega, A. M., Day, D. A., Kaser, L., Jud, W., Karl, T., Hansel, A., Hunter, J. F., Cross, E. S., Kroll, J. H., Peng, Z., Brune, W. H. and Jimenez, J. L.: In situ secondary organic aerosol formation from ambient pine forest air using an oxidation flow reactor. *Atmos. Chem. Phys.*, 16, 2943, 2016.

Paper IV





Contents lists available at ScienceDirect

Atmospheric Environment

journal homepage: www.elsevier.com/locate/atmosenv

Isoprenoid emission variation of Norway spruce across a European latitudinal transect



Ylva van Meeningen^{a,*}, Min Wang^a, Tomas Karlsson^a, Ana Seifert^a, Guy Schurgers^b, Riikka Rinnan^c, Thomas Holst^{a,c}

^a Lund University, Department of Physical Geography and Ecosystem Science, Sölvegatan 12, 223 62 Lund, Sweden

^b University of Copenhagen, Department of Geosciences and Natural Resource Management, Øster Voldgade 10, 1350 Copenhagen K, Denmark

^c University of Copenhagen, Terrestrial Ecology Section, Department of Biology, Universitetsparken 15, DK-2100 Copenhagen Ø, Denmark

HIGHLIGHTS

- Isoprenoid emission from Norway spruce were measured at seven sites in Europe.
- There were little differences in standardized emission rates across Europe.
- The emission profile differed between sites, but was less distinct for cloned trees.
- Emission patterns were potentially influenced by tree height, season and year.

ARTICLE INFO

Article history:

Received 19 April 2017

Received in revised form

5 September 2017

Accepted 25 September 2017

Available online 27 September 2017

Keywords:

Biogenic volatile organic compounds

Picea abies

Latitudinal gradient

Genetic diversity

Emission profile

ABSTRACT

Norway spruce (*Picea abies*) is one of the dominant tree species in the European boreal zone with the capacity to grow over large areas within Europe. It is an important emitter of biogenic volatile organic compounds (BVOCs), which can act as precursors of photochemical smog and ozone and contribute to the formation and growth of secondary organic aerosols (SOA) in the atmosphere.

Isoprenoid emissions were measured from Norway spruce trees at seven different sites, distributed from Ljubljana in Slovenia to Piikkiö in Finland. Four of the sites were part of a network of genetically identical spruce trees and contained two separate provenances. The remaining three sites were part of other networks which have been used to conduct studies in the European boreal zone.

There were minimal differences in the standardized emission rates between sites and across latitudes. The emission profile differed between provenances and sites, but there were not any distinct patterns which could be connected to a change in latitude. By using genetically identical trees and comparing the emission rates between sites and with genetically different trees, it was observed that the emission patterns were mostly influenced by genetics. But in order to confirm this possible stability of the relative emission profile based on genetics, more studies need to be performed.

The effects of branch height, season and variation between years on observed emission pattern variations were also investigated. There were indications of potential influences of all three factors. However, due to different experimental setups between measurement campaigns, it is difficult to draw any robust conclusions.

© 2017 The Authors. Published by Elsevier Ltd. This is an open access article under the CC BY license (<http://creativecommons.org/licenses/by/4.0/>).

1. Introduction

Biogenic volatile organic compounds (BVOCs) are emitted in large variations from different types of plants, where some of the

most prominent compound groups are isoprene (ISO, consisting of one C₅ unit), monoterpenes (MTs, consisting of two C₅ units) and sesquiterpenes (SQTs, consisting of three C₅ units) (Kesselmeier and Staudt, 1999; Holopainen, 2011). The primary functions for plants to release BVOCs are to attract pollinators, defend against herbivores and pathogens, serve as signals in plant-plant communication and to give protection against abiotic stresses such as high temperature, high irradiation or oxidative stress (Dudareva and Pichersky, 2008;

* Corresponding author.

E-mail address: ylva.van.meeningen@nateko.lu.se (Y. van Meeningen).

Laothawornkitkul et al., 2009; Vickers et al., 2009; Holopainen and Gershenson, 2010; Loreto and Schnitzler, 2010; Peñuelas and Staudt, 2010; Maffei, 2010). But once released into the atmosphere, BVOCs can influence the atmospheric chemistry and Earth's radiative balance (Di Carlo et al., 2004; VanReken et al., 2006; Beerling et al., 2007; Paasonen et al., 2013). BVOCs can act as precursors of photochemical smog and ozone, but also contribute to its destruction depending on the levels of NO_x in the atmosphere (Chameides et al., 1988; Atkinson, 2000; Peñuelas and Staudt, 2010). Furthermore, they are important in the formation and growth of secondary organic aerosols (SOA) and for enhancing the production of cloud condensation nuclei (CCN) (Claeys et al., 2004; VanReken et al., 2006; Spracklen et al., 2008; Paasonen et al., 2013; Ehn et al., 2014). Both SOA and modifications of cloud properties have the potential to affect incoming solar radiation and thus influence global warming (VanReken et al., 2006; Laothawornkitkul et al., 2009; Paasonen et al., 2013).

Forests are significant sources of BVOCs, in particular of isoprene and MTs (Kesselmeier and Staudt, 1999; Holopainen, 2011; Laffineur et al., 2011). One of the largest vegetation zones in the world is the boreal zone, consisting of approximately 33% of the total worldwide forest cover across Eurasia and Northern America (FAO, 2001). Boreal forests emit less BVOCs in comparison to temperate or tropical regions on a global scale, but are important contributors to regional emission budgets (Guenther et al., 1995, 2012; Acosta Navarro et al., 2014; Sindelarova et al., 2014). The emission budgets are influenced by the high reactivity rates of BVOCs, which depend on the structure of the BVOCs released and the chemical composition of the air at the local scale where BVOCs are emitted (Atkinson and Arey, 2003). The emission from the boreal zone is often characterized by MTs, but there can be considerable isoprene and SQT emissions as well (Tarvainen et al., 2007; Rinne et al., 2009). The boreal zone yields substantial amounts of SOA in the atmosphere, which plays an important role in the global radiation balance (Claeys et al., 2004; Tunved et al., 2006; Bonn et al., 2009).

Norway spruce (*Picea abies*) is one of the dominant tree species of the European boreal zone, but it is also widely distributed throughout other parts of Europe (Janson et al., 1999; Grabmer et al., 2006; Filella et al., 2007; Skjøth et al., 2008; Kivimäenpää et al., 2013). Norway spruce is a low or moderate monoterpene emitter and a low isoprene emitter (Janson et al., 1999; Kesselmeier and Staudt, 1999; Simpson et al., 1999; Grabmer et al., 2006). It has the capacity to emit BVOCs from storage structures in resin ducts, needles and the bark, but there can also be a significant contribution from *de novo* emissions (Ghirardo et al., 2010).

Leaf- and canopy scale emission models can be used to investigate the effect of BVOC emissions on atmospheric chemistry and aerosol formation. As BVOCs have different reactivity with OH radicals and ozone due to their different molecular structures (Atkinson and Arey, 2003), it is of importance to consider the composition of the emissions from different plant species (Niinemets et al., 2010). At a spatial-, biome- or global-scale, the emissions are typically determined by dividing the plants into plant functional types (PFT) for which an average emission potential has been determined. However, the emission capacities for different plant species within a PFT can vary greatly and the parameterization chosen for a PFT might vary for different models (Guenther et al., 2006; Arneth et al., 2010; Niinemets et al., 2010; Monson et al., 2012). The vegetation has a capacity to adapt their emission patterns over environmental gradients, which leads to large uncertainties between emissions and geographical location (Niinemets et al., 2010; Bourtsoukidis et al., 2012; Harrison et al., 2013) that are difficult to include in models. The observed geographic variability may be related to adaptation to local growing

conditions, hybridization or to existing genetic variation (Staudt et al., 2004; Bäck et al., 2012; Steinbrecher et al., 2013), but may also be affected by microclimatic conditions, adaptations at different canopy heights and by seasonal development (Keenan et al., 2009; Niinemets et al., 2010; Grote et al., 2013).

The importance and impact of genetic diversity and growing condition adaptations on the BVOC emission patterns has been highlighted by several studies. Nerg et al. (1994) studied Scots pine (*Pinus sylvestris*) seedlings grown at different latitudes in Estonia and Finland, and reported latitudinal effects on terpene concentration in pine shoots. Bäck et al. (2012) measured BVOC emission from Scots pine trees and found that there existed different chemotypes attributed to genetic variation within the same stand. Persson et al. (2016) measured genetically identical trees of English oak (*Quercus robur*), European beech (*Fagus sylvatica*) and Norway spruce and found that the relative compound contribution remained fairly stable between individuals of the same species. These studies highlight an existing uncertainty regarding the importance of genetic variation for observed BVOC emissions relative to the effect of local environmental conditions across latitudes (Kesselmeier and Staudt, 1999; Bäck et al., 2012; Persson et al., 2016).

The aims for this study are (I) to investigate the potential variability for the emission rates of Norway spruce across a latitudinal transect in Europe and (II) to examine how the observed emission patterns are influenced by genetic diversity and height within the canopy, but also time of season and variation between years will be considered.

2. Methods

2.1. Site descriptions

Measurements were performed at seven sites along a latitudinal transect across Europe, stretching from Ljubljana in Slovenia to Piikkiö in Finland (Fig. 1). The sites were chosen as they represent both the boreal ecosystem and cover a wide range where spruce has the capacity to grow. It is a collaboration of four separate



Fig. 1. The location of the seven study sites within Europe.

projects with different measurement campaigns, where one to five campaigns were performed per site. Each campaign lasted between one and three weeks. The details of location, tree height, tree age, sampling date, number of performed campaigns, measurement year, annual average temperature ($^{\circ}\text{C}$), annual total precipitation (mm), average Photosynthetically Active Radiation (PAR) and average temperature ($^{\circ}\text{C}$) during campaigns can be found in Table 1.

Four of the sites, namely Ljubljana (Slovenia), Grafath (Germany), Taastrup (Denmark) and Piikkiö (Finland), are part of the International Phenological Garden (IPG) network in Europe which have been used to perform long-term phenological observations on naturally occurring plant species (Chmielewski et al., 2013). The advantage of the network is that all plants are clones, which means the genetic variation between plants is negligible. Ljubljana, Grafath and Piikkiö were established between 1962 and 1965, whilst Taastrup was begun in 1971 (www.agrar.hu-berlin.de). Within the IPG network, there are two provenances of Norway spruce which are divided into early spruce (SE), with an early budburst, and late spruce (SL) which experiences budburst approximately one week later.

The remaining sites did not contain genetically identical trees, but are part of other networks used to perform studies in the European boreal zone. Hyltemossa research station is located in southern Sweden, whilst Norunda research station is located about 30 km north of Uppsala in Sweden. Both sites are run by the Integrated Carbon Observation System in Sweden (ICOS). Hyltemossa is dominated by Norway spruce with a small fraction of Downy birch and Scots pine (www.icos-sweden.se), whilst Norunda is part of a boreal forest dominated by 80–123-years old Norway spruce and

Scots pine (Lagergren et al., 2005). The site in Skogaryd is located in south-western Sweden, approximately 50 km from the west coast and covers an area of roughly 30 km². The site is part of Swedish Infrastructure for Ecosystem Science (SITES) (Shendryk et al., 2014) and mainly contains coniferous trees, dominated by Norway spruce and Scots Pine (Wallin et al., 2015) (Fig. 1).

2.2. BVOC measurement techniques

For the IPG network sites and Hyltemossa, samples were collected from needle chambers with a volume of 270 cm³ and which were connected to a portable infra-red gas analyzer (IRGA; 6400–22L lighted conifer chamber; LI-6400, LICOR, Lincoln, NE, USA). The needle twigs were acclimated to 1000 $\mu\text{mol m}^{-2} \text{s}^{-1}$ PAR and 400 $\mu\text{mol CO}_2 \text{ mol}^{-1}$ air for approximately one hour before BVOC sampling. Relative humidity was maintained close to ambient conditions between 50 and 65% by removing excess water vapor from the ingoing air stream when necessary. Leaf temperatures were kept constant between 10 and 15 $^{\circ}\text{C}$ in October and 20–30 $^{\circ}\text{C}$ in April–August, based on the anticipated average daily temperature. Sample air was collected from the chamber outlet.

The measurements in Skogaryd and Norunda were performed on a single tree and used 13-L cylindrical and transparent chambers consisting of Teflon and stainless steel (Haapanala et al., 2009). To avoid stress induced emissions from the trees, the chambers were installed one day before the measurements were initiated. Purge air was continuously flowing into the chambers with a flow rate of 4–6 l/min. Temperature and humidity were measured inside and outside the chambers (Campbell Scientific CS215, USA) together

Table 1

The study sites with their coordinates, approximate tree heights, the age of trees, number of trees measured with the number of collected samples given in parenthesis, the months when measurements were taken including the number of performed campaigns in parenthesis, study years, average annual temperatures, total precipitation, average Photosynthetically Active Radiation (PAR) inside the chambers during measurement campaigns and average temperatures inside the chamber during the measurements.

Study site and coordinates	Tree heights (m)	Tree age (yr)	No of trees and samples	Measurement months and no. of campaigns	Study years	Temperature ($^{\circ}\text{C}$)	Precipitation (mm)	PAR in chambers ($\mu\text{mol m}^{-2} \text{s}^{-1}$)	Temperatures in chambers ($^{\circ}\text{C}$)
Ljubljana 46°04'N, 14°30'E	17	52	3 (17)	May (1)	2014	10.9 ^a	1362 ^a	1000	17.8
Ljubljana 46°04'N, 14°30'E	17	53	3 (21)	Oct (1)	2015	10.9 ^a	1362 ^a	1000	12.5
Ljubljana 46°04'N, 14°30'E	17	54	3 (51)	Apr–May (3)	2016	10.9 ^a	1362 ^a	1000	18.5
Grafath 48°18'N, 11°17'E	2.5, 20	5, 51	6 (50)	Jun (1)	2014	8.5 ^b	877 ^b	1000	25.7
Grafath 48°18'N, 11°17'E	3, 20	7, 53	4 (22)	Jun (1)	2016	8.5 ^b	877 ^b	1000	22.8
Taastrup 55°40'N, 12°18'E	15	42	4 (76)	Jul–Aug (1)	2013	7.5 ^c	583 ^c	1000	20.2
Taastrup 55°40'N, 12°18'E	15	43–45	4 (70)	Jul (3)	2014 –2016	7.5 ^c	583 ^c	1000	20.9
Hyltemossa 56°06'N, 13°25'E	14–18	30	4 (27)	Jul (1)	2016	8.0 ^d	800 ^d	1000	20.8
Skogaryd 58°23'N, 12°09'E	25	53	1 (40)	Oct (1)	2015	6.2 ^e	709 ^e	134	8.9
Norunda 60°05'N, 17°29'E	25	119	1 (90)	Jun (1)	2014	5.4 ^f	520 ^f	250	17.8
Norunda 60°05'N, 17°29'E	25	119	1 (73)	Jul (1)	2014	5.4 ^f	520 ^f	289	29.0
Piikkiö 60°23'N, 22°30'E	12	49	4 (19)	Jul–Aug (1)	2014	5.9 ^g	698 ^g	1000	24.2

^a = <http://meteo.arso.gov.si>.

^b = <http://www.wetter-by.de>.

^c = Jensen et al., 1997.

^d = <http://www.icos-sweden.se>.

^e = Alexandersson and Eggertsson Karlström, 2001.

^f = Aubinet et al., 2010.

^g = <http://en.ilmatietaenlaitos.fi>.

with PAR (Li-Cor Li-190, USA). In Skogaryd, two chambers were mounted on a scaffold at two heights (2.5 m and 3.5 m). In Norunda, one chamber was installed 20.0 m above the ground, whilst another chamber measured the emission rates at a lower level (3.0 m in June and 11.0 m in July).

In all campaigns, a hydrocarbon trap (Alltech, Associates Inc., USA) containing MnO₂-coated copper nets was fixed between the ambient air inlet and the chamber inlet to absorb all the VOCs and ozone from the incoming air stream. Sample air passed through stainless steel cartridges (Markes International Limited, Llantrisant, UK) packed with adsorbents Tenax TA (a porous organic polymer) and Carbograph 1TD (graphitized carbon black). The air samples were extracted by using flow-controlled pocket pumps (Pocket Pump, SKC Ltd., Dorset, UK). The sampling flow rate was 200 ml min⁻¹ and the collected volume for each sample was between 5 and 6 L. Blank samples were also collected in order to acknowledge possible background contamination in the ambient air. After BVOC measurements were performed, the needles inside the chambers were harvested, dried until the biomass weight was constant and weighed to get the dry weight (g(dw)). All measurements were performed during daytime (8:00–17:00).

A total of 556 cartridges were collected and analyzed. All cartridges were sealed with Teflon-coated brass caps and stored at 3 °C until analysis. For all sites except Norunda, the BVOCs samples were analyzed by gas chromatograph-mass spectrometer following thermal desorption at 250 °C at the University of Copenhagen (for details, see van Meeningen et al., 2016). For standardization, pure standard solutions of isoprene, α -pinene, camphene, δ -phellandrene, limonene, eucalyptol, γ -terpinene, linalool, aromadendrene and α -humulene in methanol (Fluka, Buchs, Switzerland) were injected into adsorbent cartridges in a stream of helium. When quantifying BVOCs without a standard solution, α -pinene was used for MTs and α -humulene was used for SQTs. The chromatograms from the analysis were identified with the mass spectra in the NIST library and analyzed with the MSD Chemstation Data Analysis software (G1701CA C.00.00 21 Dec 1999; Agilent Technologies, Santa Clara, CA, USA). For the samples collected in Norunda, the analysis of sample tubes was done by the Finnish Meteorological Institute (Atmospheric Composition Unit, Helsinki, Finland). The samples were desorbed at 300 °C, and the standard solutions were camphene, 3-carene, 1,8-cineol, limonene, linalool, myrcene, α -pinene, β -pinene, terpinolene, longicyclene, isolongifolene, β -caryophyllene, aromadendrene, α -humulene, 2-methyl-3-buten-2-ol (MBO), *p*-cymene and bornylacetate. Isoprene was calibrated using a gaseous standard.

2.3. Normalization of BVOC emission rates

The BVOC emission rate (*E*) from all of the samples was defined by the mass of compound per dry biomass weight and time (Hakola et al., 2003):

$$E = (C_2 - C_1) \times F \times m^{-1} \quad (1)$$

where *E* is the emission rate (in $\mu\text{g}(\text{dw})^{-1} \text{h}^{-1}$), *C*₂ is the concentration of compound in the sample ($\mu\text{g} \text{L}^{-1}$), *C*₁ is the VOC concentration in the inlet air ($\mu\text{g} \text{L}^{-1}$, here considered to be zero, as the incoming air was filtered free of VOCs), *F* is the air flow rate into the chamber ($\text{L} \text{min}^{-1}$), and *m* is the dry weight of the needle biomass (g). In order to make comparisons between emission spectra and amounts from different sites, all emission rates were normalized to standard light and temperature conditions (PAR, 1000 $\mu\text{mol} \text{m}^{-2} \text{s}^{-1}$ and *T*_s, 303 K). The algorithm for light dependent compounds presented by Guenther et al. (1993) was used for isoprene and is expressed as:

$$I = I_s C_T C_L \quad (2)$$

where *I* is the emission rate at a given leaf temperature and flux of PAR. *I*_s is the standardized emission rate at standard light and temperature conditions. *C*_T and *C*_L are the temperature and light correction factors, calculated by the following equations:

$$C_L = \frac{\alpha C_{L1} \text{PAR}}{\sqrt{1 + \alpha^2 \text{PAR}^2}} \quad (3)$$

and

$$C_T = \frac{\exp\left(\frac{C_{T1}(T-T_s)}{RT_s T}\right)}{1 + \exp\left(\frac{C_{T2}(T-T_M)}{RT_s T}\right)} \quad (4)$$

where *R* (8.314 J K⁻¹ mol⁻¹) is the ideal gas constant and α (0.0027), *C*_{L1} (1.066), *C*_{T1} (95 000 J mol⁻¹), *C*_{T2} (230 000 J mol⁻¹) and *T*_M (314 K) are empirical coefficients (Guenther et al., 1993). For monoterpenes and sesquiterpenes, the algorithm for temperature dependent compounds by Guenther et al. (1993) was used and is described as:

$$M = M_s \exp^{\beta(T-T_s)} \quad (5)$$

where *M* is the monoterpene or sesquiterpene emission rate at a given leaf temperature, whilst β (0.09 K⁻¹) is an empirical coefficient.

2.4. Statistical analysis

The significant difference between sites, provenances and years was analyzed by a Kruskal-Wallis test on all of the different groups. If the test resulted in significant differences, a Mann-Whitney *U* test followed by Bonferroni correction was performed to determine significant groups. Differences in the emission rates between different heights were tested using Mann-Whitney *U*-tests.

Partial least squares regression (PLS) was performed to investigate possible connections between factors such as ambient and past average temperatures, height, latitude, PAR and season (*X*-variables) and the emitted BVOCs (*Y*-variables). Season was defined as the number of active growing days where the average daily temperature had exceeded 5 °C for five consecutive days. Analysis was performed using SIMCA (Umetrics, version 13.0.3.0, Umeå, Sweden).

3. Results

3.1. Latitudinal BVOC emission profiles and influential environmental factors

The total average normalized emission rate of BVOC was $2.74 \pm 2.96 \mu\text{g}(\text{dw})^{-1} \text{h}^{-1}$ (mean \pm standard deviation), of which MT ($1.50 \pm 1.91 \mu\text{g}(\text{dw})^{-1} \text{h}^{-1}$) was the most commonly emitted BVOC group followed by isoprene ($0.94 \pm 1.84 \mu\text{g}(\text{dw})^{-1} \text{h}^{-1}$) and SQTs ($0.30 \pm 0.88 \mu\text{g}(\text{dw})^{-1} \text{h}^{-1}$). The average release of isoprene, MTs and SQTs between sites are in line with previous studies on Norway spruce (Table 2). The sites Taastrup, Skogaryd and Norunda had different emission rates in comparison to remaining study sites. Taastrup had a higher total MT emission, due to high emission rate contribution from needle branch measurements done in 2013. Skogaryd had a total emission which was a fifth of the average total emission rate from all measured sites. But it should be noted that the site was only visited in October, whilst the other sites had a

Table 2

The average normalized emission rate (in $\mu\text{g g(dw)}^{-1} \text{h}^{-1}$) of isoprene (ISO), monoterpenes (MT) and sesquiterpenes (SQT) from different sites, months and heights within the canopy. Emission rates are reported from this study and from other studies done on Norway spruce together with the empirical coefficient (β -value) used for MTs and SQTs (β -value for SQT in the parenthesis). For this study, the β empirical coefficient is based on a value given by Guenther et al. (1993). The emission rates are mean (standard deviation) and n.d. stands for no data available.

Site	Country (Latitude)	Month	Height (m)	ISO (\pm std)	MT (\pm std)	SQT (\pm std)	β -value for MT and SQT	Source
Ljubljana	SI (46°04')	Apr–May	1–2	0.31 (0.29)	1.17 (1.46)	0.50 (1.28)	0.09 (0.09)	This study
Grafrath	DE (48°18')	Jun	1–2	0.64 (0.92)	1.60 (1.24)	0.10 (0.29)	0.09 (0.09)	This study
Taastrup	DK (55°40')	Jul	1–2	0.51 (0.78)	1.96 (1.95)	0.33 (0.84)	0.09 (0.09)	This study
Taastrup	DK (55°40')	Jul	5.5	0.06 (0.23)	3.81 (3.83)	0.55 (1.18)	0.09 (0.09)	This study
Taastrup	DK (55°40')	Jul	12.5	0.10 (0.31)	4.35 (3.42)	0.09 (0.21)	0.09 (0.09)	This study
Hylte-mossa	SE (56°06')	Jul	1–2	0.43 (0.12)	1.25 (1.14)	0.34 (0.38)	0.09 (0.09)	This study
Skogaryd	SE (58°23')	Oct	2.5–3.5	0.11 (0.61)	0.29 (0.25)	n.d.	0.09 (0.09)	This study
Norunda	SE (60°05')	Jun	3	3.79 (3.48)	1.51 (1.19)	0.23 (0.20)	0.09 (0.09)	This study
Norunda	SE (60°05')	Jul	11	2.96 (2.65)	0.95 (0.41)	0.73 (0.38)	0.09 (0.09)	This study
Norunda	SE (60°05')	Jun–Jul	20	0.98 (1.25)	0.59 (0.36)	0.17 (0.22)	0.09 (0.09)	This study
Piikkiö	FI (60°23')	Jul	1–2	0.10 (0.08)	1.47 (1.52)	0.17 (0.19)	0.09 (0.09)	This study
Fichtel-gebirge	DE (50°08')	Jul–Aug	12	0.32/1.7 ^a	0.5	n.d.	0.1	Grabmer et al., 2006
Ulfborg	DK (56°16')	Aug	12	0.5	3	n.d.	0.03–0.16	Christensen et al., 2000
Järvelja	EE (58°16')	Sep–Oct	16	n.d.	0.48–0.6	0.09–0.13	0.08–0.12 (0.09–0.17)	Bourtsoukidis et al., 2014
Jadraås	SE (60°48')	May–Jul	2	n.d.	0.7–4.4	n.d.	0.07	Janson, 1993
Asa	SE (57°)	May–Jun	n.d.	0.38	0.27	n.d.	0.16	Janson and de Serves, 2001
Hyytiälä	FI (61°51')	Jan–Oct	n.d.	<0.1–1.2	0.1–1.4	<0.1–0.5	0.09	Hakola et al., 2003
Hyytiälä	FI (61°51')	Jul–Aug	2	n.d.	0.55–12	0–0.1	n.d.	Yassaa et al., 2012
Hyytiälä	FI (61°51')	Apr–Aug	2	0.06	<0.1	<0.08	0.01–0.19 (0.02–0.06)	Hakola et al., 2017

^a Emissions are standardized according to different algorithms.

majority of their measurements taken between May and August. Norunda had the highest emission of isoprene, mostly originating from the lower parts within the canopy (Table 2).

A total of 23 terpene compounds were detected from the measurement sites, which were isoprene, 17 MTs and five SQTs. The most emitted compounds from a majority of the sites were α - and β -pinene and limonene. Other compounds with high emission rates were camphene and 3-carene. Early spruce had in general a higher emission of α - and β -pinene whilst late spruce emitted more isoprene and limonene. For the sites Hyltemossa and Skogaryd, about a third of the emissions came from pinene, whilst Norunda had high emission rates of isoprene. Average isoprene emissions for Grafrath was $0.64 \mu\text{g g(dw)}^{-1} \text{h}^{-1}$ and for Norunda $2.58 \mu\text{g g(dw)}^{-1} \text{h}^{-1}$, which was significantly higher in comparison to the majority of the study sites ($P < 0.05$). MT emissions from Norunda were $1.02 \mu\text{g g(dw)}^{-1} \text{h}^{-1}$, which was significantly less in comparison to Grafrath ($1.60 \mu\text{g g(dw)}^{-1} \text{h}^{-1}$). Taastrup had an average MT emission of $2.63 \mu\text{g g(dw)}^{-1} \text{h}^{-1}$, which was higher compared to Ljubljana ($1.17 \mu\text{g g(dw)}^{-1} \text{h}^{-1}$) and Norunda. Average SQT emissions were significantly lower for Grafrath ($0.10 \mu\text{g g(dw)}^{-1} \text{h}^{-1}$) and Norunda ($0.38 \mu\text{g g(dw)}^{-1} \text{h}^{-1}$) in comparison to the other sites. In regards to separate compounds, Taastrup had high emission rates of pinene ($0.91 \mu\text{g g(dw)}^{-1} \text{h}^{-1}$) and low emission rates of camphene ($0.13 \mu\text{g g(dw)}^{-1} \text{h}^{-1}$), whilst Norunda differed in 3-carene emission due to low emission rates ($<0.01 \mu\text{g g(dw)}^{-1} \text{h}^{-1}$). Limonene emission varied most between sites (Fig. 2).

There were little changes in the emission patterns of specific compounds with changes in latitude. Within the IPG network, the contribution of limonene in relation to the total BVOC emission increased slightly with latitude; from 12% in Ljubljana to 23% in Piikkiö. The relative emission of pinene on the other hand ranged between 16 and 23% between samples and was fairly similar between the IPG sites. For the sites Hyltemossa, Skogaryd and Norunda, the relative percentage of limonene was lower, with 16% of the total emission at Hyltemossa and 7–8% for Skogaryd and Norunda. For total BVOC emission, α -pinene and β -pinene had a relative contribution of 30–32% for Hyltemossa and Skogaryd and 10% for Norunda. In the case of Norunda, isoprene contributed with 64% to the total emission. But if only MTs were considered, the relative

compound contribution of pinene would be in range of both Hyltemossa and Skogaryd. Fig. 3 shows the average emission profile of individual MTs for each of the sites.

As the emission rates and emission profiles varied between the study sites, a PLS was used to investigate if there was any specific climatic factor which had a higher tendency to affect the observed emission patterns. It should be noted that the aim of this PLS-analysis was to investigate the connection between the compound emissions (isoprene, MTs and SQTs) and the climatic conditions experienced on site, and not to build a good prediction model for each of the studied compounds. The PLS-analysis revealed that the samples were separated according to latitude and measurement height on the y-axis and temperature on the x-axis (Fig. 4a). Height and latitude were strongly correlated. In Fig. 4a, data from higher latitudes and canopy heights are positioned towards the bottom whilst lower latitudes and canopy heights are positioned at the upper part of the figure. On the x-axis of this figure, data points with higher temperatures are positioned to the right whilst lower temperatures are positioned to the left. The number of active growing days (season) was not as strong driver as temperature on the x-axis, but is part in separating sites with measurements taken in October (Ljubljana and Skogaryd in 2015) from the sites where measurements were done in the middle of the summer (Fig. 4a). The PLS-analysis also revealed that the individual compounds are poorly explained by the model (Fig. 4b); the included climatic factors explained 7.8% of the total emission variation (Fig. 4).

3.2. The influence of genetics on observed BVOC emission patterns

The sites within the IPG network were used to study how the BVOC emissions from Norway spruce might have adapted to local growing conditions without considering genetic variation. Grafrath was significantly different ($P < 0.05$) from the other sites in regards to its isoprene emissions. The average emission from Grafrath ($0.64 \mu\text{g g(dw)}^{-1} \text{h}^{-1}$) was two to four times higher in comparison to all remaining sites and provenances, except for late spruce in Taastrup ($0.50 \mu\text{g g(dw)}^{-1} \text{h}^{-1}$). The isoprene emission rate from early spruce at Taastrup ($0.22 \mu\text{g g(dw)}^{-1} \text{h}^{-1}$) was low and significantly different from Ljubljana ($0.32 \mu\text{g g(dw)}^{-1} \text{h}^{-1}$) and

a) Isoprene						b) Monoterpenes						c) Sesquiterpenes								
Site	N	P	H	T	G	L	Site	N	P	H	T	G	L	Site	N	P	H	T	G	L
L						X	L						X	L						X
G							L							L						
T							L							L						
H							L							L						
P							L							L						
N	X						L							L						
d) Pinene						e) Limonene						f) Camphene								
Site	N	P	H	T	G	L	Site	N	P	H	T	G	L	Site	N	P	H	T	G	L
L						X	L						X	L						X
G							L							L						
T							L							L						
H							L							L						
P							L							L						
N	X						L							L						
g) 3-carene																				
Site	N	P	H	T	G	L														
L						X														
G																				
T																				
H																				
P																				
N	X																			

Fig. 2. Statistically significant differences between measurement sites Ljubljana (L), Grafath (G), Taastrup (T), Piikkiö (P), Hyltemossa (H) and Norunda (N). Statistics were done on the summarized emission of isoprene (a), monoterpenes (b), sesquiterpenes (c), pinenes (d), limonene (e), camphene (f) and 3-carene (g) across measurement sites. A grey box indicates a statistical difference ($P < 0.05$) between the two sites for a particular BVOC group or compound. All measurements performed in April and October were excluded from the dataset, which means that the site Skogaryd was not included in the statistical analysis. Statistical analysis was performed by doing a Kruskal-Wallis test and when it was statistically significant it was followed by Mann-Whitney U test with Bonferroni correction.

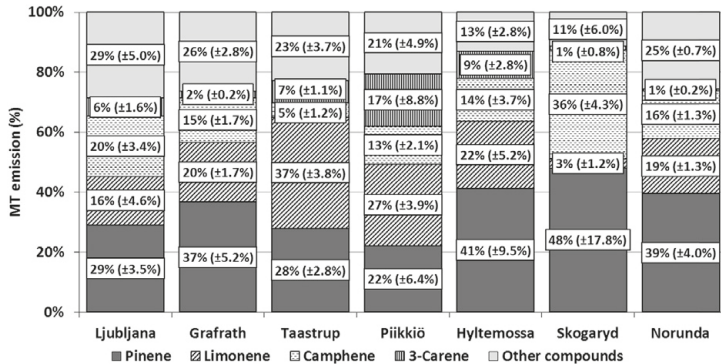


Fig. 3. Individual MT compound contribution to the total emission of MTs (mean \pm SE) from the measurement sites Ljubljana (Slovenia), Grafath (Germany), Taastrup (Denmark), Piikkiö (Finland), Hyltemossa (Sweden), Skogaryd (Sweden) and Norunda (Sweden). Other compounds include tricyclene, α -thujene, sabinene, α -phellandrene, α -terpinene, β -phellandrene, eucalyptol, ocimene, γ -terpinene, terpinolene and linalool.

Grafath. Total MT emission from early spruce in Grafath ($1.88 \mu\text{g g(dw)}^{-1} \text{h}^{-1}$) and late spruce in Taastrup ($2.95 \mu\text{g g(dw)}^{-1} \text{h}^{-1}$) were significantly different from Ljubljana ($1.17 \mu\text{g g(dw)}^{-1} \text{h}^{-1}$) and late spruce in Piikkiö ($0.70 \mu\text{g g(dw)}^{-1} \text{h}^{-1}$) due to higher average MT rates (Fig. 5). There were no significant differences in SQT emissions. In regards to separate compounds, late spruce in Taastrup had higher emission rates of α -pinene ($1.44 \mu\text{g g(dw)}^{-1} \text{h}^{-1}$) and lower emission rates of limonene ($0.82 \mu\text{g g(dw)}^{-1} \text{h}^{-1}$) in comparison to many of the other sites (Fig. 5). There were no significant emission differences between sites for camphene and 3-carene.

The importance of genetics and latitudinal adaptation was further investigated by comparing the emission pattern variation between genetically identical trees and genetically different trees

over similar latitudinal ranges. The sites Taastrup and Piikkiö were chosen for comparing genetically identical sites and the sites Hyltemossa and Norunda for the genetically different sites. These four sites were chosen as the latitudinal differences between sites are relatively similar, with approximately one latitude degree difference between the two sites compared. For Norunda, the emission rate from 20 m up in the canopy was used for the comparison.

For early and late spruce in Taastrup ($n = 25$) and Piikkiö ($n = 19$), there were significant differences ($P < 0.05$) in the emission of isoprene, 3-carene, limonene, other compounds, total MT emission and the total BVOC emission. However, if only late spruce was considered ($n = 19$ for Taastrup and $n = 10$ for Piikkiö), then there were no statistical differences ($P > 0.05$). This comparison could not be done for early spruce as there was only one tree

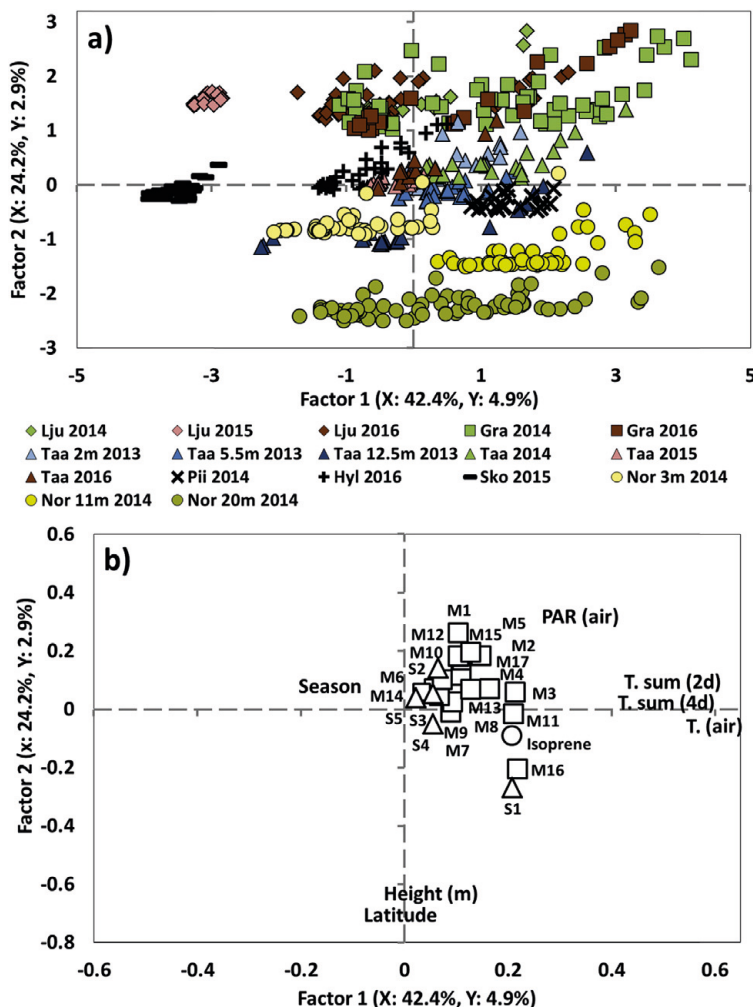


Fig. 4. Partial least squares regression (PLS) on the biogenic volatile organic compound emissions (circle in the loading plot (b) = isoprene; squares = monoterpenes (M); triangles = sesquiterpenes (S) from the different latitudinal sites, height within the canopy and measurement years. The scores of the factors (a) are shown together with the loading variables (b). The variance explained of the independent data (X) and dependent data (Y) are shown within the parenthesis. The independent variables shown in the loading plot (b) were ambient temperature ($^{\circ}\text{C}$), average temperature over the past two and four days ($^{\circ}\text{C}$), daily ambient Photosynthetically Active Radiation (PAR), height within the canopy (m), latitude and season. Season was defined as the number of active growing days where the average daily temperature had exceeded 5°C for five consecutive days. Dependent variables were the compounds isoprene (ISO), tricyclene (M1), α -thujene (M2), α -pinene (M3), camphene (M4), sabinene (M5), β -pinene (M6), myrcene (M7), α -phellandrene (M8), 3-carene (M9), α -terpinene (M10), limonene (M11), β -phellandrene (M12), eucalyptol (M13), ocimene (M14), γ -terpinene (M15), terpinolene (M16), linalool (M17), caryophyllene (S1), β -farnesene (S2), α -farnesene (S3), α -humulene (S4) and *cis*- α -bisabolene (S5).

available in Taastrup and too few measurements from Piikkiö. For the sites Hyltemossa ($n = 27$) and Norunda ($n = 72$), there were significant differences ($P < 0.05$) in the emissions of isoprene, 3-carene, other compounds and total emission of MTs. When the genetically identical trees from Taastrup and Piikkiö were

compared with the emissions from Hyltemossa and Norunda, all compounds except for the total BVOC emission were significantly different, with an average emission rate of 2.76 ± 1.88 and $1.73 \pm 1.55 \mu\text{g g(dw)}^{-1} \text{h}^{-1}$ for Taastrup and Piikkiö and 1.76 ± 1.36 and $1.75 \pm 1.59 \mu\text{g g(dw)}^{-1} \text{h}^{-1}$ for the Hyltemossa and Norunda.

Isoprene										Monoterpenes									
Site	SLP	SEP	SLT	SET	SLG	SEG	SLL	SEL		Site	SLP	SEP	SLT	SET	SLG	SEG	SLL	SEL	
SEL								X		SEL									X
SLL							X			SLL							X		
SEG						X				SEG						X			
SLG					X					SLG					X				
SET				X						SET				X					
SLT			X							SLT			X						
SEP		X								SEP		X							
SLP	X									SLP	X								

α -pinene										Limonene									
Site	SLP	SEP	SLT	SET	SLG	SEG	SLL	SEL		Site	SLP	SEP	SLT	SET	SLG	SEG	SLL	SEL	
SEL								X		SEL									X
SLL							X			SLL							X		
SEG						X				SEG						X			
SLG					X					SLG					X				
SET				X						SET				X					
SLT			X							SLT			X						
SEP		X								SEP		X							
SLP	X									SLP	X								

Fig. 5. Statistically significant differences between measurement sites Ljubljana (L), Grafarth (G), Taastrup (T) and Piikkiö (P) and between provenances of early spruce (SE), with an early budburst, and late spruce (SL) with a budburst approximately one week later. A grey box indicates a statistical difference ($P < 0.05$) between the two sites for a particular BVOC group or compound. All measurements performed in April and October were excluded from the dataset. Statistical analysis was performed by doing a Kruskal-Wallis test and when this was statistically significant it was followed by Mann-Whitney U test with Bonferroni correction.

3.3. The impact of height

At Taastrup (2013) and Norunda (2014), samples were taken at different heights within the canopy in order to investigate possible emission pattern variations. Focus has been on the emissions of isoprene, MT, SQT and dominant MT compounds (α -pinene, β -pinene, camphene, 3-carene and limonene) from different canopy heights (Table 3). For early spruce in Taastrup, there was a significant difference ($P < 0.05$) for limonene emission, between canopy level of 2.0 m ($2.47 \mu\text{g g(dw)}^{-1} \text{h}^{-1}$) in comparison to 5.5 m ($1.38 \mu\text{g g(dw)}^{-1} \text{h}^{-1}$). Camphene emissions were higher at 2.0 m ($0.07 \mu\text{g g(dw)}^{-1} \text{h}^{-1}$) in comparison to 12.5 m ($0.02 \mu\text{g g(dw)}^{-1} \text{h}^{-1}$). The remaining compounds showed no statistical difference ($P > 0.05$) between canopy heights. For late spruce in Taastrup, camphene emission was significantly lower at 2.0 m ($0.01 \mu\text{g g(dw)}^{-1} \text{h}^{-1}$) than at 12.5 m ($0.1 \mu\text{g g(dw)}^{-1} \text{h}^{-1}$), whilst limonene emission was lower at 2.0 m ($0.57 \mu\text{g g(dw)}^{-1} \text{h}^{-1}$) than at 12.5 m ($2.32 \mu\text{g g(dw)}^{-1} \text{h}^{-1}$) and at 5.0 m ($0.69 \mu\text{g g(dw)}^{-1} \text{h}^{-1}$) than at 12.5 m. For Norunda, all BVOC emissions between 3.0 m and 20.0 m height within the canopy were significantly different. The emissions of isoprene ($3.79 \mu\text{g g(dw)}^{-1} \text{h}^{-1}$) and MT ($1.51 \mu\text{g g(dw)}^{-1} \text{h}^{-1}$) at 3.0 m height were higher in comparison to the emissions at 20.0 m above the ground (isoprene $0.98 \mu\text{g g(dw)}^{-1} \text{h}^{-1}$ and MT $0.60 \mu\text{g g(dw)}^{-1} \text{h}^{-1}$). The total MT emission was not significantly different for canopy levels of 11.0 m and 20.0 m, but there was a significant difference for the compounds β -pinene ($0.1 \mu\text{g g(dw)}^{-1} \text{h}^{-1}$ for 11.0 m and $<0.01 \mu\text{g g(dw)}^{-1} \text{h}^{-1}$ for 20.0 m) and 3-carene. It should be noted though that no 3-carene emission was on 11.0 m due to a high 3-carene concentration in the blank samples (Table 3).

3.4. Indications of annual and seasonal emission pattern fluctuation

Within the IPG network, Ljubljana and Grafarth were visited in 2014 and 2016 at approximately the same time within the growing season. Comparisons between years were done on the main BVOC groups and the emission rates were not significantly different

($P > 0.05$) between measurement years. Taastrup was visited between June and August in 2013–2016. Isoprene emission was significantly different for both 2013 ($0.19 \mu\text{g g(dw)}^{-1} \text{h}^{-1}$) and 2015 ($1.12 \mu\text{g g(dw)}^{-1} \text{h}^{-1}$) in comparison to remaining measurement years ($P < 0.05$). In 2013, the emission of isoprene was low in comparison to the remaining measurement years, whilst 2015 had a higher emission rate. MT emission was significantly different in 2013 ($4.17 \mu\text{g g(dw)}^{-1} \text{h}^{-1}$) and between 2014 ($1.57 \mu\text{g g(dw)}^{-1} \text{h}^{-1}$) and 2015 ($0.69 \mu\text{g g(dw)}^{-1} \text{h}^{-1}$) ($P < 0.05$). Both provenances of spruce had MT emission rate three to four times as high in 2013 as the average emission rate in the other years. There were also differences in MT emission rates between 2014 and 2015, where the average emissions in 2014 were higher in comparison to the emission rates in 2015 (Fig. 6).

In regards to seasonal development, most of the BVOC measurements were taken between May and August, but for Ljubljana (2015) and Skogaryd, measurements were performed in October. The average standardized emission rates in October were approximately a third to a sixth of the total average standardized emission rates measured between May and July (Table 1; Fig. 6). For Ljubljana, where the emission profile in October and May were compared, early spruce had a higher contribution to the total emission of camphene (43.1%) and limonene (23.72%) in October, whilst in May there was a higher contribution of isoprene (17.64%) and SQTs (23.6%). Late spruce had a higher emission of isoprene (43.06%) and SQT (36.02%) in October and a higher contribution to the total emission of pinenes (20.48%) and other compounds (24.83%, which for Ljubljana were tricyclene, terpenines, eucalyptol and linalool) in May. Both provenances showed a decrease in the total emission contribution of other compounds, but without a decrease in the number of emitted compounds (data not shown).

4. Discussion

4.1. Separating latitudinal adaptation from genetic diversity

Norway spruce and Scots pine are important BVOC emission contributors in European boreal ecosystems (Rinne et al., 2009). In

Table 3

The p-values of Mann-Whitney *U* test for the standardized emission rate (in $\mu\text{g g(dw)}^{-1} \text{h}^{-1}$) of isoprene (ISO), monoterpenes (MT) and sesquiterpenes (SQT) and dominant MT compounds from different canopy heights in Taastrup (2.0 m, 5.5 m and 12.5 m) and Norunda (3.0 m, 11.0 m, 20.0 m). SE stands for early spruce and SL for late spruce. The hyphen marks compounds where there was a lack of data on one of the measurement heights. Statistics were not performed between height levels of 3.0 m and 11.0 m at the Norunda site due to a difference in measurement months between mentioned height levels.

Terpene	Taastrup (SE)			Taastrup (SL)			Norunda	
	2.0 m–5.5 m	2.0 m–12.5 m	5.5 m–12.5 m	2.0 m–5.5 m	2.0 m–12.5 m	5.5 m–12.5 m	3.0 m–20 m	11.0 m–20.0 m
ISO	0.66	0.35	0.21	0.82	0.83	0.83	<0.01	0.35
MT	0.13	0.24	0.98	0.65	0.07	0.05	<0.01	0.79
SQT	0.24	0.97	0.19	1.00	1.00	1.00	<0.01	<0.01
α -Pinene	0.10	0.19	0.93	1.00	0.35	0.44	<0.01	0.46
β -Pinene	0.40	0.35	0.94	1.00	0.77	0.77	<0.01	<0.01
Camphene	0.07	<0.01	0.28	0.86	0.02	0.05	<0.01	0.07
3-Carene	0.66	0.61	0.90	0.42	0.48	0.35	<0.01	–
Limonene	0.03	0.19	0.88	0.10	<0.01	<0.01	<0.01	0.64

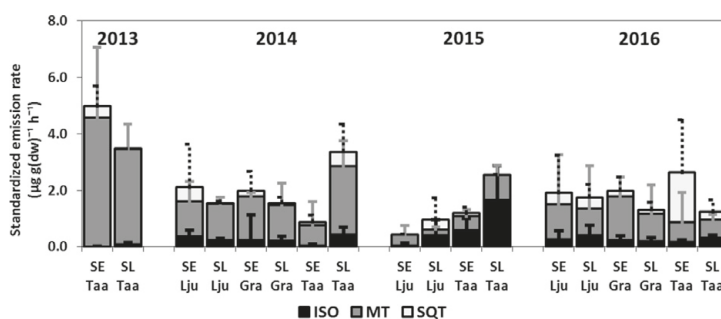


Fig. 6. The average standardized emission rates (in $\mu\text{g g(dw)}^{-1} \text{h}^{-1}$) of isoprene (ISO), monoterpenes (MT) and sesquiterpenes (SQT) from Ljubljana (Lju), Grafath (Gra) and Taastrup (Taa) for provenances and years. SE stands for early spruce and SL for late spruce, where early spruce has a budburst pattern approximately one week earlier than late spruce. The error bars shows the standard deviation for each BVOC group.

comparison to Scots pine, less emission studies have been undertaken on Norway spruce despite it being one of the most common coniferous tree species growing in Europe (Rinne et al., 2009; Yassaa et al., 2012). This study presents the average standardized emission rates of Norway spruce within the European boreal zone, but also over a larger latitudinal range across Europe. The emission rates across the sites were in range of other earlier studies (Janson, 1993; Christensen et al., 2000; Janson and de Servis, 2001; Hakola et al., 2003; Grabmer et al., 2006; Yassaa et al., 2012; Bourtsoukidis et al., 2014; Hakola et al., 2017) and there was minimal emission rate difference between the southernmost site and the northernmost site. Taastrup, Skogaryd and Norunda were sites which differed most from the other sites in regards to their emission patterns. Even though these sites are located in the northern range of this study, the observed emission rate differences are not necessarily due to their geographical location. The total MT emission rate at Taastrup in 2013 was higher and significantly different from the emission rates at the other sites. The measurement years between 2014 and 2016 were in range of the other visited sites. BVOC emission at Skogaryd was only measured in October and had lower emission rates in comparison to sites measured during the growing season. Norunda had the highest average isoprene emission, with high emission rates at 3.0 m and 11.0 m in the canopy. This is most likely due to a strong emission response during high irradiation events in different parts of the canopy.

Apart from limonene, the emission rates of other compounds in the southernmost sites Ljubljana and Grafath were not significantly different from each other. The spruce tree in Norunda

differed most from the trees in the remaining sites, both in regards to BVOC emission groups and for separate compounds. One reason could be that the tree in Norunda was standing in a much denser forest in comparison to the other sites, leading to a possible difference in shade acclimation.

Both local climate and genetic diversity have been shown to impact observed emission pattern fluctuations (Komenda and Koppmann, 2002; Semiz et al., 2007; Niinemets et al., 2010; Bäck et al., 2012; Steinbrecher et al., 2013), but it can be difficult to separate latitudinal adaptations and genetics apart. By using the IPG network, it was possible to further investigate the impact of possible adaptations to local growing conditions from two provenances of spruce without considering genetic diversity. The two provenances of Norway spruce were slightly different in regards to their emission profiles. Whilst early spruce had a higher relative emission of α - and β -pinene, late spruce emitted more isoprene and limonene. Apart from limonene emission, which increased slightly with increasing latitude, there were no distinct emission pattern changes within the same provenance and between IPG sites. This relative compound similarity across latitudes would suggest that the genetic material of the tree determines the emission profile of the compounds and that adaptation to local growing conditions do not happen instantly, but may have developed over generations.

The importance of genetic diversity was further investigated by comparing the BVOC emissions of genetically identical trees from Taastrup and Piikkio with genetically different trees in Hyltemossa and Norunda. When all sites were compared, there was a statistical difference for all compounds and sites except for the total amount

of BVOC emissions. But when the same comparison was performed on genetically identical trees, there were significant differences for all compounds and sites. These results highlight that the sites show less of a difference in emission patterns with a change in latitude, most likely due to acclimation to local weather and growing conditions. The non-significant difference between sites and genetically identical trees further suggest that adaptation to local environment do not happen instantly, but may take place over a longer time. In order to confirm this possible similarity of the relative emission profile, similar emission comparisons with more sites and over a longer latitudinal range are suggested.

The potential similarity in the total emission rates across a latitudinal gradient and relative emission profile might be of use in atmospheric emission models. In general for many emission models, the emission potentials are calculated for isoprene, the sum of all MTs and the sum of all SQTs as they represent a significant emission proportion from trees (Arneeth et al., 2010; Niinemets et al., 2010). The results presented here provide average standardized emission rates of these three compound groups from spruce over a vast latitudinal range. However, for models which focus on atmospheric chemistry, it is important to also consider the emission profile, as the reactivity of compounds varies by several orders of magnitude due to their molecular structure (Atkinson and Arey, 2003; Niinemets et al., 2010). As the composition might vary due to short-term environmental impacts and genetic diversity between trees, it is difficult to give specific emission ranges of different compounds. However, the observed similarity of emission rates between IPC network sites, which also have had the possibility to acclimate to the local growing conditions, show that the composition seen at different sites can be considered to remain fairly stable with the progression of time.

4.2. Observed BVOC emission patterns in relation to height, season and year

Apart from the studied effects of latitudinal adaptation and genetic diversity on observed emission pattern fluctuations, the effect of measurement height within the canopy, change with season and yearly differences have also been investigated.

In Taastrup and Norunda, emissions were measured at three levels within the canopy. Whilst Taastrup only showed emission pattern differences between levels for a few compounds, Norunda showed statistically significant differences both for compound groups and separate compounds for all measured canopy heights. A possible explanation for the dissimilarity in emission response could be the amount of shade adaptation at different heights and sites. Persson et al. (2016) explained that the insignificant emission difference between canopy heights in Taastrup could be caused by the wide spacing between trees in the phenological garden. This results in relatively high levels of irradiation at lower canopy levels, which minimizes the difference in light adaptation between needle branches from the upper and lower parts of the canopy. In Norunda, the trees were planted with less space in between trees and therefore have quite distinct differences in available light at different canopy levels. Furthermore, the shape and the color of the needles in Norunda were different between canopy heights, with thicker, greener and a higher percentage of newly produced shoots at the upper canopy in comparison to lower levels.

The emission pattern change in regards to time of season has shown to have a substantial effect on observed emission rates (Janson, 1993; Hakola et al., 2003, 2012, 2017; Tarvainen et al., 2005). Seasonality has also shown to influence not only the emission amounts, but also changing the compounds' emission profile (Janson, 1993; Hakola et al., 2003). The majority of the measurements in this study were performed between May and August,

which is in the middle of the growing season. But in Ljubljana and Skogaryd in 2015, measurements were performed in October which is outside the main growing season. In comparison to both the emission differences between campaigns within Ljubljana and between the remaining sites, the emission rates in October were less than one third of the emissions reported during the middle of the growing season. The trees in Ljubljana also showed a change in emission profile for both provenances of spruce and season. Early spruce changed from high emissions of isoprene and SQT in May to emitting a higher relative contribution of camphene and limonene in October. Late spruce had high relative compound contribution of pinenes and other compounds in May and emitted more isoprene and SQT in October. However, even though the emission profile changed with the progression of the season, the number of compounds emitted did not change considerably. Skogaryd has only been measured in October and as it is unknown what the emission capacities are during summer season, which makes comparisons of emission profile with other sites unrealistic. However, the differences in emission patterns with remaining sites points to a potential influence of season which would be recommended to study further.

Apart from a seasonal change in BVOC emission patterns, there might also be differences between measurement years (Hakola et al., 2017). Hakola et al. (2012) compared the emissions from a boreal forest in Hyttälä between seasons and years. They found that apart from summer, when the emission differences were rather small, the emission profile could differ between measurement years. A similarity between summer season emissions was also indicated in this study for Ljubljana and Grafath, which showed no significant difference between measurement years. But as only two summer seasons were compared, the emission similarities during the summer period in general cannot be quantified. For Taastrup, measurements were conducted for four years in a row at approximately the same time in July. For the total emission rates, the emissions were on average higher in 2013 compared to the other years. For the summer season of 2013, Persson et al. (2016) reported a distinct period without rainfall which might have caused drought stress to the spruce trees. Even though the volumetric water content of the soil was not measured, other indications such as dry needles shedding from lower branches whilst being handled suggested that the trees were in some state of water shortage. In a study by Lappalainen et al. (2009) in a coniferous forest, MT concentrations started to decline soon after a summer drought. This drop in emissions might be connected to senescence or needle shedding. The emission rates also differed between measurement years. In 2013, the emission of isoprene was significantly lower in comparison to other measurement years, whilst MTs were higher. 2015 was also a year which differed from remaining measurement years, with high isoprene emissions and lower MT emissions. In relation to other measurement years, 2015 was almost 2 °C colder than average for July (data not shown) and this may have had an influence on the observed emission patterns. Even though the reasons for variable emission patterns only can be speculated in this case, there are indications that past weather events might have had an influence on the emission pattern variations between years.

4.3. Uncertainties related to BVOC measurements from chosen sites and the latitudinal gradient

Several sites which are part of different measurement campaigns were studied in order to get a better representation of the possible growing range of Norway spruce. The inclusion of different measurement campaigns made it possible to investigate different influential aspects of the emission variation, such as genetic

diversity, latitudinal adaptations, potential emission differences between summer and autumn, height within the canopy and between measurement years. But as the different measurement campaigns were not originally set to cover all of the above mentioned aspects, the amount of data collected is not sufficient to quantify their separate importance on observed BVOC emissions. Furthermore, the inclusion of different chamber measurement techniques between studies adds further uncertainty to emission variations between sites. The needle chambers used together with LI-6400 has a disadvantage that the plant needs to be handled for each sample, which might increase the risk of mechanical stress induced emissions. The disadvantage of the transparent branch chambers is that the climatic conditions inside the chamber are more difficult to control, which might have indirectly provided with more stress to the branch inside the chamber due to different climatic conditions.

Apart from the influence of genetic diversity, adaptations to different growing conditions, height, season and measurement year on observed BVOC emissions, the emissions have also been influenced by other factors which have not been thoroughly studied in this setup. In the performed PLS analysis, only 7.8% of the emissions could be explained by temperature, PAR, height, latitude and time of season. Factors which were not included in the analysis but which have shown visible effects on the emission rates are drought, heat, herbivore attack and mechanical damage of the needle twigs or branches. Therefore, more studies investigating how the emission patterns in situ are influenced by these short-term effects would be needed.

In order to compare the emission rates between sites, all measurements were normalized according to the algorithms presented by Guenther et al. (1993). For the normalization of monoterpenes and sesquiterpenes, a β -value of 0.09 was used. But it has been shown by Duhl et al. (2008) that the β -value could be different between SQTs and MTs when the standardized emissions are calculated. Previous results have indicated that β for SQTs could be in the range 0.05–0.29 (Duhl et al., 2008). However, since many factors need to be taken into account when choosing an appropriate β -value, such as plant species, season and specific compounds, it is hard to decide which value should be used. For the studies reported in Table 2, the β -value for MTs is between 0.01 and 0.19 and for SQTs 0.02–0.17. As the main purpose of this study was to compare the emission pattern variability for spruce influenced by latitude, genetics and height, the same value for both MTs and SQTs was chosen to simplify the analysis.

5. Conclusions

Norway spruce is an important coniferous source of BVOCs which can be found over a large range in Europe. This study measured the emission rates of genetically identical and genetically different Norway spruce trees at seven European sites. The results showed that the standardized emission rates from different sites within Europe did not vary considerably with a change in latitude. The emission profile differed between provenances and sites, but the emission profile difference was less distinct for genetically identical trees. The study suggests that the spruce isoprenoid emission is potentially more determined by genetic diversity than by adaptation to local growth conditions. This possible stability in isoprenoid emissions could be used to improve the parameterization in different emission models.

It was also indicated that the observed emission rates were influenced by canopy height, time of season and measurement years. But due to different experimental setups between measurement campaigns, it is not possible to quantify the effect of the separate factors. More comprehensive measurements involving the

effect of canopy height, season and measurement years would be needed in order to better understand the emission pattern fluctuations.

Acknowledgements

The authors would like to acknowledge Michelle Schollert Reneerkens and Gosha Sylvestre at the University of Copenhagen and Hannele Hakola and Heidi Hellén at the Finnish Meteorological Institute for performing the BVOC sample analysis. We thank David Allbrand and Sven-Olof Andersson for their contribution with the field work in Skogaryd and Anders Båth and Irene Lehner for their help with the field work in Norunda. We would also like to thank Per-Erik Isberg at the department of Statistics in Lund for his advice in statistics. All campaigns were funded by FORMAS (2012–727), VR (2011–3190) and BECC.

References

- Acosta Navarro, J.C., Smolander, S., Struthers, H., Zorita, E., Ekman, A.M.L., Kaplan, J.O., Guenther, A., Arneth, A., Ripplien, I., 2014. Global emissions of terpenoid VOCs from terrestrial vegetation in the last millennium. *J. Geophys. Res. Atmos.* 119, 6867–6885. <https://doi.org/10.1002/2013JD021238>.
- Alexander, H., Eggertsson Karlström, C., 2001. *Temperaturer och nederbörden i Sverige 1961–90: Referensnormaler—utgåva 2. Meteorologi 99. Swedish Meteorological and Hydrological Institute, Norrköping (in Swedish)*.
- Arneth, A., Stith, S., Bondeau, A., Butterbach-Bahl, K., Foster, P., Gedney, N., de Noblet-Ducoudré, N., Prentice, I.C., Sanderson, M., Thonicke, K., Wania, R., Zaehe, S., 2010. From biota to chemistry and climate: towards a comprehensive description of trace gas exchange between the biosphere and atmosphere. *Biogeosciences* 7, 121–149. <https://doi.org/10.5194/bg-7-121-2010>.
- Atkinson, R., 2000. Atmospheric chemistry of VOCs and NOx. *Atmos. Environ.* 34, 2063–2101. [https://doi.org/10.1016/S1352-2310\(99\)00460-4](https://doi.org/10.1016/S1352-2310(99)00460-4).
- Atkinson, R., Arey, J., 2003. Gas-phase tropospheric chemistry of biogenic volatile organic compounds: a review. *Atmos. Environ.* 37, 197–219. [https://doi.org/10.1016/S1352-2310\(03\)00391-1](https://doi.org/10.1016/S1352-2310(03)00391-1).
- Aubinet, M., Feigenwinter, C., Heinesch, B., Bernhofer, C., Canepa, E., Lindroth, A., Montagnani, L., Rebmann, C., Sedlak, P., Van Gorsel, E., 2010. Direct advection measurements do not help to solve the night-time CO2 closure problem: evidence from three different forests. *Agric. For. Meteorol.* 150, 655–664.
- Beerling, D.J., Nicholas, H.C., Pyle, J.A., Raven, J.A., 2007. Critical issues in trace gas biogeochemistry and global change. *Phil. Trans. R. Soc. A* 365, 1629–1642. <https://doi.org/10.1098/rsta.2007.2037>.
- Bonn, B., Boy, M., Kulmala, M., Groth, A., Trawny, K., Borchert, S., Jacoby, S., 2009. A new parameterization for ambient particle formation over coniferous forests and its potential implications for the future. *Atmos. Chem. Phys.* 9, 8079–8090. <https://doi.org/10.5194/acp-9-8079-2009>.
- Bourtsoukidis, E., Bonn, B., Dittmann, A., Hakola, H., Hellén, H., Jacoby, S., 2012. Ozone stress as a driving force of sesquiterpene emissions: a suggested parameterisation. *Biogeosciences* 9, 4337–4352. <https://doi.org/10.5194/bg-9-4337-2012>.
- Bourtsoukidis, E., Bonn, B., Noe, S.M., 2014. On-line field measurements of BVOC emissions from Norway spruce (*Picea abies*) at the hemiboreal SMEAR-Estonia site under autumn conditions. *Boreal Environ. Res.* 19, 153–167.
- Bäck, J., Aalto, J., Henriksson, M., Hakola, H., He, Q., Boy, M., 2012. Chemodiversity of a Scots pine stand and implications for terpene air concentrations. *Biogeosciences* 9, 689–702. <https://doi.org/10.5194/bg-9-689-2012>.
- Chameides, W.L., Lindsay, R.W., Richardson, J., 1988. The role of biogenic hydrocarbons in urban photochemical smog: Atlanta as a case study. *Science* 241, 1473–1475.
- Chmielewski, F.-M., Heider, S., Moryson, S., 2013. International phenological observation networks: concept of IPG and GPM. In: Schwartz, M.D. (Ed.), *Phenology: an Integrative Environmental Science*. Springer Science + Business Media B.V., pp. 137–153. https://doi.org/10.1007/978-94-007-6925-0_8.
- Christensen, C.S., Hummelshøj, P., Jensen, N.O., Larsen, B., Lohse, C., Pilegaard, K., Skov, H., 2000. Determination of the terpene flux from orange species and Norway spruce by relaxed eddy accumulation. *Atmos. Environ.* 34, 3057–3067.
- Claeys, M., Graham, B., Vas, G., Wang, W., Vermeylen, R., Pashynska, V., Cafmeyer, J., Guyon, P., Andreae, M.O., Artaxo, P., Maenhaut, W., 2004. Formation of secondary organic aerosols through photooxidation of isoprene. *Science* 303, 1173–1176. <https://doi.org/10.1126/science.1092805>.
- Di Carlo, P., Brune, W.H., Martinez, M., Harder, H., Leshner, R., Ren, X., Thornberry, T., Carroll, M.A., Young, V., Shepson, P.B., Riemer, D., Apel, E., Campbell, C., 2004. Missing OH reactivity in a forest: evidence for unknown reactive biogenic VOCs. *Science* 304, 722–725. <https://doi.org/10.1126/science.1094392>.
- Duhl, T.R., Helmig, D., Guenther, A., 2008. Sesquiterpene emissions from vegetation: a review. *Biogeosciences* 5, 761–777. <https://doi.org/10.5194/bg-5-761-2008>.
- Dudareva, N., Pichersky, E., 2008. Metabolic engineering of plant volatiles. *Curr. Opin. Biotechnol.* 19, 1–9. <https://doi.org/10.1016/j.copbio.2008.02.011>.

- Ehn, M., Thornton, J.A., Kleist, E., Sipilä, M., Junninen, H., Pullinen, I., Springer, M., Rubach, F., Tillmann, R., Lee, B., Lopez-Hilfiker, F., Andres, S., Acir, I.-H., Rissanen, M., Jokinen, T., Schobesberger, S., Kangasluoma, J., Kontkanen, J., Nieminen, T., Kurtén, T., Nielsen, L.B., Jørgensen, S., Kjaergaard, H.G., Canagaratna, M., Maso, M.D., Berndt, T., Petäjä, T., Wahner, A., Kerminen, V.-M., Kulmala, M., Worsnop, D.R., Wildt, J., Mentel, T.F., 2014. A large source of low-volatility secondary organic aerosol. *Nature* 506, 476–479. <https://doi.org/10.1038/nature13032>.
- FAO, 2001. Global Forest Resources Assessment 2000. FAO Forestry paper 140.
- Filella, I., Wilkinson, M.J., Llusia, J., Hewitt, C.N., Peñuelas, J., 2007. Volatile organic compounds emissions in Norway spruce (*Picea abies*) in response to temperature changes. *Physiol. Plant.* 130, 58–66. <https://doi.org/10.1111/j.1399-3054.2007.00881.x>.
- Ghirardo, A., Koch, K., Taipale, R., Zimmer, L., Schnitzler, J.-P., Rinne, J., 2010. Determination of *de novo* and pool emissions of terpenes from four common boreal/alpine trees by ¹³C₂ labelling and PTR-MS analysis. *Plant, Cell Environ.* 33, 781–792. <https://doi.org/10.1111/j.1365-3040.2009.02104.x>.
- Grabner, W., Kreuzwieser, J., Wisthaler, A., Fojcar, C., Graus, M., Rennenberg, H., Steigner, D., Steinbrecher, R., Hansel, A., 2006. VOC emissions from Norway spruce (*Picea abies* L. [Karst]) twigs in the field—results of a dynamic enclosure study. *Atmos. Environ.* 40, 128–137. <https://doi.org/10.1016/j.atmosenv.2006.03.043>.
- Grote, R., Monson, R.K., Niinemets, Ü., 2013. Leaf-level models of constitutive and stress-driven volatile organic compound emissions. In: Niinemets, Ü., Monson, R.K. (Eds.), *Biology, Controls and Models of Tree Volatile Organic Compound Emissions*. Springer Dordrecht, pp. 315–355.
- Guenther, A.B., Zimmerman, P.R., Harley, P.C., Monson, R.K., Fall, R., 1993. Isoprene and monoterpene emission rate variability: model evaluations and sensitivity analyses. *J. Geophys. Res.* 98, 12609–12617. <https://doi.org/10.1029/93JD00527>.
- Guenther, A., Hewitt, C.N., Erickson, D., Fall, R., Geron, C., Graedel, T., Harley, P., Klinger, L., Lerdau, M., McKay, W.A., Pierce, T., Scholes, B., Steinbrecher, R., Tallamraju, R., Taylor, J., Zimmerman, P., 1995. A global model of natural volatile organic compound emissions. *J. Geophys. Res.* 100, 8873–8892.
- Guenther, A., Karl, T., Harley, P., Wiedinmyer, C., Palmer, P.I., Geron, C., 2006. Estimates of global terrestrial isoprene emissions using MEGAN (model of emissions of gases and aerosols from nature). *Atmos. Chem. Phys.* 6, 3181–3210. <https://doi.org/10.5194/acp-6-3181-2006>.
- Guenther, A.B., Jiang, X., Heald, C.L., Sakulyanontvittaya, T., Duhl, T., Emmons, L.K., Wang, X., 2012. The model of emissions of gases and aerosols from nature version 2.1 (MEGAN2.1): an extended and updated framework for modeling biogenic emissions. *Geosci. Model Dev.* 5, 1471–1492. <https://doi.org/10.5194/gmd-5-1471-2012>.
- Haapanala, S., Ekberg, A., Hakola, H., Tarvainen, V., Rinne, J., Hell, H., 2009. Mountain birch – potentially large source of sesquiterpenes into high latitude atmosphere. *Biogeosciences* 6, 2709–2718.
- Hakola, H., Tarvainen, V., Laurila, T., Hiltunen, V., Hellen, H., Keronen, P., 2003. Seasonal variation of VOC concentrations above a boreal coniferous forest. *Atmos. Environ.* 37, 1623–1634.
- Hakola, H., Hellén, H., Hemmälä, M., Rinne, J., Kulmala, M., 2012. In situ measurements of volatile organic compounds in a boreal forest. *Atmos. Chem. Phys.* 12, 11665–11678. <https://doi.org/10.5194/acp-12-11665-2012>.
- Hakola, H., Tarvainen, V., Praplan, A.P., Jaars, K., Hemmälä, M., Kulmala, M., 2017. Terpenoid and carbonyl emissions from Norway spruce in Finland during the growing season. *Atmos. Chem. Phys.* 17, 3357–3370. <https://doi.org/10.5194/acp-17-3357-2017>.
- Harrison, S.P., Morfopoulos, C., Dani, K.G.S., Prentice, I.C., Arneeth, A., Atwell, B.J., Barkley, M.P., Leishman, M.R., Loreto, F., Medlyn, B.E., Niinemets, Ü., Possell, M., Peñuelas, J., Wright, I.J., 2013. Volatile isoprenoid emissions from plastid to planet. *New Phytol.* 197, 49–57. <https://doi.org/10.1111/nph.12021>.
- Holopainen, J.K., Gershenson, J., 2010. Multiple stress factors and the emission of plant VOCs. *Trends Plant Sci.* 15, 176–184. <https://doi.org/10.1016/j.tplants.2010.01.006>.
- Holopainen, J.K., 2011. Can forest trees compensate for stress-generated growth losses by induced production of volatile compounds? *Tree Physiol.* 31, 1356–1377. <https://doi.org/10.1093/treephys/tp111>.
- Janson, R.W., 1993. Monoterpene emissions from Scots pine and Norwegian spruce. *J. Geophys. Res.* 98, 2839–2850.
- Janson, R., De Serves, C., Romero, R., 1999. Emission of isoprene and carbonyl compounds from a boreal forest and wetland in Sweden. *Agric. For. Meteorol.* 98–99, 671–681. [https://doi.org/10.1016/S0168-1923\(99\)00134-3](https://doi.org/10.1016/S0168-1923(99)00134-3).
- Janson, R., de Serves, C., 2001. Acetone and monoterpene emissions from the boreal forest in northern Europe. *Atmos. Environ.* 35, 4629–4637. [https://doi.org/10.1016/S1352-2310\(01\)0160-1](https://doi.org/10.1016/S1352-2310(01)0160-1).
- Jensen, L.S., Mueller, T., Magid, J., Nielsen, M.E., 1997. Temporal variation of C and N mineralization, microbial biomass and extractable organic pools in soil after oilseed rape straw incorporation in the fields. *Soil Biol. Biochem.* 29, 1043–1055.
- Keenan, T., Niinemets, Ü., Sabate, S., Gracia, C., Peñuelas, J., 2009. Process based inventory of isoprenoid emissions from European forests: model comparisons, current knowledge and uncertainties. *Atmos. Chem. Phys.* 9, 4053–4076. <https://doi.org/10.5194/acp-9-4053-2009>.
- Kesselmeier, J., Staudt, M., 1999. Biogenic Volatile Organic Compounds (VOC): an overview on emission, physiology and ecology. *Atmos. Chem. Phys.* 3, 23–88.
- Kivimänpää, M., Riikonen, J., Ahonen, V., Tervahauta, A., Holopainen, T., 2013. Sensitivity of Norway spruce physiology and terpenoid emission dynamics to elevated ozone and elevated temperature under open-field exposure. *Environ. Exp. Bot.* 90, 32–42. <https://doi.org/10.1016/j.envexpbot.2012.11.004>.
- Komenda, M., Koppmann, R., 2002. Monoterpene emissions from Scots pine (*Pinus sylvestris*): field studies of emission rate variabilities. *J. Geophys. Res.* 107, 1–25. <https://doi.org/10.1029/2001JD000691>.
- Laffner, Q., Aubinet, M., Schoon, N., Amelynck, C., Müller, J.-F., Dewulf, J., Van Langenhove, H., Steppe, K., Simpraga, M., Heinesch, B., 2011. Isoprene and monoterpene emissions from a mixed temperate forest. *Atmos. Environ.* 45, 3157–3168. <https://doi.org/10.1016/j.atmosenv.2011.02.054>.
- Lagergren, F., Eklundh, L., Grelle, A., Lundblad, M., Mölder, M., Lankreijer, H., Lindroth, A., 2005. Net primary production and light use efficiency in a mixed coniferous forest in Sweden. *Plant, Cell Environ.* 28, 412–423.
- Lothawornkitkul, J., Taylor, J.E., Paul, N.D., Hewitt, C.N., 2009. Biogenic volatile organic compounds in the Earth system. *New Phytol.* 183, 27–51. <https://doi.org/10.1111/j.1469-8137.2009.02859.x>.
- Lappalainen, H.K., Sevanto, S., Bäck, J., Ruuskanen, T.M., Kolari, P., Taipale, R., Rinne, J., Kulmala, M., Hari, P., 2009. Day-time concentrations of biogenic volatile organic compounds in a boreal forest canopy and their relation to environmental and biological factors. *Atmos. Chem. Phys.* 9, 5447–5459. <https://doi.org/10.5194/acp-9-5447-2009>.
- Loreto, F., Schnitzler, J.-P., 2010. Abiotic stresses and induced BVOCs. *Trends Plant Sci.* 15, 154–166. <https://doi.org/10.1016/j.tplants.2009.12.006>.
- van Meeningen, Y., Schurgers, G., Rinnan, R., Holst, T., 2016. BVOC emissions from English oak (*Quercus robur*) and European beech (*Fagus sylvatica*) along a latitudinal gradient. *Biogeosciences* 13, 6067–6080.
- Maffei, M.E., 2010. Sites of synthesis, biochemistry and functional role of plant volatiles. *South Afr. J. Bot.* 76, 612–631. <https://doi.org/10.1016/j.sajb.2010.03.003>.
- Monson, R.K., Grote, R., Niinemets, Ü., Schnitzler, J.-P., 2012. Modeling the isoprene emission rate from leaves. *New Phytol.* 195, 541–559. <https://doi.org/10.1111/j.1469-8137.2012.04204.x>.
- Nerg, A., Kainulainen, P., Vuorinen, M., Hansa, M., Holopainen, J.K., Kurkela, T., 1994. Seasonal and geographical variation of terpenes, resin acids and total phenolics in nursery grown seedlings of Scots pine (*Pinus sylvestris* L.). *New Phytol.* 128, 703–713.
- Niinemets, Ü., Monson, R.K., Arneeth, A., Ciccioli, P., Kesselmeier, J., Kuhn, U., Noe, S.M., Peñuelas, J., Staudt, M., 2010. The leaf-level emission factor of volatile isoprenoids: caveats, model algorithms, response shapes and scaling. *Biogeosciences* 7, 1809–1832. <https://doi.org/10.5194/bg-7-1809-2010>.
- Paasonen, P., Asmi, A., Petäjä, T., Kajos, M.K., Äijälä, M., Junninen, H., Holst, T., Abbatt, J.P.D., Arneeth, A., Birmili, V., van der Gon, H.D., Hamed, A., Hoffer, A., Laakso, L., Laaksonen, A., Leaitch, W.R., Plass-Dülmer, C., Pryor, S.C., Räisänen, P., Swietlicki, E., Wiedensohler, A., Worsnop, D.R., Kerminen, V.-M., Kulmala, M., 2013. Warming-induced increase in aerosol number concentration likely to moderate climate change. *Nat. Geosci.* 6, 438–442. <https://doi.org/10.1038/ngeo1800>.
- Peñuelas, J., Staudt, M., 2010. BVOCs and global change. *Trends Plant Sci.* 15, 133–144. <https://doi.org/10.1016/j.tplants.2009.12.005>.
- Persson, Y., Schurgers, G., Ekberg, A., Holst, T., 2016. Effects of intra-genotypic variation, variance with height and time of season on BVOC emissions. *Meteorol. Z.* 25, 377–388. <https://doi.org/10.1127/mz/2016/0674>.
- Rinne, J., Bäck, J., Hakola, H., 2009. Biogenic volatile organic compound emissions from the Eurasian taiga: current knowledge and future directions. *Boreal Environ. Res.* 14, 807–826.
- Semiz, G., Hejari, J., Isik, K., Holopainen, J.K., 2007. Variation in needle terpenoids among *Pinus sylvestris* L. (Pinaceae) provenances in Turkey. *Biochem. Syst. Ecol.* 35, 652–661.
- Shendryk, I., Hellström, M., Klemetsson, L., Kljun, N., 2014. Low-Density LIDAR and optical imagery for biomass estimation over boreal forest in Sweden. *Forests* 5, 992–1010. <https://doi.org/10.3390/f5050992>.
- Simpson, D., Winiwarter, W., Borjesson, C., Cinderyby, S., Ferreira, A., Guenther, A., Hewitt, C.N., Janson, R., Khalil, M.A.K., Owen, S., Pierce, T.E., Puxbaum, H., Shearer, M., Skiba, U., Steinbrecher, R., Tarrason, L., Oquist, M.G., 1999. Inventory emissions from nature in Europe. *J. Geophys. Res.* 104, 8113–8152.
- Sindelarova, K., Granier, C., Bouarar, I., Guenther, A., Tilmes, S., Stavrakou, T., Müller, J.-F., Kuhn, U., Stefani, P., Knorr, W., 2014. Global data set of biogenic VOC emissions calculated by the MEGAN model over the last 30 years. *Atmos. Chem. Phys.* 14, 9317–9341. <https://doi.org/10.5194/acp-14-9317-2014>.
- Skjøth, C.A., Geels, C., Hvidberg, M., Hertel, O., Brandt, J., Frohn, L.M., Hansen, K.M., Hedegård, G.B., Christensen, J.H., Moseholm, L., 2008. An inventory of tree species in Europe—an essential data input for air pollution modelling. *Ecol. Model.* 217, 292–304. <https://doi.org/10.1016/j.ecolmodel.2008.06.023>.
- Spracklen, D.V., Bonn, B., Carslaw, K.S., 2008. Boreal forests, aerosols and the impacts on clouds and climate. *Phil. Trans. R. Soc. A* 366, 4613–4626. <https://doi.org/10.1098/rsta.2008.0201>.
- Staudt, M., Mir, C., Joffre, R., Rambal, S., Bonin, A., Landais, D., Lumaret, R., 2004. Isoprenoid emissions of *Quercus* spp. (*Q. suber* and *Q. ilex*) in mixed stands contrasting in interspecific genetic introgression. *New Phytol.* 163, 573–584. <https://doi.org/10.1111/j.1469-8137.2004.01140.x>.
- Steinbrecher, R., Contran, N., Gugerli, F., Schnitzler, J.-P., Zimmer, L., Menard, T., Günthard-Goerg, M.S., 2013. Inter- and intra-specific variability in isoprene production and photosynthesis of Central European oak species. *Plant Biol.* 15, 148–156. <https://doi.org/10.1111/j.1438-8677.2012.00688.x>.
- Tarvainen, V., Hakola, H., Hellén, H., Bäck, J., Kulmala, M., 2005. Temperature and light dependence of the VOC emissions of Scots pine. *Atmos. Chem. Phys.* 5,

- 989–998.
- Tarvainen, V., Hakola, H., Rinne, J., Hellén, H., Haapanala, S., 2007. Towards a comprehensive emission inventory of terpenoids from boreal ecosystems. *Tellus* 59B, 526–534. <https://doi.org/10.1111/j.1600-0889.2007.00263.x>.
- Tunved, P., Hansson, H.-C., Kerminen, V.-M., Ström, J., Dal Maso, M., Lihavainen, H., Viisanen, Y., Aalto, P.P., Komppula, M., Kulmala, M., 2006. High natural aerosol loading over boreal forests. *Science* 312, 261–263.
- VanReken, T.M., Greenberg, J.P., Harley, P.C., Guenther, A.B., Smith, J.N., 2006. Direct measurement of particle formation and growth from the oxidation of biogenic emissions. *Atmos. Chem. Phys.* 6, 4403–4413. <https://doi.org/10.5194/acp-6-4403-2006>.
- Vickers, C.E., Gershenson, J., Lerdau, M.T., Loreto, F., 2009. A unified mechanism of action for volatile isoprenoids in plant abiotic stress. *Nat. Chem. Biol.* 5, 283–291. <https://doi.org/10.1038/nchembio.158>.
- Wallin, M.B., Weyhenmeyer, G.A., Bastviken, D., Chimel, H.E., Peter, S., Sobek, S., Klemetsson, L., 2015. Temporal control on concentration, character and export of dissolved organic carbon in two hemiboreal headwater streams draining contrasting catchments. *J. Geophys. Res. – Biogeosciences* 120, 832–846. <https://doi.org/10.1002/2014JG002814>.
- Yassaa, N., Song, W., Lelieveld, J., Vanhatalo, A., Bäck, J., Williams, J., 2012. Diel cycles of isoprenoids in the emissions of Norway spruce, four Scots pine chemotypes, and in Boreal forest ambient air during HUMPPA-COPEC-2010. *Atmos. Chem. Phys.* 12, 7215–7229. <https://doi.org/10.5194/acp-12-7215-2012>.

Web references

- Humboldt University of Berlin, https://www.agrar.hu-berlin.de/en/institut-en/departments/dntw-en/agrarmet-en/phaenologie/ipg/lpg_net (last accessed: 24th of February, 2017).
- ICOS Sweden, <http://www.icos-sweden.se/> (last accessed: 22nd of February, 2017).
- Slovenian Environment Agency, <http://meteo.arso.gov.si/met/en/> (last accessed: 1st of March, 2017).
- Agrarmeteorologie Bayern, <http://www.wetter-by.de> (last accessed: 1st of March, 2017).
- Finnish Meteorological Institute, <http://en.ilmatieteenlaitos.fi/> (last accessed: 1st of March, 2017).

**Avhandlingar från Institutionen för naturgeografi och ekosystemanalys (INES),
Lunds universitet**

**Dissertations from Department of Physical Geography and Ecosystem Science,
University of Lund**

Martin Sjöström, 2012: Satellite remote sensing of primary production in semi-arid Africa.

Zhenlin Yang, 2012: Small-scale climate variability and its ecosystem impacts in the sub-Arctic.

Ara Toomanian, 2012: Methods to improve and evaluate spatial data infrastructures.

Michał Heliasz, 2012: Spatial and temporal dynamics of subarctic birch forest carbon exchange.

Abdulghani Hasan, 2012: Spatially distributed hydrological modelling: wetness derived from digital elevation models to estimate peatland carbon.

Julia Bosiö, 2013: A green future with thawing permafrost mires?: a study of climate-vegetation interactions in European subarctic peatlands. (Lic.)

Anders Ahlström, 2013: Terrestrial ecosystem interactions with global climate and socio-economics.

Kerstin Baumanns, 2013: Drivers of global land use change: are increasing demands for food and bioenergy offset by technological change and yield increase? (Lic.)

Yengoh Genesis Tambang, 2013: Explaining agricultural yield gaps in Cameroon.

Jörgen Olofsson, 2013: The Earth: climate and anthropogenic interactions in a long time perspective.

David Wårlind, 2013: The role of carbon-nitrogen interactions for terrestrial ecosystem dynamics under global change: a modelling perspective.

Elin Sundqvist, 2014: Methane exchange in a boreal forest: the role of soils, vegetation and forest management.

Julie Mari Falk, 2014: Plant-soil-herbivore interactions in a high Arctic wetland: feedbacks to the carbon cycle.

Finn Hedefalk, 2014: Life histories across space and time: methods for including geographic factors on the micro-level in longitudinal demographic research. (Lic.)

Sadegh Jamali, 2014: Analyzing vegetation trends with sensor data from earth observation satellites.

Cecilia Olsson, 2014: Tree phenology modelling in the boreal and temperate climate zones : timing of spring and autumn events.

Jing Tang, 2014: Linking distributed hydrological processes with ecosystem vegetation dynamics and carbon cycling: modelling studies in a subarctic catchment of northern Sweden.

Wenxin Zhang, 2015: The role of biogeophysical feedbacks and their impacts in the arctic and boreal climate system.

Lina Eklund, 2015: “No Friends but the Mountains”: understanding population mobility and land dynamics in Iraqi Kurdistan.

Stefan Olin, 2015: Ecosystems in the Anthropocene: the role of cropland management for carbon and nitrogen cycle processes.

Thomas Möckel, 2015: Hyperspectral and multispectral remote sensing for mapping grassland vegetation.

Hongxiao Jin, 2015: Remote sensing phenology at European northern latitudes: from ground spectral towers to satellites.

Bakhtiyor Pulatov, 2015: Potential impact of climate change on European agriculture: a case study of potato and Colorado potato beetle.

Christian Stiegler, 2016: Surface energy exchange and land-atmosphere interactions of Arctic and subarctic tundra ecosystems under climate change.

Per-Ola Olsson, 2016: Monitoring insect defoliation in forests with time-series of satellite based remote sensing data: near real-time methods and impact on the carbon balance.

Jonas Dalmayne, 2016: Monitoring biodiversity in cultural landscapes: development of remote sensing- and GIS-based methods.

Balathandayuthabani Panneer Selvam, 2016: Reactive dissolved organic carbon dynamics in a changing environment: experimental evidence from soil and water.

Kerstin Engström, 2016: Pathways to future cropland: assessing uncertainties in socio-economic processes by applying a global land-use model.

Finn Hedefalk, 2016: Life paths through space and time: adding the micro-level geographic context to longitudinal historical demographic research.

Ehsan Abdolmajidi, 2016: Modeling and improving Spatial Data Infrastructure (SDI).

Giuliana Zanchi, 2016: Modelling nutrient transport from forest ecosystems to surface waters.

Florian Sallaba, 2016: Biophysical and human controls of land productivity under global change: development and demonstration of parsimonious modelling techniques.

Norbert Pirk, 2017: Tundra meets atmosphere: seasonal dynamics of trace gas exchange in the High Arctic.

Minchao Wu, 2017: Land-atmosphere interactions and regional Earth system dynamics due to natural and anthropogenic vegetation changes.

Niklas Boke-Olén, 2017: Global savannah phenology: integrating earth observation, ecosystem modelling, and PhenoCams.

Abdulhakim M. Abdi, 2017: Primary production in African drylands: quantifying supply and demand using earth observation and socio-ecological data.

Nitin Chaudhary, 2017: Peatland dynamics in response to past and potential future climate change.

Ylva van Meeningen, 2017: Is genetic diversity more important for terpene emissions than latitudinal adaptation?: using genetically identical trees to better understand emission fluctuations across a European latitudinal gradient.

Patrik Vestin, 2017: Effects of forest management on greenhouse gas fluxes in a boreal forest.

Mohammadreza Rajabi, 2017: Spatial modeling and simulation for disease surveillance.

Jan Blanke, 2018: European ecosystems on a changing planet: integrating climate change and land-use intensity data.

Min Wang, 2018: Characteristics of BVOC emissions from a Swedish boreal forest: using chambers to capture biogenic volatile organic compounds (BVOCs) from trees and forest floor.

Wilhelm Dubber, 2018: Natural and social dimensions of forest carbon accounting.

Emma Johansson, 2018: Large-Scale Land Acquisitions as a Driver of Socio-Environmental Change: From the Pixel to the Globe.

Helen Eriksson, 2018: Harmonisation of geographic data: between geographic levels, hierarcic structures and over time. (Lic.)

Zhendong Wu, 2018: Modelling the terrestrial carbon cycle: drivers, benchmarks, and model-data fusion.

Zhanzhang Cai, 2019: Vegetation observation in the big data era: Sentinel-2 data for mapping the seasonality of land vegetation.

Fabien Rizinjirabake, 2019: Dissolved organic carbon in tropical watersheds: linking field observation and ecohydrological modelling.

Jeppé Ågård Kristensen, 2019: Biogeochemistry in Subarctic birch forests: perspectives on insect herbivory.

Yanzi Yan, 2019: The role of hydrological cycle in forest ecosystems: flow path, nutrient cycling and water-carbon interaction.

George Oriangi, 2019: Urban resilience to climate change shocks and stresses in Mbale municipality in Eastern Uganda.

Alex Paulo Lubida, 2019: Investigating spatial data infrastructure planning in Tanzania using system modelling and social concepts.

Weiming Huang, 2020: Geospatial data and knowledge on the Web: knowledge-based geospatial data integration and visualisation with Semantic Web technologies.

Oskar Löfgren, 2020: Remote sensing of grassland communities: integrated effects of soil nutrients and habitat age.

Altaaf Mechiche-Alami, 2020: Food security in a changing climate: the role of cropland intensification and land acquisitions across Africa.

Helen Eriksson, 2020: Harmonisation of 3D geodata – a prerequisite for a digital information flow for applications in the planning and building sector.

Augustus Aturinde, 2020: GIS and Health: Enhancing Disease Surveillance and Intervention through Spatial Epidemiology.

Geert Hensgens, 2020: Dissolved organic matter dynamics across terrestrial and aquatic systems: sources, chemistry and microbial processing.

Enass Said Al-Kharusi, 2021: Broad-Scale Patterns in CDOM and Total Organic Matter Concentrations of Inland Waters – Insights from Remote Sensing and GIS.

Tetiana Svystun, 2021: Understanding the environmental regulation of tree phenology.

Pearl Mzobe, 2021: Bearing the brunt of warming: Interactions between carbon and hydrology in northern Sweden.

Tomas Karlsson, 2021: The variability in Salix BVOC emissions and possible consequences for managed SRC plantations.

